Order Number 9235737

Thermal desorption and decomposition of hazardous organic compounds: I. Mass transfer of benzene and chlorobenzene in soil matrices. II. Oxidation and pyrolysis of 1,1,1-trichloroethane in methane/oxygen/argon

Wu, Yo-ping, Ph.D.

New Jersey Institute of Technology, 1992

U·M·I
300 N. Zeeb Rd.
Ann Arbor, MI 48106

THERMAL DESORPTION AND DECOMPOSITION OF HAZARDOUS ORGANIC COMPOUNDS
I: MASS TRANSFER OF BENZENE AND CHLOROBENZENE IN SOIL MATRICES
II: OXIDATION AND PYROLYSIS OF 1,1,1-TRICHLOROETHANE IN METHANE/OXYGEN/ARGON

by
Yo-ping Wu

A Dissertation
Submitted to the Faculty of New Jersey Institute of Technology
in Partial Fulfillment of the Requirements for the Degree of
Doctor of Philosophy
Department of Chemical Engineering, Chemistry,
and Environmental Science
May 1992

APPROVAL PAGE

Thermal Desorption and Decomposition of Hazardous Organic Compounds
I: Mass Transfer of Benzene and Chlorobenzene in Soil Matrices
II: Oxidation and Pyrolysis of 1,1,1-Trichloroethane in Methane/Oxygen/Argon

by
Yo-ping Wu

Dr. Joseph W. Bozzelli, Dissertation Advisor
Distinguished Professor of Chemical Engineering,
Chemistry and Environmental Science, NJIT

Dr. Dana E. Knox, Committee Member
Professor of Chemical Engineering,
Chemistry and Environmental Science, NJIT

Dr. Gordon Lewandowski, Committee Member
Professor and Chairperson of Chemical Engineering,
Chemistry and Environmental Science, NJIT

Dr. Henry Shaw, Committee Member
Professor of Chemical Engineering,
Chemistry and Environmental Science, NJIT

Dr. Namunu J. Meegoda, Committee Member
Professor of Civil and Environmental Engineering, NJIT

ABSTRACT

Thermal Desorption and Decomposition of Hazardous Organic Compounds

I: Mass Transfer of Benzene and Chlorobenzene in Soil Matrices

II: Oxidation and Pyrolysis of 1,1,1-Trichloroethane in Methane/Oxygen/Argon

by

Yo-ping Wu

I: Mass Transfer of Benzene and Chlorobenzene in Soil Matrices

Experimental measurements on several apparatus were used in conjunction with chromatographic theory to study the thermal adsorption and desorption of organic vapors on soil with different particle sizes for analysis mass transfer parameters and heat of adsorption. Benzene (C_6H_6) and chlorobenzene (C_6H_5Cl) were tested on soil with 0.55, 0.46, 0.36, and 0.225 mm average particle sizes. Sample injection volumes for organic compounds were studied to ensure linearity of gas chromatography. Equilibrium constants were strongly dependent on temperature but not on particle size. Heats of adsorption, determined from the slope of the plot of Van't Hoff's equation, were −16.08 for C_6H_6 and −19.48 kcal/mole for C_6H_5Cl. An analysis of second central moment showed that mass transfer resistance of larger molecules like C_6H_6 and C_6H_5Cl was not strongly dependent on temperature within the ranges of this study and for this soil matrix.

Results from continuous adsorption and desorption experiments showed that temperature and inlet flow rate affect effluent concentration. The temperature effect on the effluent concentration of C_6H_6 became less significant for temperatures above 220 ^oC.

The results from an analytical solution and numerical analysis using orthogonal collocation method showed excellent coincidence. The numerical approach was therefore chosen to model experimental results. This model includes axial dispersion coefficients, intraparticle diffusion coefficient, film mass transfer

coefficients plus the adsorption equilibrium constant and shows good agreement at higher temperatures; but shows slower transfer through the bed for the effluent concentration of organics on soil at lower temperature.

II: Oxidation and Pyrolysis of 1,1,1-Trichloroethane in Methane/Oxygen/Argon

The thermal decomposition of 1,1,1-trichloroethane in methane/oxygen mixtures and argon bath gas was carried out at 1 atmosphere total pressure in tubular flow reactors. The thermal degradation of 1,1,1-trichloroethane and methane was analyzed systematically over the temperature range of 500 to 800°C, with average residence times of 0.05 to 2.5 seconds. Five reactant ratio sets, in three different diameter flow reactors, were studied.

It was found that the 99% decay of the 1,1,1-trichloroethane at 1 second residence time occurs at about 600°C for all the reactant ratio sets. The major products for 1,1,1-trichloroethane decomposition were 1,1-dichloroethylene and HCl. Oxygen (maximum 4.5%) had almost no effect on the initial decay rates of 1,1,1-trichloroethane in our study. Formation of CH_2CCl_2 as a major product from CH_3CCl_3 increased with increasing temperature to a maximum near 600°C at 1.0 sec residence time, and was independent of O_2/CH_3CCl_3 reactant ratio from 0 to 9. It then drops quickly with increasing temperature and increased O_2 partial pressure. Faster decay of compounds, such as C_2H_3Cl, C_2H_2, C_2H_4 and C_2HCl which were formed at lower temperatures, occurred when the reactor temperature was increased above 650°C, and higher oxygen levels were present in the mixture. At higher ratios of O_2 to CH_4, it was observed that lower temperatures were needed to form CO and CO_2. The major products at temperature above 750°C are HCl, C_2HCl, and non-chlorinated hydrocarbons C_2H_2, C_2H_4, CO and CO_2.

Increasing the surface to volume ratio of the quartz reactor accelerated the decomposition of the reactants, but had no effect on distribution of major products.

A detailed kinetic reaction mechanism was developed and used to model the experimental results. The mechanism consists of 339 elementary reactions with both forward and reverse rate constants based on thermochemical principles. A sensitivity analysis of the model was done to show the most important reactions in the mechanism.

Rate constants obtained for initially important decomposition of 1,1,1-trichloroethane over the temperature range 500 - 1000°C are:

	A(sec^{-1})	Ea(kcal/mole)
$CH_3CCl_3 \rightarrow CH_2CCl_2 + HCl$	3.35E+13	51.2
$CH_3CCl_3 \rightarrow CH_3CCl_2 + Cl$	4.59E+14	66.6

Transition state theory was utilized for isomerization reactions and Quantum Kassel theory was used to account for fall-off in unimolecular dissociation reaction and in reactions of adducts formed from addition, combination or insertion reactions.

BIOGRAPHICAL SKETCH

Author: Yo-ping Wu

Degree: Doctor of Philosophy

Date: May, 1992

Undergraduate and Graduate Education:

- Doctor of Philosophy, New Jersey Institute of Technology, Newark, NJ, May, 1992
- Master of Science in Chemical Engineering, New Jersey institute of Technology, Newark, NJ, May, 1989
- Bachelor of Science in Chemical Engineering, Tunghai University, Taichung, Taiwan, R.O.C., July, 1986

Major: Chemical Engineering

Presentations and Publications:

Wu, yo-ping. "Thermal Decomposition of 1,1,1-Trichloroethane-Methane-Oxygen Mixture in Tubular Flow Reactor", with J. W. Bozzelli, AIChE 1989 National Meeting, Aug., 1989, Philadelphia, PA.

Wu, yo-ping. "Thermodynamic Insights on Pathways to Formation of Chlorinated Dioxins and Dibenzofurans", with J. W. Bozzelli and E. R. Ritter, Chemosphere, Vol. 23, Nos. 8-10, pp1221-1232, 1991.

Wu, yo-ping. "Mass Transfer of Hazardous Organic Compounds in Soil Matrices Experiment and Model", with J. I. Dong and J. W. Bozzelli, Combust. Sci. and Tech., in press, 1992.

Wu, yo-ping. "Thermodynamic Analysis of Selected Pathways to Formation of Chlorinated Dioxins and Dibenzofurans", with R. Magee, E. R., Ritter and J. W. Bozzelli, manuscript submitted Environ. Sci. and Tech.

Wu, yo-ping. "High Temperature Oxidation of 1,1,1-Trichloroethane, A Comparison of Experiments with Detailed Model", with M. J. Thomson, C. P. Koshland, D. Lucass, R. Sawyer and J. W. Bozzelli, Western State Section/The Combustion Institute, 1992 Spring Meeting, March, 1992, Oregon State University, Corvallis, Oregon.

Wu, yo-ping. "Study of Adsorption-Desorption of Hazardous Organic Compounds on Soil Matrices from Gas Chromatography", with T. -H. Lay and J. W. Bozzelli, International Conference on Hazardous Waste Management, Atlantic City, NJ, May, 1992.

Positions Held:

9/87 - 5/92 Research Assistant, NJIT
Air Pollution Control Laboratory
Department of Chemical Engineering,
Chemistry and Environmental Science,

7/86 - 8/87 Teaching Associate, Tunghai University, Taichung, Taiwan, R.O.C.
Department of Chemical Engineering

This dissertation is dedicated to
my wife, Hui-tzu and my parents

ACKNOWLEDGEMENTS

I wish to express my appreciation to Dr. Joseph W. Bozzelli, my advisor, not only for his professional guidance but also for his encouragement and kindnesses. I am deeply indebted to him for the opportunities which he made available to me.

I would also like to thank my dissertation committee members, Dr. Dana Knox, Dr. Gordon Lewandowski, Dr. Henry Shaw and Dr. Namunu Meegoda for their careful review and comments.

It is my pleasure to thank Dr. Edward Ritter, Dr. Join-In Dong and Dr. Yang Soo Won who shared their experiences with me and helped me with GC/MS analysis during their stays at NJIT. In addition, I like to acknowledge my co-workers at NJIT, Dustin Ho, Hank Chiang and Larry Lay, for having dealt with me as a colleague, which has made my time at NJIT much more enjoyable and productive. Special thanks go to Yi-min Gao and Dr. Dana Knox for their help on the use of mercury porosimeter.

I am deeply grateful to my wife, Hui-tzu, and my parents for their love and support.

TABLE OF CONTENTS

I: Mass Transfer of Benzene and Chlorobenzene in Soil Matrices

LIST OF TABLES

SECTION I

SECTION II

LIST OF FIGURES

SECTION I

SECTION II

SECTION I
Mass Transfer of Benzene and Chlorobenzene in Soil Matrices

1. INTRODUCTION

The negative connotation associated with incineration as a hazardous waste disposal process, as perceived by the public, has resulted in a strong desire for alternative technologies (1,2,3,4). One of the current incineration applications is for treatment of soils contaminated with hazardous organic substances. These substances have been known to threaten human health through pathways such as: evaporation of organic compounds into the ambient atmosphere or contamination of surface and ground waters via transport through the soil which then impacts drinking water and aquatic organisms (5,6,7).

Estes et. al. (4) have reported that adsorption and desorption of organic compounds by soil particles is one of the more important factors governing complex process of transport of contaminants through the environment. Lighty et. al. (2,3) further reported that adsorption and desorption of contaminants in the soil particles during incineration is a important factor.

A number of treatment technologies for the decontamination of soils have been tried. These include: incineration of the entire soil mass, thermal desorption with secondary collection or treatment, biological treatment, photo-degradation, solidification, electrokinetic methods, vacuum extraction-volatilization and soil aeration. Most of these treatment methods involve a component of contaminant desorption. Among these, thermal desorption with purge, is considered one of the most feasible technologies as an alternate to incineration. It shows a high degree of effectiveness for a wide range of volatile and semi-volatile organics and combines reasonable energy and equipment costs with relatively rapid process times. The most recent US EPA listing of techniques applied to Superfund sites (8) lists 3 completed, 8 in design and 2 pre-design processes utilizing thermal desorption.

Recent studies have emphasized that a fundamental study of the adsorption

and desorption of contaminant organic compounds on soil matrices can contribute considerably to understanding the relevant thermodynamic and mass transfer processes (9,10). Two studies on mass transfer of these hazardous chemicals in soil matrices have and lead to development of an initial fundamental model for use in optimization of the operation of incineration systems, such as rotary kilns (10,11). In spite of increasing acceptance and application of thermal desorption treatment for soil decontamination and reclamation, there is little known about the mass transfer principles of organic contaminants through the heated soil matrices. More importantly, little is known about limitations of the process with respect to mass transfer properties of target organic compounds, or soil types and the relation of these to operating parameters.

The main objective of this study is to elucidate mass transfer mechanisms and equilibrium behavior of volatile organic substances in soil matrices using chromatographic types of experiments and theory. We plan to apply these parameters and mass transfer model to experiments on thermal desorption of organics with our labortary scale rotary kiln. In this study we report the results of adsorption and desorption of organic compounds on several particle sizes of a dried local (NJIT) soil.

2. LITERATURE REVIEW

Delineation and remediation of subsurface contamination have become a major focus of environmental science during the past few years (12). The introduction of chemicals into the environment may come from process effluents, spills, transportation, dumping, and release from landfill or storage facilities (13). In fiscal year of 1988, EPA issued a total 111 Records of Decisions (RODs) requiring control of site contamination sources. Among 74 treatment technologies, 22 cases used incineration/thermal destruction, 18 cases employed solidification/ stabilization/neutralization, 10 cases on vacuum extraction, 7 cases on volatilization/soil aeration, 7 cases utilized soil washing/flushing and so on (14).

There have been a number of efforts to understand the behavior of chemical substances in soil environment. Jury et. al. (15) have studied the transport and loss of soil-applied organic chemical, such as pesticide. They presented a simple procedure for determining the relative behavior of chemicals under prototype conditions. Valverde-Garcia et. al. (16) studied the adsorption of thiram and dimethoate, which are pesticides used for control of plant parasitic organisms, on Almeria soils. They concluded that the adsorption of thiram on Almeria soils is about threefold higher than that corresponding to dimethoate.

Dragun(17) has reported that the organic carbon content of the soil components is a primary factor governing the adsorption of organic chemicals. A number of studies, related to this concept, have been made experimentally(4,18-22) and theoretically(23,24) to understand the behavior of organic substances in complex soil environment. In spite of research on the mechanism of transport and equilibria of chemical substances in soil under environmental conditions, little effort has been made to study the behavior of organics in soil matrices from the process of decontamination using incineration or other thermal treatment technologies.

The group of Pershing and Lighty(2,3) has done research on the process of soil decontamination using incineration and thermal desorption technologies. They used a particle-characterization reactor to experimentally observe the desorption and diffusion behavior for p-xylene(2). They studied the desorption on several adsorbents at ambient temperature, indicating that more porous material (e.g. clays) show stronger retention curves in the desorption of p-xylene. They also observed the temperature effect on the desorption rate of p-xylene by varying the temperature of the soil bed. They concluded that desorption rate is a strong function of soil types and temperature is an important factor in desorbing the contaminated soil. In the consecutive experiments (3), they utilized bed-characterization reactor to measure mass change during experiment. They also utilized batch-type rotary kiln simulator to compare its desorption rate with those of the other two reactors. They found that the desorption rate of their rotary kiln simulator is between those of the other two reactors.

Rhue and Rao (25) have reviewed the applications of gas chromatographic technologies for characterizing vapor sorption on soils. They reviewed the current status of physicochemical measurements by gas chromatography, the use of soil and other natural materials for gas chromatographic columns, and the use of water as a liquid phase in gas chromatography. They reported that the sorption effect, the effects of isotherm curvature and pressure gradient on changes in peak shape during elution must be taken into consideration to prevent errors in the derived isotherm. They also pointed out that although a number of studies have used GC retention data to derive an adsorption isotherm for volatile organic compounds (VOCs), questions remain concerning the reproducibility of the isotherms on different columns and what factors effect isotherms derived from the soil columns.

The studies of VOC sorption on water films using GC appear to have been restricted to relatively high water contents and to dilute VOC concentrations.

Wood et. al. (26) used batch equilibrium and column miscible displacement techniques to investigate the influence of methanol on the sorption and transport of naphthalene, phenanthrene and the herbicide diuron in a sandy surface soil. They showed equilibrium sorption constants have an inverse, log-linear dependence on the volume fraction of methanol for sorption these three organic solutes from binary mixed solvent.

Smith et. al. (27) investigated the sorption of trichloroethene (TCE) vapor to vadose-zone soil above a contaminated water-table aquifer at Picatinny Arsenal in Morris County, NJ. They reported that soil-moisture content suppresses sorption of TCE vapor to soil up to saturation soil moisture content. Above saturation soil moisture content and soil uptake of TCE vapor is attributed largely to partition into soil organic matter. They found the moisture content of soil collected from the vadose-zone was greater than the saturation soil content, which implies that adsorption of TCE by the mineral fraction of the vadose-zone soil should be small relative to the partition uptake by soil's organic matter. They also reported that the ratio of the concentration of TCE on the vadose-zone soil to its concentration in the soil gas is 1-3 orders of magnitude greater than the ratio predicted using assumed of equilibrium conditions.

Dong(11) has utilized the chromatographic response analysis to study the mass transfer mechanism of organic contamination in single particle size soil matrices. The equilibrium constants have been found to be strongly dependent on temperature and showed good linearity from the plot of Van't Hoff equation. He also studied the adsorption isotherms of several organic chemical in soil matrices. The adsorption isotherms showed good linearity at the lower concentrations and

the slopes decreased with increasing temperature. Dong also developed an initial model with both an analytical solution and a numerical solution using orthogonal collocation method, to predict the transient mass transfer in a soil column. Sensitivity analysis was performed to analyze the effects of the mass transfer parameters and showed that axial dispersion coefficients, intraparticle diffusion coefficients and equilibrium constants have the most significant effects on the concentration profile in the soil column system.

3. MODEL DEVELOPMENT

A. Method of Analysis by Chromatography

Chromatographic response analysis, which incorporates axial dispersion, external diffusion (gas-to-particle surface), intraparticle diffusion and adsorption, was derived by Kubin(28) and Kucera (29). A significant number of applications have been applied both with this technique experimentally and theoretically(30-45). Many authors have used different definitions and different mass transfer mechanisms for their analysis. We, therefore, need to verify the appropriate expressions which are to be applied to experiment or model.

The basic mass transfer steps incorporated in the mathematical model for the chromatographic response of a packed soil column in this study are:

1. Axial dispersion of components along the column axis.
2. Diffusion from the main fluid phase to the external surface of the adsorbent particle (external film diffusion).
3. Diffusion through the pore space of the particles (internal diffusion).
4. The adsorption process of component between gas phase of the intraparticle pore space and particle surface.

The major assumptions where the following equations are based are:

1. The particle diameter is small in comparison with the overall column length.
2. The column is macroscopically uniform.
3. The adsorption equilibrium relationship is linear.

With these restrictions the basic equations to describe the packed soil column can be set up as follows:

Mass balance for the gas phase in the column:

$$\frac{\partial C}{\partial t} - D_z \frac{\partial^2 C}{\partial z^2} - v\frac{\partial C}{\partial z} = \frac{3(1-\theta_b)}{\theta_b R_p} N_{Rp} \tag{3-1}$$

where $N_{Rp} = D_p(\frac{\partial C_i}{\partial r})_{r=Rp} = k_f(C - C_i|_{Rp})$ (3-2)

and the mass balance inside the particles:

$$\theta_p \frac{\partial C_i}{\partial t} + (1-\theta_p)\frac{\partial C_p}{\partial t} = D_p(\frac{\partial^2 C_i}{\partial r^2} + \frac{2}{r}\frac{\partial C_i}{\partial r}) \tag{3-3}$$

with initial and boundary conditions:

$$C_i|_{t=0} = 0 \tag{3-4}$$

$$C(0, 0 \le t \le \tau) = C_0 \tag{3-5}$$

$$C(0, t > \tau) = 0 \tag{3-6}$$

$$C(\infty, t) = 0 \tag{3-7}$$

$$C(z, 0) = 0 \tag{3-8}$$

$$\left.\frac{\partial C_i}{\partial r}\right|_{r=0} = 0 \tag{3-9}$$

where C= sorbate concentration in the interparticle space in the column, g/cm^3

C_i = sorbate concentration in the intraparticle pore space, g/cm^3

C_o = sorbate concentration in the square pulse input, g/cm^3

C_p = sorbate concentration in the solid phase, g/cm^3

D_z = axial dispersion coefficient, cm^2/sec.

D_P = intraparticle diffusion coefficient, cm^2/sec.

k_f = mass transfer coefficient in the external film of particle, cm/sec.

K_a = adsorption equilibrium constant defined by

$$K_a = (1-\theta_p)\, C_p / \theta_p\, C_i \tag{3-10}$$

Rp = radius of a particle, cm.

r = distance from the center of a particle in the radial direction, cm

t = time, sec.

τ = time for the input square pulse, sec.

v = linear velocity of the carrier gas in the interparticle space, cm/sec.

z = distance from the inlet of the column, cm

θ_b = interparticle void fraction in the column

θ_p = intraparticle void fraction inside particles

Eq.(3-3) can be manipulated with the equilibrium constant defined in Eq.(3-10) to give

$$\theta_p(1+K_a)\frac{\partial C_i}{\partial t} = D_p\left(\frac{\partial^2 C_i}{\partial r^2} + \frac{2}{r}\frac{\partial C_i}{\partial r}\right) \tag{3-11}$$

If the Laplace transform of the variables with respect to time are $\overline{C}$and $\overline{C_i}$, Eq. (3-1) with (3-2), (3-4 to 3-9) and (3-11) may be written

$$D_z\frac{\partial^2\overline{C}}{\partial z^2} - v\frac{\partial\overline{C}}{\partial z} - \frac{3(1-\theta_b)}{\theta_b R_p}\overline{N}_{Rp} = p\overline{C} \tag{3-12}$$

$$\overline{N}_{Rp} = D_p\left(\frac{\partial\overline{C}_i}{\partial r}\right)_{r=Rp} = k_f(\overline{C} - \overline{C}_i|_{Rp}) \tag{3-13}$$

$$D_p\left(\frac{\partial^2\overline{C}_i}{\partial r^2} + \frac{2}{r}\frac{\partial\overline{C}_i}{\partial r}\right) = \theta_p(1+K_a)p\overline{C_i} \tag{3-14}$$

$$\left.\frac{\partial\overline{C}_i}{\partial r}\right|_{r=0} = 0 \tag{3-15}$$

$$\overline{C}(0) = \frac{C_0}{p}(1-\exp^{-p\tau}) \tag{3-16}$$

$$\overline{C}(\infty) = 0 \tag{3-17}$$

solving Eq.(3-14) and applying the boundary condition (3-15),

$$\overline{C_i} = \frac{B(z)}{r}\sinh(\alpha r) \tag{3-18}$$

$$\text{where } \alpha = \sqrt{\frac{\theta_p(1+K_a)}{D_p}p} \tag{3-19}$$

substituting this equation into (3-13) and rearranging,

$$\overline{C}=\frac{B(z)}{R_pB_1}[\phi(p)\cosh\phi(p)-(1-B_1)\sinh\phi(p)] \tag{3-20}$$

where $B_1=\frac{k_fR_p}{D_p}$ and $\phi(p)=R_p\alpha$.

Replacing the expression for $\overline{N_{Rp}}$ into Eq.(3-12) using Eq.(3-20),

$$D_z\frac{\partial^2}{\partial z^2}B(z)-v\frac{\partial}{\partial z}B(z)-G(p)B(z)=0 \tag{3-21}$$

where $G(p)=p+\frac{3(1-\theta_b)}{\theta_b}\frac{B_1D_p}{R_p^2}[1-\frac{B_1}{A_0(p)+B_1}]$ (3-22)

$$A_0(p)=\phi(p)\coth\phi(p)-1 \tag{3-23}$$

Solving Eq.(3-21) by using the boundary condition (3-17),

$$B(z)=B_0\exp[\frac{v}{2D_z}(1-\sqrt{1+\frac{4D_z}{v^2}G(p)})z] \tag{3-24}$$

combining Eq. (3-24) with Eq. (3-20) and applying the boundary condition (3-16), we have the solution for C in the Laplace domain:

$$\overline{C}=\frac{C_0}{p}[1-\exp(-p\tau)]\exp(-\lambda z) \tag{3-25}$$

where $\lambda=\frac{v}{2D_z}[\sqrt{1+\frac{4D_z}{v^2}G(p)}-1]$. (3-26)

Though it does not appear feasible to invert the transform, it is possible to obtain an explicit expression for the moments of the chromatographic peaks leaving the packed column directly from Eq.(3-25).

Using Van der Laan's theorem, the moments of chromatographic curves are defined as

$$M_n=(-1)^n\lim_{p\to 0}[\frac{d^n}{dp^n}\overline{C}] \tag{3-27}$$

where $M_n = \int_0^\infty Ct^n dt$ (3-28)

The n-th absolute moment is then given as:

$$\mu_n = \frac{M_n}{M_0} = \frac{\int_0^\infty Ct^n dt}{\int_0^\infty C dt} \tag{3-29}$$

and the n-th central moment is given as:

$$\mu'_n = \frac{\int_0^\infty C(t-t_1)^n dt}{\int_0^\infty C dt} \tag{3-30}$$

where $t_1 = \mu_1$ equals first absolute moment or an average retention time of the component in the column.

Hence, the first absolute moment is given by

$$\mu_1 = \frac{M_1}{M_0} = \frac{-\lim_{p\to 0}\frac{d\bar{C}}{dp}}{\lim_{p\to 0}\bar{C}} \tag{3-31}$$

By L'Hospital's rule,

$$M_0 = \lim_{p\to 0}\bar{C} = \tau C_0 \exp(-\lambda z) \tag{3-32}$$

$$M_1 = -\lim_{p\to 0}\frac{d\bar{C}}{dp} = C_0\tau[\lim_{p\to 0}(\frac{\tau}{2} + z\frac{d\lambda}{dp})\exp(-\lambda z)] \tag{3-33}$$

Again, applying L'Hospital's rule on the $\lim_{p\to 0}(\frac{d\lambda}{dp})$ in Eq. (3-33), we finally can obtain

$$\lim_{p\to 0}(\frac{d\lambda}{dp}) = \frac{1}{v}[1 + \frac{1-\theta_b}{\theta_b}\theta_p(1+K_a)] \tag{3-34}$$

substituting Eq.(3-34) back to Eq.(3-33), we have

$$M_1 = C_0\tau[\frac{\tau}{2} + \frac{L}{v}(1 + \frac{1-\theta_b}{\theta_b}\theta_p(1+K_a)]\exp(-\lambda L) \tag{3-35}$$

where z=L at the column outlet.

Then the first absolute moment μ_1 can be obtain as

$$\mu_1 = \frac{M_1}{M_0} = \frac{\tau}{2} + \frac{L}{v}[1 + \frac{1-\theta_b}{\theta_b}\theta_p(1+K_a)] \tag{3-36}$$

Proceeding in the same way, the second central moment is given by

$$\mu'_2 = \frac{\int_0^\infty C(t-\mu_1)^2 dt}{\int_0^\infty C dt} = \frac{M_2}{M_0} - \mu_1^2 \tag{3-37}$$

where

$$M_2 = \lim_{p\to 0}\frac{d^2\overline{C}}{dp^2} = C_0 \lim_{p\to 0}\{[\frac{\tau^3}{3} + L\tau^2\frac{d\lambda}{dp} + L^2\tau(\frac{d\lambda}{dp})^2 - L\tau\frac{d^2\lambda}{dp^2}]\exp(-\lambda L)\} \tag{3-38}$$

In solving this equation, we need expressions for the derivative form of λ.

$$\frac{d^2\lambda}{dp^2} = -\frac{2D_z}{v^3}[1 + \frac{4D_z}{v^2}G(p)]^{-3/2}(\frac{dG}{dp})^2 + \frac{1}{v}[1 + \frac{4D_z}{v^2}G(p)]^{1/2}\frac{d^2G}{dp^2} \tag{3-39}$$

After manipulating the equations by limiting the value of p to zero in Eq. (3-38), the following expressions are obtained:

$$\lim_{p\to 0}\frac{d^2G}{dp^2} = -(\frac{2}{3}\frac{R_p}{k_f} + \frac{2}{15}\frac{R_p^2}{D_p})\frac{1-\theta_b}{\theta_b}[\theta_p(1+K_a)]^2 \tag{3-40}$$

and then

$$\lim_{p\to 0}\frac{d^2\lambda}{dp^2} = \frac{-2D_z}{v^3}[1 + \frac{1-\theta_b}{\theta_b}\theta_p(1+K_a)]^2 - \frac{1}{v}(\frac{2}{3}\frac{R_p}{k_f} + \frac{2}{15}\frac{R_p^2}{D_p})\frac{1-\theta_b}{\theta_b}[\theta_p(1+K_a)]^2 \tag{3-41}$$

substituting Eq.(3-34) and (3-41) into (3-38), we have

$$\begin{aligned} M_2 = C_0\{&\frac{\tau^3}{3} + \frac{L\tau^2}{v}[1 + \frac{1-\theta_b}{\theta_b}\theta_p(1+K_a)] + (\frac{L^2\tau^2}{v^2} + \frac{2L\tau D_z}{v^3}) \\ &[1 + \frac{1-\theta_b}{\theta_b}\theta_p(1+K_a)]^2 + \frac{L\tau}{v}(\frac{2}{3}\frac{R_p}{k_f} + \frac{2}{15}\frac{R_p^2}{D_p})\frac{1-\theta_b}{\theta_b}[\theta_p(1+K_a)]^2\}\exp(-\lambda L) \end{aligned} \tag{3-42}$$

substituting Eq.(3-36) and (3-42) into Eq.(3-37) gives the second central moment, μ'_2 as:

$$\mu'_2=\frac{\tau^2}{12}+\frac{2LD_z}{v^3}[1+\frac{1-\theta_b}{\theta_b}\theta_p(1+K_a)]^2+(\frac{R_p}{k_f}+\frac{R_p^2}{5D_p})[\frac{2L}{3v}\frac{1-\theta_b}{\theta_b}\theta_p^2(1+K_a)^2] \quad (3\text{-}43)$$

Experimental chromatographic curves of the effluent from the packed column can be used to evaluate the moments μ_1 and μ'_2. The first absolute moment physically describes the average retention time or center of mass of the chromatographic peak. The experimental chromatographic curve can be evaluated by the computer program using the equation as:

$$\mu_1=\frac{\int_0^\infty Ctdt}{\int_0^\infty Cdt}=\frac{\sum_{t=0}^{t=\infty} tC}{\sum_{t=0}^{t=\infty} C} \quad (3\text{-}44)$$

The second central moment, μ'_2, signifies the variance of the chromatographic response i.e. the experimental data and for the computer calculation, μ'_2 can be written as

$$\mu'_2=\frac{\int_0^\infty C(t-\mu_1)^2dt}{\int_0^\infty Cdt}=\frac{\sum_{t=0}^{t=\infty} t^2C}{\sum_{t=0}^{t=\infty} C}-\mu_1^2 \quad (3\text{-}45)$$

B. Theoretical Prediction of Effluent Concentration of a Packed Soil Column

Mathematical solutions for the adsorption column have been presented for special cases. For example, Rosen (46) solved the problem when only intraparticle diffusion is significant. Rosen (46,47) also considered the combined effects of intraparticle and external diffusion. Rasmuson and Neretnieks (48) extended the

solution of Rosen (46) to include longitudinal dispersion. The analytical solution of the adsorption column considering longitudinal dispersion, intraparticle diffusion and film mass transfer resistance were tried and shown to be appropriate in the studies of Rasmuson and Neretnieks (48) and Rasmuson (49). A simplified form of their result is used here with some modification of the parameter terms and with the assumption of a fast adsorption rate.

The concentration, C(z,t), of the adsorbing gas as a function of time and axial position in the packed column can be obtained by solving the equation set for a chromatographic column, Eq. (3-1) to (3-3). The only difference between this case and that of the chromatographic column is the boundary condition for chromatographic column, Eq. (3-5) and (3-6), should be replaced by

$$C(0, t > 0) = C_0 \tag{3-46}$$

which describes the concentration from the inlet as maintained constant.

Final solution is as follows:

$$u(z,t) = \frac{1}{2} + \frac{2}{\pi}\int_0^\infty \exp\left(\frac{1}{2}Pe - \sqrt{\frac{\sqrt{(z^2x')^2 + (z^2y')^2} + z^2x'}{2}}\right)\sin\left(y\lambda^2 - \sqrt{\frac{\sqrt{(z^2x')^2 + (z^2y')^2} + z^2x'}{2}}\right)\frac{d\lambda}{\lambda} \tag{3-47}$$

where $z^2x' = Pe(\frac{1}{4}Pe + \delta H_1)$ (3-48)

$$z^2y' = \delta Pe\left(\frac{2}{3}\frac{\lambda^2}{R_1} + H_2\right) \tag{3-49}$$

$$H_1 = \frac{H_{D1} + \upsilon(H_{D1}^2 + H_{D2}^2)}{(1 + \upsilon H_{D1})^2 + (\upsilon H_{D2})^2} \tag{3-50}$$

$$H_2 = \frac{H_{D2}}{(1 + \upsilon H_{D1})^2 + (\upsilon H_{D2})^2} \tag{3-51}$$

$$H_{D1} = \lambda\left(\frac{\sinh 2\lambda + \sin 2\lambda}{\cosh 2\lambda - \cos 2\lambda}\right) - 1 \tag{3-52}$$

$$H_{D2} = \lambda\left(\frac{\sinh 2\lambda - \sin 2\lambda}{\cosh 2\lambda - \cos 2\lambda}\right) \tag{3-53}$$

and λ variable of integration, with parameters as follow:

$$y = \frac{2D_p t}{KR_p^2} \qquad Pe = \frac{Lv}{D_z}$$

$$K = \theta_p + \theta_p K_a \qquad m = \frac{\theta_b}{1-\theta_b}$$

$$R_1 = \frac{K}{m} \qquad \delta = \frac{\gamma L}{mv}$$

$$\upsilon = \frac{\gamma R_p}{3k_f} \qquad \gamma = \frac{3D_p}{R_p^2}$$

In order to obtain the infinite integral term in Eq.(3-47), a numerical method was utilized. A QDAGI subprogram of IMSL software, which uses Gauss-Kornrod rule to estimate the integral and the error (50), was utilized for this integration in semi-infinite interval. The detailed FORTRAN program of this solution method is listed in Appendix I-2.

A numerical approach using the orthogonal collocation method has been derived by Dong (11). Dong has briefly described the matrices development which is required for the simulation using orthogonal collocation method and the developed matrices were verified in Dong's work. The verification from Dong shows that a matrix of 8 x 8 in the axial direction and that of 7 x 7 in the radial direction of soil particle are determined to be sufficient in this numerical solution. The numerical model, which was initially developed by Dong, has been modified in order to generate the output data file for graphic use. This numerical simulation program and the developed matrices combined with IVPAG subprogram, which

utilizes the Adams-Moulton or the Gear Integration Method, of IMSL software in the NJIT DEC VAX/VMS system can then perform the mathematics for determination of concentration profiles in the adsorption/desorption of soil packed column system. The program for the numerical simulation is listed in Appendix I-3.

4. EXPERIMENTAL METHODS

A. Soil Equilibrium Test

The soil equilibrium test system consists of an injection unit, a six-port gas sampling valve, a ten-way gas sampling valve, an equilibrium chamber and a magnetically-coupled micropump for circulation of the gases through the system and is outlined in Figure 4-1. A magnetically-coupled metering gear pump (Cole Parmer, Concord, CA) and speed controller (Cole Parmer model 2630) are used to circulate the gas at low flow rates. Speed controller setting was calibrated by using soap film flowmeter (Hewlett-Packard). The injection unit was wrapped by heating tape and maintained at 150 ^{o}C , which is high enough to vaporize the organic chemicals in this study.

The equilibrium chamber was made of conical aluminum flages, aluminum adapters, aluminum centering rings with viton O-rings and aluminum clamps connecting these components, which are generally used in vacuum devices. The soil bed was secured by placing phosphor-bronze 49 mm diameter screens from mini-sieve inserts (Bel-Artt Products, Pequannock, N.J.) between the centering ring. Mesh number of sieves is 120. Amount of soil loaded between the screens for each run is about 10 grams. The soil used was pretreated in a separate oven at 200°C for 16 hours and then cooled in a glass desiccator. A K-type thermocouple was installed at the center of soil bed to monitor soil bed temperature and connected to a thermocouple meter.

System components including a ten-way valve with loops and equilibrium chamber were installed in a gas chromatograph (Varian 3700) oven which is used as a constant temperature bath. Vacuum was connected to the system to evacuate any remaining hazardous organic compound after each run.

Prior to the equilibrium tests, vacuum was applied to the system, then pure nitrogen gas was allowed to fill the system to 1 atmosphere pressure. Two hours were needed to allow the soil bed to reach a stable test temperature after the soil was loaded. 0.5 μL unit of organic compound was injected using micro syringes into the injection unit for the adsorption phase. The system was then allowed to reach equilibrium (at least one hour). Gas phase concentration was then determined by sampling gas through the six-port sampling valve (with 1 cc. sampling loop, heated at 170 ^{o}C) to the on-line FID detector. The concentration of both phases were then calculated by the mass balance. Addition units of the target organic compound were then applied to the system after each sampling with this process repeated until a satisfactory adsorption isotherm was obtained.

The desorption experiment are carried out after the adsorption experiment was performed. The position of ten-way valve was switched to replace a known volume (20 cc) of gas phase in the system with pure nitrogen. The system was allowed to reach its new equilibrium and then gas phase concentration was determined through the sampling valve by the FID detector. This procedure is similar to that of the adsorption experiments replacing the organic containing vapor phase with equal volumes of pure N_2, were repeated until a desorption isotherm was obtained.

B. Plug Deposition Experiment

A gas chromatograph and a data acquisition system are utilized for the chromatographic response analysis experiment. Figure 4-2 shows a diagram of the plug deposition experiment. The gas chromatograph used here is Shimadzu model GC 8A. Signals generated by the flame ionization detector were collected in a Hewlett Packard integrator HP3396A (1/5 sec. per signal) and then converted to

digital data and stored in IBM PC/XT through a RS-232-C cable. A PASCAL computer program is used to analyze the digital data and evaluated the average retention time and the variance of the chromatographic peak. A detailed PASCAL program listing can be found in Appendix I-1.

Organic soil was taken from Newark, N.J. ground surface, cleaned using tap water and baked in the oven at 200 ^{o}C overnight. The soil was also analyzed by X-Ray diffraction for determination of mineral fractions. Further specifies on characterization of the soil can be found in tables in Chapter 5. The treated soil was separated into particle size classes by sieves (U.S. standard Testing Sieve, ASTM-11, Soil Test, I.L.). The average particle size of the soil taken as the diameter of the equivalent spherical particle for this study are D= 0.55, 0.463, 0.363, and 0.225 mm. The properties of soil particles are listed in Table 5-3. The sieved soil was packed in a 0.21 in (5.33 mm) ID stainless steel tube (length = 24 in). The soil bed was then placed inside GC oven and heated up to 350 ^{o}C for at least 24 hours. Chemicals chosen in this study are C_6H_6 and C_6H_5Cl.

The organic compound was kept in ice bath (0°C) to ensure constant vapor pressure. A fixed volume of vapor (5 μL for C_6H_6 and 25 μL for C_6H_5Cl) was taken by a gas tight syringe (CR- 700 series, Hamilton Co.) and then injected onto the head of the soil column. Pure nitrogen gas served as carrier. Temperature was changed in 20 ^{o}C increments and flow was varied from 5 to 30 ml/min at each temperature. The target organic remaining in the soil column after one hour operation at the specific temperature and flow rate was purged by increasing temperature (ca. 100 ^{o}C higher than the operating temperature). Flow rate was varied to enable measurement of mass transfer coefficients. The dead volume, which is 1.31 cm^3, of the system was determined from the retention

time of the chromatographic peak by direct connection of the tubing (exclude the soil column) to the FID.

C. Soil Column Adsorption/Desorption Experiment

The experimental apparatus for adsorption/desorption are similar to that for the plug deposition experiment. An outline of this system is illustrated in Figure 4-3. The only difference between these two experiments is the injection unit. The injection unit for this experiment contains a six-way gas sampling valve and a glass impinger containing the target compound. The six-way valve was wrapped by heating tape and temperature fixed at 150°C. A moderate flow of nitrogen gas was allowed to flow through the glass impinger, which contain the target compound and was kept in an ice bath (0°C), to supply constant concentration of the target organic compound in the gas stream to the soil column. Soil columns used in this experiment are identical to those used for the plug deposition experiment.

For the adsorption stage, the six-way gas sampling valve is turned to the contamination (inject) position after the soil column in the GC oven reaches the desired operating temperature. Continuous signal from the FID was then recorded until the outlet concentration of the column reached an asymptotic value. Bunched digital data was then transferred from the HP3396A integrator to the IBM PC/XT for further analysis.

Desorption experiments started by changing the six-way valve position to bypass the saturator after the adsorption stage was observed. This allowed pure N_2 to flow into the saturated soil column. The same data management procedure used in the adsorption process was then followed to obtain the data for desorption experiments.

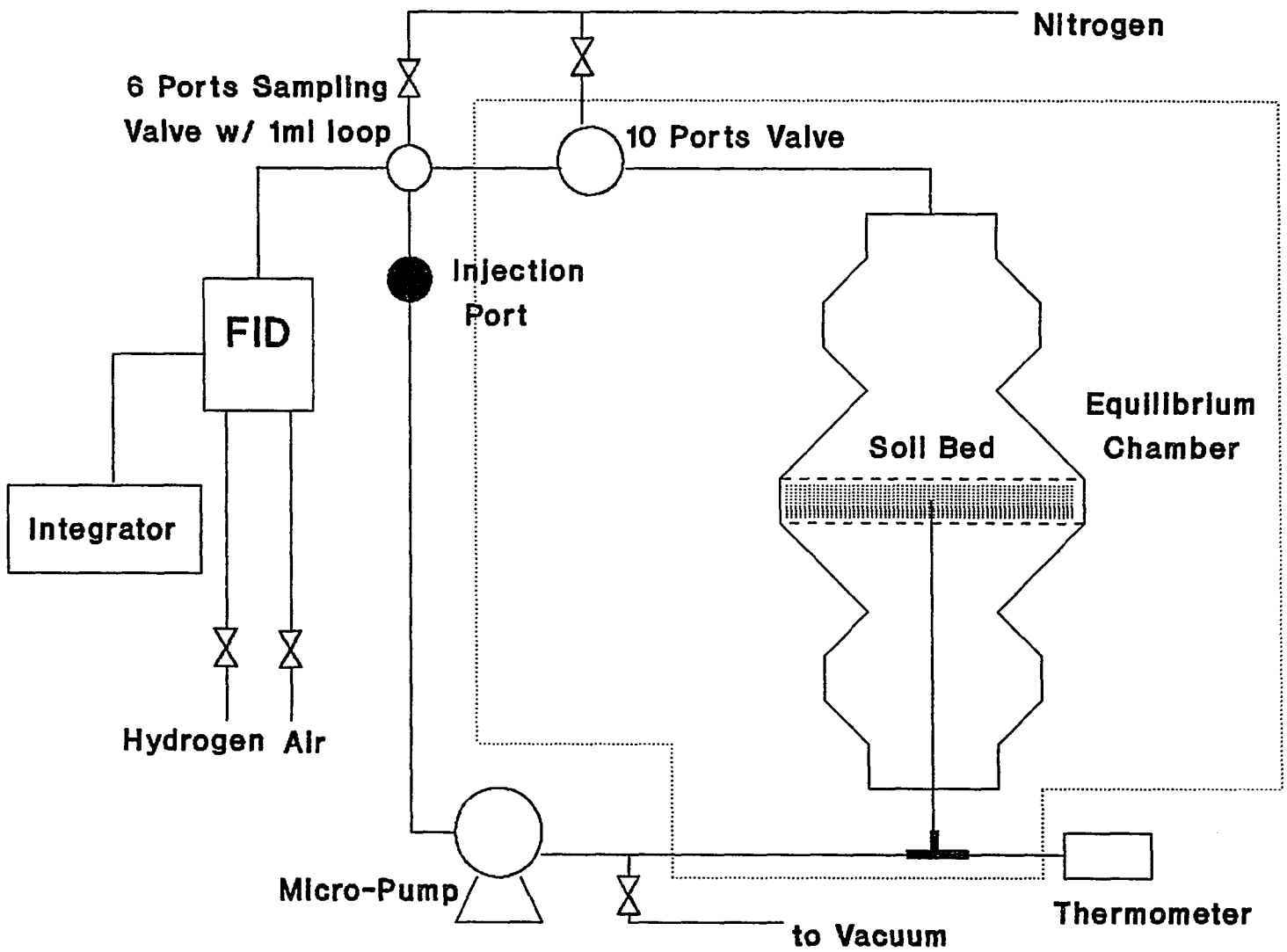

Figure 4-1. Soil Equilibrium System

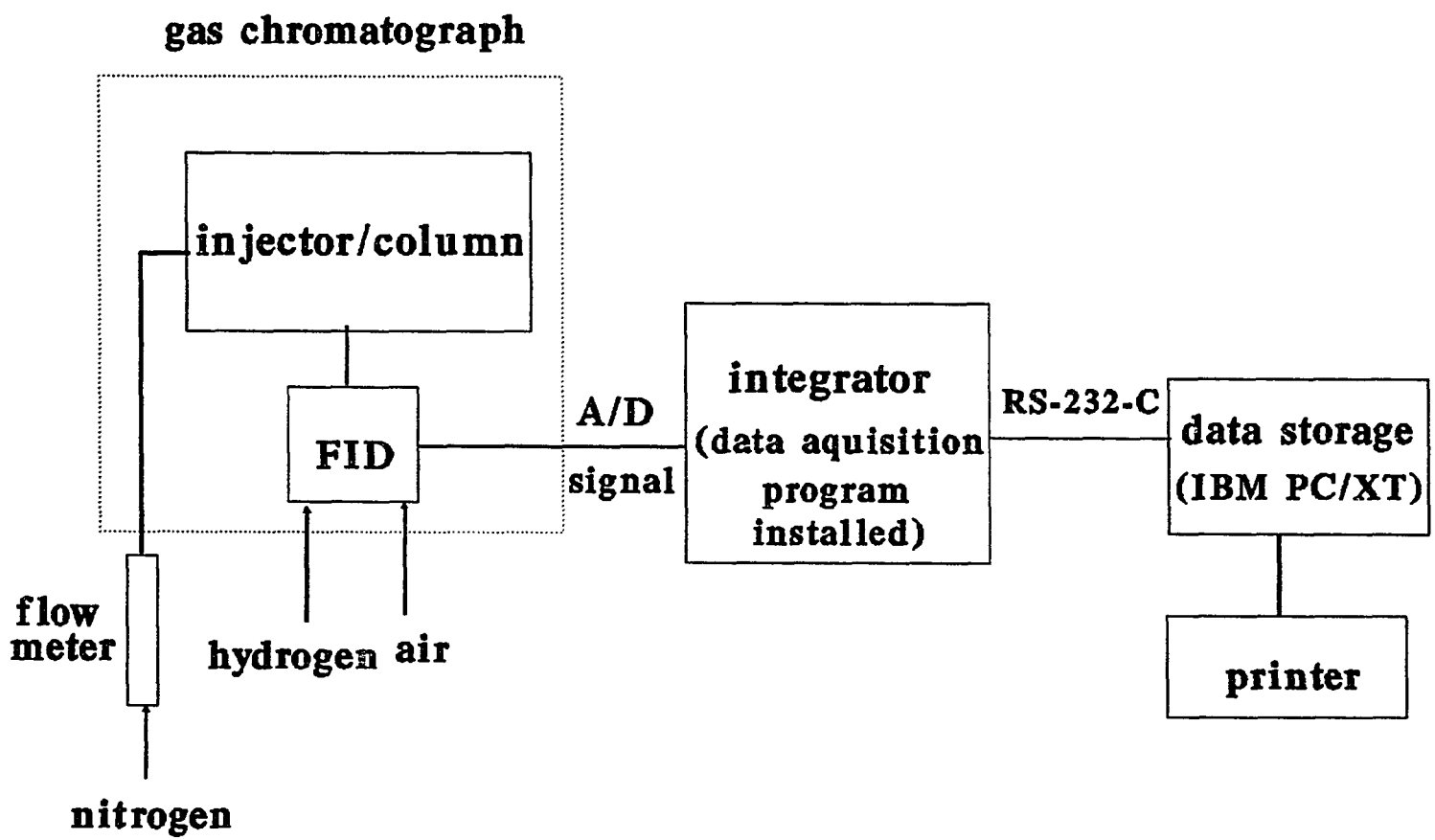

Figure 4-2. System Outline of Equipment for Plug Flow Deposition Experiments

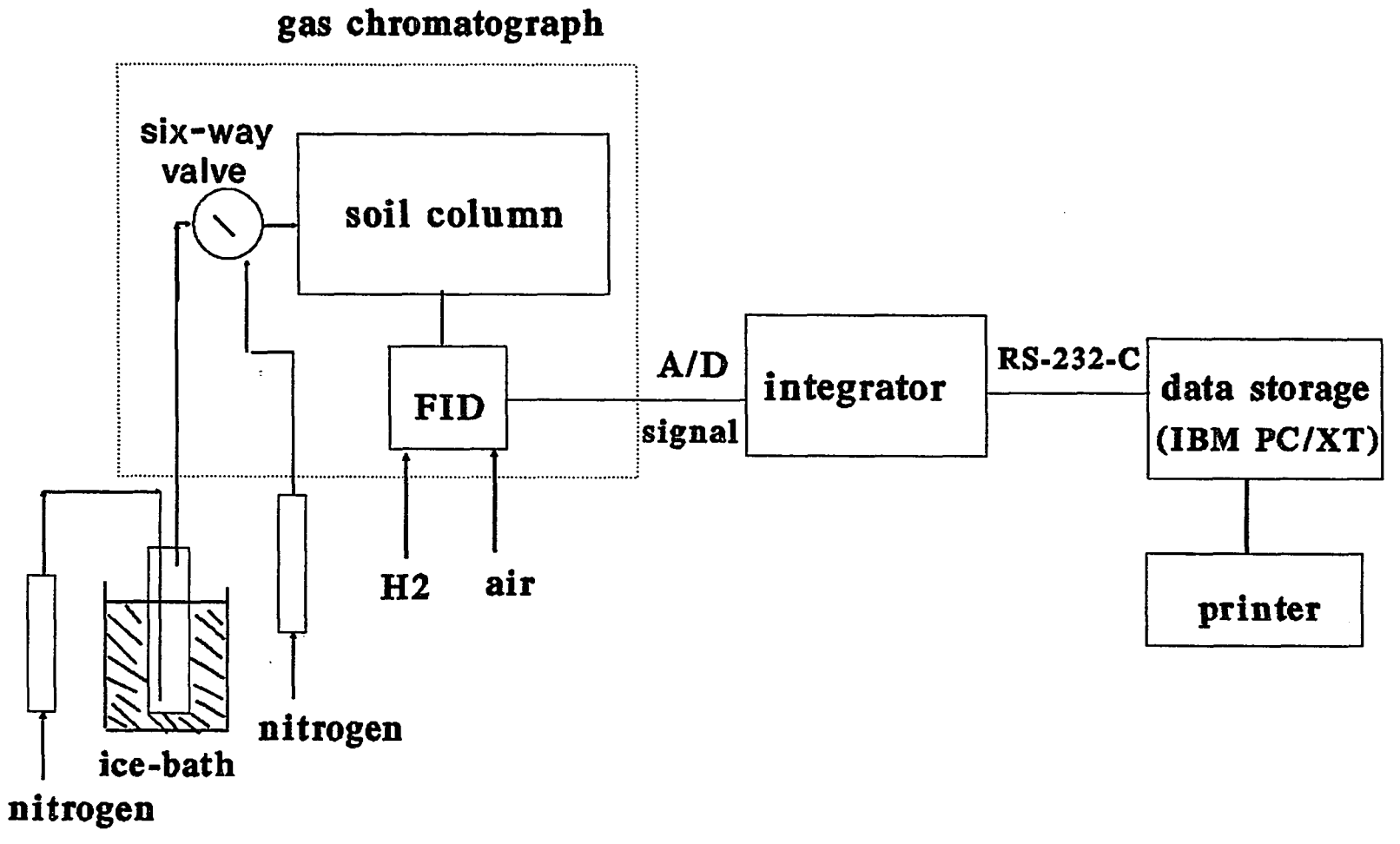

Figure 4-3. Outline of Experimental Apparatus for Soil Contamination/Decontamination

5. RESULTS AND DISCUSSION

The stock soil used in this work was taken from a location within the New Jersey Institute of Technology campus at Newark, New Jersey. Preparation and primary treatment are detailed in Hornsby(51). Particle size distribution of stock soil was determined using sieves and a mechanical shaker (Humbolt Manufacturing Co.) and is listed in Table 5-1. Stock soil has also been analyzed by Labtech Corp., Fairfield, New Jersey, using emission spectroscopy and X-ray diffraction. This analysis shows the major elements of stock soil are Si, Al, X, Fe, K, Mg, and Mn as listed in Table 5-2.

Table 5-3 lists the properties of the stock soil used in the study. The average density, 2.48 g/cm^3, was determined by water displacement, which followed the Standard Test Method for Specific Gravity of Soils (ASTM D854-83). The intraparticle porosity of particles was determined using mercury porosimetry, and it has an average value at 0.22. The average particle diameter chosen in this study are 0.55, 0.463, 0.363 and 0.225 mm. The columns used for plug deposition experiment and breakthrough measurements are 61 cm x 0.53 mm i.d. stainless steel tube.

Organic compounds used in this experiment are C_6H_6 and C_6H_5Cl. Table 5-4 tabulates their physical properties with parameters for vapor pressure calculation. The vapor pressure (P_{vp}) are determined by using the Antoine vapor-pressure equation (52). To relate the vapor pressure to concentration using the ideal gas law, for example, 5μL of the vapor phase of C_6H_6 at 0°C (273 K) will gives 7.1E-9 gmole.

A. Equilibrium Adsorption Results

The equilibrium test system, as described in Chapter 4, is further characterized in Table 5-5. Preliminary calibrations were performed to measure the gas flow rates

in the equilibrium chamber and the relationship between target compound concentration in the chamber and corresponding response peak areas from gas chromatography. Figure 5-1 demonstrates that the gas flow rate and superficial linear velocity across the soil bed corresponds linearly to the reading on the speed controller of the magnetically coupled micropump. Figure 5-2 shows the calibration curves for C_6H_6 and C_6H_5Cl, i.e. the relationship between concentration and gas chromatographic peak area in the empty reactor system. These response curves are quite linear, which indicated that there is no systematic effect or error throughout the operations.

The speed controller was fixed at reading 4 (ca. 5.7 cm^3/min) for all experiments, this supplied uniform gas flow (0.29 cm/min) across the soil bed. Figure 5-3 shows the adsorption isotherm for C_6H_6 on the NJIT soil at 120 and 160 ^oC. The isotherm of C_6H_6 shows the linear relationship at the lower concentrations for both temperatures. Figure 5-4 shows the adsorption isotherm for C_6H_5Cl on soil at 120 and 160 ^oC. From data in Figure 5-4, it is clear that the linear zone for C_6H_5Cl is easier to identify than for C_6H_6. Slopes of the linear zone tend to decrease with increasing temperature for both organics, which indicate that the organic molecules favor transfer to gas phase, as expected, with higher temperature. Figure 5-3 and 5-4 also show the results from the desorption experiments of C_6H_6 and C_6H_5Cl, respectively. In these operations, as shown in figures, the concentrations of solid phase remain a relatively high value even as the gas phase concentration decreases which implies that the desorption of C_6H_6 and C_6H_5Cl is very slow at 160^oC and below.

Due to the temperature limitation of the O-ring seals in the equilibrium chamber, it is not recommended to operate the system at temperatures higher than 180 ^oC. In order to obtain the adsorption isotherm at higher temperature, we

employed the method derived from the gas chromatography (54-57). The operation procedures are almost the same as those in plug deposition experiments, except here the injection size (dose) is varied from 2.5 to 300 μL(vapor phase at 0 °C) for C_6H_6 and 5 to 50 μL(vapor phase at 0 °C) for C_6H_5Cl. The amount adsorbed by the soil particles is obtained from the difference in the measurements from the packed column (soil bed) and the bypass.

Figures 5-5 and 5-6 show the adsorption isotherm for C_6H_6 and C_6H_5Cl on soil column at 220 °C. The isotherm of C_6H_6 shows a linear relationship at lower concentration and the ratio of solid phase concentration to gas phase concentration tended to decrease as concentration increased. The adsorption isotherm of C_6H_5Cl exhibits a linear isotherm over the entire concentration range as shown in Figure 5-6. This is because the concentration of C_6H_5Cl from 6.7E-10 to 6.7E-9 mole is relatively low and remains in the low concentration region relative to C_6H_6 from 1.4E-8 to 4.3E-7 mole.

The purpose of adsorption isotherm study is to validate the assumptions used in the mathematical model and to use these results to verify that a linear adsorption relationship holds at low concentrations.

B. Plug Deposition Experiments

A series of linearity tests have been performed to ensure the pulse injection volume into the packed soil column are reasonable, i.e. that no column overloading or other artifact effects occur. Figure 5-7 is the plot of a series of these linearity tests for C_6H_5Cl at 220 °C and linear velocity 4.23 cm/sec. Figure 5-8 is the linearity test for C_6H_6 at 200 °C and linear velocity 3.93 cm/sec. The samples of the organic compounds were taken from the vapor phase where liquid vapor was maintained with the liquid was held at 0 °C in an ice bath to ensure the constant

vapor pressure. It is clear from data in Figures 5-7 and 5-8, that the sample injection volume has almost no influence on the shape of the chromatograph for sample volume less than 100 μL for C_6H_5Cl and 20 μL for C_6H_6. Sample volumes chosen for plug deposition experiments are 25 μL for C_6H_5Cl and 5 μL for C_6H_6, which are well within the linear region of our experimental setup and this implies that linear chromatographic theory can be applied.

The moment analysis technique can be used to analyze the chromatographic response in a soil matrix column as discussed in Chapter 3. Since the output signal data from the flame ionization detector can be transferred from the integrator to an IBM PC/XT, it is possible to evaluate the first absolute moment and second central moment by a computer program. This program, listed in Appendix 1, written in Turbo Pascal was used to calculated the center of mass and the variance for the chromatographic peak. The first absolute moment for the center of mass can be obtained from equation (3-36) and rearranging it, as follow:

$$\frac{\mu - \frac{L}{v}(1+\alpha\beta)}{\alpha\beta} = \frac{L}{v}K_a \tag{5-1}$$

where $\alpha = \frac{\theta_b}{1-\theta_b}$, $\beta = \theta_p$ and $\mu = \mu_1 - \frac{\tau}{2}$.

By plotting $\frac{\mu - \frac{L}{v}(1+\alpha\beta)}{\alpha\beta}$ (which is denoted as Y in the tables and figures) vs $\frac{L}{v}$ from Eq.(5-1), the slope is equal to the equilibrium constant K_a. Figure 5-9 shows a typical plot for C_6H_6 for test at average particle diameter 0.46 mm column. Figure 5-10 shows a typical plot of C_6H_5Cl through a soil column which has average particle diameter 0.55 mm over temperatures from 220 ^oC to 280 ^oC. It is apparent that the linearity requirement is fulfilled for all testing temperatures as

shown. The values of adsorption equilibrium constant K_a determined from the slopes of the lines are given in Table 5-10 and 5-11. Figure set 5-11 illustrates the dependence of μ from C_6H_6 on L/v for all particle sizes at various temperature. The dependence of μ from C_6H_5Cl on L/v for all particle sizes is shown in Figure set 5-12. Schneider and Smith (31) and Andrieu and Smith (35) have showed that there is no particle size effect on the first moment result for the adsorption of gases on silica gel and activated carbon. From the experimental results on four different particle sizes, as shown in Figure sets 5-11 and 5-12, the reduced first absolute moments are linear with respect L/v as expected. This indicating that there is also no particle size effect on the first absolute moment for the soil adsorption because according to Eq. (5-1) the results should not be a function of particle size but only of the adsorption equilibrium constant K_a. Summarized results of this experiment are listed in Table 5-6 (for C_6H_6) and Table 5-7 (C_6H_5Cl). As one can see from these figures and tables, the equilibrium constants (K_a) decrease as temperature increases, as expected.

It is also useful to show the effect of varied injection doses on first and second moments to verify the reproducibility. Figure 5-13 shows the effect of C_6H_5Cl doses on these moments at 220°C. The first and second moments remain constant as doses increased up to 50μL as shown.

The Van't Hoff equation,

$$\frac{Ka}{T} = \left(\frac{K_a}{T}\right)_0 EXP\left(-\frac{\Delta H}{RT}\right) \tag{5-2}$$

can be utilized to determine the temperature dependency on equilibrium constants by plotting $\ln(K_a/T)$ vs 1/T. Figure 5-14 is such plot according to the Van't Hoff equation for C_6H_5Cl and C_6H_6 for all particle sizes. The heat of adsorption ΔH can be obtained from the slope of the straight line. The observed values of ΔH_{ads} for C_6H_6 is −15.89 kcal/mole and −18.86 kcal/mole for C_6H_5Cl. Since there are no

literature data we know of on heat of adsorption for these compounds on the soil we used, it is difficult to compare heat of adsorption from this study with the literature value. Table 5-8 lists the heat of adsorption of C_6H_6 on varies adsorbents. Our experimental value for C_6H_6 is similar to those on 13X molecular sieve which has an Al_2O_3 chemical base and as our soil has a significant amount of clay, which contains fine alumina and silica particulate, we feel these results are reasonable validate of our theory and experimental procedures.

The corresponding expression to obtain axial dispersion and mass transfer resistance can be derived from a combination from Eq.(3-36) and (3-43):

$$\frac{\sigma^2 L}{2\mu^2 v} = \frac{D_z}{v^2} + \frac{1}{\alpha}\left(\frac{R_p^2}{15D_p} + \frac{R_p}{3k_f}\right)\left[1 + \frac{1}{\alpha\beta(1+K_a)}\right]^{-2} \tag{5-3}$$

where $\sigma^2 = \mu'_2 - \frac{\tau^2}{12}$. Applying Eq. (5-3), plots of $\frac{\sigma^2 L}{2\mu^2 v}$ vs. $\frac{1}{v^2}$, allow the axial dispersion coefficient D_z to be obtained from the slope of the plot. The intraparticle diffusion coefficient D_p can be derived from the value of the intercept with use of an empirical equation (45) for determination of film mass transfer coefficient k_f. Equilibrium constants, K_a, needed in this calculation can be obtained from the first moment analysis. Analysis results for the estimation of mass transfer parameters with varied gas phase flow rates are summarized in Table 5-6 and 5-7. Figure 5-15 shows a typical plot for the calculation of mass transfer parameters for C_6H_6 on 0.463 mm average particle diameter at varied temperature. Figure 5-16 shows a example of such plot for C_6H_5Cl from 0.55 mm average particle diameter soil column. Figure sets 5-17 and 5-18 show the dependence of the second central moment on particle size at varied temperatures for C_6H_6 and C_6H_5Cl, respectively. It is hard to classify the temperature effect on

the second central moment for the same particle size as shown in Figures 5-15, 16, 17 and 18. One also can plot the intercept from the these plots vs. R_p^2 (where R_p is the radius of the particles, cm) to show the particle size effect here if there is one. This is shown in Figure 5-19 for C_6H_6 and Figure 5-20 for C_6H_5Cl. The data from these two figures show that the mass transfer coefficients are insensitive to the particle size for both compounds. These results are similar to those of Kumar et. al. (44) who have shown that when molecules are too large to penetrate the lattice of the soil particle, the mass transfer resistance is small and insensitive to temperature.

In order to obtain intraparticle diffusion coefficients, D_p, the mass transfer coefficient for the mass transfer resistance film, k_f, on the outer surface of particles should be first estimated using empirical equation(45). The appropriate dimensionless group characterizing film mass transfer is the Sherwood number, defined by $Sh \equiv 2R_p k_f/D_m$, which is analog of the Nusselt number for heat transfer. The limiting value of Nusselt number for low Reynolds number flows is 2.0, and this should also be applicable to Sherwood numbers. Ranz and Marshall have derived a correlation from the results of an experimental study of mass transfer rate for freely falling solid spheres:

$$Sh = \frac{2k_f R_p}{D_m} = 2.0 + 0.6 Sc^{1/3} Re^{1/2} \tag{5-4}$$

which has been widely applied to packed beds. This equation implies that the Sherwood number approaches a limiting value of 2.0 at low velocity. This is the regime of our experiments.

As shown in Eq (5-4), the molecular diffusivity data, D_m, need to be obtained to estimate the film mass transfer. The Chapman-Enskog equation (58) can be utilized for accurate estimation of the molecular diffusivity. For a binary

gas mixture

$$D_m = \frac{0.00158T^{3/2}(1/M_A + 1/M_B)^{1/2}}{P\sigma_{AB}^2\Omega(\varepsilon/kT)} \tag{5-5}$$

where D_m= molecular diffusivity, cm^2/sec

T = temperature, K

M_A,M_B= molecular weights

P= pressure, 1 atm in this study

σ_{AB}= 1/2 (σ_A+σ_B) is the collision diameter from Lennard-Jones potential, Å

$\varepsilon = \sqrt{\varepsilon_A \varepsilon_B}$ is the Lennard-Jones force constant, erg

k = Boltzmann constant

Ω = a function of ε/kT, (dimensionless)

Calculated molecular diffusivities with corresponding parameters which are required for Eq. (5-5) are listed in Table 5-9. Film mass transfer coefficient, k_f, can then be calculated by plugging D_m into Eq. (5-4). A calculated k_f, intraparticle diffusion coefficient, can then be obtained by utilizing the intercept values from the plots of Eq. (5-3). Tables 5-10 and 5-11 summarize the mass transfer parameter calculation results from this study for C_6H_6 and C_6H_5Cl, respectively. The adsorption equilibrium constants, K_a, decrease with increasing temperature as expected and illustrated in these two tables. K_a's for C_6H_5Cl are much higher than those for C_6H_6 at the same temperature. The results in Figures 5-15, 16, 17 and 18, indicate that it is difficult to distinguish any temperature effect on axial dispersion coefficient D_z and intraparticle diffusion coefficient D_p. It is also difficult to see the effect of particle size on D_z and D_p. This lack of result may caused by the differences between particle sizes utilized in this study are not significant or that the organic compound being relative large (Lennard-Jones

kinetic diameter is 5.27 Å for C_6H_6 and 5.95 Å for C_6H_5Cl) to penetrate the lattice of the soil particle.

C. Effluent Concentration of Soil Columns

As described in Chapter 3-B, an analytical solution for the adsorption of organics (contamination process) on a soil column was utilized to calculate the breakthrough curves, enabling the comparison of the analytical solution results with numerical simulation and experimental results. A FORTRAN program, which has been modified from the initial model of Dong's work (11), was developed to perform this calculation. The QDAGI subroutine from the IMSL package was utilized. This program was executed on the NJIT DEC VAX/VMS V5.3-1 system. The input data for this program include column dimensions and gas velocity. The equilibrium constant, axial dispersion coefficient, intraparticle diffusion coefficient and film mass transfer coefficient were input as obtained from the moment analysis. The program for the analytical solution is listed in Appendix I-2.

A numerical method to describe the adsorption and desorption behavior inside an adsorption column using the orthogonal collocation method was described in Chapter 3-B. This method was utilized to simulate the adsorption and desorption processes of organic compounds in a soil packed column and to compare its results with experimental results and to validate our model.

Dong (11) has briefly described the matrices development which is required for the simulation using orthogonal collocation method. The developed matrices have also been verified in Dong's work. The verification from Dong shows that a matrix of 8 x 8 in the axial direction and of 7 x 7 in the radial direction of the particle are determined to be sufficient in this numerical solution. The numerical

model, which was initially developed by Dong, has been modified in order to generate the output data file for graphic use. This numerical simulation program and the developed matrices combined with the IVPAG subprogram from the IMSL package in the NJIT DEC VAX/VMS system can then perform the mathematical determination of concentration profiles in the adsorption/desorption of soil packed column system. The program for the numerical simulation was listed in Appendix I-3.

For the purpose of comparison with analytical solution, six collocation points for both the intraparticle radial coordinate (radial direction inside the particles) and the axial direction of the column were selected in the numerical solution. Both results from analytical and numerical solutions are compared in Figure set 5-21 to show the breakthrough curves in the column. The curves from both approaches, as shown in Figure set 5-21, show essentially identical results and thus validate that the numerical approach can be utilized for further analysis.

The experimental breakthrough curve measurements are performed on 0.463 and 0.225 mm average particle diameter columns for several flow rate settings. The dimension for these columns are the same as those in the plug deposition experiments. The temperature setting for breakthrough curve measurements on C_6H_6 are 200, 220, 240 ^oC, and 220, 240, 260^oC for C_6H_5Cl.

Figures 5-22 and 5-23 show that there is little effect of particle size on the effluent concentration of C_6H_6 and C_6H_5Cl, respectively. The different particle sizes have almost no effect on the effluent concentration of either C_6H_6 or C_6H_5Cl. Figure 5-24 shows the temperature effect on the adsorption phase of C_6H_6 at same inlet flow setting. Figures 5-25 and 5-26 show similar plots only for the desorption phase for C_6H_6 and C_6H_5Cl, respectively. The breakthroughs and desorptions occur earlier at higher temperature for both compounds as expect.

Figure 5-25 also shows that the differences of desorption of C_6H_6 appear to be less significant at temperature above 220 ^oC. Figure 5-27 shows that the desorption of C_6H_5Cl with different flow settings at 260 ^oC. Here the higher flow rate does remove the organic compound faster or easier than the low flow rate.

The mass transfer parameters which are obtained from the moment analysis can now utilized to simulated the outlet concentration in the processes of adsorption and desorption of the soil packed column. We base our modeling on the numerical approach. The simulated (model) results are compared with the experimental data from breakthrough curve measurements on soil columns as shown in Figure sets 5-28 and 5-29. The results from the numerical approach all show slower breakthrough than experiments on both adsorption and desorption cases from the comparisons of the effluent concentration for C_6H_6,. Although the differences become smaller as linear velocity increases, there still exists a small delay in the numerical approach results.

The numerical approach for C_6H_5Cl match the experimental results quite well for two different linear velocities for adsorption and desorption cases at 260 ^oC as shown in Figure 5-29-a to 5-29-d. The numerical approach also show slower breakthrough than the experimental data for C_6H_5Cl at lower temperatures, e.g. 240 ^oC as in Figure 5-29-e and 5-29-f.

The differences between experimental and numerical result might come from the experimental errors of the data obtained from the plug deposition experiments at lower temperatures, which have shown has some deviations on the average retention time and variance in plug deposition experiments, or there might be some additional organic-particle interactions at lower temperature between soil and C_6H_6 or C_6H_5Cl which needs to be take into account.

We note that both these molecules are aromatic systems with significant π

bond networks. It is possible that alkane and other saturated molecules (as opposed to unsaturated with π bonds) may serve the theory better. This result will be tested and if validated we will need to account for π bond adsorption further in important molecules like larger PAH's (Polycyclic Aromatic Hydrocarbons) for particle thermal desorption.

Table 5-1. Particle Size Distribution of NJIT Stock Soil

Particle Diameter (microns)	Mesh Size	Mass (g)	% of Total
-	> 100	2000	6.9
150	100	2910	10.0
212	70	480	1.7
250	60	3200	11.0
425	40	7060	24.3
-	< 40	13400	46.1
total		29050	100

Table 5-2. Emission Spectrographic Analysis Results of NJIT Stock Soil

Element	Range of Percent by Mass
Al	>10 %
B	0.001-0.01 %
Ba	0.01-0.1 %
Ca	1.0-10.0 % (H)
Cr	0.001-0.1 %
Cu	0.001-0.01 %
Fe	1.0-10.0 %
K	1.0-10.0 %
Mg	0.1-1.0 %
Mn	0.1-1.0 % (L)
X	>10 %
Ni	0.001-0.01 %
Si	>10 %
Sr	0.001-0.01 %
Ti	0.1-10.0 %
V	0.001-0.01 %
Zn	0.01-0.1 %
Zr	0.001-0.1 %

Note:

1. (H) and (L) indicate high and low end of range.
2. Results are semiquantitative. Accuracy and sensitivity are element and matrix dependent.

Table 5-3. Properties of NJIT Stock Soil

Mesh No.	Avg. Particle Diameter(mm)	Density* (g/cm^3)	Particle Porosity**	Void Fraction of Soil Bed
30/35	0.55	2.501	0.231	0.531
35/40	0.463	2.470	0.221	0.498
40/50	0.363	2.473	0.218	0.462
50/100	0.225	2.481	0.21	0.442
	overall	2.48	0.22	

* Density was measured by water displacement follow the ASTM D854 instruction.

** Particle porosity was measured by the mercury porosimetry

Table 5-4. Property Data of C_6H_6 and C_6H_5Cl

Compound	M.W.	Boiling Pt. (°C)	Density @25°C	ANTA	ANTB	ANT C	P_{vp}* @0°C (mmHg)
C_6H_6	78.11	80	0.879	15.9008	2788.51	-52.36	26.34
C_6H_5Cl	112.56	132	1.107	16.0676	3295.12	-55.66	2.49

* vapor pressure (P_{vp}) was calculated by Antoine vapor-pressure equation (52):

$$\ln(P_{vp}) = ANTA - ANTB/(T + ANTC)$$

with vapor pressure in mmHg and T in K.

Table 5-5. Characteristics of Soil Equilibrium System

Void Volume of System	
Chamber (exclude soil bed) :	119.6 cc
Copper loop :	20 cc
	(49 in. long x 1/4 o.d.)
Soil bed :	15.7 cc
1/8" copper tube :	3.2 cc
1/8" S.S tube :	3.0 cc
1/4" S. S. tube :	3.4 cc
Total volume:	164.9 cc
Soil Bed:	
Diameter:	5.0 cm
Depth:	0.8 cm
Soil loading:	~ 10 gram

Table 5-6. Experimental Results of C6H6 on NJIT Soil from Chromatographic Analysis and Calculation for First Absolute Moment and Second Central Moment Plots

Soil Particle Diameter: 0.55 mm Temp. 180 °C

Scale	l. vel (cm/sec)	Rt (min)	Variance (min^2)	Corr. Rt (min)	Y (min)	L/v (min)	$10/v^2$ sec^2/cm	$\sigma^2L/2\mu^2v$ (sec)
1.5	2.09	18.4731	19.9661	18.4302	90.858	0.4872	2.2964	0.8591
2	2.77	15.1671	16.4240	15.1348	74.815	0.3668	1.3015	0.7889
2	2.77	15.5486	16.8151	15.5163	76.757	0.3668	1.3015	0.7685
2.5	3.77	12.5089	12.0653	12.4852	61.917	0.2698	0.7045	0.6266
2.5	3.77	11.9913	11.6837	11.9676	59.282	0.2698	0.7045	0.6604
3	4.71	11.4803	11.2386	11.4614	57.034	0.2157	0.4501	0.5536
3	4.71	11.6992	11.6200	11.6802	58.148	0.2157	0.4501	0.5511
4.5	6.14	6.4689	4.1252	6.4544	31.850	0.1655	0.2651	0.4918
4.5	6.14	7.2502	5.5150	7.2357	35.827	0.1655	0.2651	0.5232

Soil Particle Diameter: 0.55 mm Temp. 200 °C

Scale	l. vel (cm/sec)	Rt (min)	Variance (min^2)	Corr. Rt (min)	Y (min)	L/v (min)	$10/v^2$ sec^2/cm	$\sigma^2L/2\mu^2v$ (sec)
1	1.62	15.0366	15.2800	14.9812	72.434	0.6293	3.8314	1.2852
1	1.62	15.0465	15.2435	14.9911	72.484	0.6293	3.8314	1.2805
1.5	2.18	8.4568	5.1375	8.4158	40.001	0.4666	2.1064	1.0153
1.5	2.18	8.0092	4.5643	7.9681	37.723	0.4666	2.1064	1.0062
2	2.89	6.6679	3.7793	6.6370	31.649	0.3513	1.1938	0.9041
2.5	3.93	5.2019	2.4474	5.1792	24.792	0.2584	0.6462	0.7073
2.5	3.93	5.1916	2.3648	5.1689	24.740	0.2584	0.6462	0.6862
4.5	6.41	3.1968	1.0789	3.1829	15.238	0.1585	0.2432	0.5065
4.5	6.41	3.0548	0.8700	3.0409	14.515	0.1585	0.2432	0.4475

Table 5-6. (cont'd)
Soil Particle Diameter: 0.55 mm Temp. 220 °C

Scale	l. vel (cm/sec)	Rt (min)	Variance (min^2)	Corr. Rt (min)	Y (min)	L/v (min)	$10/v^2$ sec^2/cm	$\sigma^2L/2\mu^2v$ (sec)
1	1.68	7.2819	3.9408	7.2287	33.123	0.6038	3.5270	1.3657
1	1.68	7.4802	3.9252	7.4270	34.132	0.6038	3.5270	1.2886
1.5	2.27	4.1273	1.2417	4.0879	18.084	0.4477	1.9390	0.9976
1.5	2.27	4.3092	1.3738	4.2698	19.010	0.4477	1.9390	1.0116
2	3.02	3.5676	1.0348	3.5379	15.958	0.3370	1.0989	0.8356
2	3.02	3.5865	1.0062	3.5569	16.055	0.3370	1.0989	0.8039
2.5	4.10	2.8226	0.6422	2.8007	12.748	0.2480	0.5948	0.6089
2.5	4.10	2.6216	0.5794	2.5998	11.725	0.2480	0.5948	0.6375
3	5.13	2.3947	0.4840	2.3772	10.895	0.1982	0.3801	0.5091
3	5.13	2.4020	0.5258	2.3845	10.932	0.1982	0.3801	0.5497
4.5	6.68	1.4276	0.1980	1.4142	6.273	0.1521	0.2239	0.4517
4.5	6.68	1.4656	0.2086	1.4522	6.466	0.1521	0.2239	0.4512

Soil Particle Diameter: 0.55 mm Temp. 240 °C

Scale	l. vel (cm/sec)	Rt (min)	Variance (min^2)	Corr. Rt (min)	Y (min)	L/v (min)	$10/v^2$ sec^2/cm	$\sigma^2L/2\mu^2v$ (sec)
1	1.75	4.2314	1.2132	4.1803	17.747	0.5802	3.2574	1.2076
1.5	2.36	2.3919	0.4516	2.3540	9.364	0.4302	1.7908	1.0507
1.5	2.36	2.4553	0.5281	2.4174	9.686	0.4302	1.7908	1.1652
2.5	4.27	1.4375	0.1837	1.4165	5.760	0.2383	0.5494	0.6540
2.5	4.27	1.8011	0.2470	1.7802	7.611	0.2383	0.5494	0.5569
4.5	6.95	0.9479	0.0970	0.9350	3.870	0.1462	0.2068	0.4864
4.5	6.95	0.8662	0.0841	0.8533	3.454	0.1462	0.2068	0.5064

Soil Particle Diameter: 0.55 mm Temp. 260 °C

Scale	l. vel (cm/sec)	Rt (min)	Variance (min^2)	Corr. Rt (min)	Y (min)	L/v (min)	$10/v^2$ sec^2/cm	$\sigma^2L/2\mu^2v$ (sec)
1.5	2.46	1.5806	0.1670	1.5442	5.339	0.4141	1.6590	0.8678
1.5	2.46	1.6434	0.1904	1.6070	5.659	0.4141	1.6590	0.9138
2.5	4.43	0.9077	0.0574	0.8875	3.121	0.2294	0.5089	0.5005
2.5	4.43	0.9141	0.0568	0.8939	3.154	0.2294	0.5089	0.4876

Table 5-6. (cont'd)
Soil Particle Diameter: 0.463mm Temp. 180 °C

Scale	l. vel (cm/sec)	Rt (min)	Variance (min^2)	Corr. Rt (min)	Y (min)	L/v (min)	$10/v^2$ sec^2/cm	$\sigma^2L/2\mu^2v$ (sec)
1.5	2.29	16.0276	19.3862	15.9847	69.180	0.4433	1.9010	1.0089
2	3.05	14.5517	16.4124	14.5194	63.216	0.3337	1.0774	0.7794
2	3.05	14.2088	15.8445	14.1765	61.680	0.3337	1.0774	0.7893
2.5	4.14	11.8458	11.3859	11.8221	51.616	0.2455	0.5832	0.6000
2.5	4.14	11.1030	11.5205	11.0793	48.288	0.2455	0.5832	0.6913
3	5.18	9.3247	9.1368	9.3057	40.613	0.1962	0.3726	0.6212
3	5.18	10.4131	11.1574	10.3941	45.489	0.1962	0.3726	0.6080
4.5	6.75	8.2122	7.8269	8.1976	35.899	0.1506	0.2195	0.5263
4.5	6.75	8.6957	8.3709	8.6811	38.065	0.1506	0.2195	0.5019

Soil Particle Diameter: 0.463mm Temp. 200 °C

Scale	l. vel (cm/sec)	Rt (min)	Variance (min^2)	Corr. Rt (min)	Y (min)	L/v (min)	$10/v^2$ sec^2/cm	$\sigma^2L/2\mu^2v$ (sec)
1	1.78	14.9273	16.0693	14.8719	63.486	0.5726	3.1717	1.2479
1	1.78	16.6603	17.7075	16.6050	71.250	0.5726	3.1717	1.1031
1.5	2.39	6.4548	3.6220	6.4137	26.406	0.4245	1.7437	1.1212
1.5	2.39	6.7925	3.7321	6.7515	27.919	0.4245	1.7437	1.0426
2	3.18	6.4188	3.9197	6.3879	26.865	0.3196	0.9882	0.9210
2	3.18	6.0995	3.6000	6.0686	25.435	0.3196	0.9882	0.9372
2.5	4.32	4.9074	2.5172	4.8847	20.594	0.2351	0.5349	0.7442
2.5	4.32	5.1398	2.7880	5.1171	21.635	0.2351	0.5349	0.7511
4.5	7.05	3.4890	1.4815	3.4751	14.777	0.1443	0.2013	0.5309
4.5	7.05	3.5492	1.5550	3.5353	15.047	0.1443	0.2013	0.5384

Table 5-6. (cont'd)
Soil Particle Diameter: 0.463mm Temp. 220 °C

Scale	l. vel (cm/sec)	Rt (min)	Variance (min^2)	Corr. Rt (min)	Y (min)	L/v (min)	$10/v^2$ sec^2/cm	$\sigma^2L/2\mu^2v$ (sec)
1	1.85	7.8919	4.9198	7.8388	32.106	0.5493	2.9196	1.3193
1	1.85	7.7274	4.4208	7.6743	31.369	0.5493	2.9196	1.2368
1.5	2.50	3.5787	1.1315	3.5393	13.624	0.4073	1.6051	1.1033
1.5	2.50	3.8225	1.2269	3.7831	14.716	0.4073	1.6051	1.0471
2	3.32	3.5497	1.0515	3.5201	14.089	0.3066	0.9097	0.7805
2	3.32	3.4026	1.0561	3.3729	13.430	0.3066	0.9097	0.8537
2.5	4.51	2.6174	0.6611	2.5956	10.392	0.2256	0.4924	0.6640
2.5	4.51	2.7422	0.7467	2.7204	10.951	0.2256	0.4924	0.6828
3	5.64	2.3451	0.5739	2.3276	9.439	0.1803	0.3146	0.5729
3	5.64	2.2822	0.5078	2.2648	9.158	0.1803	0.3146	0.5355
4.5	7.35	1.7548	0.3368	1.7414	7.043	0.1384	0.1853	0.4611
4.5	7.35	2.3384	0.5227	2.3250	9.657	0.1384	0.1853	0.4014

Soil Particle Diameter: 0.463mm Temp. 240 °C

Scale	l. vel (cm/sec)	Rt (min)	Variance (min^2)	Corr. Rt (min)	Y (min)	L/v (min)	$10/v^2$ sec^2/cm	$\sigma^2L/2\mu^2v$ (sec)
1	1.93	4.3081	1.3664	4.2570	16.178	0.5279	2.6965	1.1934
1	1.93	4.3407	1.3005	4.2897	16.324	0.5279	2.6965	1.1186
1.5	2.60	2.4014	0.3736	2.3636	8.443	0.3914	1.4824	0.7844
1.5	2.60	2.3080	0.3471	2.2701	8.025	0.3914	1.4824	0.7900
2.5	4.69	1.6260	0.2274	1.6050	6.002	0.2168	0.4548	0.5737
2.5	4.69	1.9438	0.2962	1.9228	7.426	0.2168	0.4548	0.5208
4.5	7.64	1.0216	0.1006	1.0087	3.790	0.1330	0.1712	0.3942

Soil Particle Diameter: 0.463mm Temp. 260 °C

Scale	l. vel (cm/sec)	Rt (min)	Variance (min^2)	Corr. Rt (min)	Y (min)	L/v (min)	$10/v^2$ sec^2/cm	$\sigma^2L/2\mu^2v$ (sec)
2.5	4.87	1.0298	0.0728	1.0096	3.379	0.2087	0.4213	0.4461
2.5	4.87	1.0488	0.0793	1.0286	3.465	0.2087	0.4213	0.4682

Table 5-6. (cont'd)
Soil Particle Diameter: 0.363 mm Temp. 200 °C

Scale	l. vel (cm/sec)	Rt (min)	Variance (min^2)	Corr. Rt (min)	Y (min)	L/v (min)	$10/v^2$ sec^2/cm	$\sigma^2L/2\mu^2v$ (sec)
1.5	2.58	12.8265	14.7474	12.7855	48.225	0.3940	1.5018	1.0663
1.5	2.58	13.7773	16.1541	13.7362	51.956	0.3940	1.5018	1.0119
2.5	4.66	8.9134	8.3435	8.8907	33.809	0.2182	0.4607	0.6910
2.5	4.66	9.0411	9.1504	9.0184	34.310	0.2182	0.4607	0.7365
4.5	7.59	6.0199	4.7538	6.0059	22.906	0.1339	0.1734	0.5293
4.5	7.59	6.4872	5.8294	6.4732	24.739	0.1339	0.1734	0.5587
4.5	7.59	6.0842	4.8844	6.0702	23.158	0.1339	0.1734	0.5324

Soil Particle Diameter: 0.363 mm Temp. 220 °C

Scale	l. vel (cm/sec)	Rt (min)	Variance (min^2)	Corr. Rt (min)	Y (min)	L/v (min)	$10/v^2$ sec^2/cm	$\sigma^2L/2\mu^2v$ (sec)
1.5	2.69	5.6390	2.5431	5.5996	20.109	0.3780	1.3824	0.9196
1.5	2.69	5.4882	2.8992	5.4488	19.518	0.3780	1.3824	1.1072
1.5	2.69	7.3327	5.7682	7.2933	26.755	0.3780	1.3824	1.2296
1.5	2.69	7.3134	4.6507	7.2740	26.679	0.3780	1.3824	0.9967
2.5	4.86	4.5838	2.4482	4.5620	16.869	0.2094	0.4241	0.7388
2.5	4.86	4.0823	1.8748	4.0605	14.901	0.2094	0.4241	0.7142
4.5	7.92	2.9659	1.3190	2.9525	10.952	0.1284	0.1596	0.5830
4.5	7.92	2.9651	1.2121	2.9518	10.949	0.1284	0.1596	0.5360

Soil Particle Diameter: 0.363 mm Temp. 240 °C

Scale	l. vel (cm/sec)	Rt (min)	Variance (min^2)	Corr. Rt (min)	Y (min)	L/v (min)	$10/v^2$ sec^2/cm	$\sigma^2L/2\mu^2v$ (sec)
1.5	2.80	3.0216	0.8219	2.9837	9.918	0.3633	1.2768	1.0056
1.5	2.80	3.1637	0.7683	3.1258	10.476	0.3633	1.2768	0.8564
1.5	2.80	3.6294	1.1280	3.5916	12.303	0.3633	1.2768	0.9526
1.5	2.80	3.5860	1.0862	3.5482	12.133	0.3633	1.2768	0.9399
2.5	5.05	2.3891	0.6283	2.3681	8.301	0.2012	0.3917	0.6761
2.5	5.05	2.4257	0.5948	2.4047	8.444	0.2012	0.3917	0.6207
4.5	8.24	1.5020	0.2735	1.4892	5.235	0.1234	0.1474	0.4567
4.5	8.24	1.4213	0.2348	1.4084	4.918	0.1234	0.1474	0.4382

Table 5-6. (cont'd)
Soil Particle Diameter: 0.363 mm Temp. 260 °C

Scale	l. vel (cm/sec)	Rt (min)	Variance (min^2)	Corr. Rt (min)	Y (min)	L/v (min)	$10/v^2$ sec^2/cm	$\sigma^2L/2\mu^2v$ (sec)
1.5	2.91	1.9640	0.2705	1.9276	5.842	0.3496	1.1828	0.7625
1.5	2.91	1.9555	0.2615	1.9191	5.808	0.3496	1.1828	0.7436
1.5	2.91	2.1491	0.3250	2.1127	6.568	0.3496	1.1828	0.7628
2.5	5.25	1.4330	0.1872	1.4129	4.590	0.1937	0.3628	0.5443
2.5	5.25	1.4034	0.1698	1.3832	4.474	0.1937	0.3628	0.5152
4.5	8.56	0.8575	0.0720	0.8452	2.731	0.1188	0.1366	0.3588
4.5	8.56	0.9032	0.0822	0.8908	2.910	0.1188	0.1366	0.3691

Soil Particle Diameter: 0.225mm Temp. 200 °C

Scale	l. vel (cm/sec)	Rt (min)	Variance (min^2)	Corr. Rt (min)	Y (min)	L/v (min)	$10/v^2$ sec^2/cm	$\sigma^2L/2\mu^2v$ (sec)
1.5	2.69	10.7367	9.0921	10.6957	37.654	0.3773	1.3770	0.8995
1.5	2.69	11.0329	9.7485	10.9918	38.745	0.3773	1.3770	0.9131
2.5	4.87	8.1291	7.5060	8.1064	28.899	0.2090	0.4224	0.7160
2.5	4.87	7.8578	6.7229	7.8350	27.899	0.2090	0.4224	0.6865
4.5	7.93	5.0745	3.4386	5.0606	18.051	0.1282	0.1590	0.5164

Soil Particle Diameter: 0.225mm Temp. 220 °C

Scale	l. vel (cm/sec)	Rt (min)	Variance (min^2)	Corr. Rt (min)	Y (min)	L/v (min)	$10/v^2$ sec^2/cm	$\sigma^2L/2\mu^2v$ (sec)
1.5	2.81	4.6676	1.9433	4.6283	15.363	0.3620	1.2675	0.9848
1.5	2.81	4.4858	1.6858	4.4464	14.692	0.3620	1.2675	0.9256
2.5	5.07	3.7906	1.4278	3.7688	12.951	0.2005	0.3888	0.6045
2.5	5.07	3.8502	1.5178	3.8284	13.171	0.2005	0.3888	0.6228
4.5	8.27	2.3836	0.6945	2.3702	8.160	0.1230	0.1464	0.4561
4.5	8.27	2.2750	0.6224	2.2617	7.760	0.1230	0.1464	0.4489

Table 5-6. (cont'd)
Soil Particle Diameter: 0.225mm Temp. 240 °C

Scale	l. vel (cm/sec)	Rt (min)	Variance (min^2)	Corr. Rt (min)	Y (min)	L/v (min)	$10/v^2$ sec^2/cm	$\sigma^2L/2\mu^2v$ (sec)
1.5	2.92	2.6660	0.5384	2.6281	8.057	0.3479	1.1707	0.8127
2.5	5.28	2.1374	0.4525	2.1165	6.898	0.1927	0.3591	0.5837
2.5	5.28	2.0612	0.3914	2.0402	6.617	0.1927	0.3591	0.5433
4.5	8.60	1.6461	0.3082	1.6332	5.466	0.1182	0.1352	0.4097
4.5	8.60	1.3468	0.2099	1.3339	4.363	0.1182	0.1352	0.4182
4.5	8.60	1.2359	0.1441	1.2231	3.954	0.1182	0.1352	0.3414

Soil Particle Diameter: 0.225mm Temp. 260 °C

Scale	lin. Vel. (cm/sec)	Rt (min)	Variance (min^2)	Corr. Rt (min)	Y (min)	L/v (min)	$10/v^2$ sec^2/cm	$\sigma^2L/2\mu^2v$ (sec)
2.5	5.48	1.2725	0.1222	1.2523	3.747	0.1854	0.3327	0.4330
2.5	5.48	1.2535	0.1219	1.2333	3.677	0.1854	0.3327	0.4452
4.5	8.94	0.8391	0.0668	0.8268	2.514	0.1138	0.1252	0.3332
4.5	8.94	0.8296	0.0629	0.8172	2.479	0.1138	0.1252	0.3213

Table 5-7. Experimental Results of C6H5Cl on NJIT Soil from Chromatographic Analysis and Calculation for First Absolute Moment & Second Central Moment Plots

Soil Particle Diameter:0.55mm Temp. 200 °C

Scale	lin. vel (cm/sec)	Rt (min)	Variance (min^2)	Corr. Rt (min)	Y (min)	L/v (min)	$10/v^2$ sec^2/cm	$\sigma^2L/2\mu^2v$ (sec)
1.5	2.25	34.8481	48.6507	34.8071	163.34	0.4527	1.9827	0.5454
2.5	4.05	27.0571	33.2916	27.0344	127.44	0.2507	0.6082	0.3426
2.5	4.05	26.2944	43.4900	26.2717	123.81	0.2507	0.6082	0.4740
2.5	4.05	21.8954	34.9042	21.8727	102.83	0.2507	0.6082	0.5488
2.5	4.05	23.5940	33.7676	23.5713	110.93	0.2507	0.6082	0.4572
3	5.07	23.8337	35.9252	23.8156	112.39	0.2004	0.3886	0.3808
3	5.07	23.1263	36.2982	23.1081	109.01	0.2004	0.3886	0.4087
4.5	6.61	14.1281	17.2766	14.1141	66.40	0.1538	0.2289	0.4002
4.5	6.61	14.9255	18.2544	14.9116	70.21	0.1538	0.2289	0.3788

Soil Particle Diameter:0.55mm Temp. 220 °C

Scale	lin. vel (cm/sec)	Rt (min)	Variance (min^2)	Corr. Rt (min)	Y (min)	L/v (min)	$10/v^2$ sec^2/cm	$\sigma^2L/2\mu^2v$ (sec)
1	1.74	24.5477	32.8901	24.4946	113.40	0.5858	3.3198	0.9633
1	1.74	22.9766	30.4435	22.9235	105.91	0.5858	3.3198	1.0181
1.5	2.34	19.9912	31.6422	19.9518	92.62	0.4343	1.8251	1.0357
1.5	2.34	19.2484	26.0092	19.2091	89.08	0.4343	1.8251	0.9184
1.5	2.34	18.4324	19.2574	18.3930	85.19	0.4343	1.8251	0.7417
1.5	2.34	19.0301	22.3491	18.9907	88.04	0.4343	1.8251	0.8075
2	3.11	14.9918	17.8623	14.9622	69.45	0.3270	1.0344	0.7827
2	3.11	14.2988	14.9925	14.2691	66.14	0.3270	1.0344	0.7223
2.5	4.23	11.3717	12.4202	11.3499	52.72	0.2406	0.5599	0.6958
2.5	4.23	10.8079	10.6270	10.7861	50.04	0.2406	0.5599	0.6592
2.5	4.23	11.1131	10.5963	11.0913	51.49	0.2406	0.5599	0.6216
3	5.29	9.7627	8.8877	9.7453	45.35	0.1923	0.3577	0.5399
3	5.29	9.6344	7.1284	9.6170	44.74	0.1923	0.3577	0.4446
4.5	6.89	6.4450	4.1616	6.4316	29.81	0.1476	0.2107	0.4454
4.5	6.89	6.4867	4.4079	6.4733	30.01	0.1476	0.2107	0.4657

Table 5-7. (cont'd)

Soil Particle Diameter:0.55mm Temp. 240 °C

Scale	lin. vel (cm/sec)	Rt (min)	Variance (min^2)	Corr. Rt (min)	Y (min)	L/v (min)	$10/v^2$ sec^2/cm	$\sigma^2L/2\mu^2v$ (sec)
1.5	2.44	8.1753	4.6475	8.1375	36.39	0.4174	1.6856	0.8788
1.5	2.44	8.5612	4.2521	8.5234	38.23	0.4174	1.6856	0.7328
2.5	4.40	5.2250	2.5426	5.2040	23.48	0.2312	0.5171	0.6511
4.5	7.17	2.9061	0.8410	2.8932	12.98	0.1418	0.1946	0.4275
4.5	7.17	3.1402	0.9465	3.1273	14.09	0.1418	0.1946	0.4118

Soil Particle Diameter:0.55mm Temp. 260 °C

Scale	lin. vel (cm/sec)	Rt (min)	Variance (min^2)	Corr. Rt (min)	Y (min)	L/v (min)	$10/v^2$ sec^2/cm	$\sigma^2L/2\mu^2v$ (sec)
1	1.88	5.7256	1.5107	5.6764	23.94	0.5418	2.8404	0.7617
1	1.88	5.5636	1.7164	5.5145	23.17	0.5418	2.8404	0.9171
1.5	2.53	3.8872	0.8058	3.8508	16.04	0.4017	1.5615	0.6546
1.5	2.53	3.9362	0.9401	3.8998	16.28	0.4017	1.5615	0.7447
1.5	2.53	4.0451	0.9771	4.0087	16.79	0.4017	1.5615	0.7325
1.5	2.53	4.1057	1.0176	4.0693	17.08	0.4017	1.5615	0.7404
1.5	2.53	4.1259	1.0259	4.0895	17.18	0.4017	1.5615	0.7390
1.5	2.53	4.4566	0.9534	4.4202	18.76	0.4017	1.5615	0.5879
2	3.36	3.4029	0.9134	3.3755	14.35	0.3024	0.8850	0.7272
2	3.36	3.4757	0.7804	3.4482	14.70	0.3024	0.8850	0.5953
2.5	4.57	2.5681	0.5246	2.5480	10.86	0.2225	0.4790	0.5393
2.5	4.57	2.6127	0.5319	2.5925	11.08	0.2225	0.4790	0.5282
2.5	4.57	2.6682	0.5889	2.6480	11.34	0.2225	0.4790	0.5605
2.5	4.57	2.7202	0.5996	2.7001	11.59	0.2225	0.4790	0.5489
3	5.72	2.2501	0.4341	2.2340	9.62	0.1779	0.3061	0.4641
3	5.72	2.3864	0.5055	2.3703	10.27	0.1779	0.3061	0.4800
4.5	7.45	1.4577	0.1906	1.4453	6.10	0.1365	0.1803	0.3735
4.5	7.45	1.4919	0.1996	1.4795	6.27	0.1365	0.1803	0.3734

Soil Particle Diameter:0.55mm Temp. 280 °C

Scale	lin. vel (cm/sec)	Rt (min)	Variance (min^2)	Corr. Rt (min)	Y (min)	L/v (min)	$10/v^2$ sec^2/cm	$\sigma^2L/2\mu^2v$ (sec)
1.5	2.63	2.5659	0.3820	2.5308	9.83	0.3872	1.4507	0.6921
1.5	2.63	2.5894	0.4134	2.5543	9.94	0.3872	1.4507	0.7354
2.5	4.74	1.5761	0.1986	1.5567	6.18	0.2145	0.4450	0.5270
2.5	4.74	1.5541	0.1741	1.5346	6.08	0.2145	0.4450	0.4753
4.5	7.73	0.8498	0.0669	0.8379	3.24	0.1316	0.1675	0.3760
4.5	7.73	0.8506	0.0656	0.8386	3.24	0.1316	0.1675	0.3681

Table 5-7. (cont'd)

Soil Particle Diameter:0.463mm Temp. 200 °C

Scale	lin. vel (cm/sec)	Rt (min)	Variance (min^2)	Corr. Rt (min)	Y (min)	L/v (min)	$10/v^2$ sec^2/cm	$\sigma^2L/2\mu^2v$ (sec)
2	3.18	27.5201	50.4027	27.4892	121.40	0.3196	0.9882	0.6395
2.5	4.32	26.2580	66.1209	26.2353	116.24	0.2351	0.5349	0.6777
3	5.41	21.4507	48.5095	21.4325	94.98	0.1880	0.3418	0.5955
3	5.41	23.0754	59.0754	23.0573	102.26	0.1880	0.3418	0.6266
4.5	7.05	18.7656	52.7430	18.7517	83.21	0.1443	0.2013	0.6491
4.5	7.05	19.2585	57.5421	19.2445	85.42	0.1443	0.2013	0.6724

Soil Particle Diameter:0.463mm Temp. 220 °C

Scale	lin. vel (cm/sec)	Rt (min)	Variance (min^2)	Corr. Rt (min)	Y (min)	L/v (min)	$10/v^2$ sec^2/cm	$\sigma^2L/2\mu^2v$ (sec)
1	1.85	18.7194	31.8252	18.6663	80.61	0.5493	2.9196	1.5052
1.5	2.50	15.4770	22.9767	15.4376	66.93	0.4073	1.6051	1.1781
1.5	2.50	14.1607	18.6814	14.1213	61.03	0.4073	1.6051	1.1447
2	3.32	11.1490	12.6071	11.1194	48.13	0.3066	0.9097	0.9380
2	3.32	11.0471	12.8014	11.0174	47.68	0.3066	0.9097	0.9702
2.5	4.51	9.5508	10.0297	9.5290	41.45	0.2256	0.4924	0.7476
2.5	4.51	8.5559	8.7808	8.5341	37.00	0.2256	0.4924	0.8160
3	5.64	9.4016	11.5286	9.3842	41.05	0.1803	0.3146	0.7082
3	5.64	9.9196	11.6184	9.9022	43.37	0.1803	0.3146	0.6410
4.5	7.35	7.6843	8.9685	7.6709	33.61	0.1384	0.1853	0.6328
4.5	7.35	7.5147	7.7354	7.5013	32.85	0.1384	0.1853	0.5708

Soil Particle Diameter:0.463mm Temp. 240 °C

Scale	lin. vel (cm/sec)	Rt (min)	Variance (min^2)	Corr. Rt (min)	Y (min)	L/v (min)	$10/v^2$ sec^2/cm	$\sigma^2L/2\mu^2v$ (sec)
1.5	2.60	6.4466	3.8120	6.4087	26.57	0.3914	1.4824	1.0898
1.5	2.60	5.8208	3.4563	5.7830	23.76	0.3914	1.4824	1.2135
2.5	4.69	4.7417	2.2174	4.7207	19.96	0.2168	0.4548	0.6471
2.5	4.69	4.6466	2.2909	4.6256	19.53	0.2168	0.4548	0.6964
4.5	7.64	3.3273	1.2715	3.3144	14.12	0.1330	0.1712	0.4618
4.5	7.64	3.4925	1.5248	3.4797	14.86	0.1330	0.1712	0.5025

Table 5-7. (cont'd)

Soil Particle Diameter:0.225mm Temp. 220 °C

Scale	lin. vel (cm/sec)	Rt (min)	Variance (min^2)	Corr. Rt (min)	Y (min)	L/v (min)	$10/v^2$ sec^2/cm	$\sigma^2L/2\mu^2v$ (sec)
2.5	5.07	13.8374	22.9278	13.8156	49.98	0.2005	0.3888	0.7225
2.5	5.07	13.4585	20.8311	13.4367	48.58	0.2005	0.3888	0.6939
4.5	8.27	8.9140	11.8977	8.9006	32.23	0.1230	0.1464	0.5541
4.5	8.27	9.1503	13.7961	9.1369	33.10	0.1230	0.1464	0.6097

Soil Particle Diameter:0.225mm Temp. 240 °C

Scale	lin. vel (cm/sec)	Rt (min)	Variance (min^2)	Corr. Rt (min)	Y (min)	L/v (min)	$10/v^2$ sec^2/cm	$\sigma^2L/2\mu^2v$ (sec)
1.5	2.92	7.9977	4.7332	7.9598	27.71	0.3479	1.1707	0.7795
1.5	2.92	8.1962	8.2036	8.1583	28.44	0.3479	1.1707	1.2862
1.5	2.92	8.0113	6.0479	7.9734	27.76	0.3479	1.1707	0.9927
1.5	2.92	7.9580	4.6857	7.9202	27.56	0.3479	1.1707	0.7794
2.5	5.28	6.2789	4.2631	6.2579	22.16	0.1927	0.3591	0.6292
2.5	5.28	6.1001	3.3338	6.0791	21.50	0.1927	0.3591	0.5214
4.5	8.60	4.0651	2.1949	4.0523	14.38	0.1182	0.1352	0.4740
4.5	8.60	4.1028	2.2100	4.0900	14.52	0.1182	0.1352	0.4685

Soil Particle Diameter:0.225mm Temp. 260 °C

Scale	lin. vel (cm/sec)	Rt (min)	Variance (min^2)	Corr. Rt (min)	Y (min)	L/v (min)	$10/v^2$ sec^2/cm	$\sigma^2L/2\mu^2v$ (sec)
1.5	3.04	4.1399	1.3985	4.1034	13.56	0.3348	1.0845	0.8340
1.5	3.04	4.3814	1.8708	4.3450	14.45	0.3348	1.0845	0.9951
1.5	3.04	4.4745	2.0296	4.4380	14.79	0.3348	1.0845	1.0348
2.5	5.48	3.1286	1.0596	3.1084	10.59	0.1854	0.3327	0.6100
2.5	5.48	3.1003	0.8400	3.0801	10.48	0.1854	0.3327	0.4925
4.5	8.94	2.1358	0.6179	2.1234	7.29	0.1138	0.1252	0.4677

Soil Particle Diameter:0.225mm Temp. 280 °C

Scale	lin. vel (cm/sec)	Rt (min)	Variance (min^2)	Corr. Rt (min)	Y (min)	L/v (min)	$10/v^2$ sec^2/cm	$\sigma^2L/2\mu^2v$ (sec)
1.5	3.15	2.4066	0.6218	2.3715	7.23	0.3227	1.0075	1.0696
2.5	5.69	1.8156	0.3520	1.7961	5.78	0.1787	0.3091	0.5849
2.5	5.69	1.7911	0.3028	1.7716	5.69	0.1787	0.3091	0.5172
4.5	9.27	1.2117	0.1857	1.1998	3.91	0.1097	0.1163	0.4243
4.5	9.27	1.1926	0.1750	1.1807	3.84	0.1097	0.1163	0.4128

Table 5-7. (cont'd)

Soil Particle Diameter:0.463mm Temp. 260 °C

Scale	lin. vel (cm/sec)	Rt (min)	Variance (min^2)	Corr. Rt (min)	Y (min)	L/v (min)	$10/v^2$ sec^2/cm	$\sigma^2L/2\mu^2v$ (sec)
1	2.00	5.0104	1.4863	4.9613	19.44	0.5081	2.4980	0.9200
1	2.00	4.4831	1.3474	4.4340	17.08	0.5081	2.4980	1.0441
1.5	2.70	3.6461	1.0247	3.6097	14.11	0.3768	1.3733	0.8885
1.5	2.70	3.1816	0.8014	3.1452	12.03	0.3768	1.3733	0.9152
2	3.58	2.7826	0.7443	2.7552	10.79	0.2836	0.7783	0.8341
2	3.58	2.8515	0.6891	2.8241	11.10	0.2836	0.7783	0.7349
2.5	4.87	2.3064	0.5889	2.2862	9.10	0.2087	0.4213	0.7053
2.5	4.87	2.5702	0.5555	2.5501	10.28	0.2087	0.4213	0.5346
3	6.10	2.2652	0.6474	2.2491	9.16	0.1668	0.2692	0.6404
3	6.10	2.2309	0.5624	2.2148	9.01	0.1668	0.2692	0.5736
4.5	7.94	1.6531	0.2901	1.6407	6.65	0.1280	0.1586	0.4138
4.5	7.94	1.6761	0.3206	1.6637	6.75	0.1280	0.1586	0.4448

Soil Particle Diameter:0.463mm Temp. 280 °C

Scale	lin. vel (cm/sec)	Rt (min)	Variance (min^2)	Corr. Rt (min)	Y (min)	L/v (min)	$10/v^2$ sec^2/cm	$\sigma^2L/2\mu^2v$ (sec)
1.5	2.80	2.2513	0.2801	2.2161	7.94	0.3631	1.2758	0.6203
1.5	2.80	1.9824	0.3152	1.9473	6.73	0.3631	1.2758	0.9043
2.5	5.05	1.4310	0.2681	1.4116	5.22	0.2011	0.3914	0.8114
2.5	5.05	1.5175	0.2206	1.4981	5.61	0.2011	0.3914	0.5929
4.5	8.24	0.9540	0.1072	0.9421	3.54	0.1234	0.1473	0.4469

Soil Particle Diameter:0.363mm Temp. 200 °C

Scale	lin. vel (cm/sec)	Rt (min)	Variance (min^2)	Corr. Rt (min)	Y (min)	L/v (min)	$10/v^2$ sec^2/cm	$\sigma^2L/2\mu^2v$ (sec)
2.5	4.66	14.8169	36.0870	14.7941	56.97	0.2182	0.4607	1.0794
2.5	4.66	14.9383	34.5786	14.9155	57.45	0.2182	0.4607	1.0175
4.5	7.59	10.8665	19.6573	10.8526	41.92	0.1339	0.1734	0.6703
4.5	7.59	10.7510	23.0696	10.7370	41.47	0.1339	0.1734	0.8037
4.5	7.59	10.9765	22.2410	10.9626	42.35	0.1339	0.1734	0.7433

Table 5-7. (cont'd)

Soil Particle Diameter:0.363mm Temp. 220 °C

Scale	lin. vel (cm/sec)	Rt (min)	Variance (min^2)	Corr. Rt (min)	Y (min)	L/v (min)	$10/v^2$ sec^2/cm	$\sigma^2L/2\mu^2v$ (sec)
1.5	2.69	11.8249	13.6164	11.7855	44.38	0.3780	1.3824	1.1117
1.5	2.69	11.4787	12.2159	11.4393	43.02	0.3780	1.3824	1.0586
2.5	4.86	6.3588	5.9096	6.3370	23.83	0.2094	0.4241	0.9243
2.5	4.86	6.4698	6.6768	6.4479	24.27	0.2094	0.4241	1.0087
4.5	7.92	5.9227	4.4929	5.9094	22.55	0.1284	0.1596	0.4958
4.5	7.92	4.6559	3.3363	4.6425	17.58	0.1284	0.1596	0.5965
4.5	7.92	4.6620	3.6149	4.6486	17.61	0.1284	0.1596	0.6446

Soil Particle Diameter:0.363mm Temp. 240 °C

Scale	lin. vel (cm/sec)	Rt (min)	Variance (min^2)	Corr. Rt (min)	Y (min)	L/v (min)	$10/v^2$ sec^2/cm	$\sigma^2L/2\mu^2v$ (sec)
1.5	2.80	5.6166	3.1830	5.5788	20.10	0.3633	1.2768	1.1144
1.5	2.80	5.8444	2.8734	5.8066	20.99	0.3633	1.2768	0.9286
2.5	5.05	3.0709	1.1831	3.0499	10.98	0.2012	0.3917	0.7676
2.5	5.05	3.0617	1.2692	3.0408	10.94	0.2012	0.3917	0.8285
4.5	8.24	2.2008	0.6656	2.1879	7.98	0.1234	0.1474	0.5149
4.5	8.24	2.2878	0.7618	2.2749	8.32	0.1234	0.1474	0.5451

Soil Particle Diameter:0.363mm Temp. 260 °C

Scale	lin. vel (cm/sec)	Rt (min)	Variance (min^2)	Corr. Rt (min)	Y (min)	L/v (min)	$10/v^2$ sec^2/cm	$\sigma^2L/2\mu^2v$ (sec)
1.5	2.91	3.0316	0.7770	2.9952	10.03	0.3496	1.1828	0.9080
1.5	2.91	3.2181	0.9397	3.1816	10.76	0.3496	1.1828	0.9732
2.5	5.25	1.7004	0.3082	1.6802	5.64	0.1937	0.3628	0.6340
2.5	5.25	1.6685	0.2933	1.6483	5.51	0.1937	0.3628	0.6268
4.5	8.56	1.1902	0.2035	1.1779	4.04	0.1188	0.1366	0.5227
4.5	8.56	1.1895	0.1892	1.1771	4.03	0.1188	0.1366	0.4865

Table 5-8. Comparison of Heat of Adsorption of Benzene on Varied Adsorbents

Adsorbent	Heat of Adsorption* (kcal/mol)
Silica gel	8.5 - 12
Alumina	6.8
Calcined alumina	3.4
13X molecular sieve	15.5, 16.8
NJIT soil	15.89

* literature value obtained from Eberly, Jr.,P.E. J. Phys. Chem., 65, 68, 1961.

Table 5-9.
Calculation of Molecular Diffusion Coefficient for C_6H_6 and C_6H_5Cl

Compound	Temp. (K)	kT/ε_{AB}	Ω	σ_{AB}(Å)	D_m(cm^2/sec)
C_6H_6	433	2.159	1.048	4.476	0.323
	453	2.259	1.033		0.367
	473	2.359	1.018		0.414
	493	2.458	1.005		0.465
	513	2.558	0.994		0.520
	533	2.658	0.983		0.579
C_6H_5Cl	453	2.195	1.042	4.816	0.292
	473	2.292	1.028		0.330
	493	2.389	1.014		0.371
	513	2.486	1.002		0.415
	533	2.583	0.991		0.462
	553	2.680	0.98		0.512

Table 5-10.Summary of Mass Transfer Parameters Calculation Results for C_6H_6

Adsorption Equilibrium Constant (K_a)

Avg. Particle Diameter(mm)	Temperature (°C) 180	200	220	240	260
0.55	191.2	102.54	50.06	26.36	13.37
0.463	194.77	94.97	48.69	27.29	-
0.363	-	138.89	64.49	32.7	18.71
0.225	-	104.31	48.5	36.44	20.54
overall		104.3	52.12	28.62	16.51

Axial Dispersion Coefficient (D_z, cm^2/sec)

Avg. Particle Diameter(mm)	Temperature (°C) 180	200	220	240	260
0.55	1.878	2.077	2.591	2.657	3.450
0.463	2.815	1.980	2.977	2.834	-
0.363	-	3.652	3.924	4.003	3.449
0.225	-	2.711	4.324	4.036	5.390
overall	2.448	2.105	2.780	3.014	3.425

Intraparticle Diffusion Coefficient x 1E4(D_p, cm^2/sec)

Avg. Particle Diameter(mm)	Temperature (°C) 180	200	220	240	260
0.55	1.119	0.998	1.043	0.869	1.106
0.463	1.131	0.827	0.988	1.097	-
0.363	-	1.043	0.915	0.975	0.991
0.225	-	0.962	1.146	1.162	1.355

Film Mass Transfer Coefficient (k_f, cm/sec)

Avg. Particle Diameter(mm)	Temperature (°C) 180	200	220	240	260
0.55	13.334	15.060	16.916	18.908	21.039
0.463	15.857	17.909	20.117	22.485	25.019
0.363	20.232	22.849	25.666	28.688	31.921
0.225	32.595	36.812	41.351	46.220	51.428

Table 5-11.
Summary of Mass Transfer Parameters Calculation Results for C_6H_5Cl

Adsorption Equilibrium Constant (K_a)

Avg. Particle Diameter(mm)	Temperature (°C) 220	240	260	280
0.55	200.54	91.40	44.45	26.12
0.463	170.88	95.96	40.05	27.21
0.363	174.54	73.85	37.84	-
0.225	214.47	93.12	45.31	27.5
overall	186.96	82.58	42.01	24.85

Axial Dispersion Coefficient (D_z, cm^2/sec)

Avg. Particle Diameter(mm)	Temperature (°C) 220	240	260	280
0.55	2.398	2.379	1.546	2.516
0.463	3.344	4.989	2.096	2.511
0.363	3.661	3.138	4.972	-
0.225	5.206	4.721	5.219	-
overall	3.703	3.260	2.680	2.555

Intraparticle Diffusion Coefficient x 1E4(D_p, cm^2/sec)

Avg. Particle Diameter(mm)	Temperature (°C) 220	240	260	280
0.55	1.057	1.225	1.037	1.130
0.463	0.914	1.153	0.874	0.909
0.363	1.135	1.115	1.174	1.016
0.225	1.072	1.254	1.193	1.233

Film Mass Transfer Coefficient (k_f, cm/sec)

Avg. Particle Diameter(mm)	Temperature (°C) 220	240	260	280
0.55	13.494	15.087	16.790	18.608
0.463	16.047	17.941	19.967	22.128
0.363	20.474	22.890	25.475	28.232
0.225	32.986	36.879	41.043	45.485

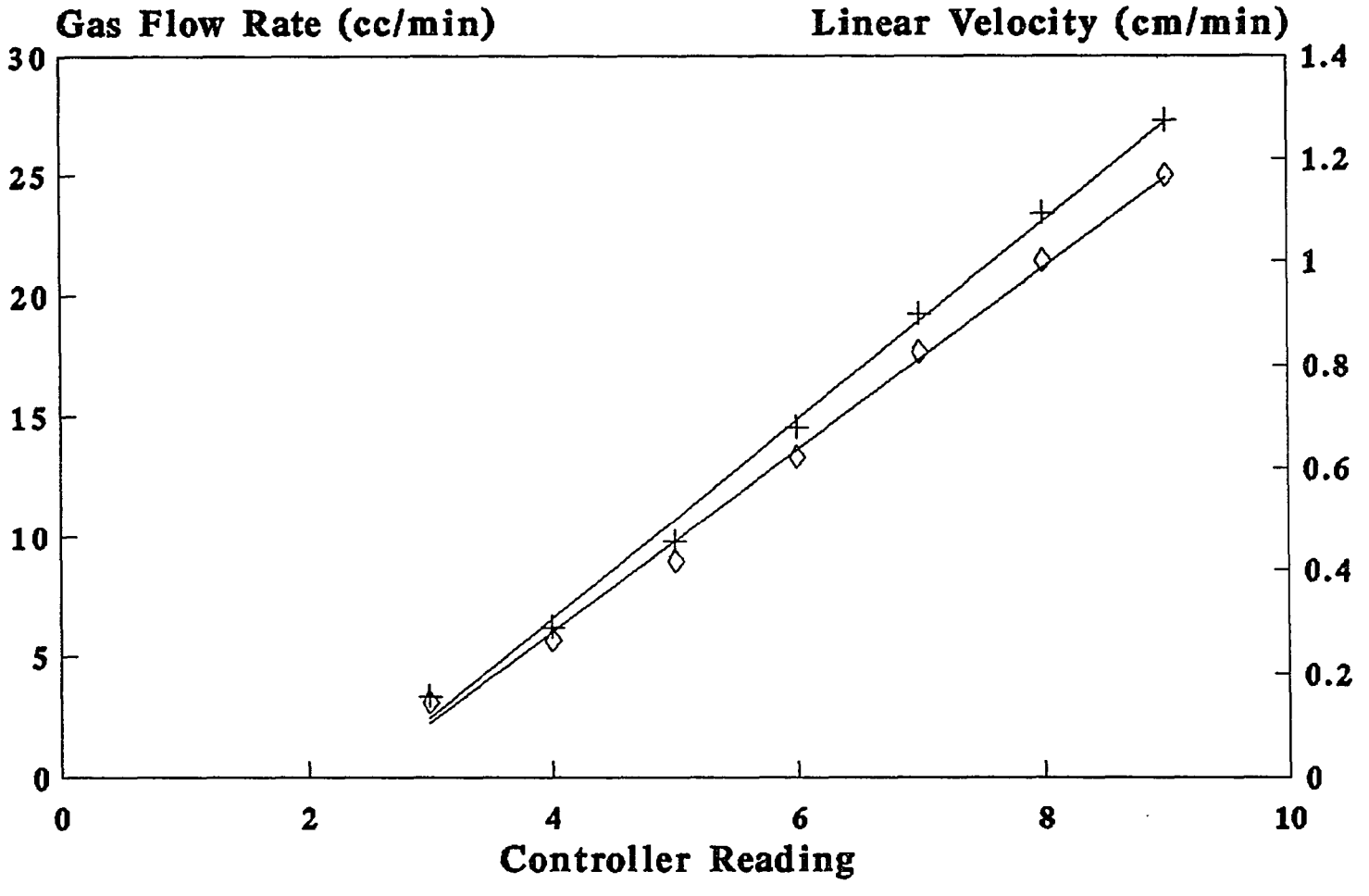

◊ Gas Flow Rate + Linear Velicity

Figure 5-1. Gas Flow Rate in Equilibrium Test System and Linear Velocity Across Soil Bed

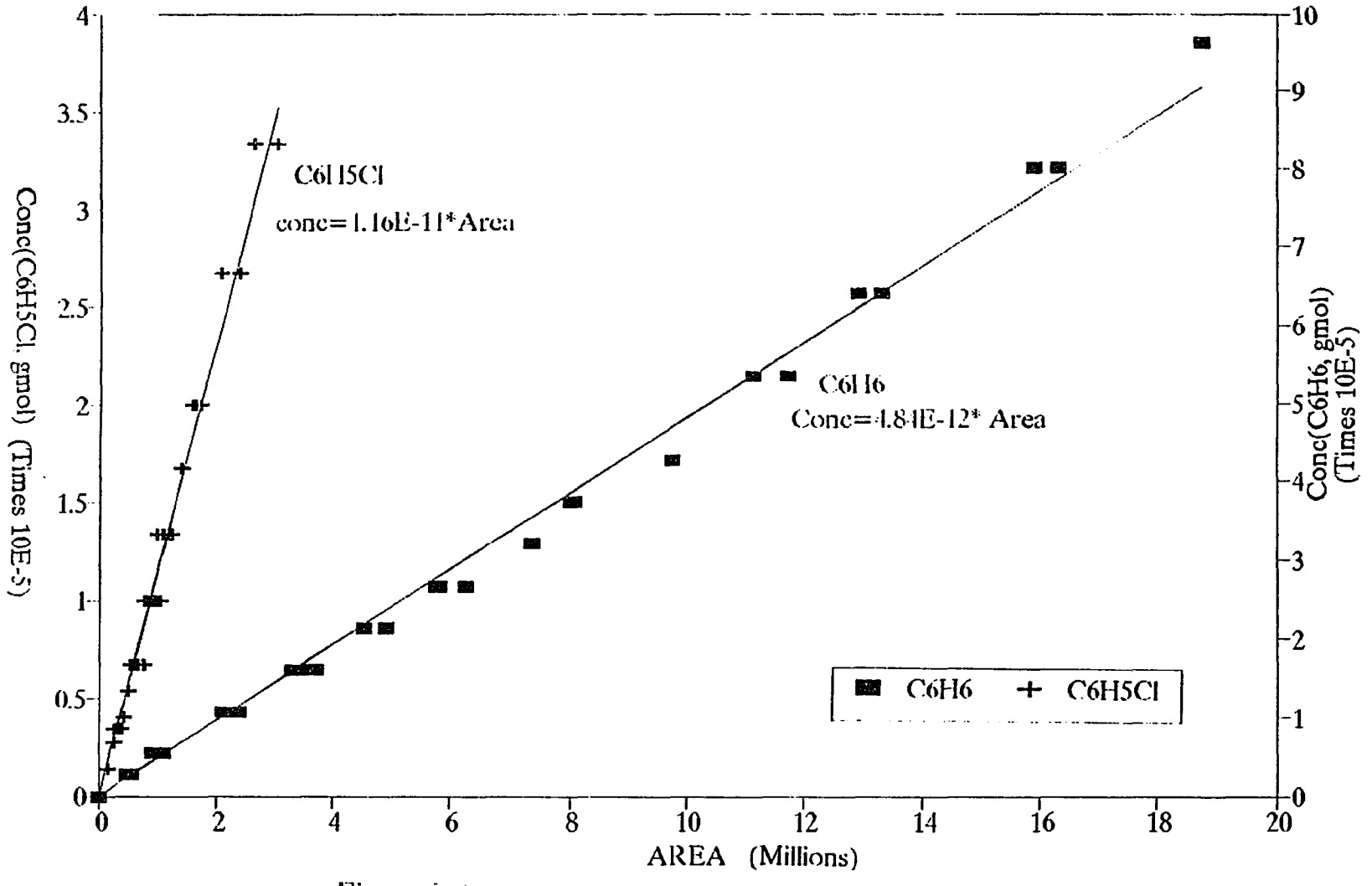

Figure 5-2. Chromatographic Response Calibration

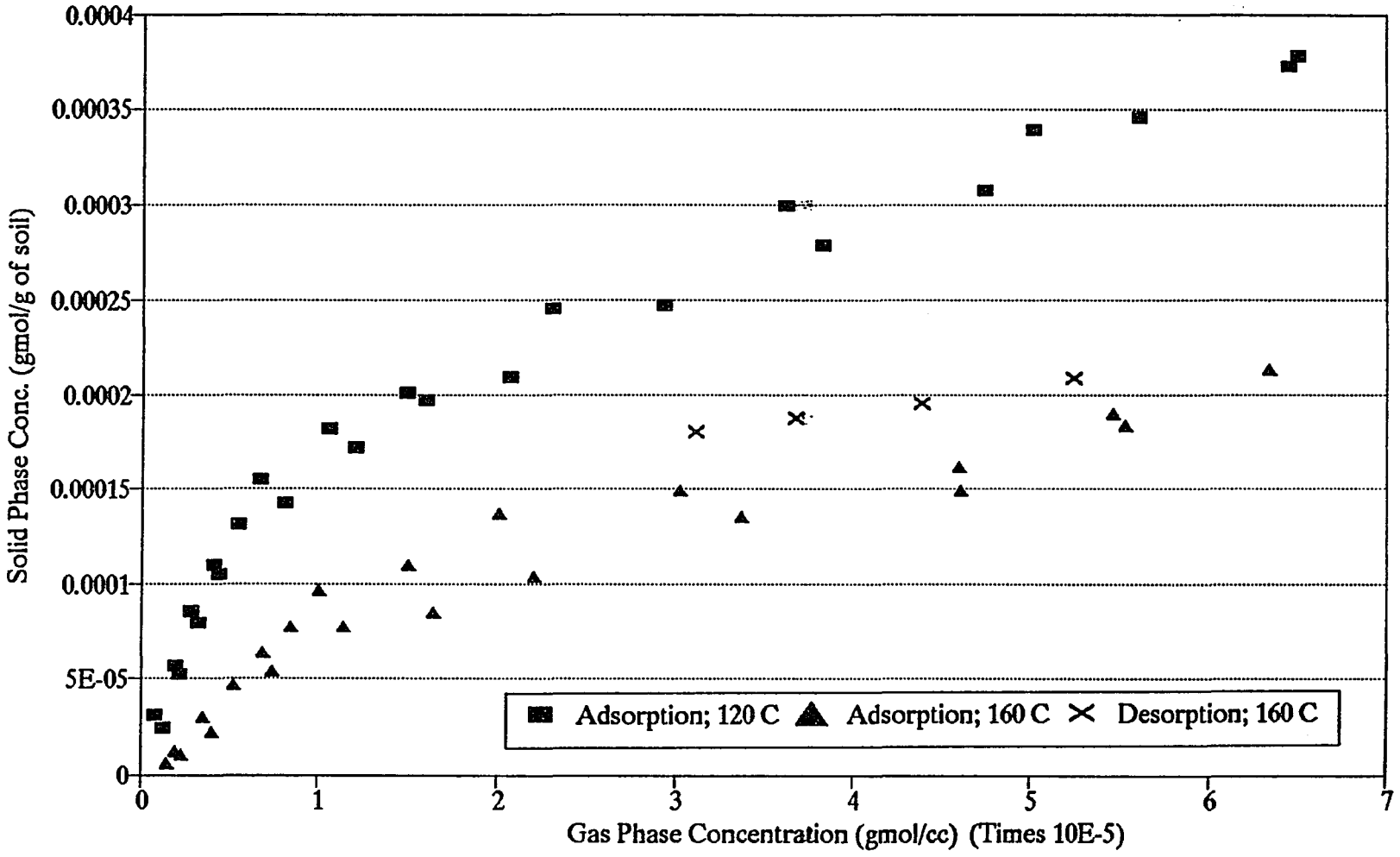

Figure 5-3 Equilibrium Test Results for
C6H6 on Soil Mesh 50/100

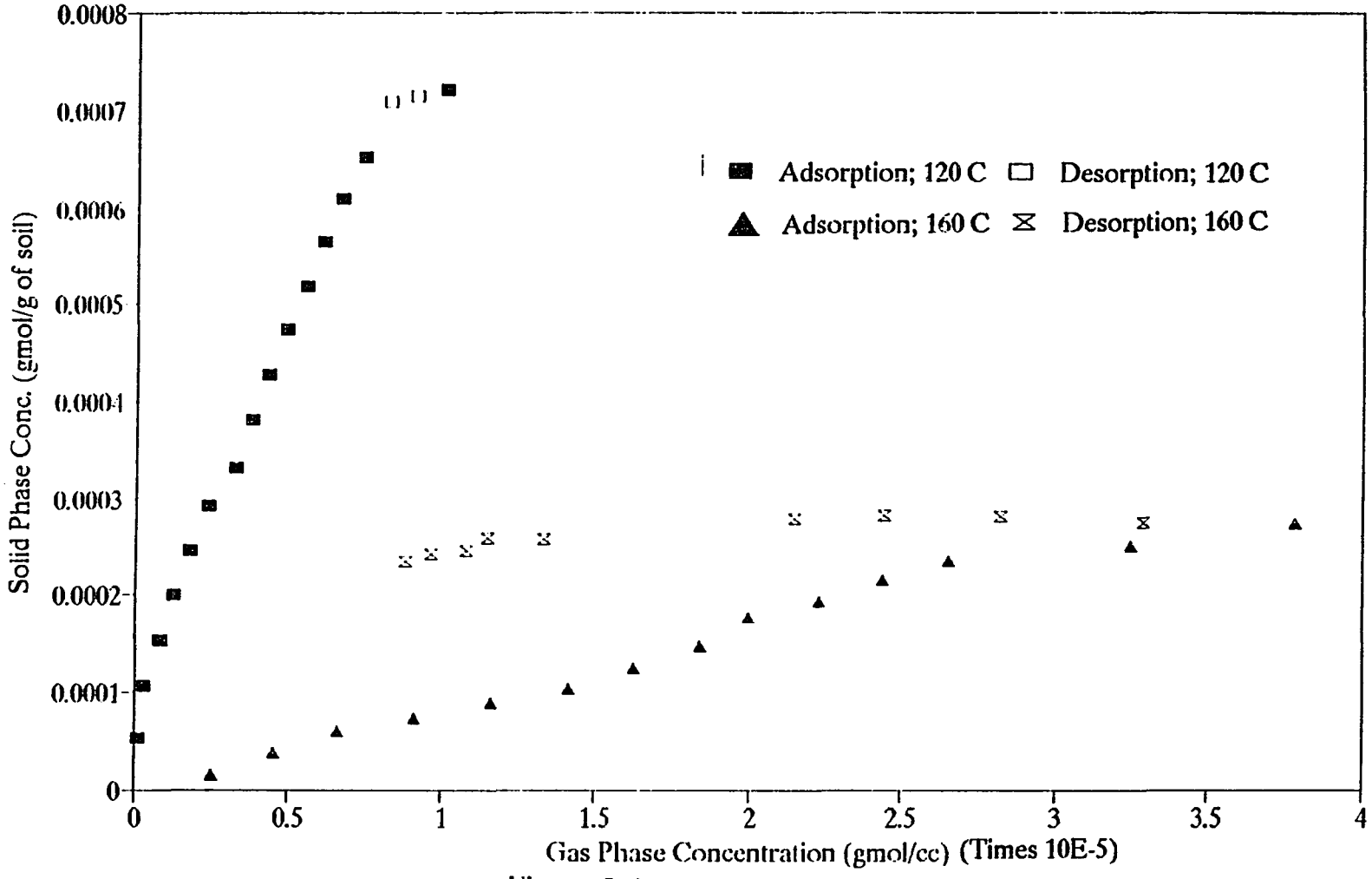

Figure 5-4. Equilibrium Test Results
C_6H_5Cl on Soil Mesh 50/100

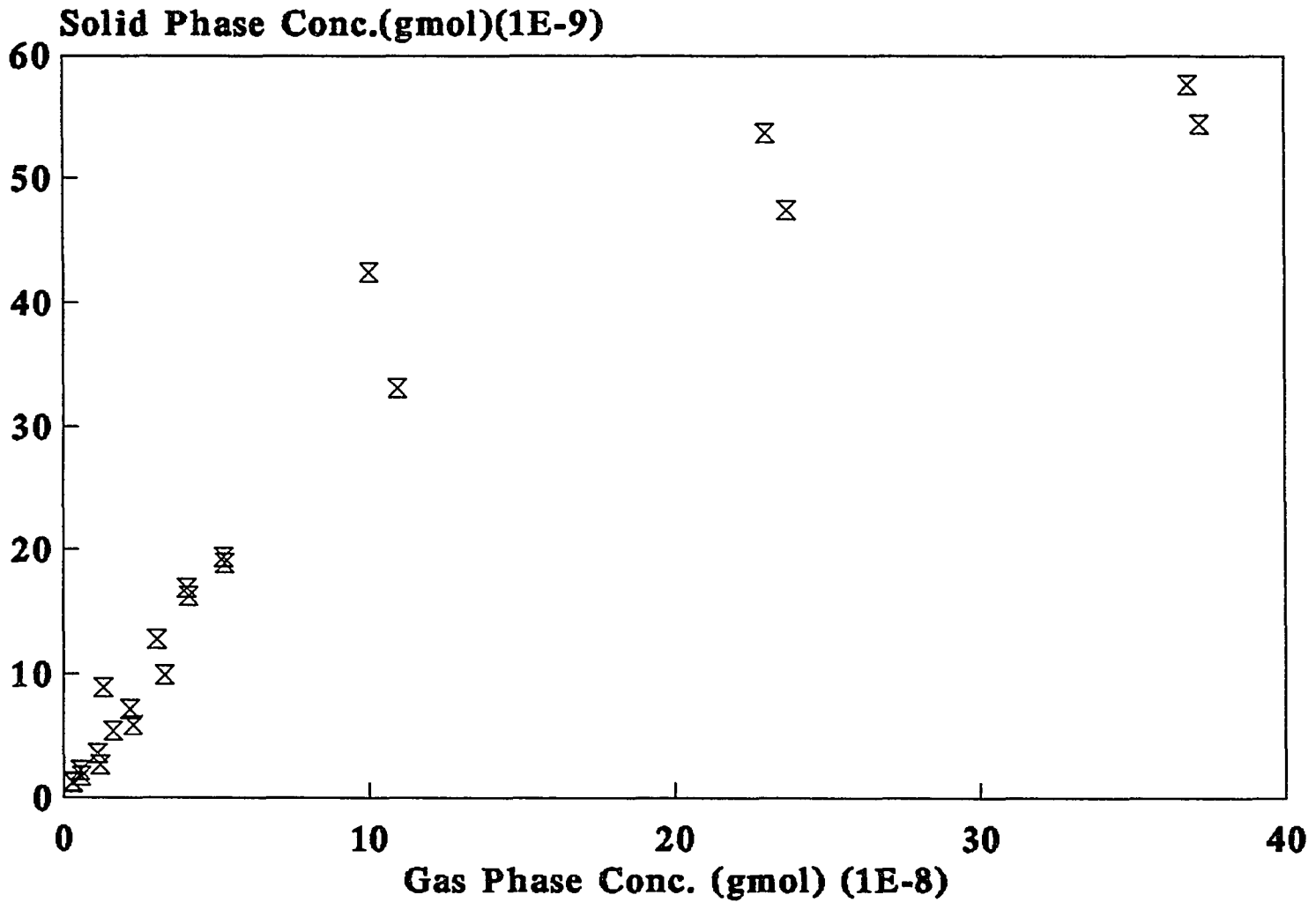

Figure 5-5. Adsorption Isotherm of C6H6 on NJIT Soil at 220C

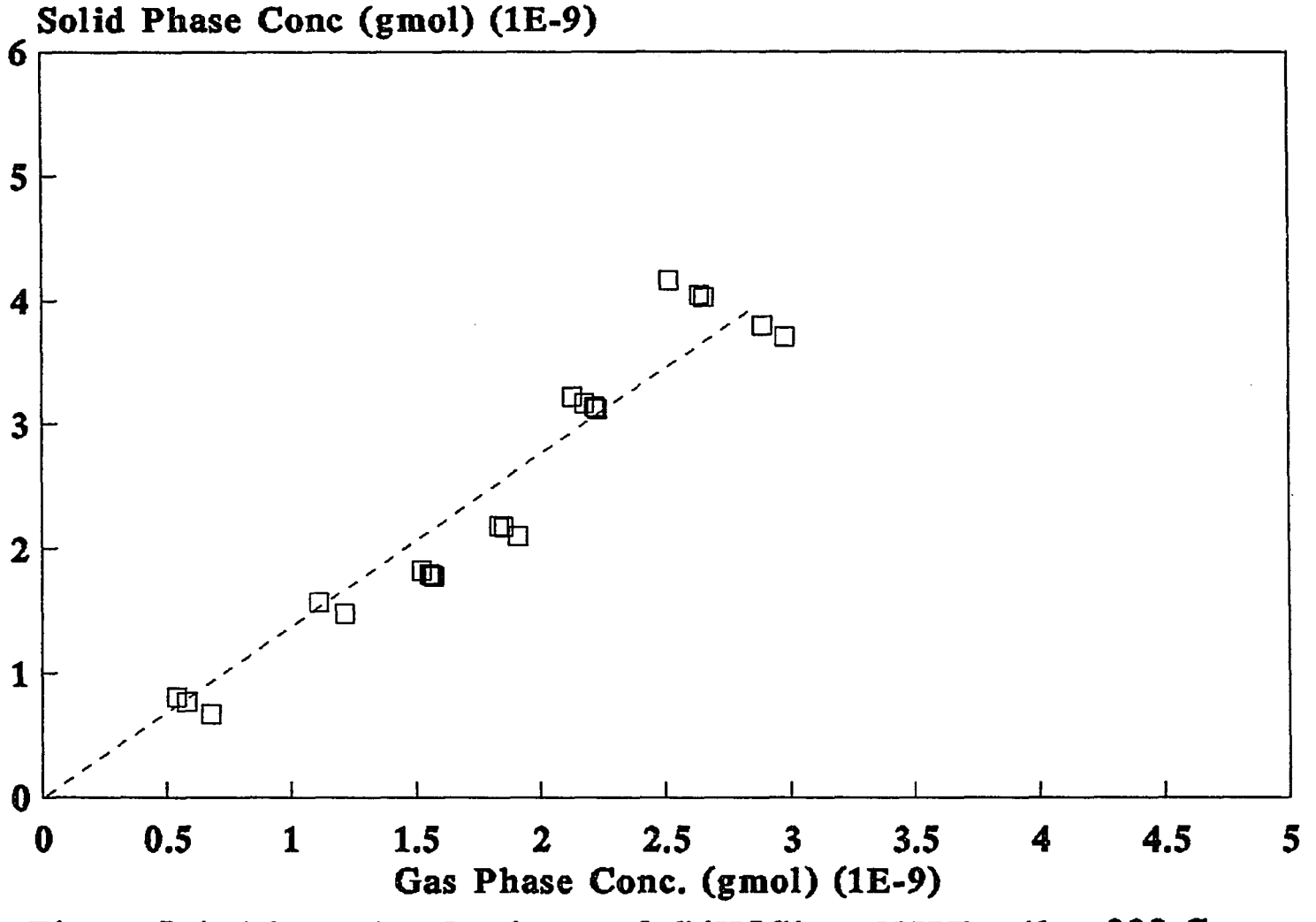

Figure 5-6. Adsorption Isotherm of C6H5Cl on NJIT soil at 220 C

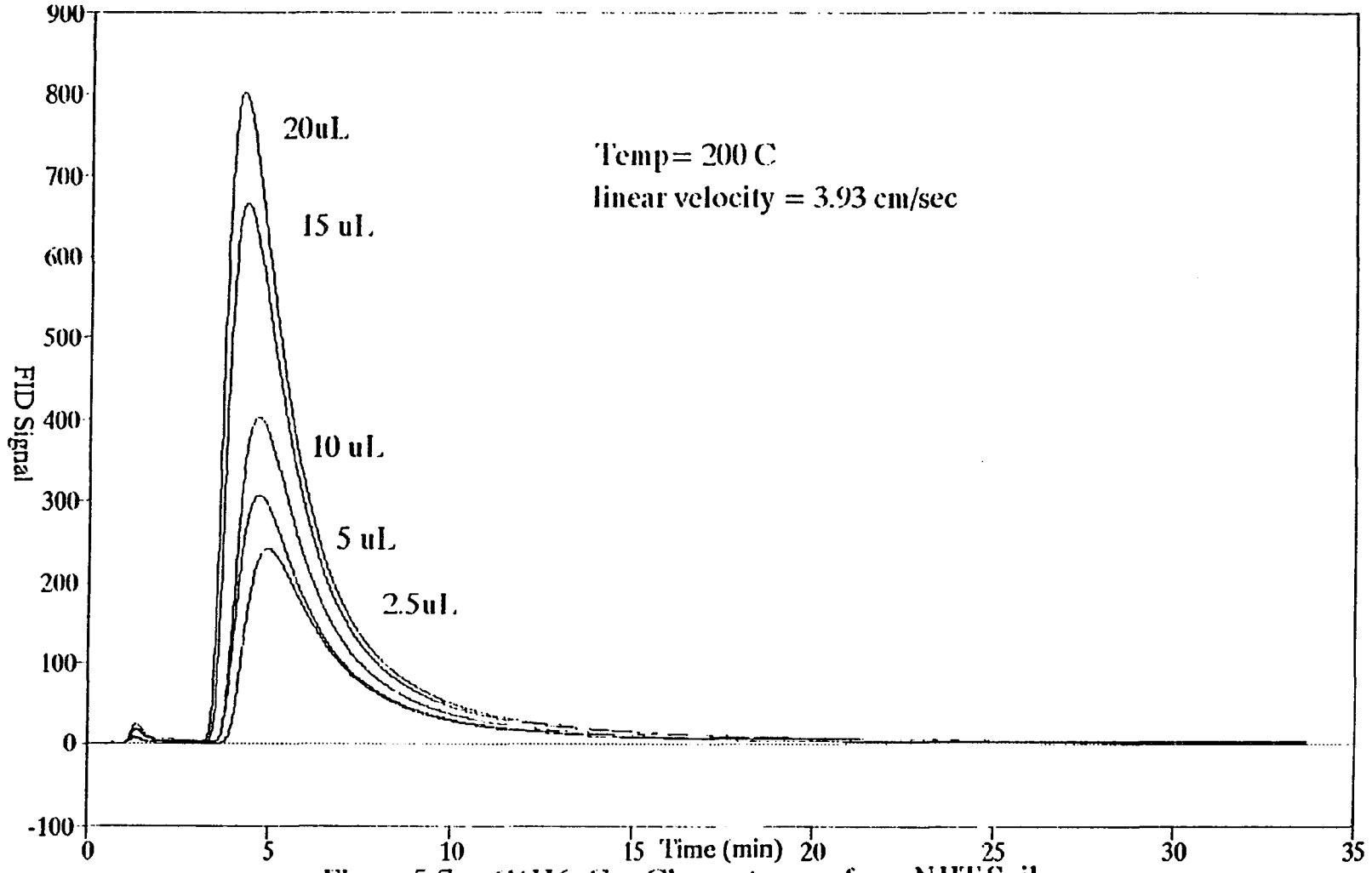

Figure 5-7. C6H6- Gas Chromatogram from NJIT Soil
varide Dose in Particle Dia.=0.55 mm

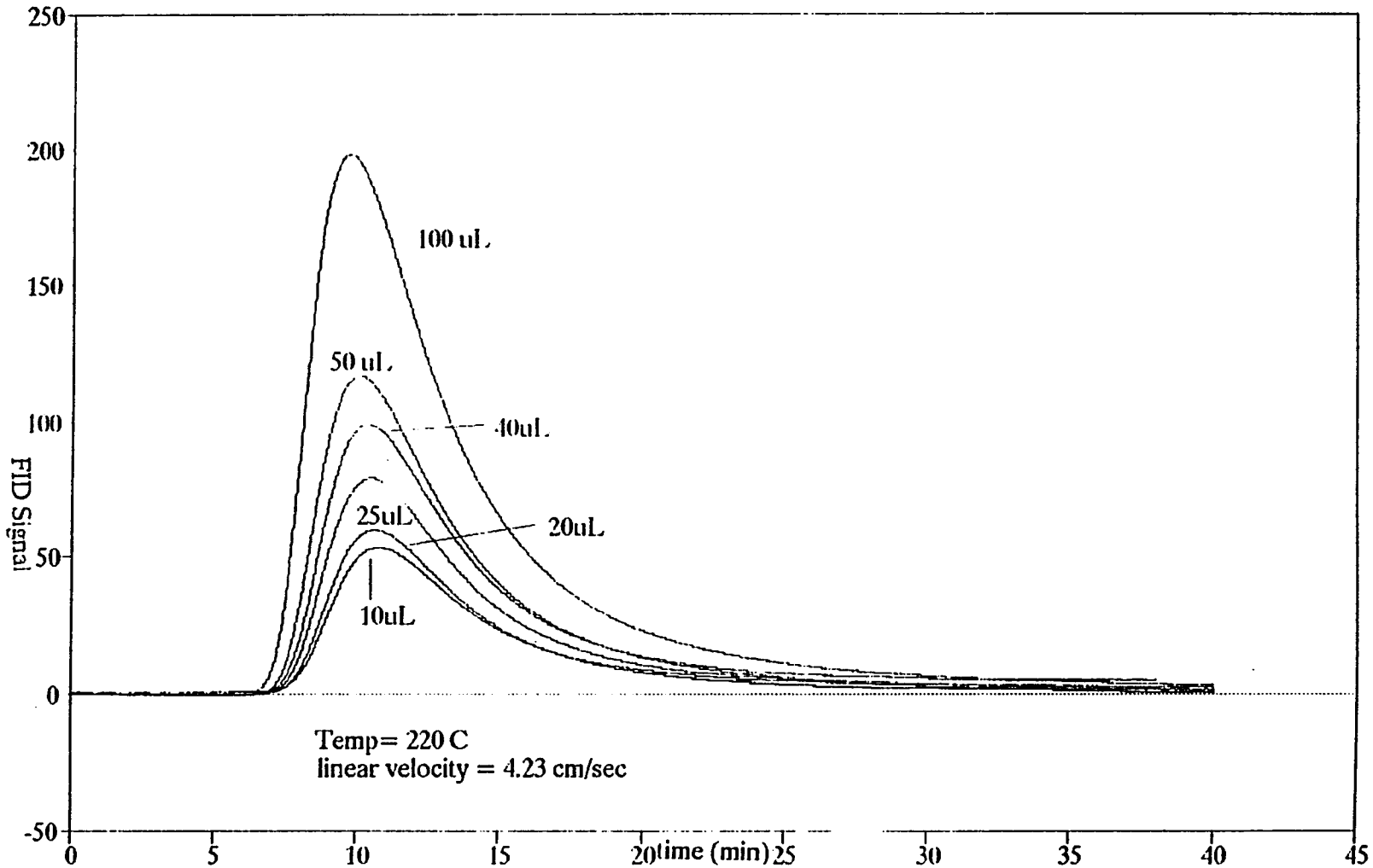

Figure 5-8. C6H5Cl- Gas Chromatogram from NJIT Soil
varied Dose in Particle Dia= 0.55 mm

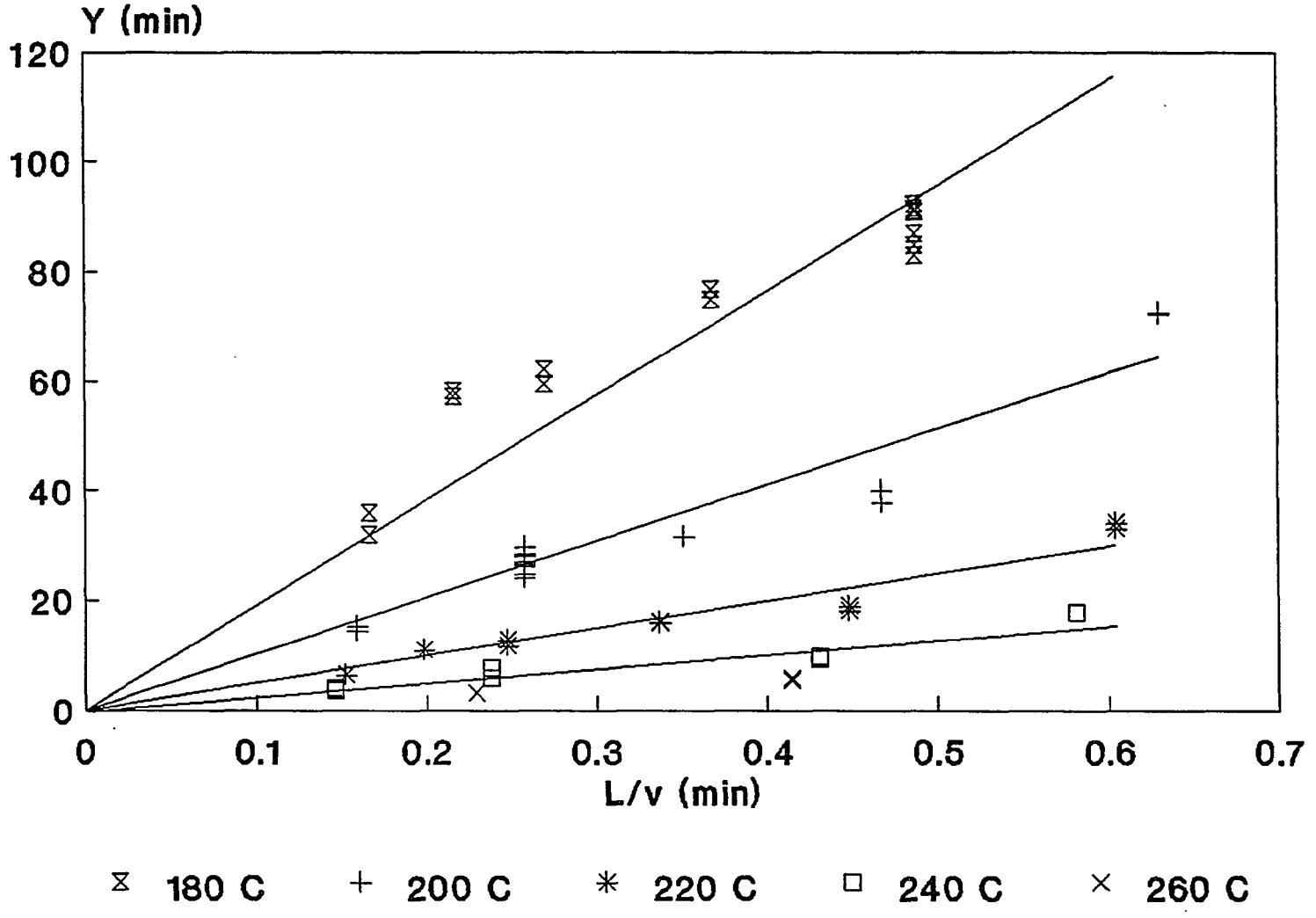

Figure 5-9. Plot for Determination of Ka for Benzene in Soil
Average Particle Diameter: 0.55 mm

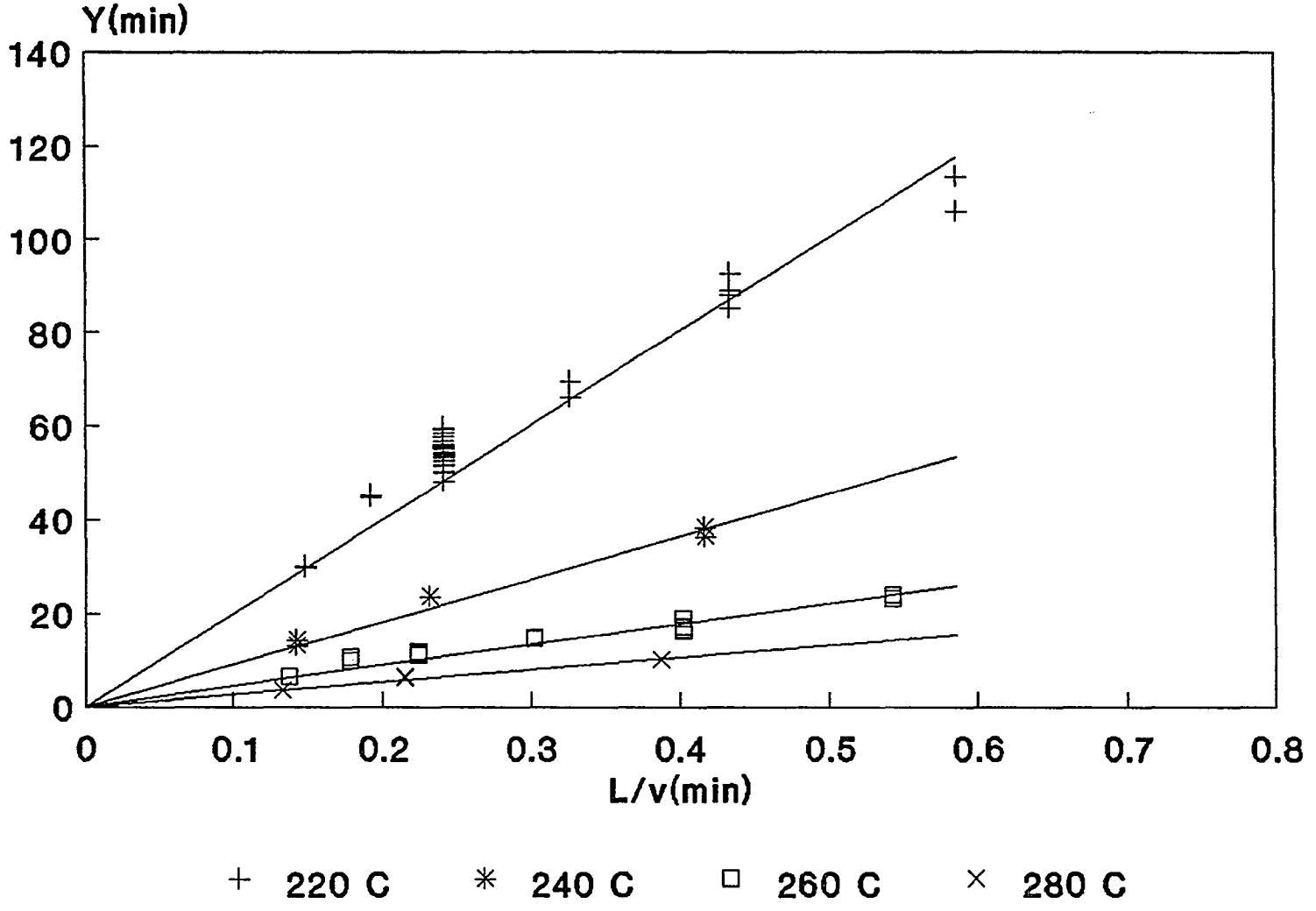

Figure 5-10. Plot for Determination of Ka for C6H5Cl on Soil
Average Particle Diameter: 0.55mm

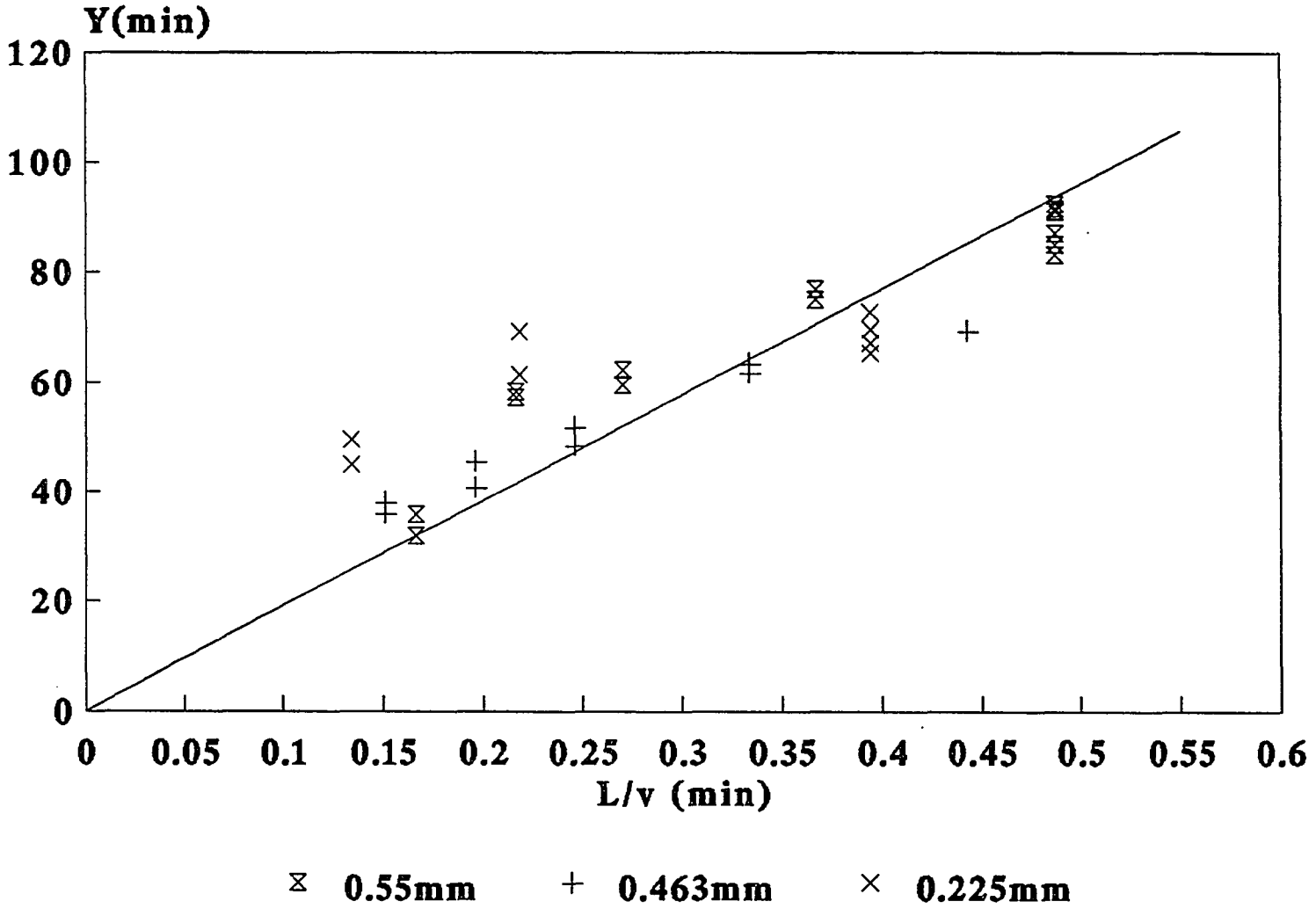

Figure 5-11-a. Dependence of First Absolute Moment on L/v for C6H6 at 180 C

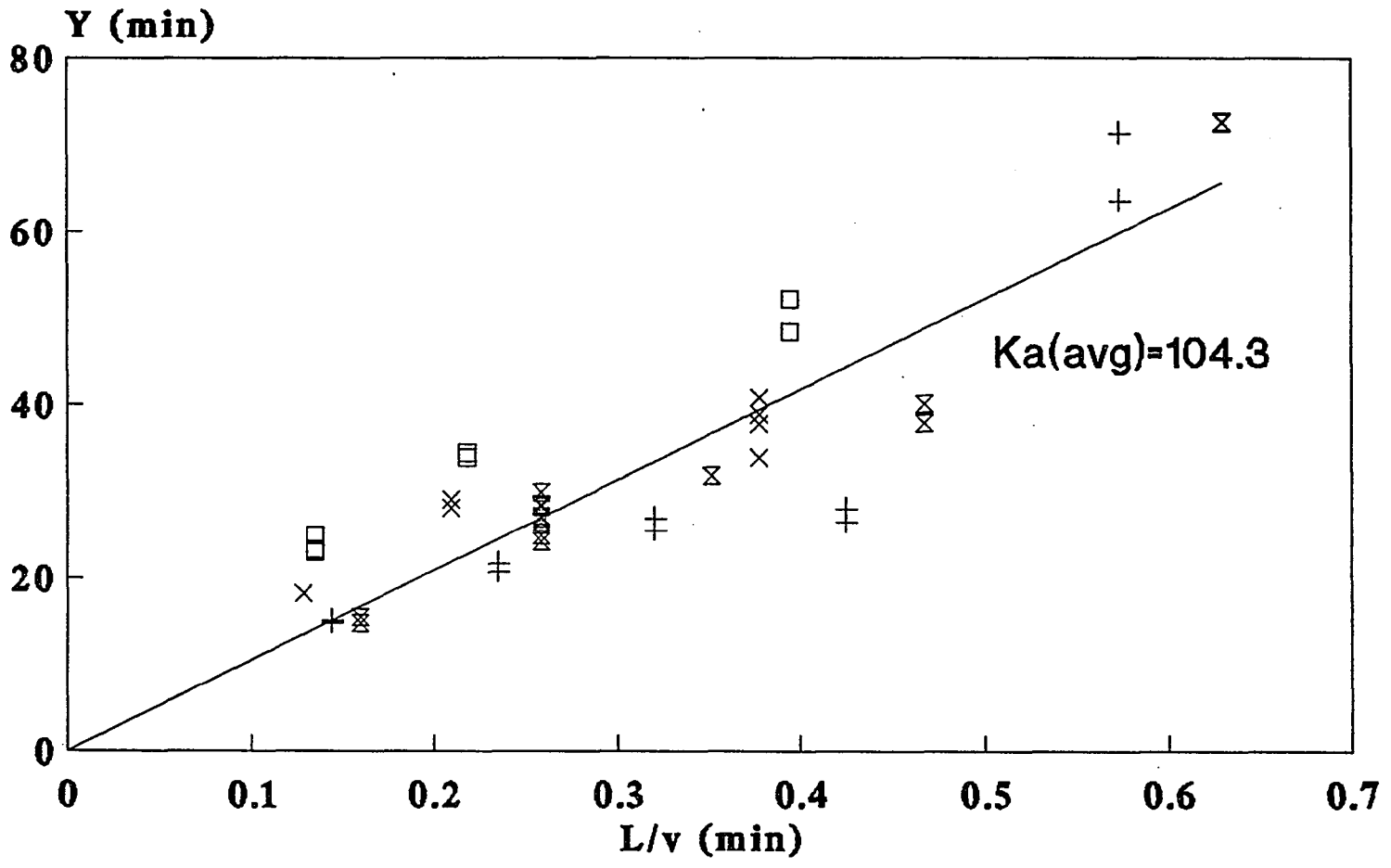

⧖ 0.55mm + 0.463mm □ 0.363mm × 0.225mm

Figure 5-11-b. Dependence of First Absolute Moment on L/v for C6H6 at 200 C

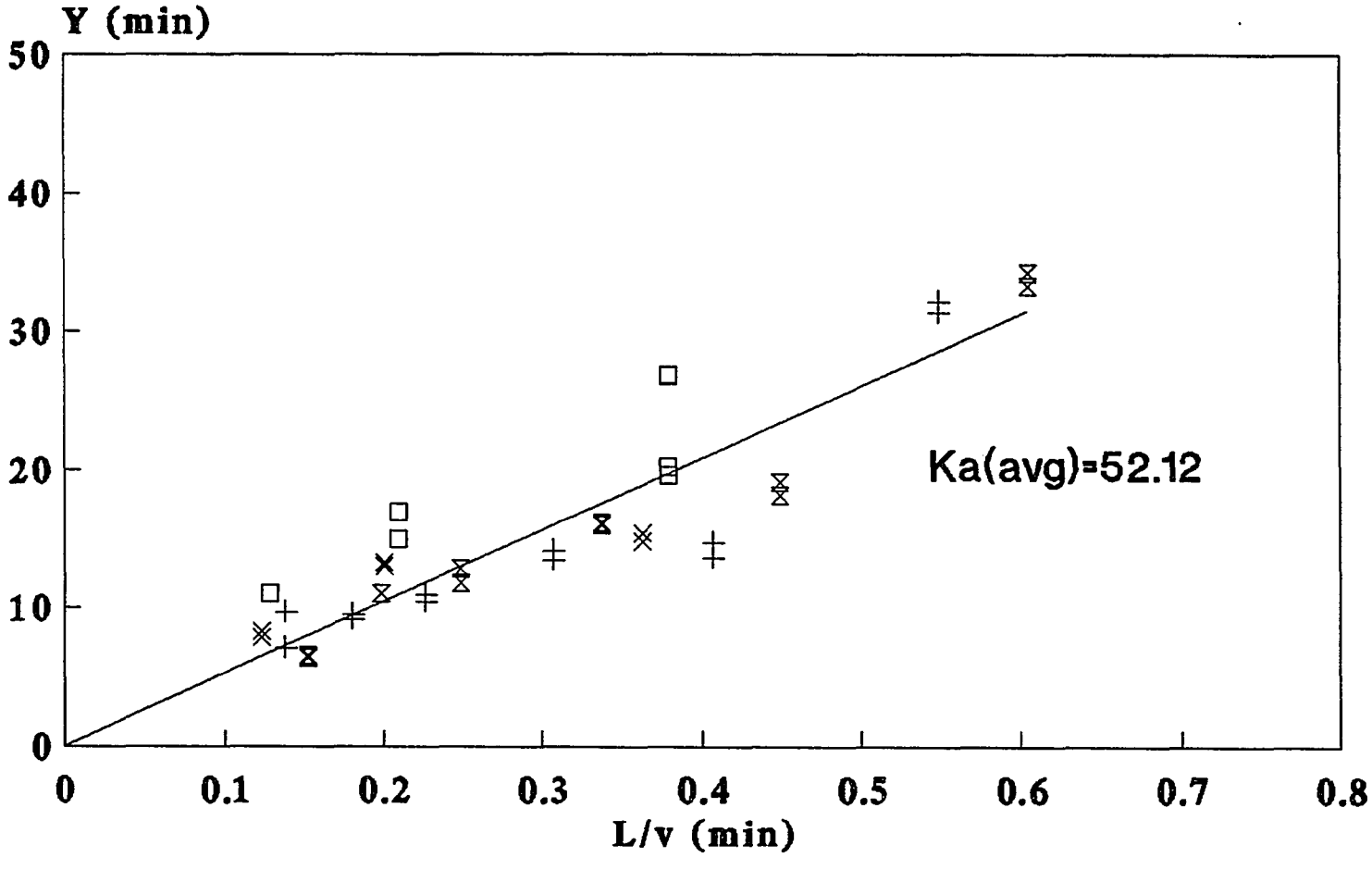

⧖ 0.55mm + 0.463mm □ 0.363mm × 0.225mm

Figure 5-11-c. Dependence of First Absolute Moment on L/v for C6H6 at 220 C

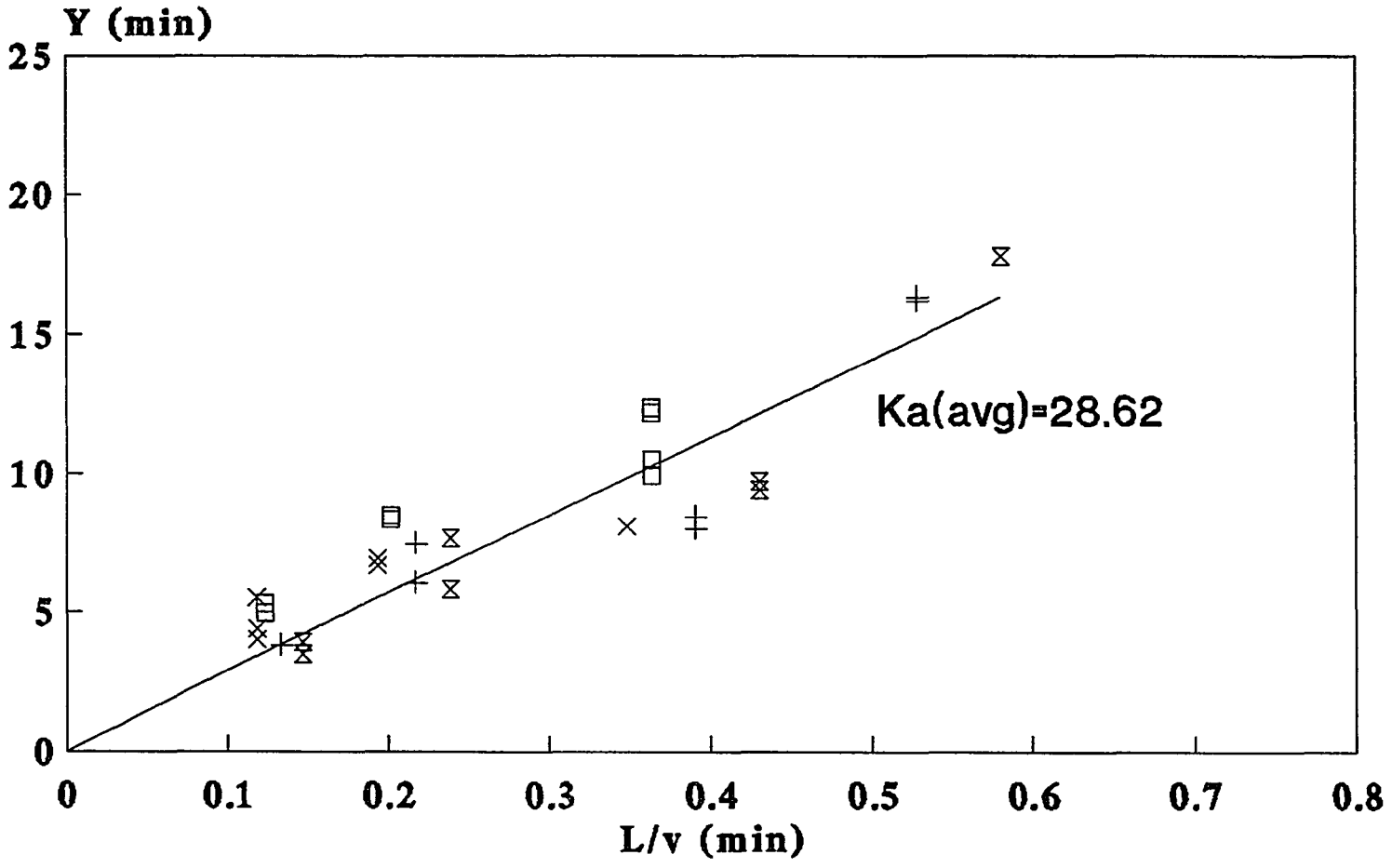

⧖ 0.55mm + 0.463mm □ 0.363mm × 0.225mm

Figuer 5-11-d. Dependence of First Absolute Moment on L/v for C6H6 at 240 C

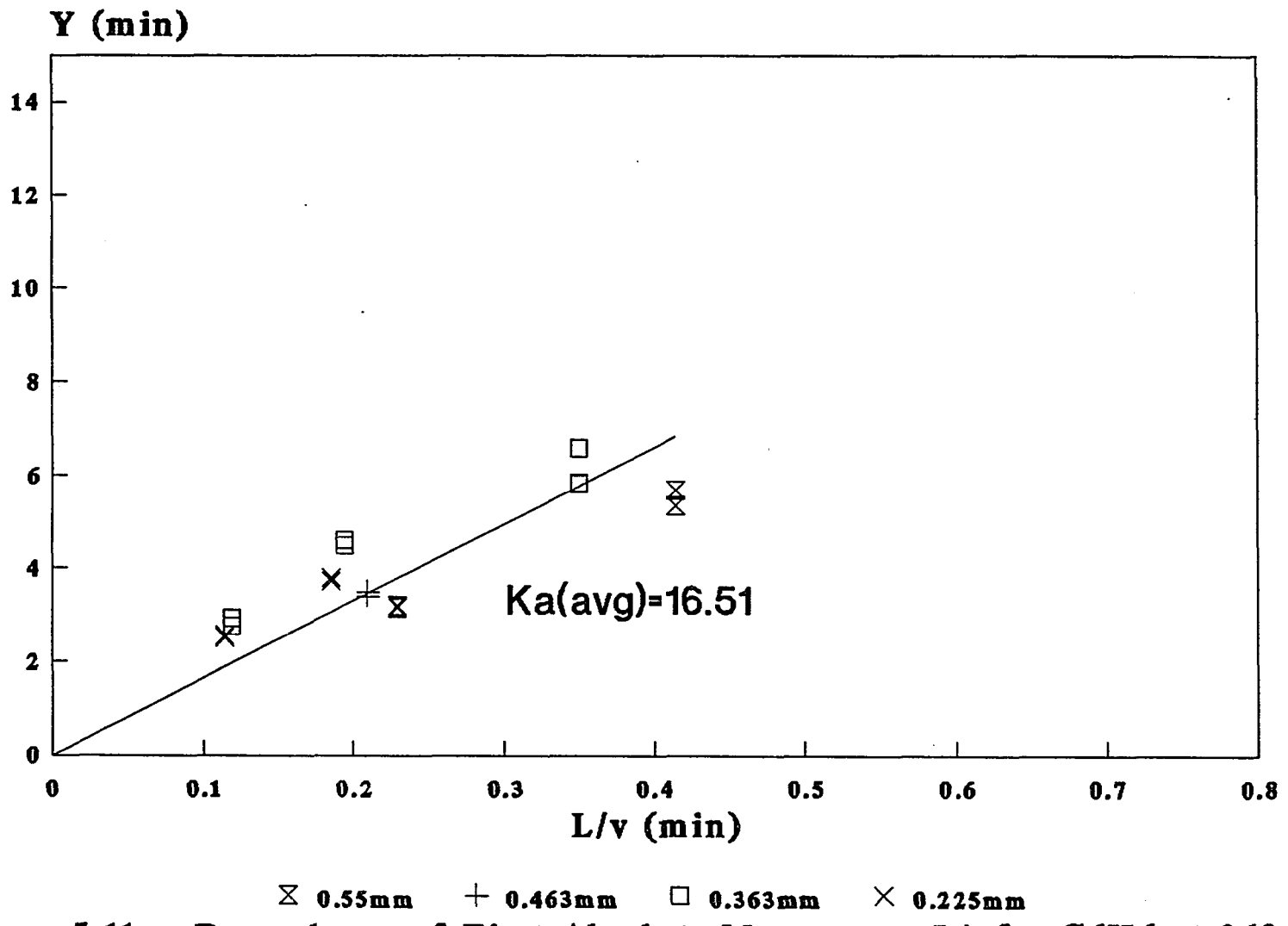

Figure 5-11-e. Dependence of First Absolute Moment on L/v for C6H6 at 260 C

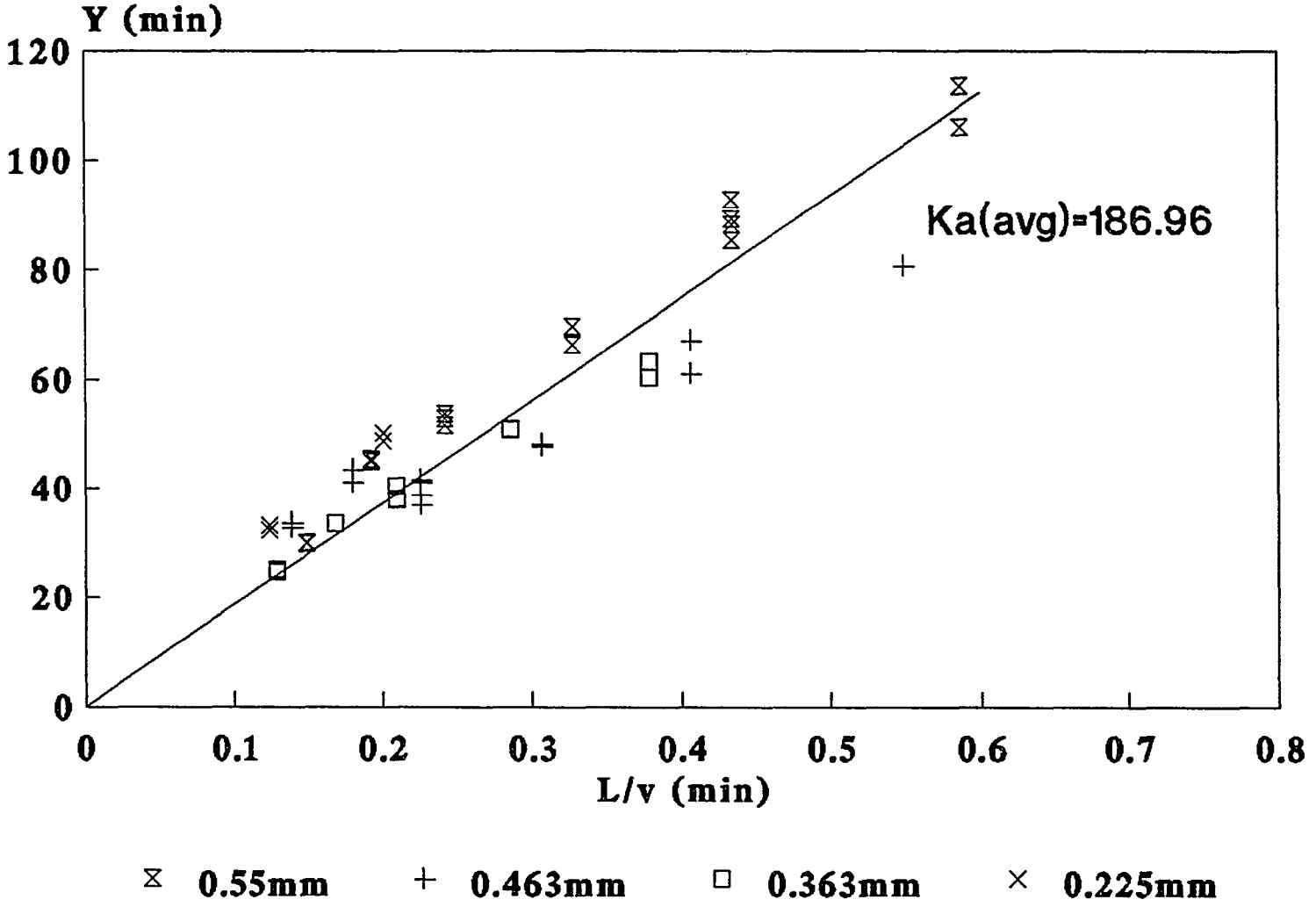

Figure 5-12-a. Dependence of 1st Absolute Moment on L/v for C6H5Cl at 220 C

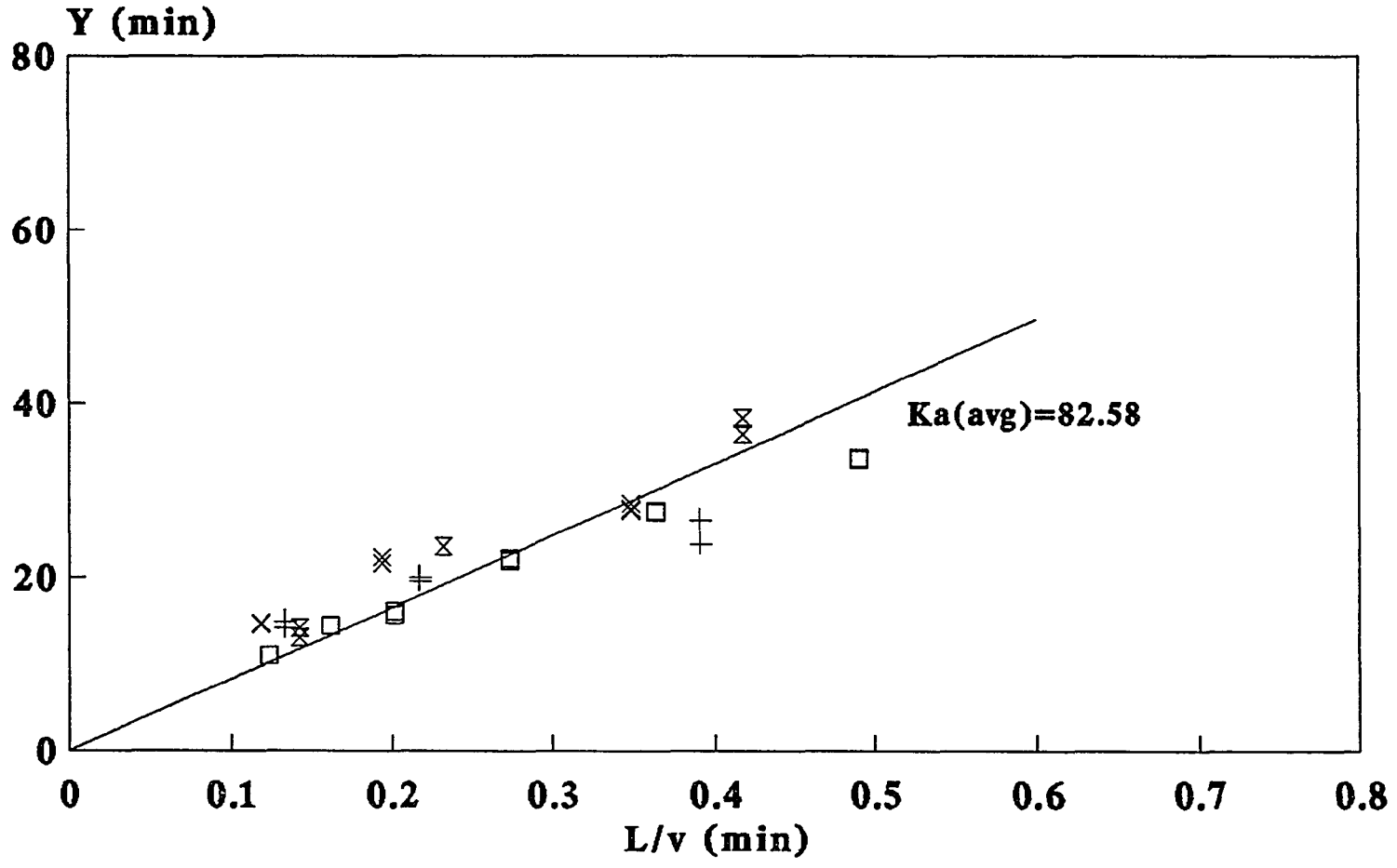

⧖ 0.55mm + 0.463mm □ 0.363mm × 0.225mm

Figure 5-12-b. Dependence of 1st Absolute Moment on L/v for C_6H_5Cl at 240 C

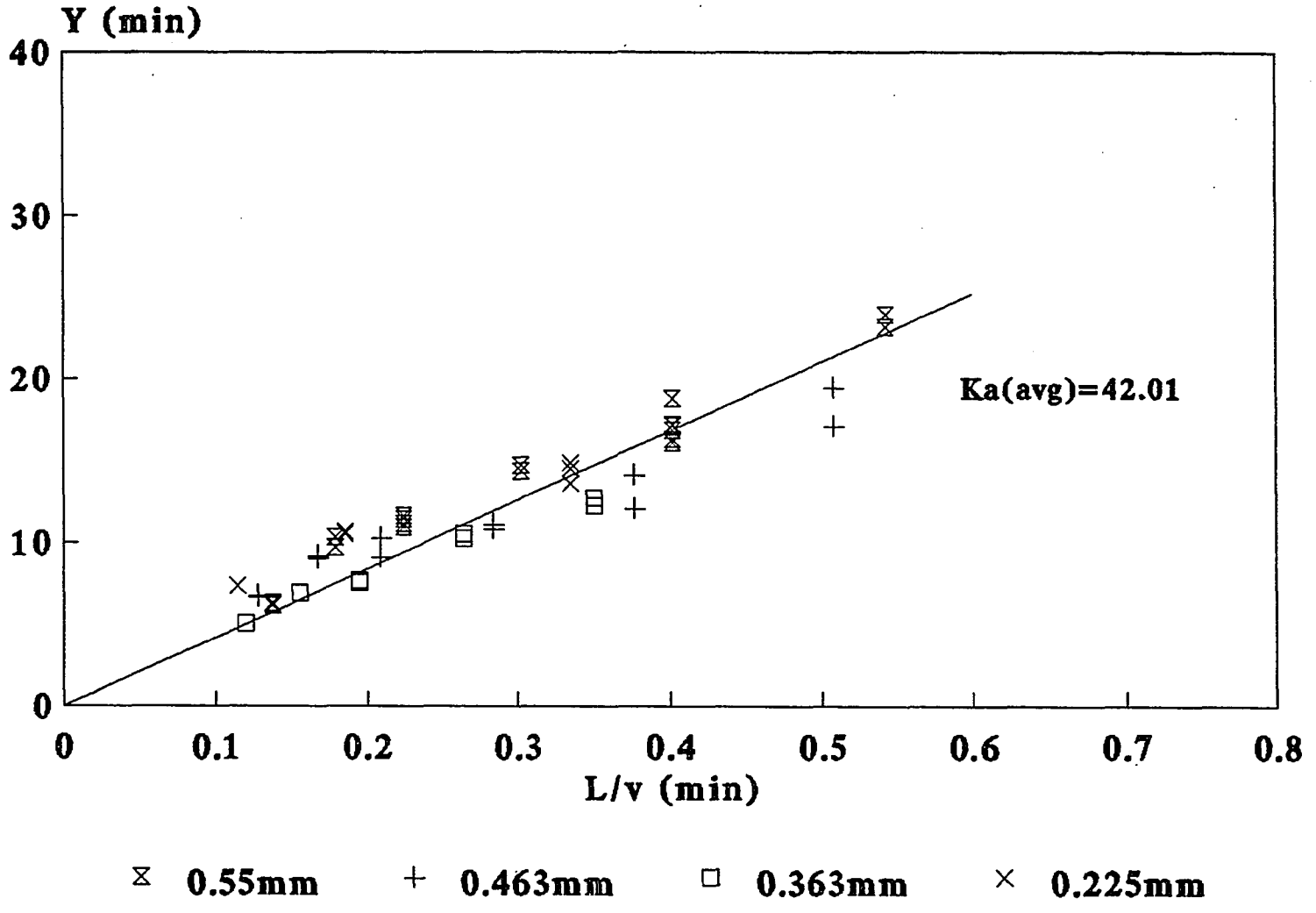

Figure 5-12-c. Dependence of 1st Absolute Moment on L/v for C6H5Cl at 260 C

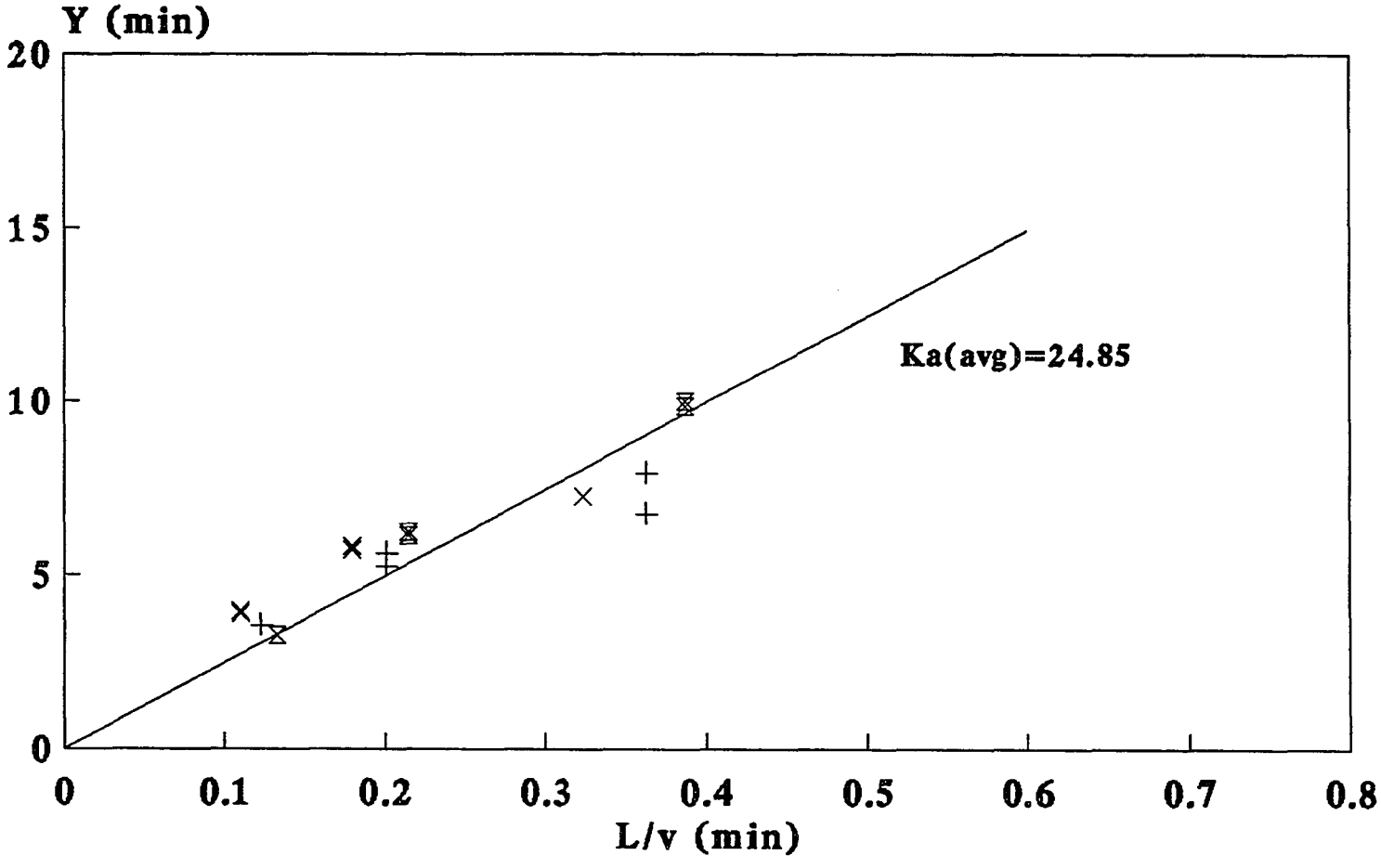

⧖ 0.55mm + 0.463mm × 0.225mm

Figure 5-12-d. Dependence of 1st Absolute Moment on L/v for C_6H_5Cl at 280 C

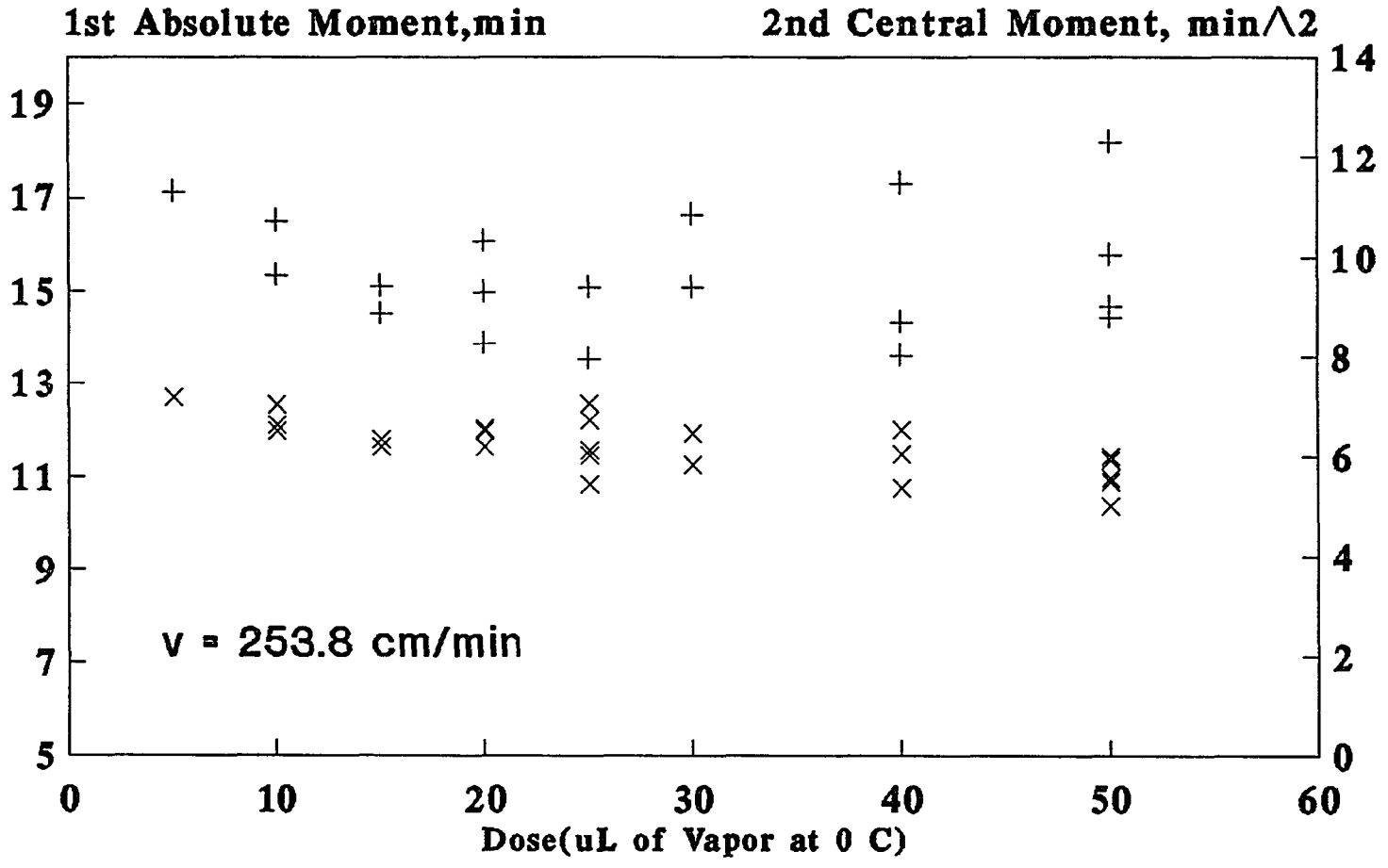

10 uL= 1.34E-9 gmole of C6H5Cl

× 1st Absolute Moment + 2nd Central Moment

Figure 5-13. Effect of C6H5Cl Dose on 1st and 2nd Moments at 220 C

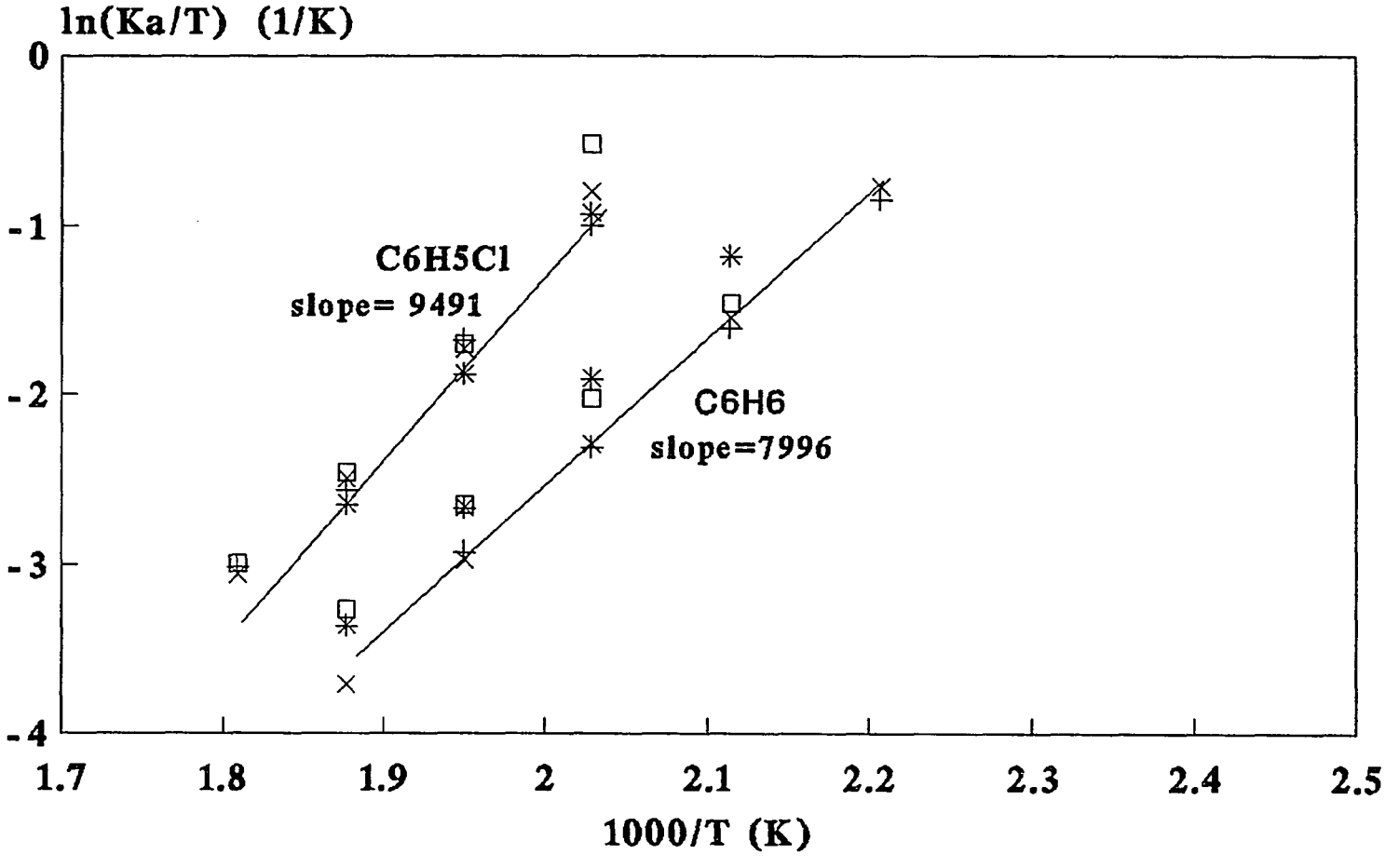

× 0.55mm + 0.463mm ✳ 0.363mm □ 0.225mm

Figure 5-14. Plot of Van't Hoff's Equation for C6H6 and C6H5Cl on NJIT Soil

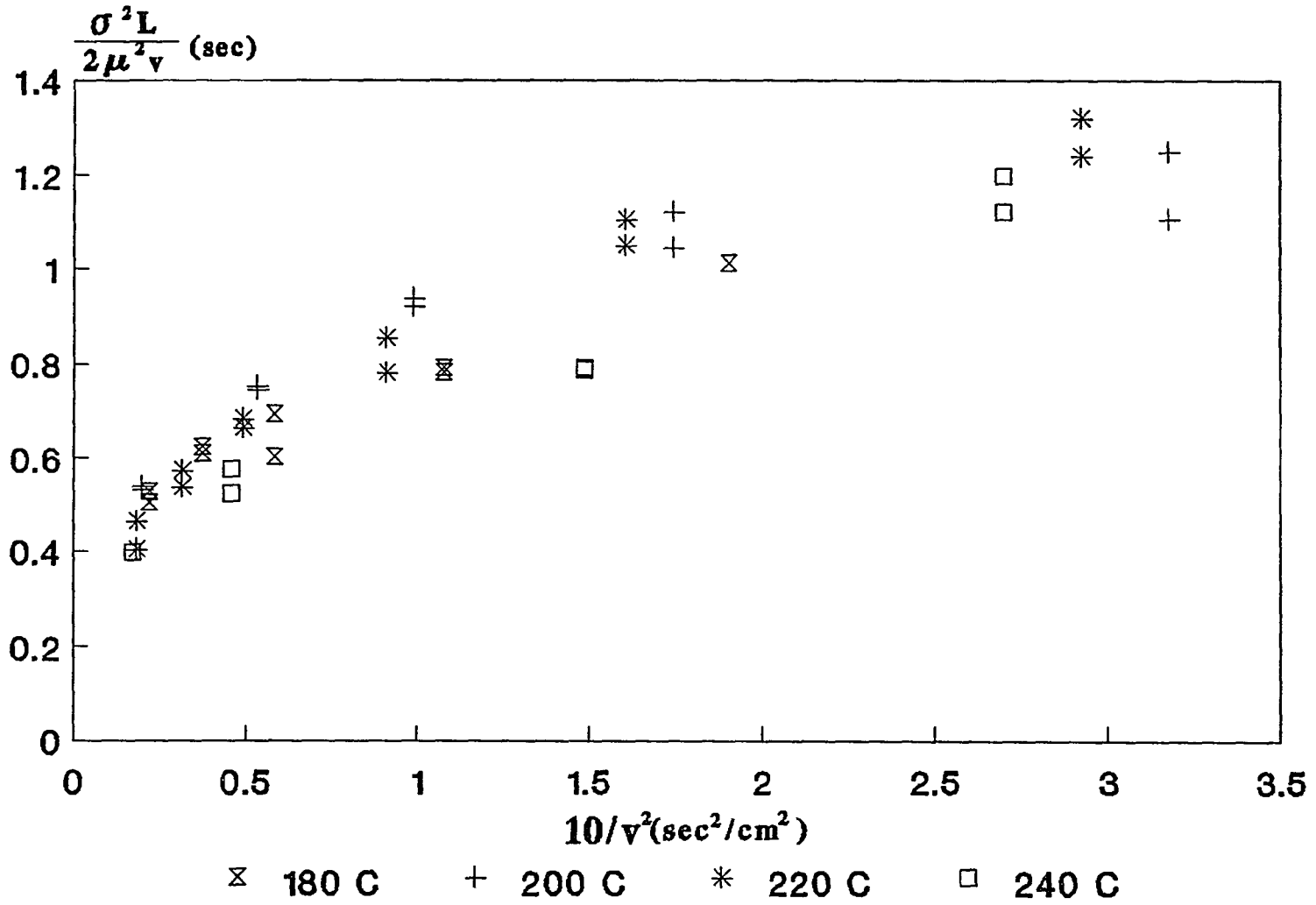

Figure 5-15. Plot for Mass Transfer Coefficients for C6H6 on Soil
Average Particle Diameter: 0.463 mm

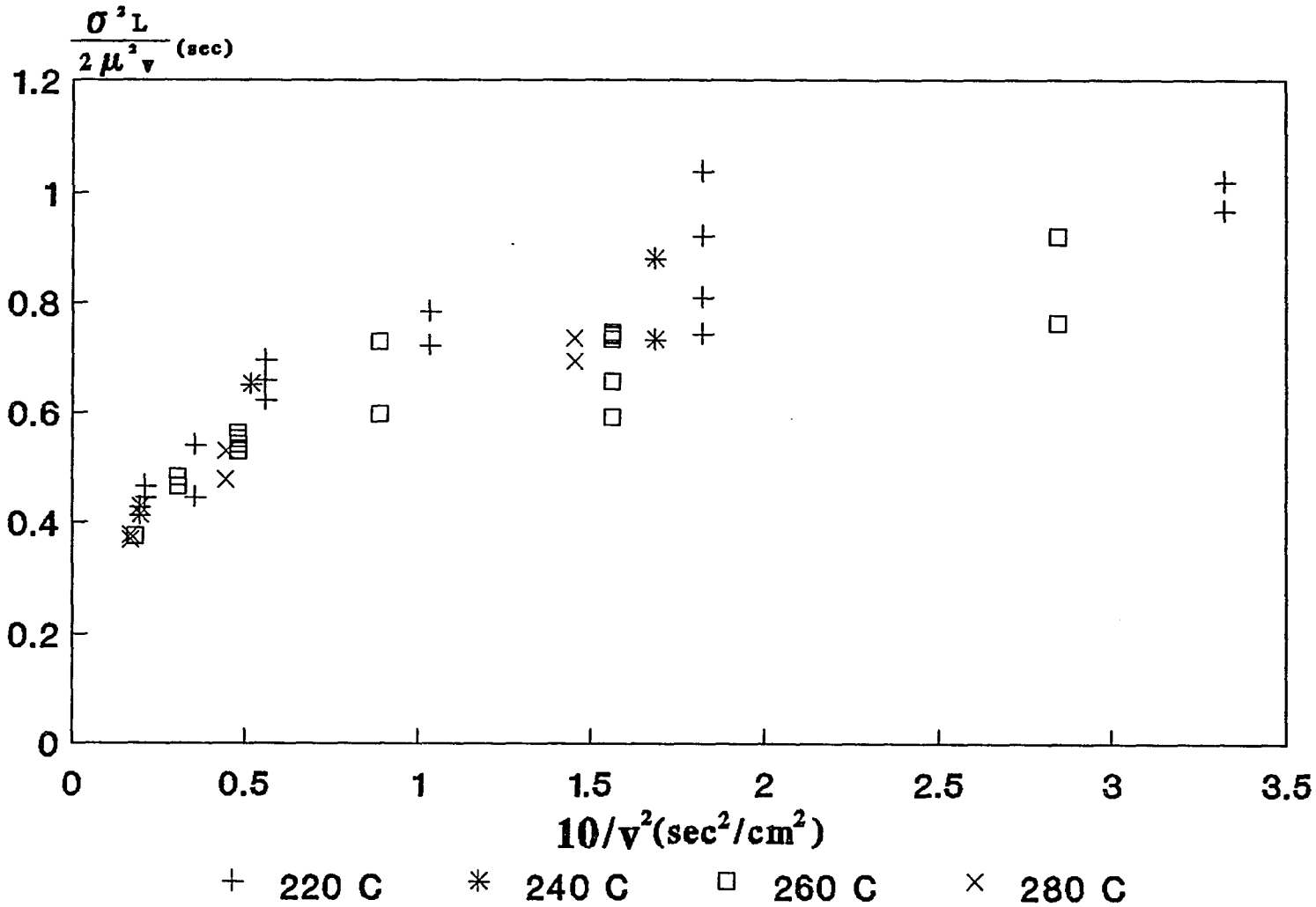

Figure 5-16. Plot for Mass Transfer Coefficients for C6H5Cl on Soil Average Particle Diameter: 0.55 mm

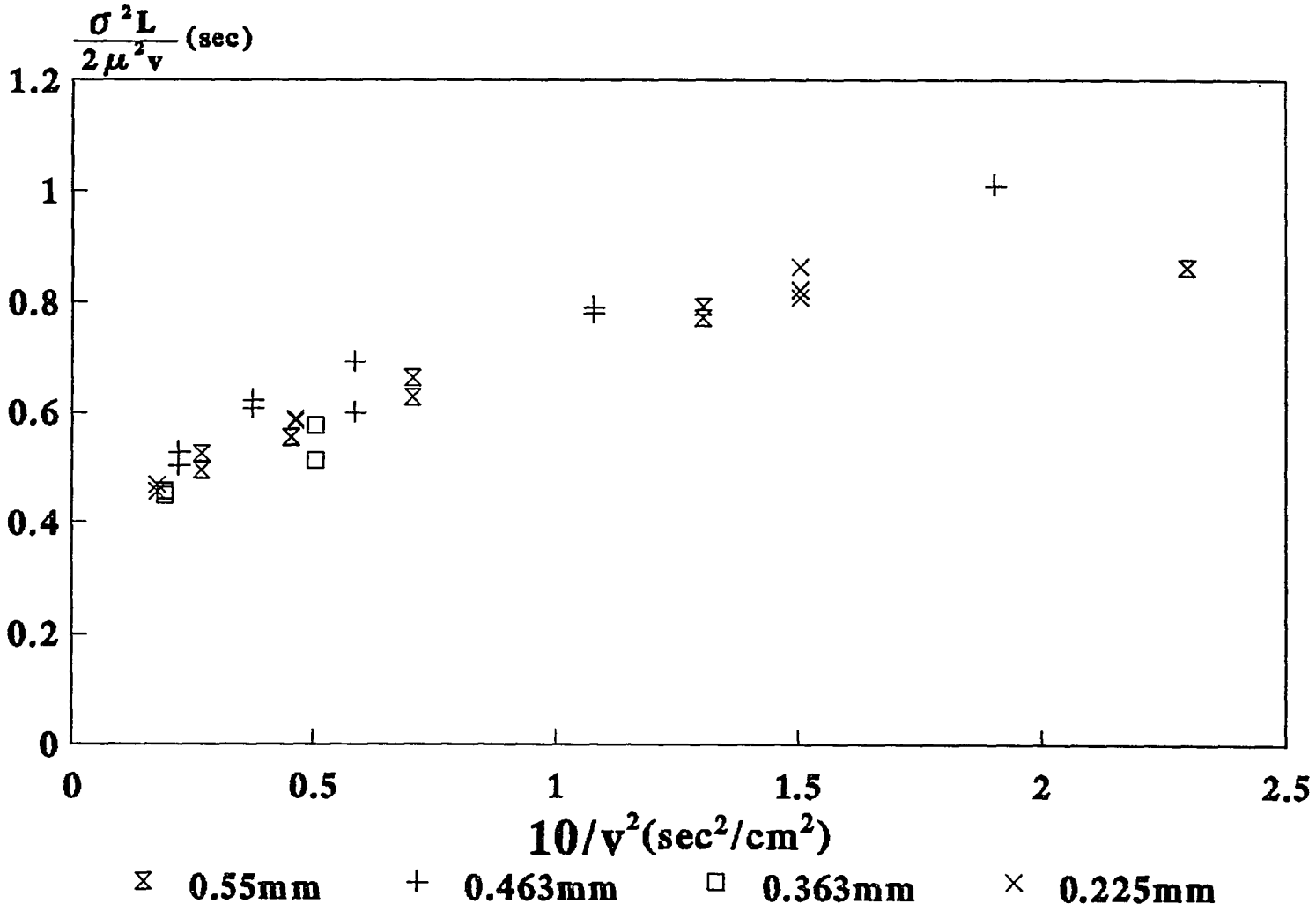

Figure 5-17-a. Plot for Mass Transfer Coefficients for C6H6 at 180 C

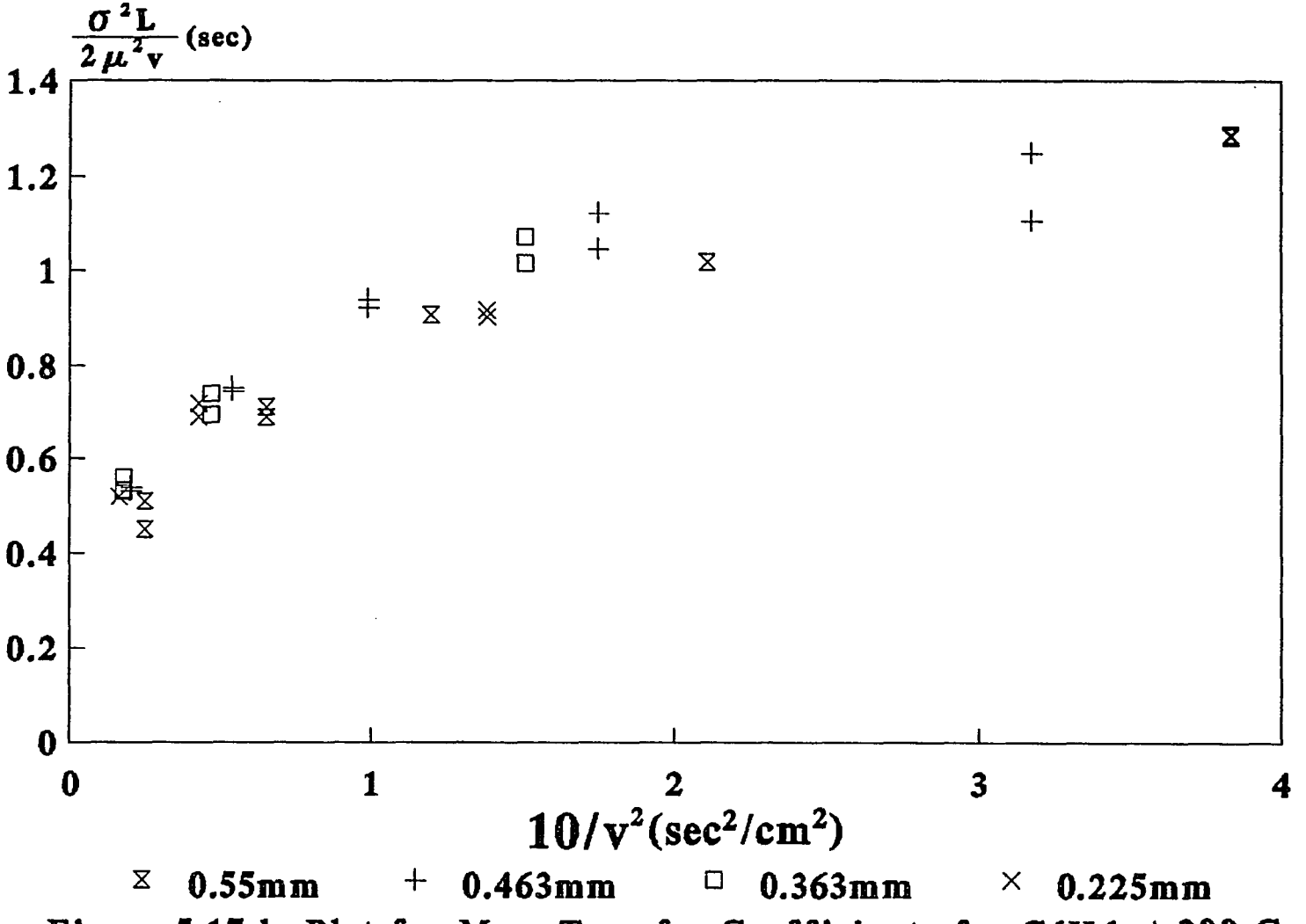

Figure 5-17-b. Plot for Mass Transfer Coefficients for C6H6 at 200 C

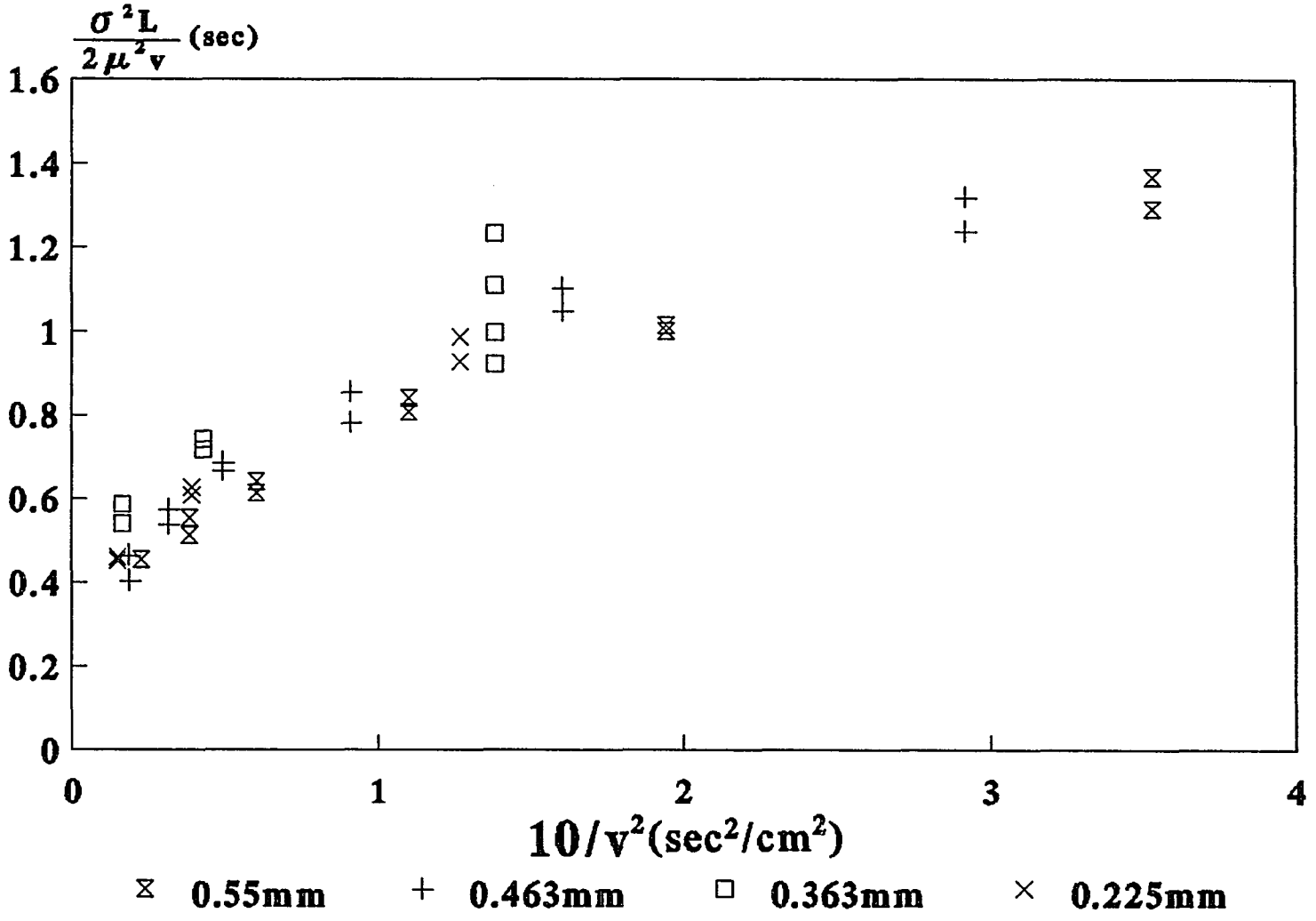

Figure 5-17-c. Plot for Mass Transfer Coefficients for C6H6 at 220 C

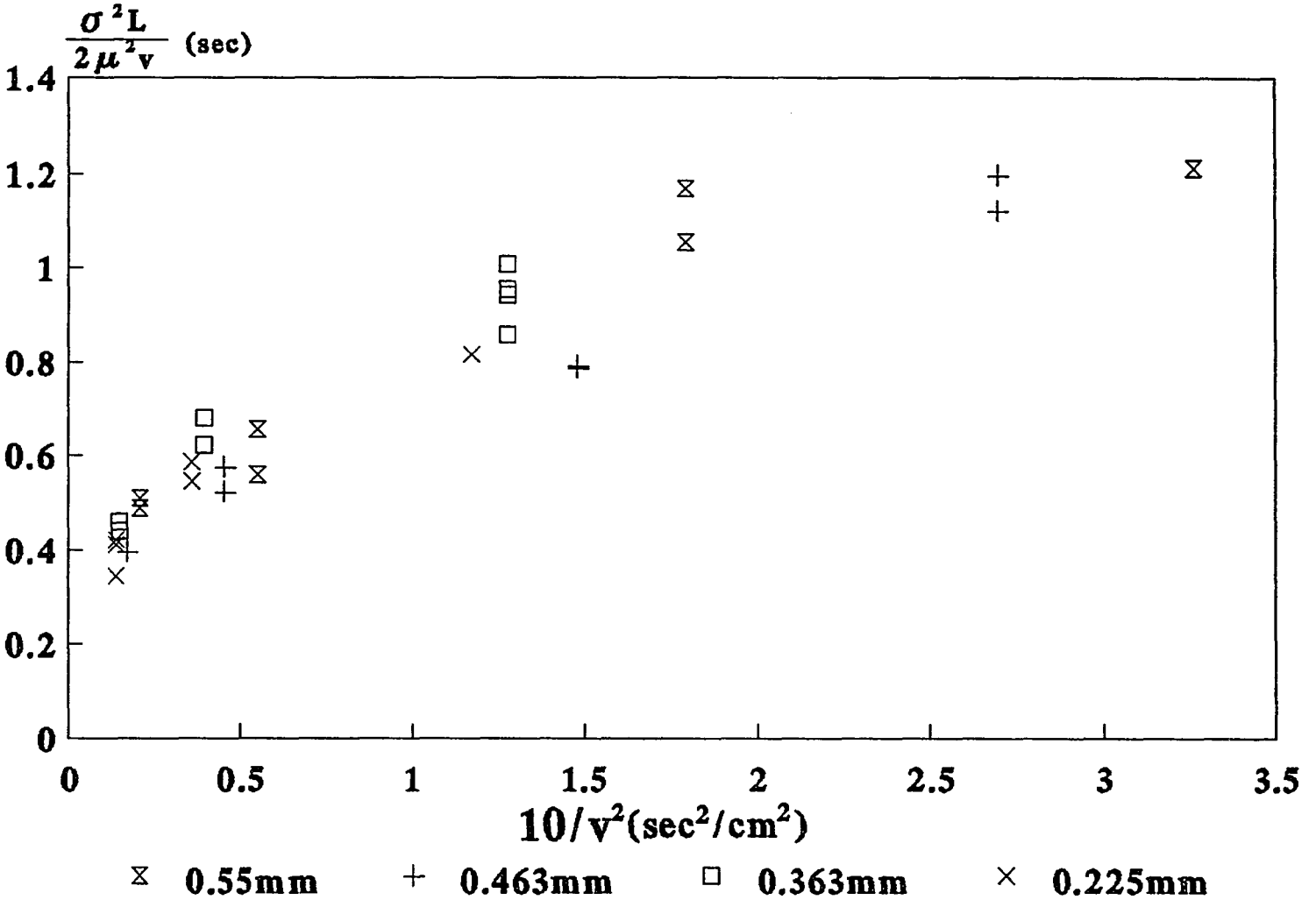

Figure 5-17-d. Plot for Mass Transfer Coefficients for C6H6 at 240 C

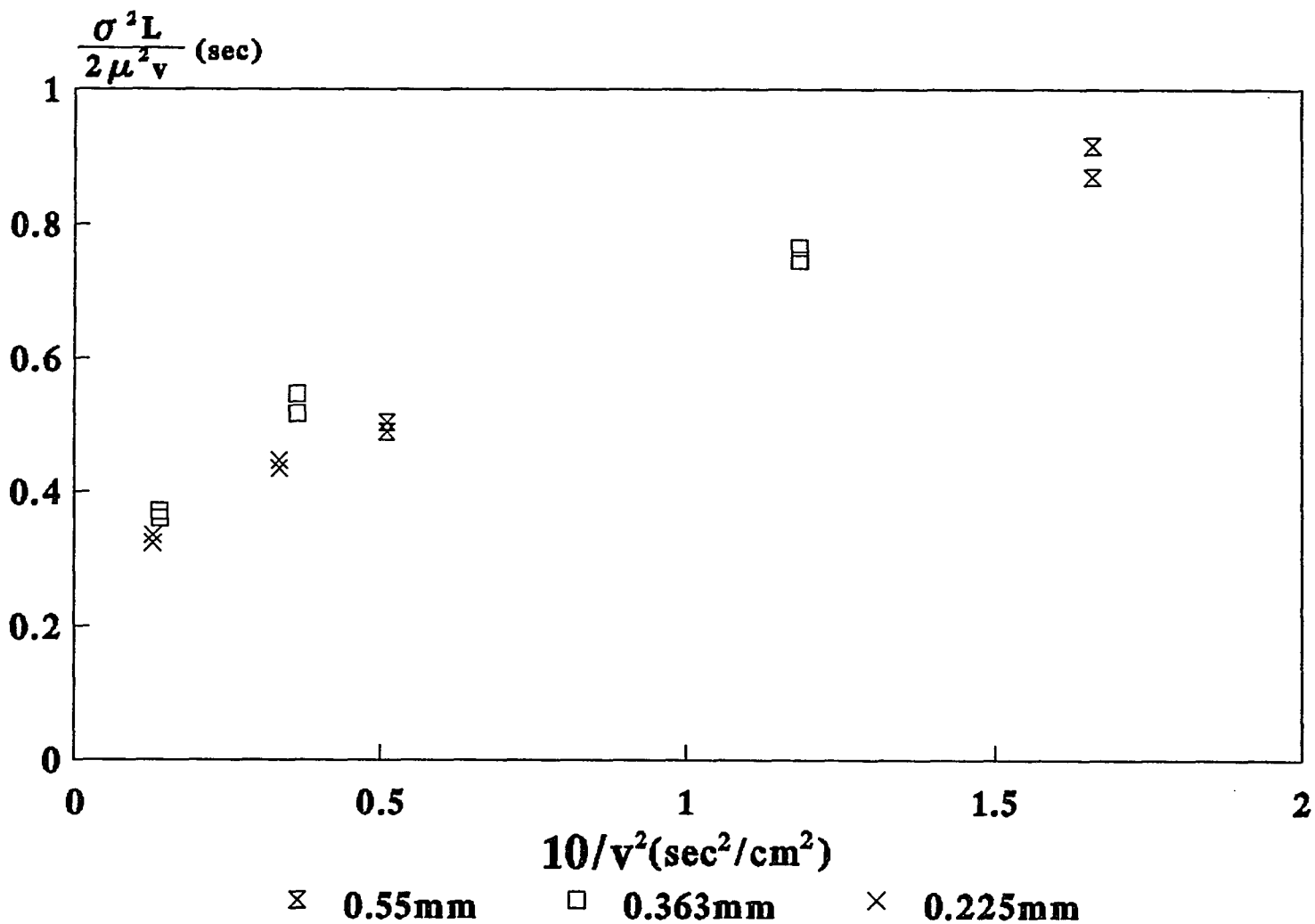

Figure 5-17-e. Plot for Mass Transfer Coefficients for C6H6 at 260 C

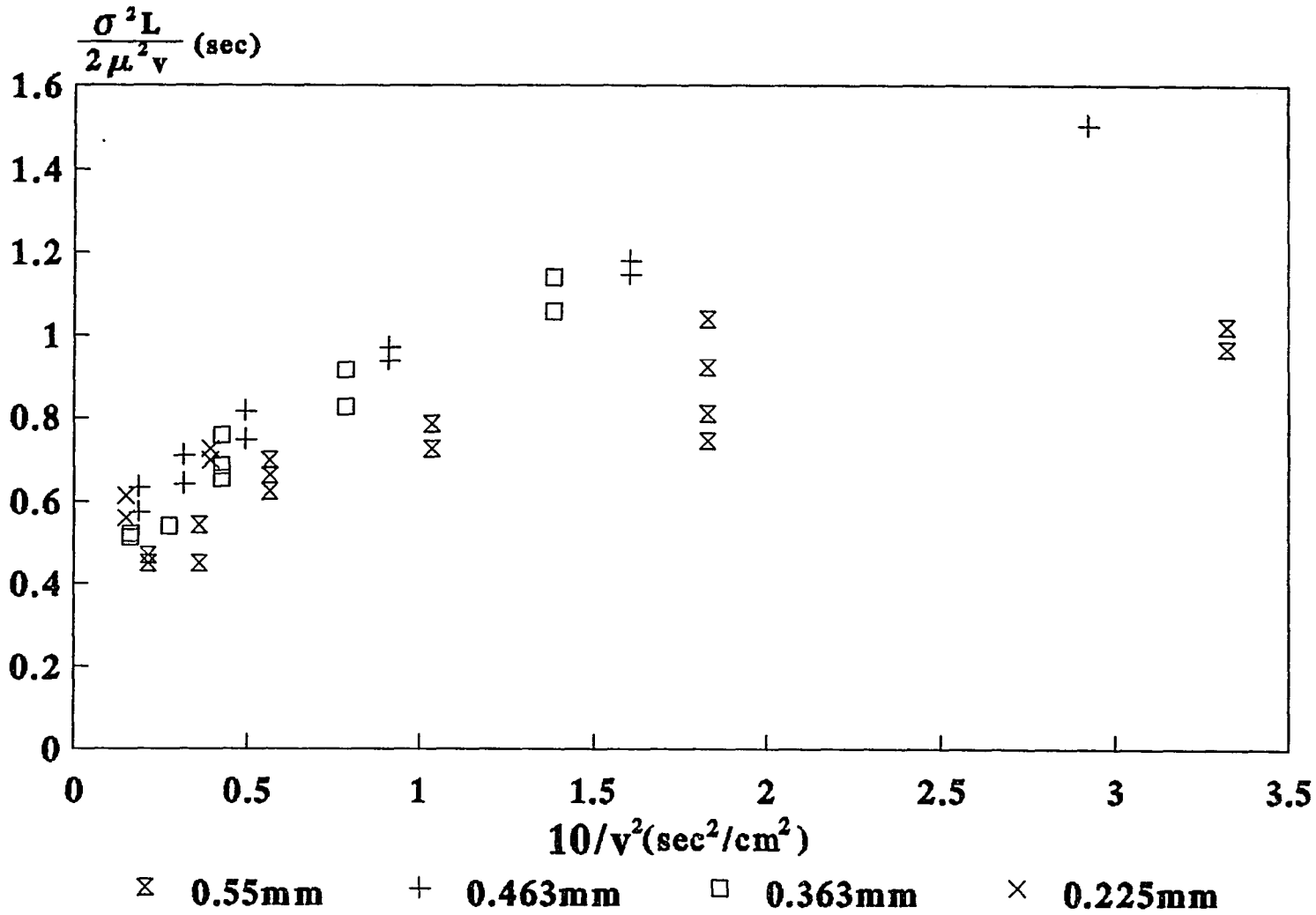

Figure 5-18-a. Plot for Mass Transfer Coefficients of C6H5Cl at 220 C

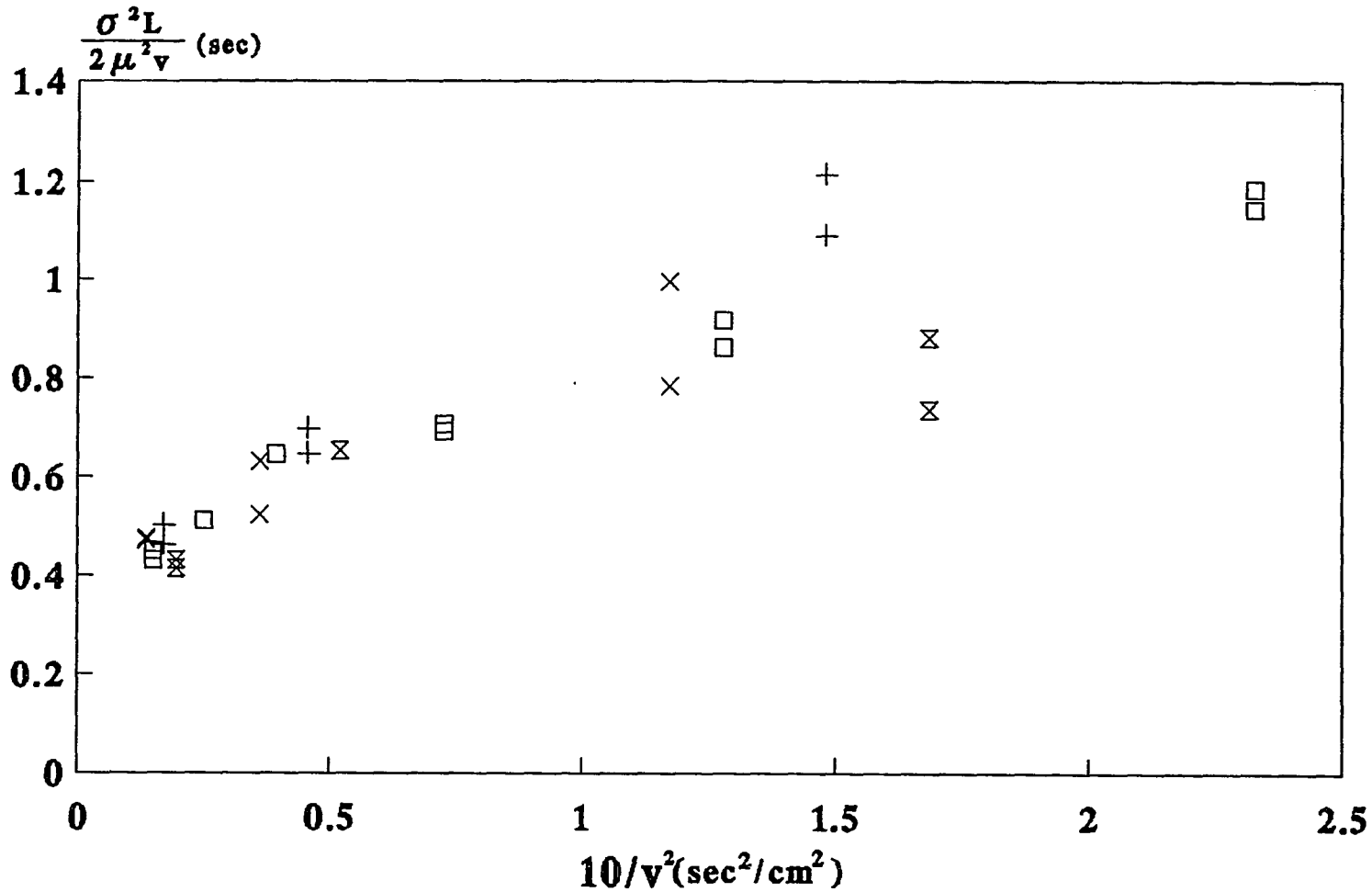

⧖ 0.55mm + 0.463mm □ 0.363mm × 0.225mm

Figure 5-18-b. Plot for Mass Transfer Coefficients of C6H5Cl at 240 C

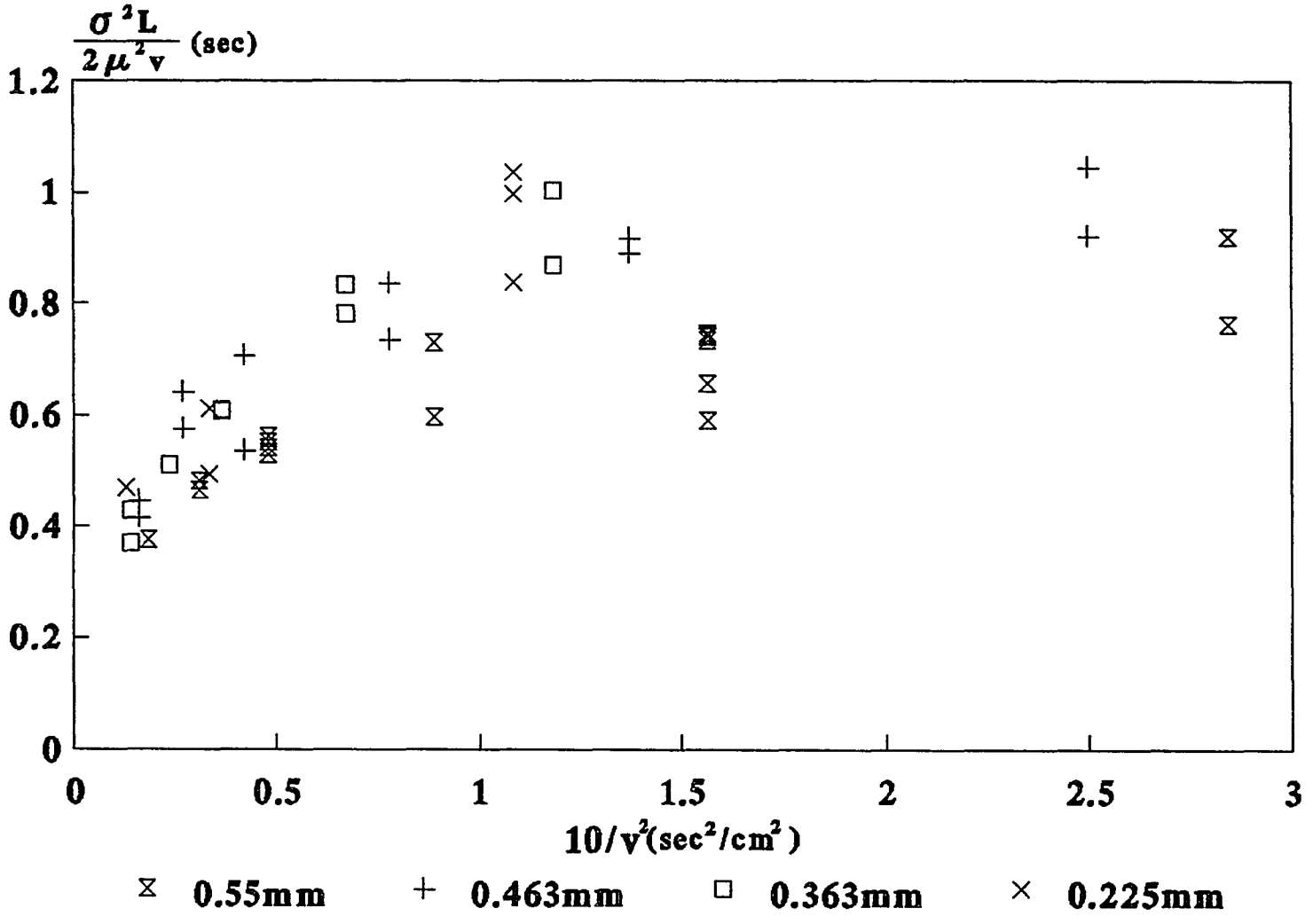

Figure 5-18-c. Plot for Mass Transfer Coefficients of C6H5Cl at 260 C

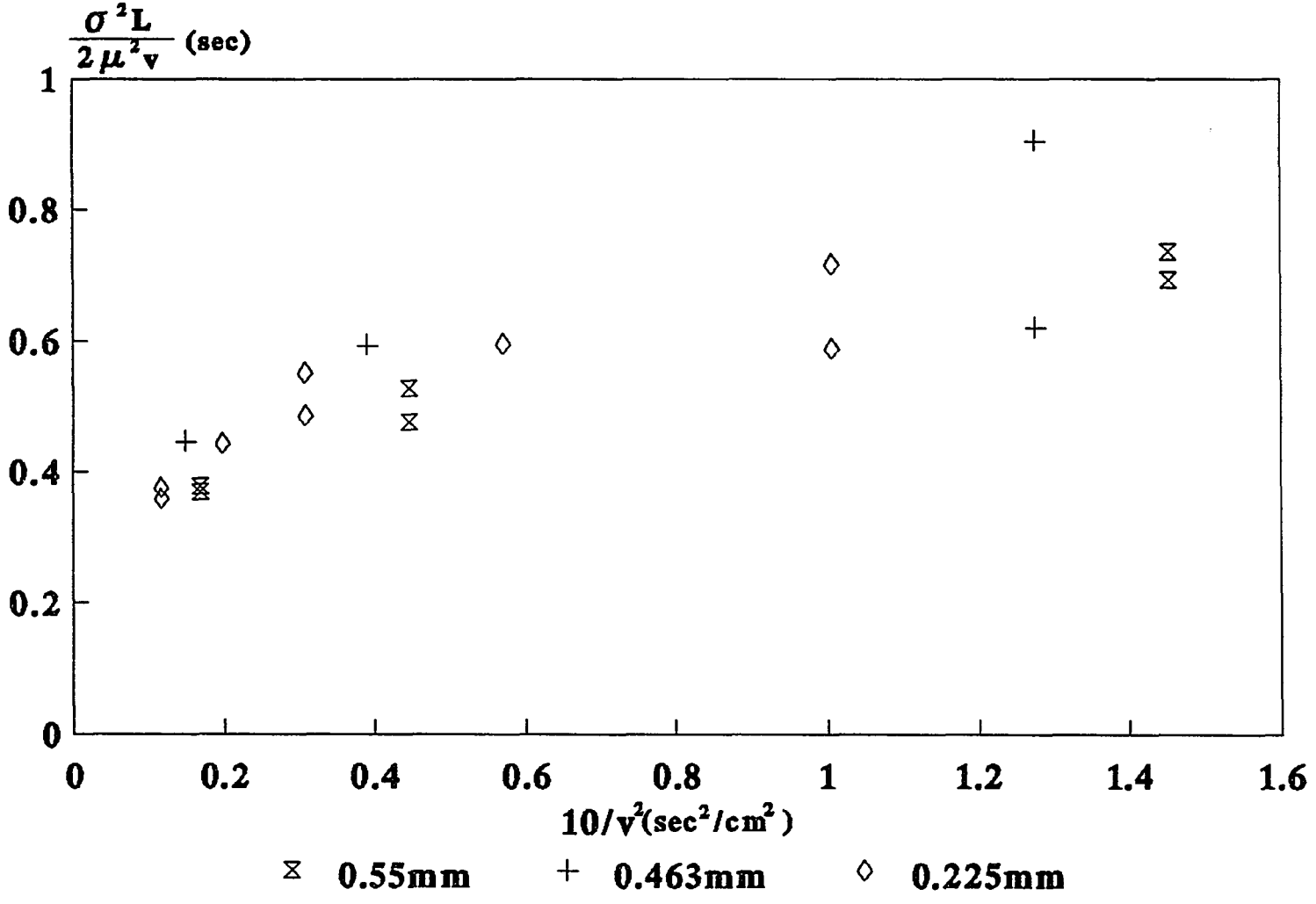

Figure 5-18-d. Plot for Mass Transfer Coefficients of C6H5Cl at 280 C

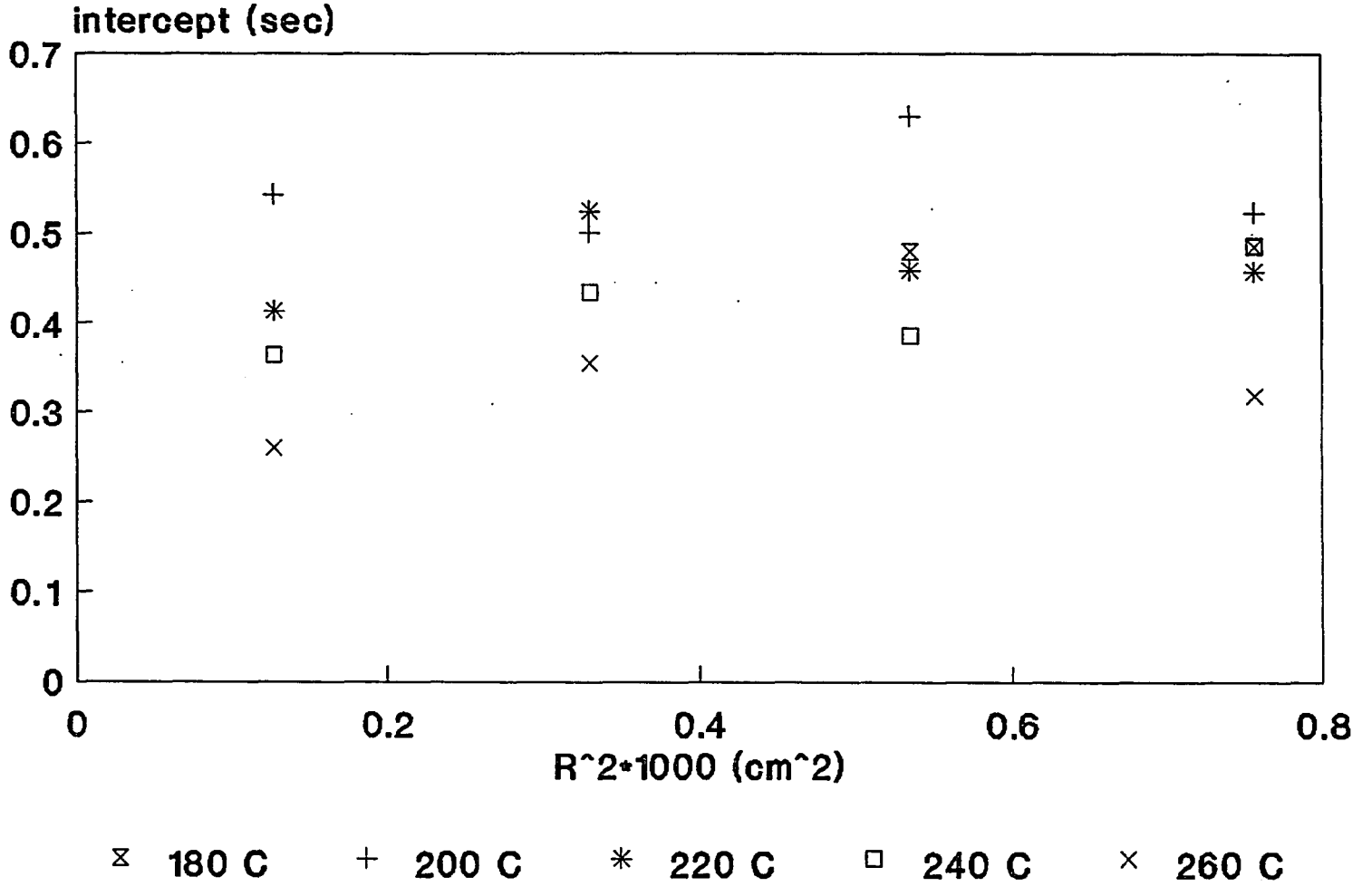

Figure 5-19. Dependence of Intercept on R^2 for C6H6

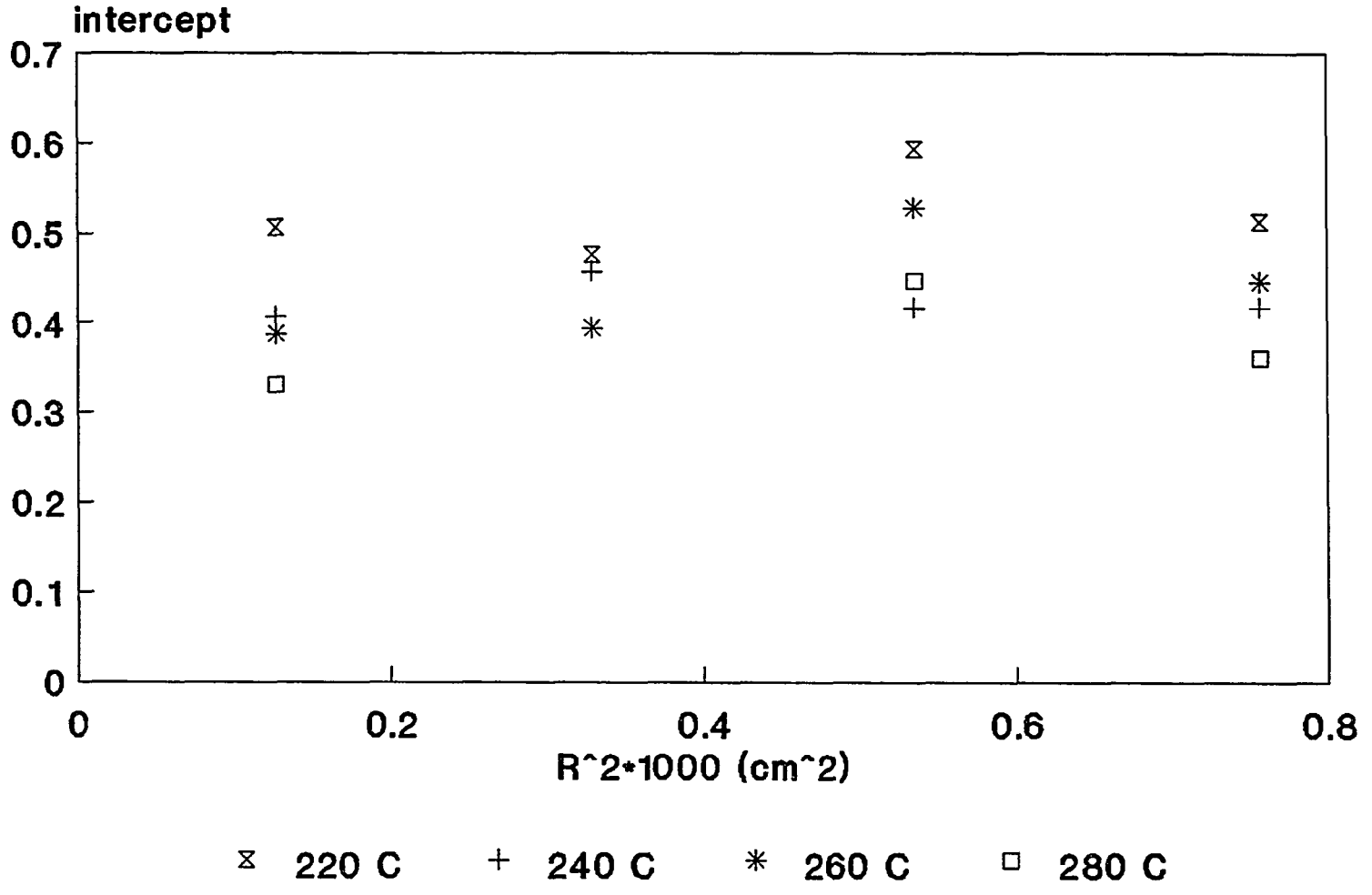

Figure 5-20. Dependence of Intercept on R^2 for C6H5Cl

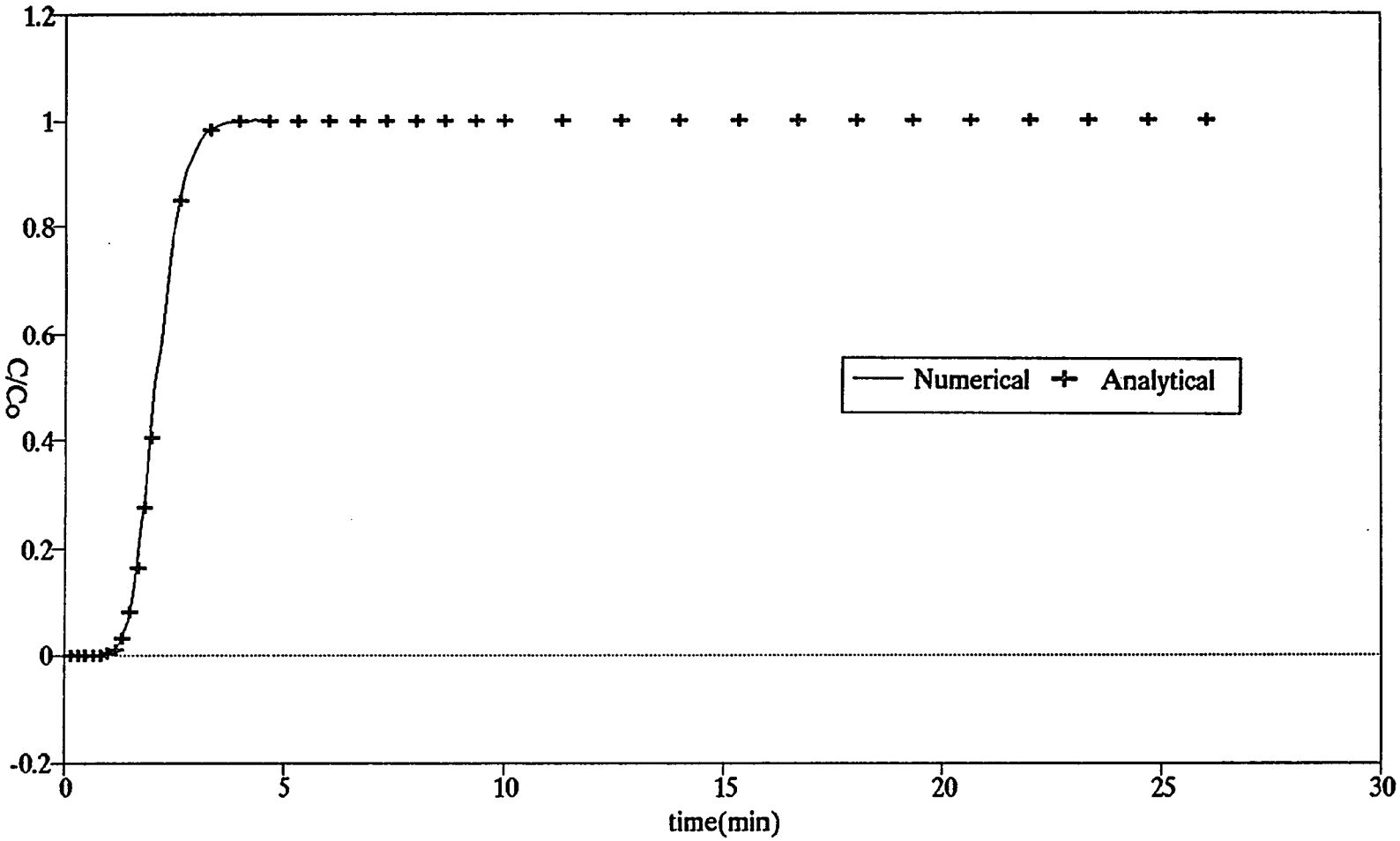

Figure 5-21-a. Effluent Concentration Comparison
C6H6, T=240C, v=3.45cm/sec, Rp=0.23mm

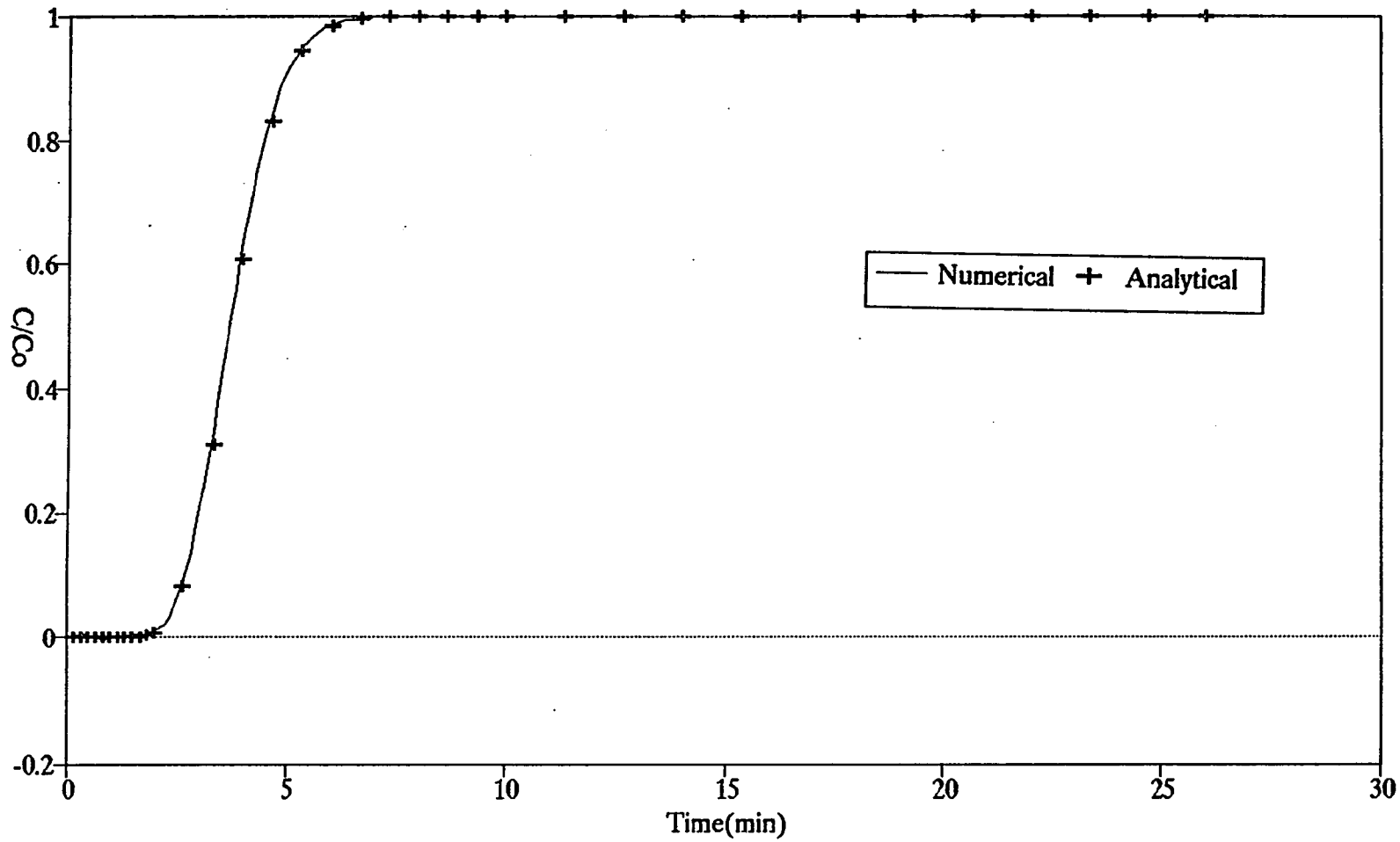

Figure 5-21-b. Effluent Concentration Comparison
C6H5Cl, T=260C, v=2.7cm/sec, Rp=0.23mm

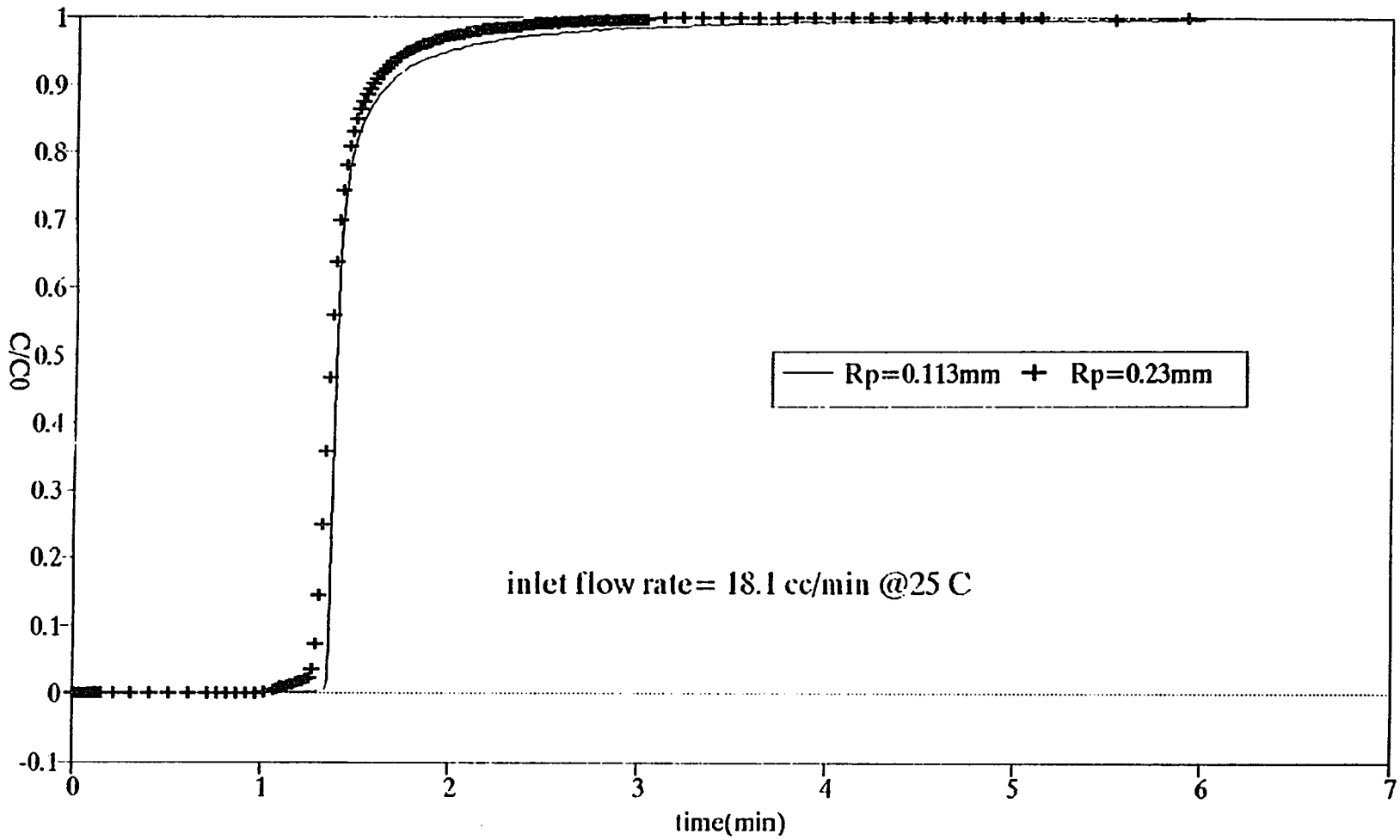

Figure 5-22 Effluent Concentration-C6H6
on Diff. Part Size Soil Column at 220C

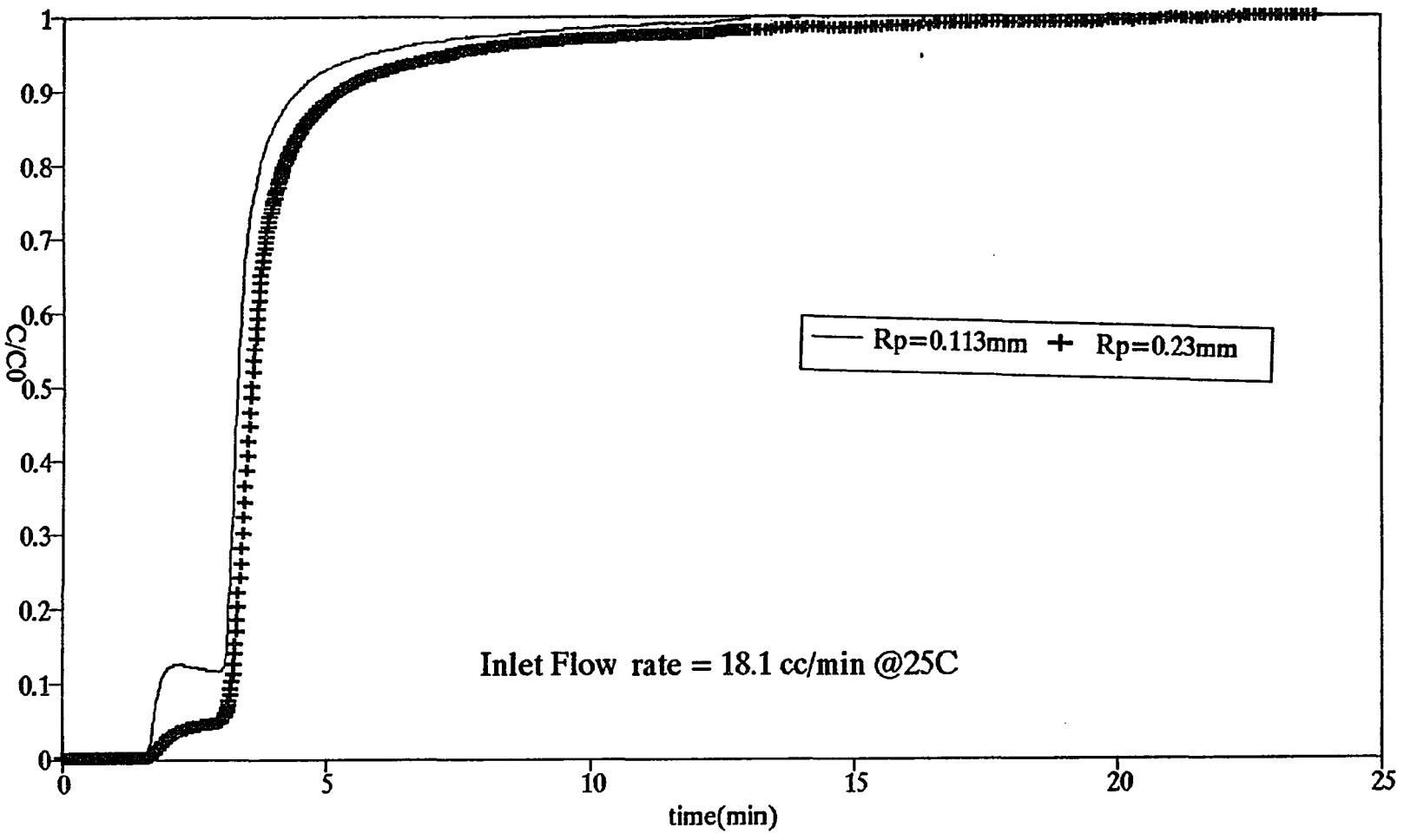

Figure 5-23 Effluent Concentration of C6H5Cl on Different Particle Size Column at 240C

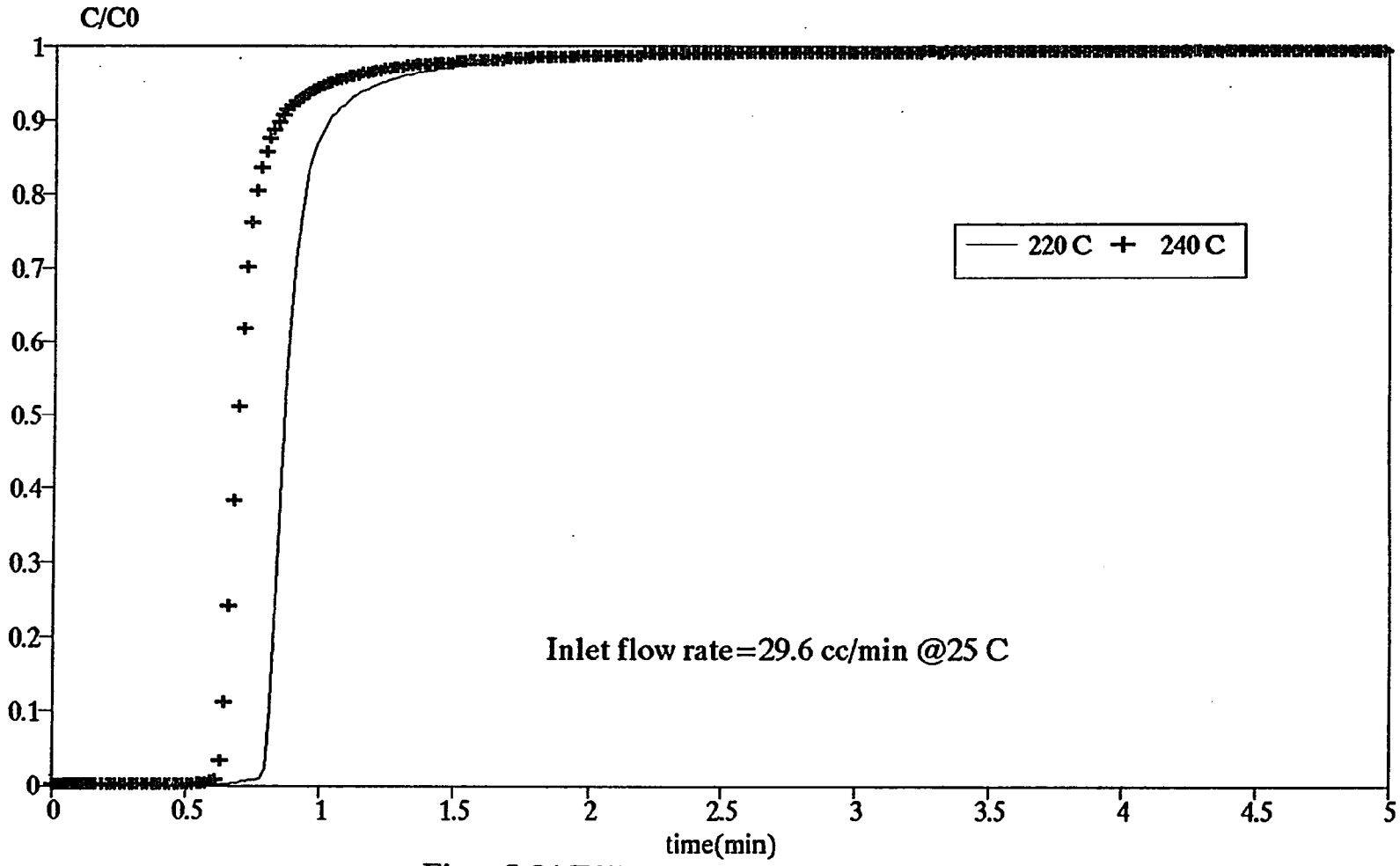

Figur 5-24 Effluent Concentration-C6H6
at Different Temperature

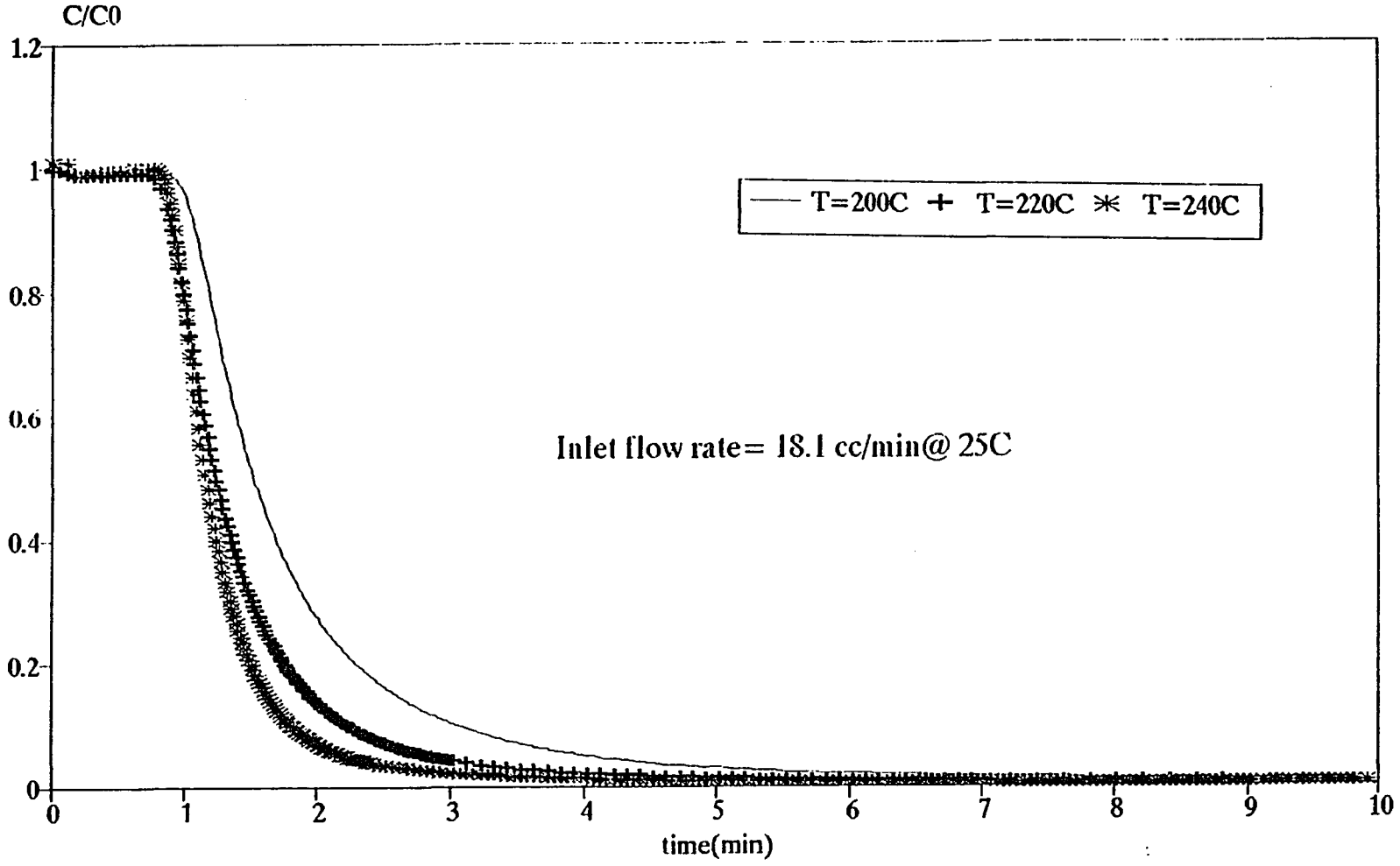

Figure 5-25 Effluent Concentration-C6H6
at Different Temperature

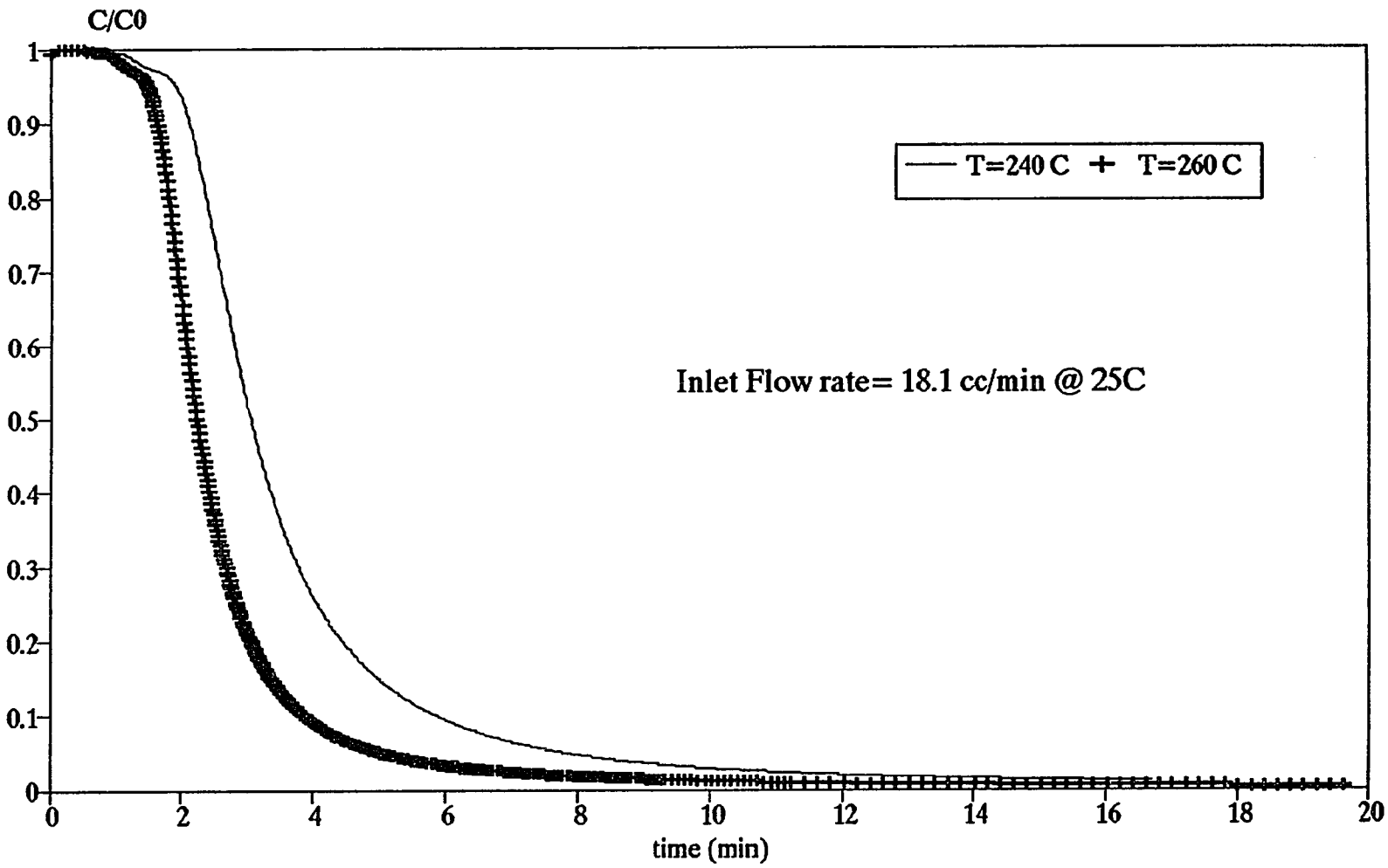

Figure 5-26 Effluent Concentration of C6H5Cl
at Different Temperatures

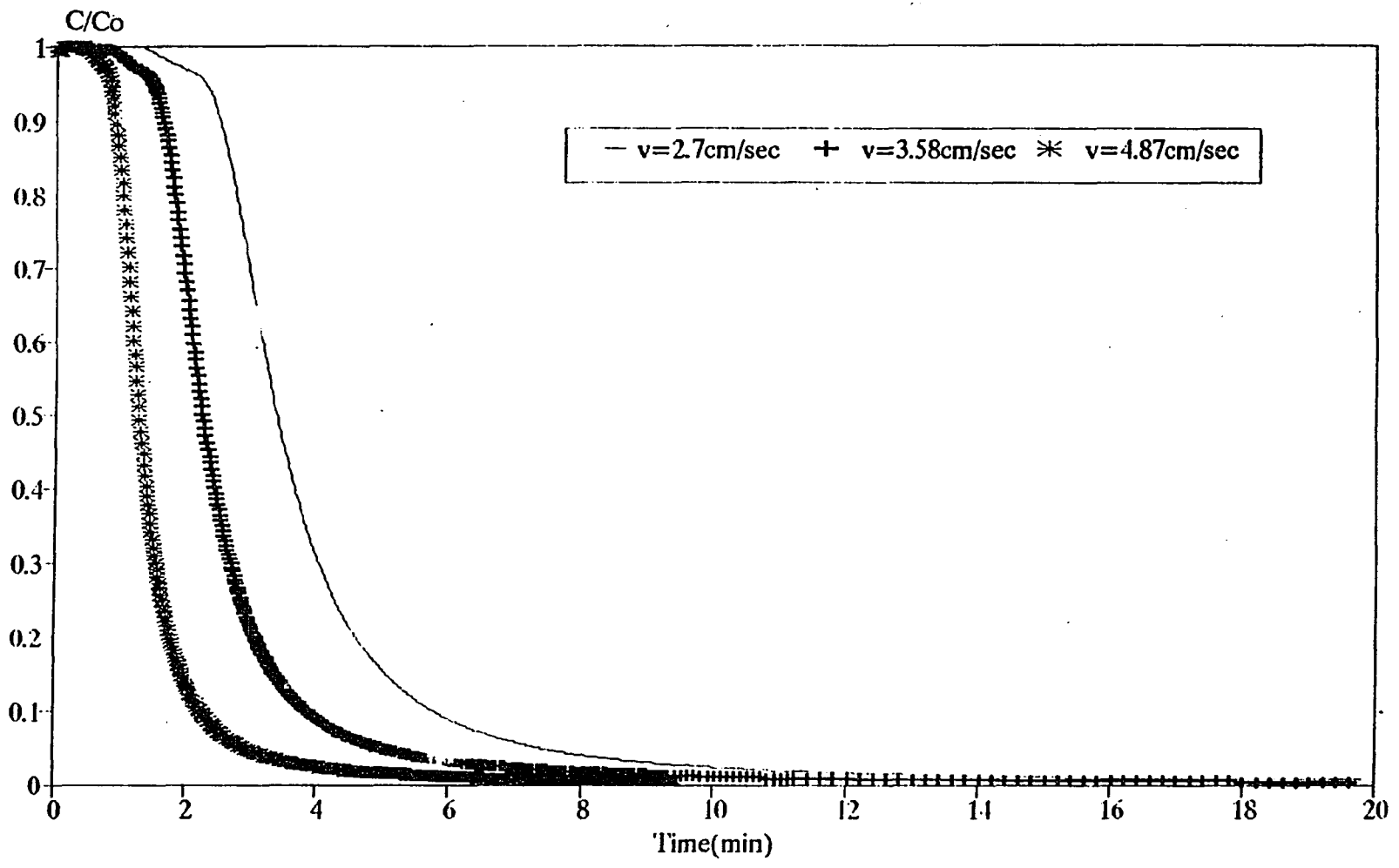

Figure 5-27. Effluent Comcentration of C6H5Cl with Different Flow Rate at 260 C

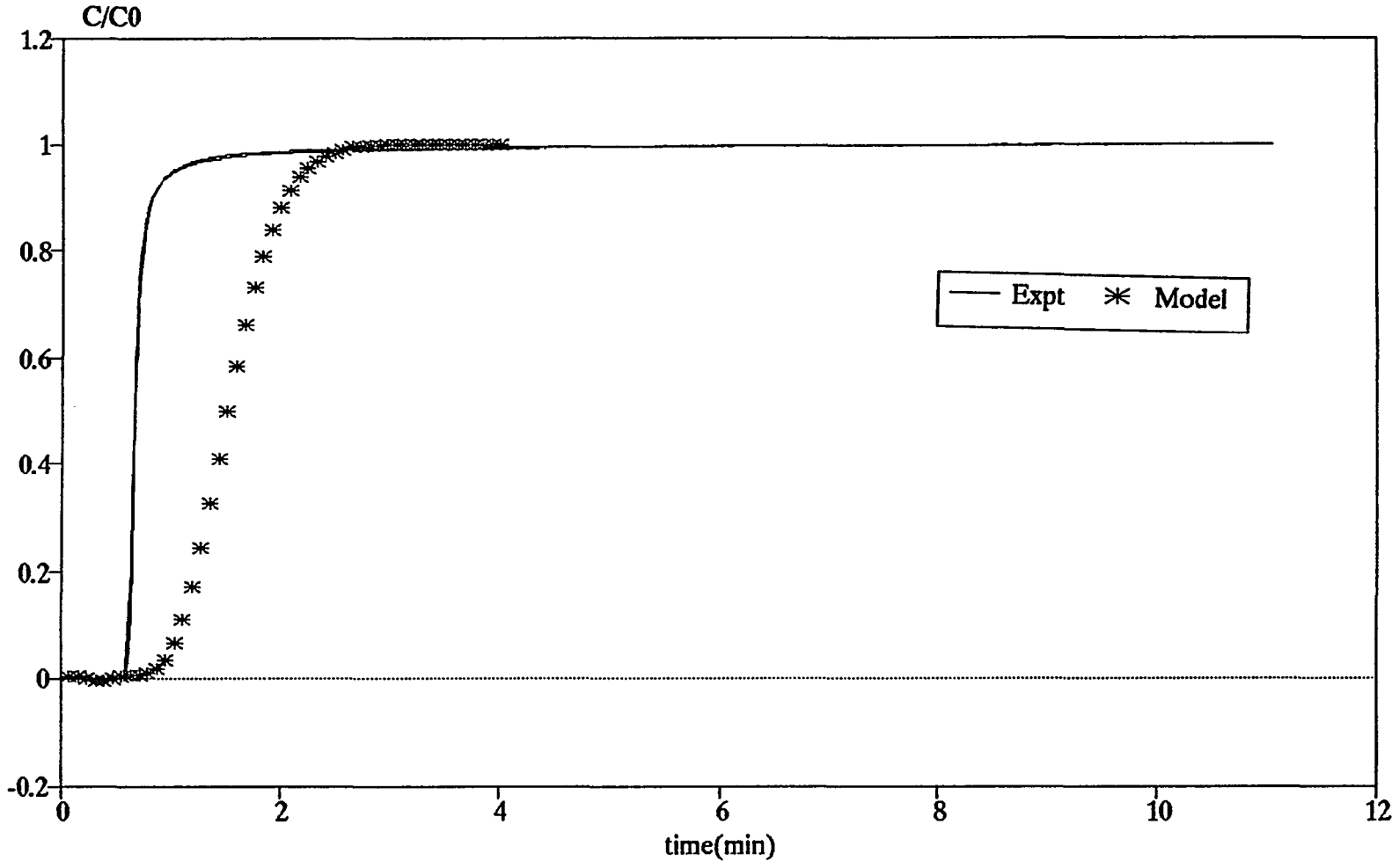

Figure 5-28-a. Effluent Concentration Comparison
C6H6, T=240C, v=4.69cm/sec, Rp=0.23mm

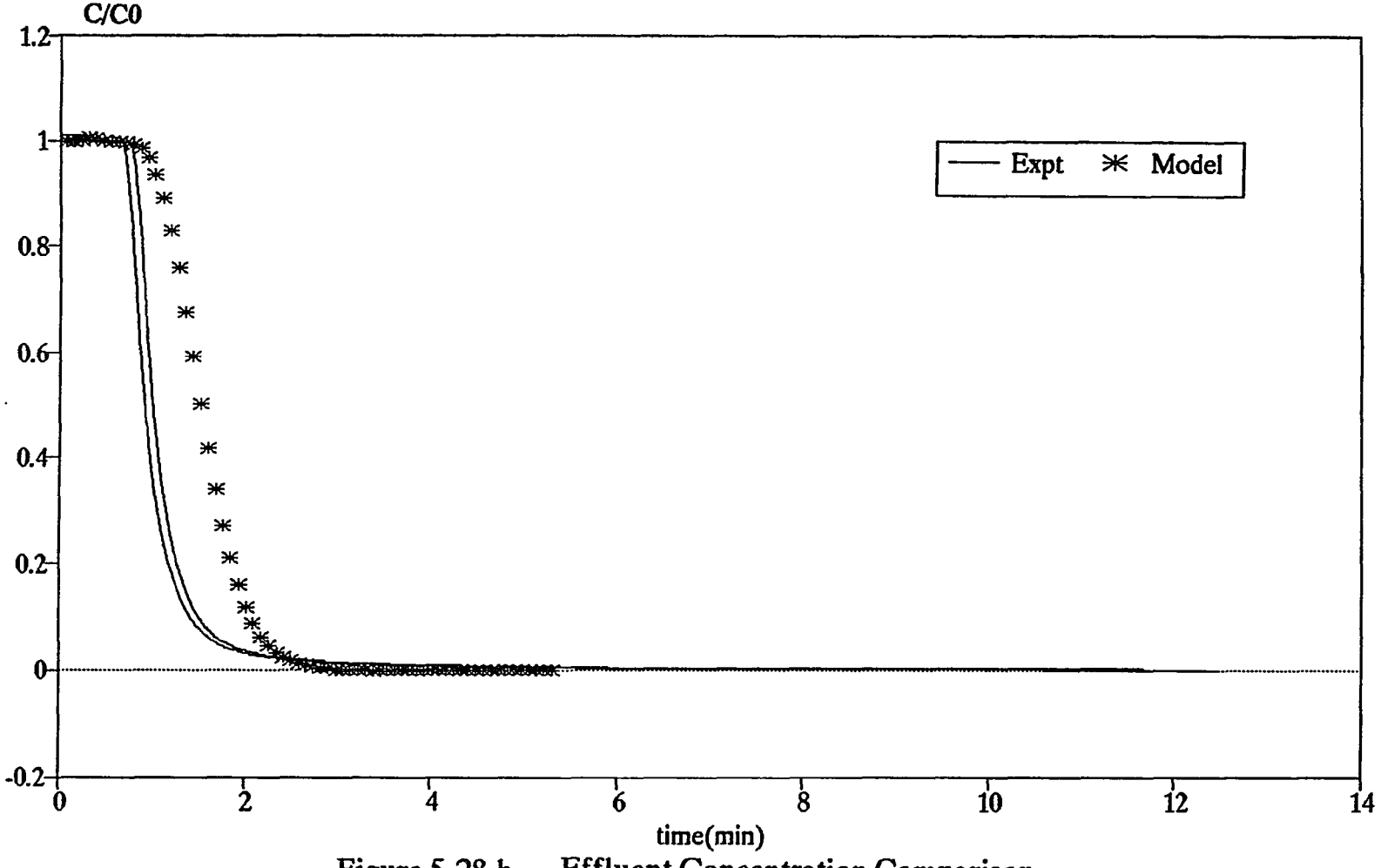

Figure 5-28-b. Effluent Concentration Comparison
C6H6, T=240C, v=4.69cm/sec, Rp=0.23mm

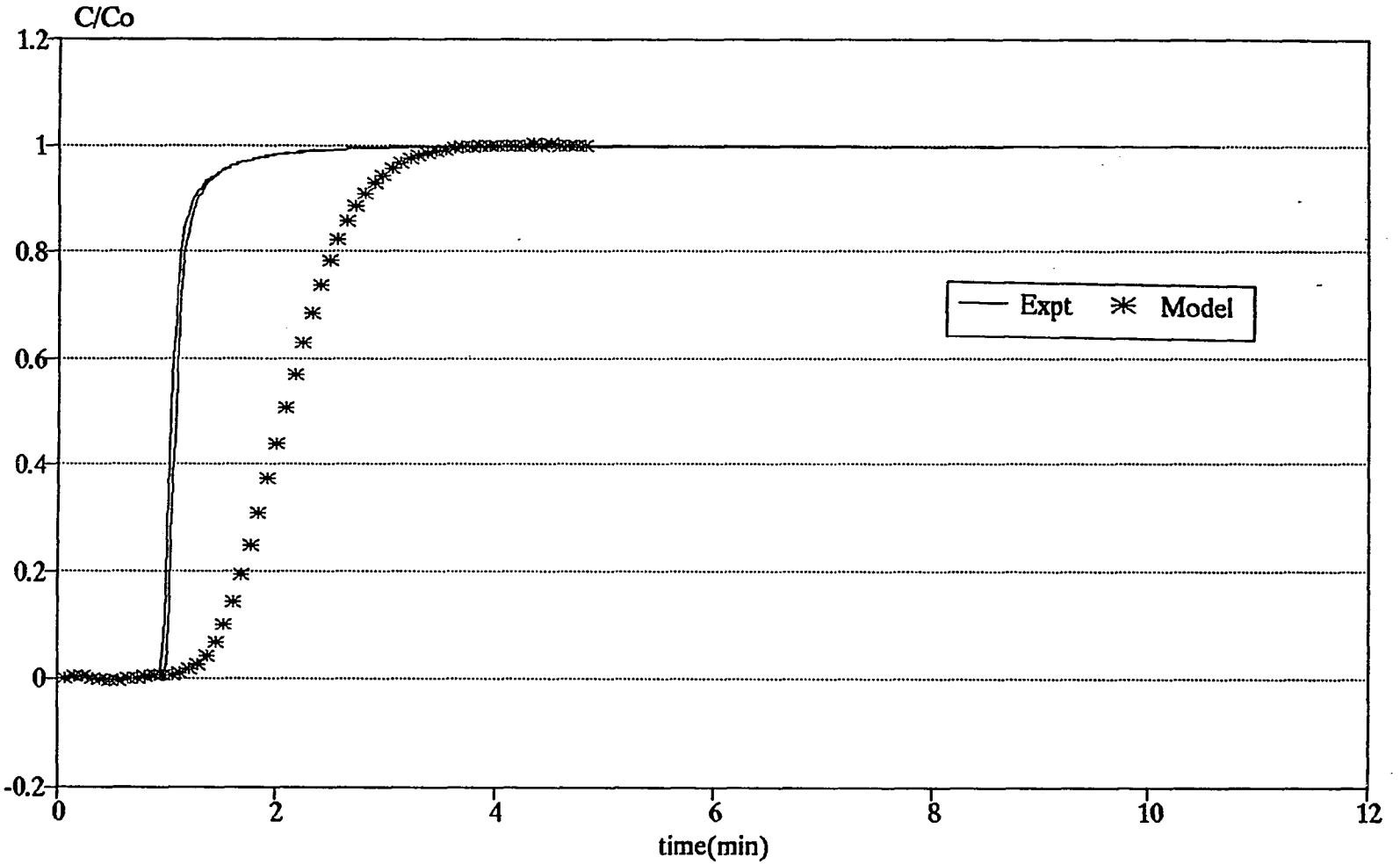

Figure 5-28-c Effluent Concentration Comparison
C6H6, T=240C, v=3.45cm/sec, Rp=0.23mm

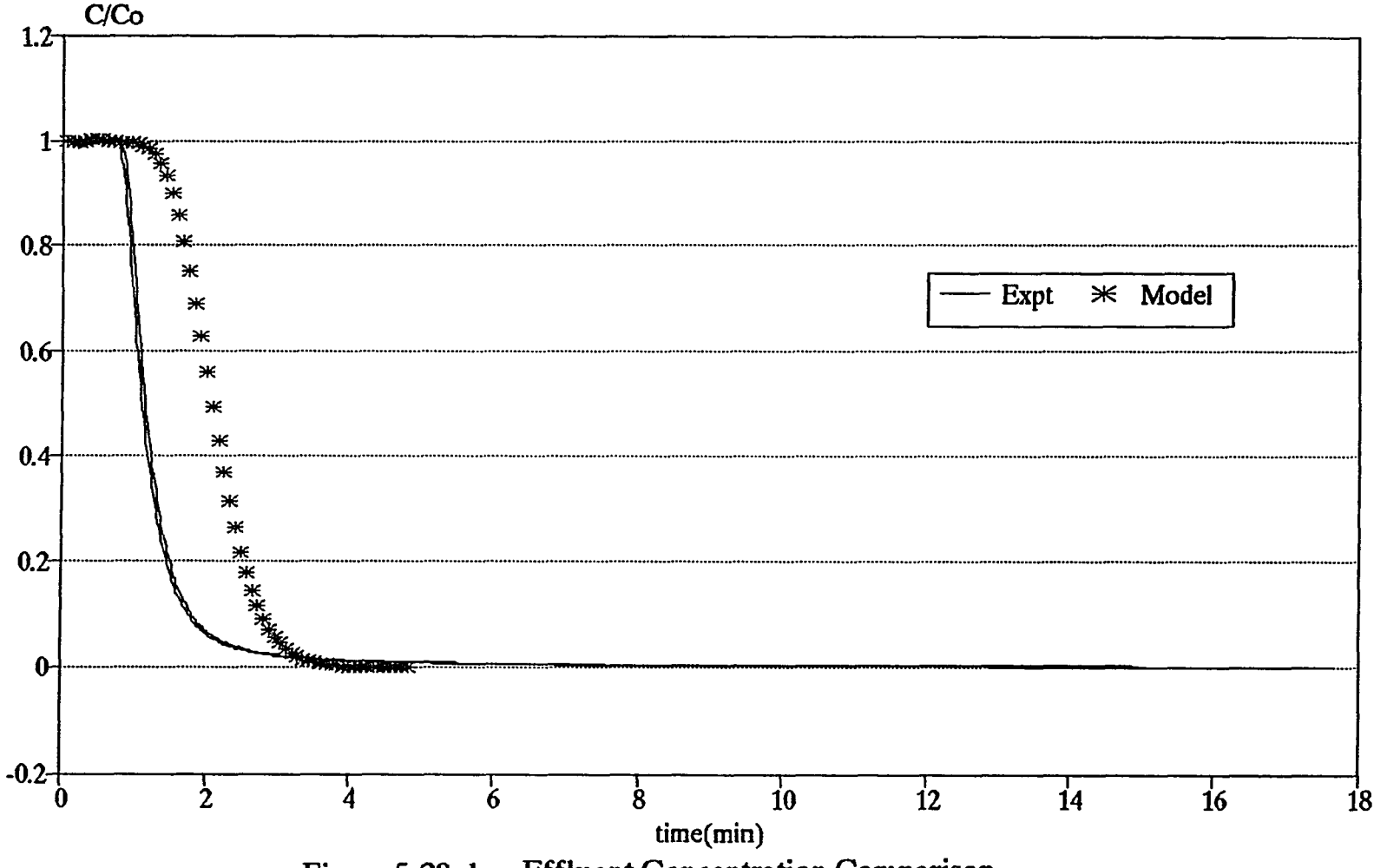

Figure 5-28-d. Effluent Concentration Comparison
C6H6, T=240C, v=3.45cm/sec, Rp=0.23mm

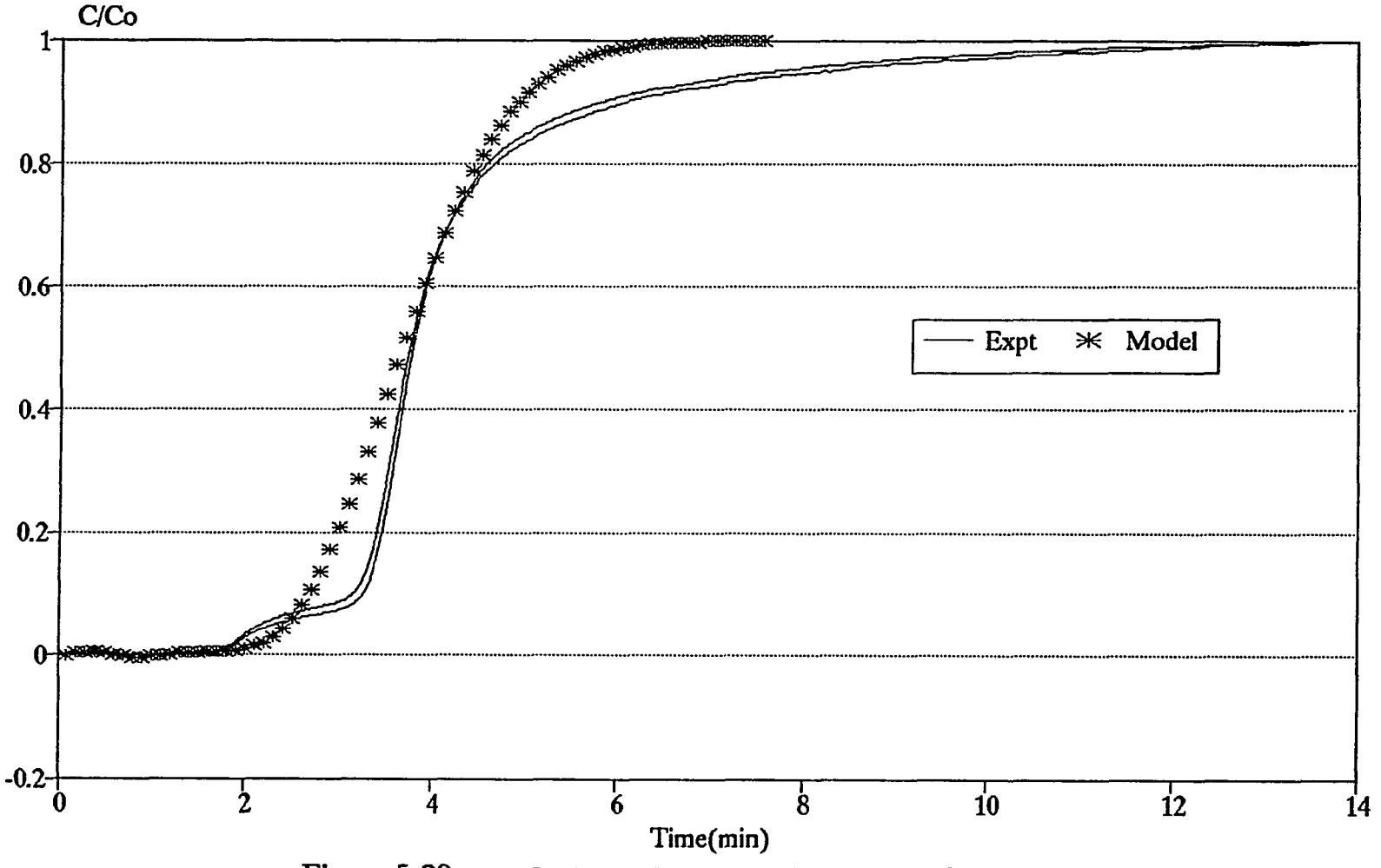

Figure 5-29-a. Effluent Concentration Comparison
C6H5Cl, T=260C, v=2.7cm/sec,Rp=0.23mm

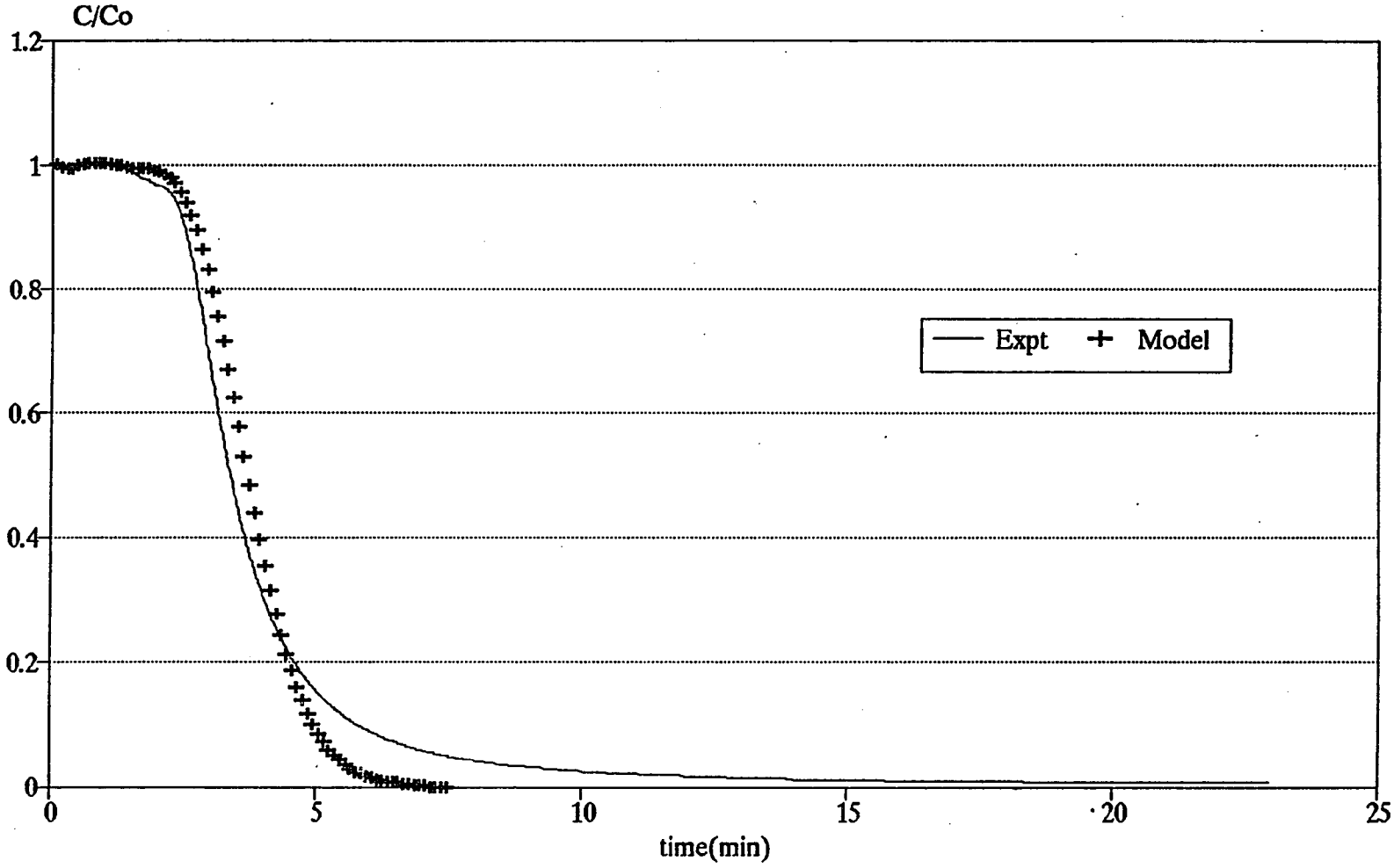

Figure 5-29-b. Effluent Concentration Comparison
C6H5Cl, T=260C, v=2.7cm/sec, Rp=0.23mm

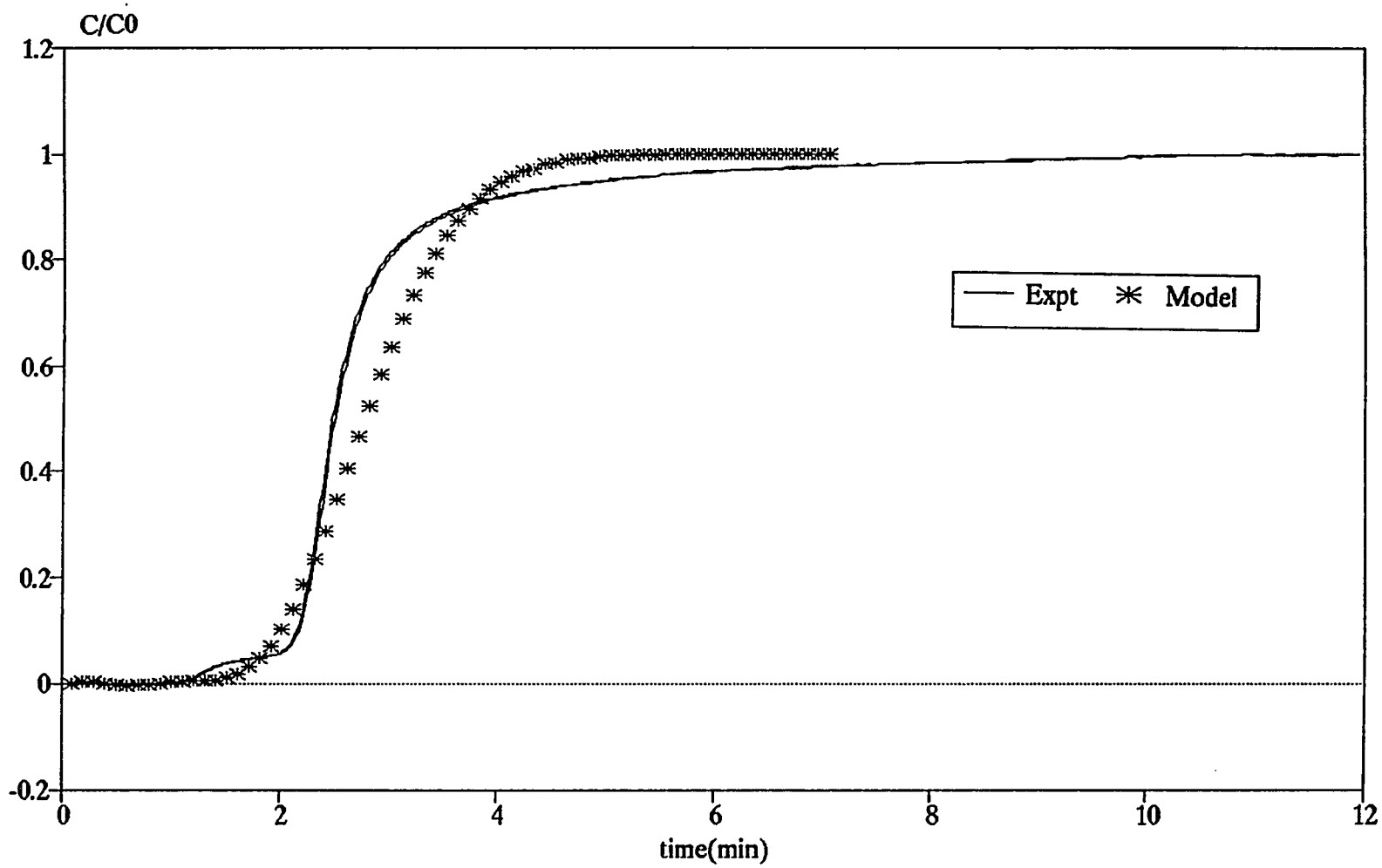

Figure 5-29-c. Effluent Concentration Comparison
C6H5Cl, T=260C, v=3.58cm/sec, Rp=0.23mm

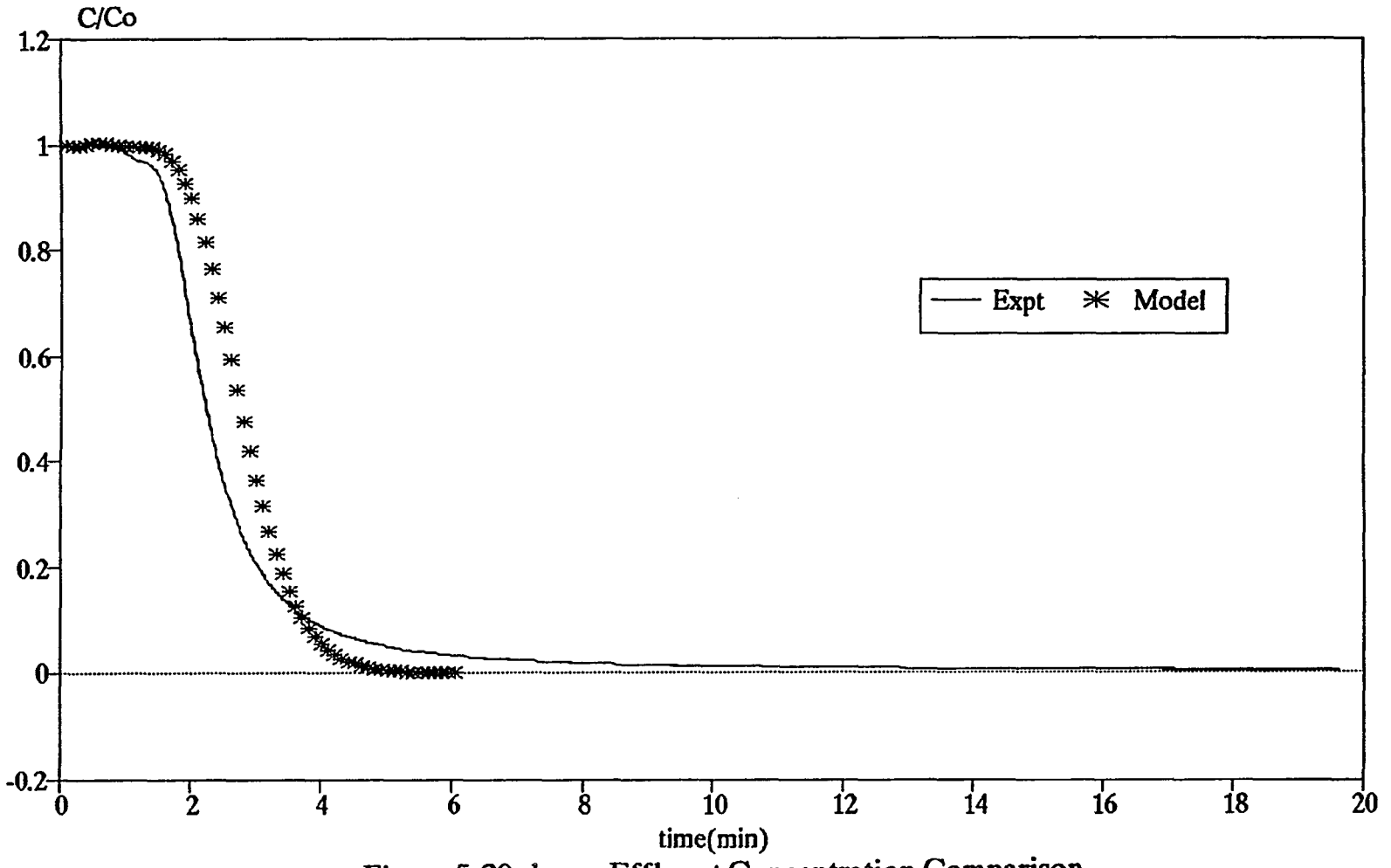

Figure 5-29-d. Effluent Concentration Comparison
C6H5Cl, T=260C, v=3.58cm/sec, Rp=0.23mm

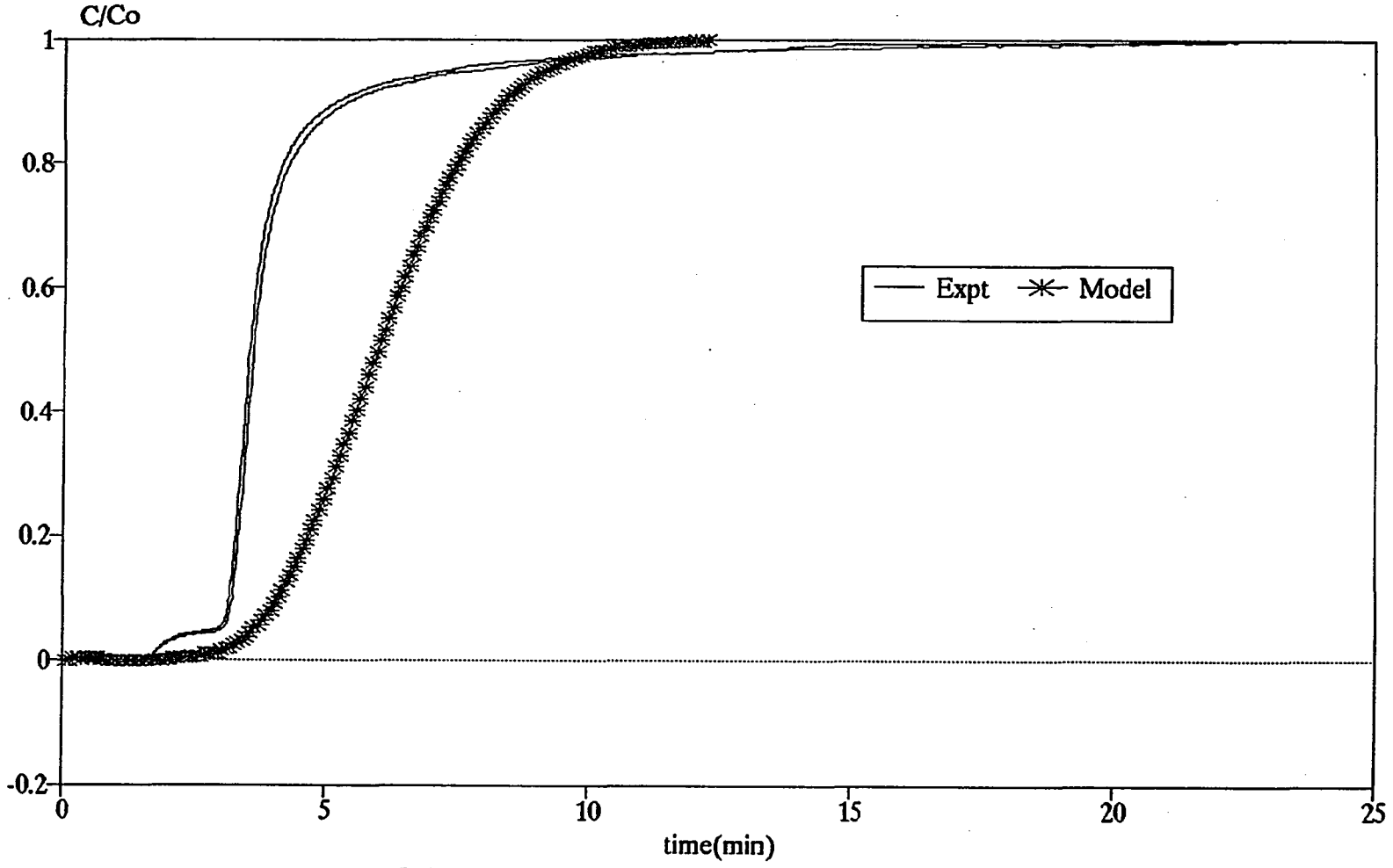

Figure 5-29-e. **Effluent Concentration Comparison**
C6H5Cl, T=240 C, v=3.45cm/sec,Rp=0.23mm

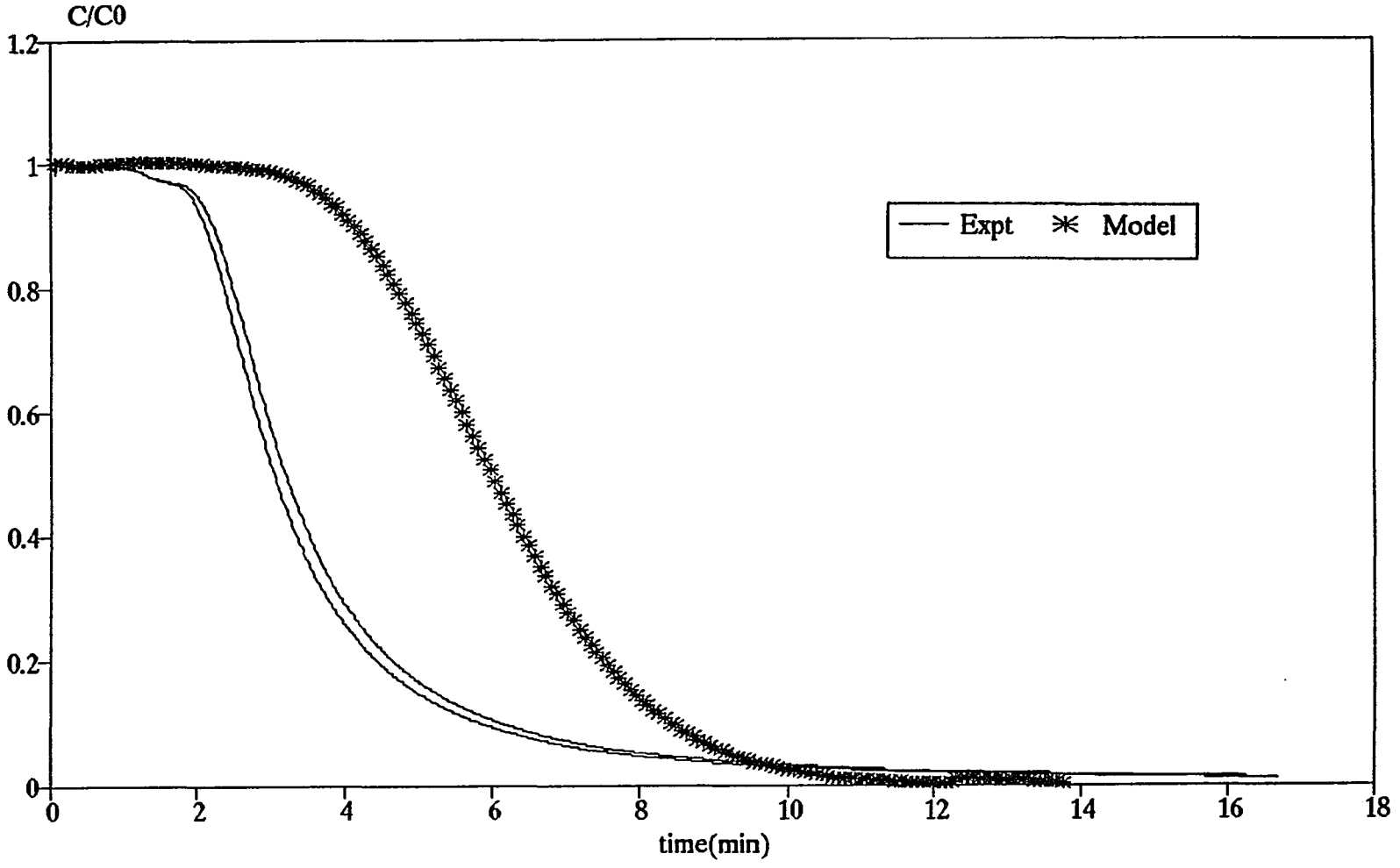

Figure 5-29-f. Effluent Concentration Comparison
C6H5Cl, T=240C, v=3.45cm/sec, Rp=0.23mm

6. CONCLUSIONS

The adsorption isotherms from the equilibrium adsorption test show good linearity at the lower concentrations and the slopes (equilibrium constants) tend to decrease with increasing temperature for C_6H_6 and C_6H_5Cl. Desorption experiments show hysteresis phenomena for C_6H_6 and C_6H_5Cl at 160 ^oC, a relative low temperature.

Chromatographic response analysis has been utilized to study the mass transfer mechanism of C_6H_6 and C_6H_5Cl in soil matrices. A sample-size test experiments were performed to examine the linearity of chromatographic system versus the quantity of organic compound inlet to the system. Sample volumes determined for plug deposition experiments are 25 μL for C_6H_5Cl and 5 μL for C_6H_6, which are well within the linear region of our experimental setup. This further verifies that linear chromatographic theory can be applied.

Equilibrium constants, heats of adsorption and mass transfer parameters in a soil matrix column system were determined at varied temperatures (180 to 260 ^oC for C_6H_6 and 220 to 280 ^oC for C_6H_5Cl). Equilibrium constants were strongly dependent on temperature and show linearity of Van't Hoff's equation plots. The observed values of heat of adsorption (ΔH_{ads}) for C_6H_6 is –15.89 kcal/mole and –18.86 kcal/mole for C_6H_5Cl. There is almost no particle size effect on equilibrium constants as expected. The analysis of second central moment shows that the mass transfer resistance is less sensitive within the temperature ranges of this study for larger molecules, like C_6H_6 and C_6H_5Cl, for this soil matrix. It is also hard to classify the particle size effect on the mass transfer resistance.

Analysis of mass transfer parameters, as discussed by Dong (11), show that axial dispersion coefficients, intraparticle diffusion coefficients and equilibrium constants have the most significant effects on the concentration profiles in the system. Estimated mass transfer coefficients were applied using both the analytical solution and the numerical approach with the orthogonal collocation method. The

results from analytical solution showed satisfactory coincidence with the numerical method. The numerical approach includes axial dispersion coefficients, intraparticle diffusion coefficient, film mass transfer coefficients and adsorption equilibrium constant match the experimental results at higher temperatures. The comparisons between numerical approach and experimental results at lower temperatures show that the numerical simulations predict a delay on the adsorption or desorption curves relative to experimental data.

Further studies on different soil matrices and organic compounds will be considered valuable to verify and improve the prediction of mass transfer behavior in the soil adsorption/desorption column.

7. BIBLIOGRAPHY

1. Evans, R. B. and G. E. Schweitzer, Environ. Sci. Technol., 18 (1984): 330A-339A.

2. Lighty, J. S., D. W. Pershing , V. A. Cundy and D. G. Linz, Nucl. Chem. Waste Manage, 8 (1988): 225.

3. Lighty, J. S., R. M. Britt, D. W. Pershing, W. D. Owens and V. A. Cundy, JAPCA, 39, 187 (1989).

4. Estes, T. S., R. V. Shah and V. L. Vilker, Environ. Sci. Technol., 22, 4 (1988): 377-381.

5. Webster, D. M., J. of Air & Waste Management Assoc., 36, 10 (1986): 1156-1163.

6. Mackay, D. M., P. V. Roberts and J. A. Cherry, Environ. Sci. Technol., 19 (1985): 384-392.

7. Koltuniak, D. L., Chem. Eng., Aug. 18 (1986): 30-31.

8. U. S. EPA/540/2-91/001, Innovative Treatment Technologies: Semi-Annual Status Report, Jan. 1991.

9. Tognotti, L., M. Flytzani-Stephanopoulos, A. F. Sarofim, H. Kopsinis and M. Stoukides, Environ. Sci. Technol., 25 (1991): 104- 109.

10. Wu, Y. -P, J. I. Dong and J. W. Bozzelli, Combust.. Sci. and Technol., in press.

11. Dong, J. -I., Doctoral Thesis, New Jersey Institute of Technology, October (1990).

12. Marrin, D. L. and H. B. Kerfoot, Environ. Sci. Technol., 22, 7 (1988): 740-745.

13. Thielen, D. R., P. S. Foreman, A. Davis and R. Wyeth, Environ. Sci. Technol., 21, 2 (1987): 145-148.

14. Porter, J. W., Chem. Eng. Progr., Apr. (1989) 16-25.

15. Jury, W. A., W. J. Farmer and W. F. Spencer, J. Environ. Qual., Vol 12, 4 (1983): 558-564, Vol. 13, 4 (1984): 567-572, 573-579, 580.

16. Valverde-Garcia, A., E. Ganzalez-Pradas, M. Villafranca-Sanchez, F. del Rey-Bueno and A. Garcai-Rodriguez, Soil Sci. Soc. Am. J., Vol. 52 (1988): 1571-1574.

17. Dragun, G., Haz. Mat'l Control. Sep./Oct. (1988): 24-43.

18. Walter, R.W. and A. Guiseppi-Elie, Environ. Sci. Technol., 22, 7 (1988): 819-825.

19. Chiou, C. T., D. E. Kile and R. M. Malcolm, Environ. Sci. Technol., 22, 3 (1988): 298-303.

20. Roger, R. D., J. C. McFarlane and A. J. Cross, Environ. Sci. Technol., 14, 4 (1980): 457-460.

21. Garbarini, D. R. and L. W. Lion, Environ. Sci. Technol., 20, 12 (1986): 1263-1269.

22. Nkedi-Kizza, P., P. S. C. Rao and A. G. Hornsby, Environ. Sci. Technol., 19, 11 (1985): 1122-1128.

23. Sabljic, A., Environ. Sci. Technol., 21, 4 (1987): 358-366.

24. Collin, M. and A. Rasmuson, Soil. Sci. Soc. Am. J., 52 (1988): 1559-1565.

25. Rhue, R. D. and P. S. C. Rao, Chemosphere, Vol. 21, Nos. 4-5 (1990): 537-556.

26. Wood. A. L., D. C. Bouchard, M. L. Brusseau and P. S. C. Rao, Chemosphere, Vol. 21, Nos. 4-5 (1990): 575-587.

27. Smith, J. A., C. T. Chiou, J. A. Kammer and D. E. Kile, Environ. Sci. Technol., 24 (1990): 676-683.

28. Kubin, M., Collection Czechoslov. Chem. Commun., 30 (1965): 1105-1118; 2901-2907.

29. Kucera, E., J. of Chromatography, 19 (1965): 237-248.

30. Kocirik, M., J. of Chromatography, 30 (1967): 495-468.

31. Schneider, P. and J. M. Smith, Am Inst. Chem. Engrs. J., 14, 5 (1968): 762-771.

32. Suzuki, M. and J. M. Smith, Chem. Eng. Sci., 26 (1071): 221-235.

33. Suzuki, M. and J. M. Smith, Chem. Eng. J., 3 (1972): 256-264.

34. Chihara, K., J. M. Smith and K. Kawazoe, Am. Inst. Chem. Engrs. J., 24, 2 (1978): 237-246.

35. Andrieu, J. and J. M. Smith, Am. Inst. Chem. Engrs. J., 26, 6 (1980): 944-948.

36. Wang, C. T. and J. M. Smith, Am. Inst. Chem. Engrs. J., 29, 1 (1983): 132-136.

37. Park, I. S., J. M. Smith and B. J. McCoy, Am. Inst. Chem. Engrs. J.,33, 7 (1987): 1102-1109.

38. Haynes, Jr., H. W. and Sarma, P. N., Am. Inst. Chem. Engrs. J., 19, 5 (1973): 1043-1046.

39. Haynes, Jr., H. W., Chem. Eng. Sci., 30 (1975): 955-961.

40. Hsu, L.-K. P. and H. W. Haynes Jr., Am. Inst. Chem. Engrs. J., 27, 1 (1981): 81-91.

41. Fu, C. C., M. S. P. Ramesh and H. W. Haynes Jr., Am. Inst. Chem. Engrs. J., 32, 11 (1986): 1848-1857.

42. Haynes, Jr., H. W., Am. Inst. Chem. Engrs. J., 32, 10 (1986): 1750-1753.

43. Ruthven, D. M. and R. Kumar, Can. J. Chem. Eng., 57 (1979): 342-348.

44. Kumar, R., R. C. Duncan and D. M. Ruthven, Can. J. Chem. Eng., 60 (1982): 493-499.

45. Ruthven, D. M. "Principles of Adsorption and Adsorption Processes", J-W & Sons (1984).

46. Rosen, J. B., J. of Chem. Phys., 20, 3 (1952): 387-394.

47. Rosen, J. B., Indust. & Eng. Chemistry, 46, 8 (1954): 1590-1594.

48. Rsamuson, A. and Neretnieks, Am. Inst. Chem. Engrs. J., 26, 4 (1980): 686-690.

49. Rasmuson, A. Am. Inst. Chem. Engrs. J., 27, 6 (1981): 1032-1035.

50. IMSL User's Manual, Math/Library (1987).

51. Hornsby, M. L., Master Thesis, New Jersey Inst. of Tech. (1987).

52. Reid, R. C., J. M. Prausnitz and B. E. Poling, "The Properties of Gases and Liquids", 4th Ed., McGraw-Hill Book Company (1988).

53. Eberly, Jr.,P. E., J. Phys. Chem., Vol. 65 (1961): 68.

54. Hori, Y. and R. Kobyashi, J. of Chem. Phys., Vol. 54, 3 (1971): 1226.

55. Kiselev, A. V. and Y. I. Yashin, "Gas-Adsorption Chromatography", Translated from Russian by Bradley, J.E.S., Plenum Press, New York-London (1969).

56. Sorial, G. A., W. H. Granville and W. O. Daly, Chem. Engr. Sci., Vol. 38, No. 9 (1983): 1517-1523.

57. Lewis, W. K., E. R. Gilliland, B. Chertow and W. P. Cadogan, Indus. Engr. Chem., Vol. 42, No. 7 (1950).

58. Hirschfelder, J. O., C. F. Curtiss and R. B. Bird, "Molecular Theory of Gases and Liquids", Wiley, New York (1954).

APPENDIX I

APPENDIX I-1.

Program List of Chromatographic Response Analysis

```
{c+}
(*program for chromatographic response analysis of     *)
(*soil column utilized the Normal Distribution         *)
(*Equations and Least Square fit to calculate           *)
(*the average retention time and variance for the       *)
(* chromatographic peaks                                *)
(* INPUT: file which contain the filenames of signal   *)
(*        data                                          *)
(* OUTPUT: 1. document file which contain the signal   *)
(*          file name,baseline value, average           *)
(*          retention time, variance, total area and    *)
(*         the time peak ended                          *)
(*         2. prn file which contain only filenames,    *)
(*            average retention time and variance       *)
(*                                                      *)
(*program written by Yo-ping G. Wu                      *)
(*Dept. of Chem. Eng., Chemistry, Environ.              *)
(*Science, New Jersey Inst. of Tech., Newark, NJ        *)

Program Area_Integrator(input,output);

  uses printer,
       crt,
       DOS;

  type ptrec = ^rectype;
       rectype = RECORD
            nx : INTEGER;
            ay,sl,ar :REAL;
            next : ptrec;
            END;
       ary = ARRAY[1..20] of REAL;
       arry1 = ARRAY [1..4,1..5] of REAL;
       arry = ARRAY[1..6] of REAL;
       strg15 = string[15];

var i, ii, inpend, j, jj, k, n, nend, nend1:INTEGER;
    count, count1, counter, peakstart: INTEGER;
    position, xtime: INTEGER;
    avgarea, avgt, avgy, delarea, delslope, deltx: REAL;
    delty, maxy, meantx, mini, py1, py2  :REAL;
    sigma, slope, sum, sumarea, sumsq, sumy :REAL;
    tarea, tareaall, tend, yarea, ybase : REAL;
    filein,filein1, fileout,fileout1:TEXT;
    namein,namein1,nameout,nameout1,nameout2 : strg15;
    head1, head2, tail1, tail2, tail3:ptrec;
    tempx, tempy, ps, px, py:ptrec;
    flag1, flag2, flag3, flag4, peak:BOOLEAN;
```

```
    key :char;

   (* PROCEDURE FOR Key check *)
   PROCEDURE chkkey;
   BEGIN                          (*check enter <ESC> or not*)
     IF (Key = #27) AND KeyPressed
      THEN key :=readkey
    ELSE Key := UpCase(Key);
   END;                                  (* END of CHKKEY *)

   (*PROCEDURE to calculate the area for each slice*)
   PROCEDURE intg;
     BEGIN
       py1:= tempy^.ay + ybase;
       py2:= tempy^.next^.ay + ybase;
       delty := py2 - py1;
       avgy:= (py1 + py2)/2 ;
       IF avgy <0 THEN
         BEGIN
           avgy:=0;
         END;     (* END of avgy < 0 *)
       deltx := tempx^.next^.nx - tempx^.nx;
       meantx := (tempx^.nx + tempx^.next^.nx)/2;
       delarea := deltx * avgy;
    END;                            (* END of PROCEDURE intg
*)

(* PROCEDURE to find the position of max peak height *)
   PROCEDURE find_max;
     BEGIN
       IF maxy <= tempy^.ay THEN
         BEGIN
           maxy := tempy^.ay;
           position := i;
         END;      (* END of maxy loop *)
       tempy := tempy^.next;
       tempx := tempx^.next;
     END;  (* END of PROCEDURE find_max *)

(* PROCEDURE for slope calculation of each bunch of data
*)
   PROCEDURE slope_cal;
     var  bunch:ary;
          newx,newy :ptrec;
     BEGIN
       newx:= tempx;
       newy := tempy;
       IF (newx <> nil ) THEN
         IF count1 < (nend-13) THEN
         BEGIN
           FOR j:= 1 to 12 DO
             BEGIN
               bunch[j]:=newy^.ay;
```

```
            newy := newy^.next;
            newx := newx^.next;
          END;    (* EoF j loop *)
        END  (* EoF IF count1 loop *)
        ELSE
          BEGIN
            FOR j := 1 to (nend-count1) DO
              BEGIN
                bunch[j] := newy^.ay;
                newy := newy^.next;
                newx := newx^.next;
              END;          (* END of j loop *)
            FOR j := (nend-count1+1) to 12 DO
              BEGIN
                bunch[j]:=0;
                newy := newy^.next;
                newx := newx^.next;
              END;     (* EoF j loop *)
          END;         (* EoF ELSE *)
        count1 := count1 +1;
        slope:= 11*(bunch[12]-bunch[1])+9*(bunch[11]-
                bunch[2])+7*(bunch[10]-bunch[3]) +
                5*(bunch[9]-bunch[4])+
                3*(bunch[8]-bunch[5])+bunch[7]-bunch[6];
        new(ps);
        ps^.sl := slope;
        ps^.next := nil;
        tail3^.next := ps;
        tail3 := ps;
        IF not peak THEN
          BEGIN
            IF (slope > 5) THEN
              BEGIN
                peak := TRUE;
                peakstart:= n-10;
                IF peakstart < 1 THEN peakstart := 1;
               END;    (* EoF IF slope *)
             n:= n+1;
          END;        (* END of IF peak *)
      tempx := tempx^.next;
      tempy := tempy^.next;
    END; (* EoF PROCEDURE slope_cal *)

(* PROCEDURE perform gauss elimination *)
PROCEDURE gauss(a1:arry1;var x:arry;n,np1:INTEGER);
  var
    ip1,ii,jj,l,nm1,kp1:INTEGER;
    temp,factor,sum:REAL;
  BEGIN
    nm1:= n-1;
    FOR k := 1 to nm1 DO
      BEGIN
        kp1 := k+1;
```

```
        l := k;
        FOR i := kp1 to n DO
          BEGIN
            IF abs(a1[i,k]) > abs(a1[l,k]) THEN l:= i;
          END;
        IF l <> k THEN
          BEGIN
            FOR j := k to np1 DO
              BEGIN
                temp := a1[k,j];
                a1[k,j]:= a1[l,j];
                a1[l,j]:= temp;
              END;
          END;
        FOR i := kp1 to n DO
          BEGIN
            factor := a1[i,k]/a1[k,k];
            FOR j := kp1 to np1 DO
              BEGIN
                a1[i,j] := a1[i,j]-factor*a1[k,j];
              END;
          END;
      END;
    x[n]:= a1[n,np1]/a1[n,n];
    ii:= nm1;
    REPEAT
        ip1:= ii + 1;
        sum := 0;
        FOR jj := ip1 to n DO
          BEGIN
            sum := sum + a1[ii,jj]* x[jj];
          END;
        x[ii] := (a1[ii,np1]-sum)/a1[ii,ii];
        ii:= ii-1;
      UNTIL ii <1;
 END;     (* END of GAUSS *)

(* PROCEDURE to find the end of the peak *)
PROCEDURE find_END;
   var
        a,sum,right:arry;
        matrix:arry1;
        ca0,ca1,ca2,fx1,fx2,fitx,fity,limit,xend:REAL;
        newx:ptrec;
        kk:INTEGER;
  BEGIN
    count:= 0;
    FOR i := 1 to 4 DO
        BEGIN
          sum [i] := 0.;
        END;
    FOR i := 1 to 3 DO
      BEGIN
```

```
        right[i] := 0.;
      END;
    FOR j := 1 to nend DO
    BEGIN
      IF j > position+10 THEN
        BEGIN
          count:= count+1;
          fitx:= tempx^.nx;
          fity:=tempy^.ay;
          FOR i:= 1 to 4 DO
            BEGIN
              sum[i] := sum[i] + exp(i*ln(fitx));
            END;
          FOR i := 1 to 3 DO
            BEGIN
              right[i]:=right[i]+fity*
                          (exp((i-1)*ln(fitx)));
            END;
        END;
      tempy := tempy^.next;
      tempx := tempx^.next;
    END;
matrix[1,1] := count;
FOR i := 1 to 3 DO
  BEGIN
    matrix[i,4]:= right [i];
    FOR j:= 1 to 3 DO
      BEGIN
        k := i + j;
        IF k <> 2 THEN matrix[i,j]:= sum[k-2];
      END;
  END;
  gauss(matrix,a,3,4);
  ca0:= a[1];
  ca1:=a[2];
  ca2:=a[3];
  WRITELN('y=',ca0:10:4,'+',ca1:10:5,'x + ',ca2:20:9,
          ' x^2');
  xend:= 1e-5 - (ca1/(2*ca2));
  tempx:=head1; tempx:=tempx^.next;
  flag4:=FALSE; flag2:=FALSE; flag3:=FALSE;
  counter:=1;
  IF ((ca2<0) and (ca1>0)) or ((ca1<0) and (ca2<0))
    THEN flag3:=TRUE;
  WHILE (not flag4) and (counter < nend) DO
     BEGIN
       IF counter > position+10 THEN flag2:=TRUE;
       IF flag2 and flag3 THEN
         BEGIN
           fx1 := tempx^.nx;
           limit := ca2*(fitx+fx1)+ ca1;
           IF (abs(limit) <= 1e-4) THEN
           BEGIN
```

```
                flag4 := TRUE;
                nend := counter;
              END;
            END
          ELSE IF flag2 THEN
            BEGIN
              IF tempx^.nx > xend THEN
                BEGIN
                  flag4 := TRUE;
                  nend := counter;
                  limit := ca2*(fitx+tempx^.nx)+ca1;
                END;
            END;
          tempx:=tempx^.next;counter:= counter+1;
        END;  mini:=limit;
    END; (* END of PROCEDURE find_end *)

(* Proceudre to obtain corresponding baseline *)
PROCEDURE ybase_cal;
  BEGIN
  tempy:=head2; tempy:=tempy^.next;
  IF peakstart > 5 THEN
    BEGIN
      FOR i := 1 to peakstart-5 DO
        BEGIN
          sumy := sumy + tempy^.ay;
          tempy := tempy^.next;
        END;
      ybase := -sumy/(peakstart-5);
    END
  ELSE
    IF peakstart > 0 THEN
    BEGIN
      FOR i := 1 to peakstart DO
        BEGIN
          sumy := sumy + tempy^.ay;
          tempy := tempy^.next;
        END;
      ybase := -sumy/peakstart;
    END
   ELSE ybase := 0;
 END; {EoF PROCEDURE ybase_cal}

(* PROCEDURE FOR loading the chromatographic signal for *)
(* calculation                                           *)
  PROCEDURE peaktran;
  BEGIN
  new(head1);new(head2);
  head1^.nx:=0; head2^.ay:=0.0;
  head1^.next:=nil; head2^.next:=nil;
  tail1:= head1; tail2:=head2;
  px := tail1;
  py:= tail2;
```

```
ps := tail3;
ybase :=0.0;  sumy:=0.;  tareaall:=0;
READLN(filein1,namein);
namein1 := namein+'.dat' ;
ASSIGN(filein, namein1);
RESET(filein);  (* input of file FOR calculation *)
i:= 1 ;
WHILE not EoF(filein) DO
  BEGIN
    new(px);
    new(py);
    READLN(filein, xtime, yarea);
    px^.nx := xtime;
    px^.next := nil;
    py^.ay := yarea;
    py^.next := nil;
    tail1^.next := px;
    tail1 := px;
    tail2^.next :=py;
    tail2 := py;
  i:= i+1;
  END;  (* END of reading the input data *)
nend := i-1 ;
sumsq := 0;
tempx:=head1; tempx:=tempx^.next;
tempy:=head2; tempy:=tempy^.next;
position := 0; maxy:= 0;
FOR i := 1 to nend-2 DO
BEGIN
  find_max;  (* call PROCEDURE FIND_MAX *)
END;
tempx:=head1; tempx:=tempx^.next;
tempy:=head2; tempy:=tempy^.next;
n:= 1;
delslope:=0;
peak := FALSE;
peakstart:=0;  count1:=0;
FOR i := 1 to nend-1 DO
BEGIN
  slope_cal;     (* call PROCEDURE SLOPE_CAL *)
END;
ybase_cal;       (* call proceudre YBASE_CAL *)
tarea := 0;
tempx:=head1; tempx:=tempx^.next;
tempy:=head2; tempy:=tempy^.next;
WHILE  tempx^.next <> nil DO
  BEGIN
    intg;     (* call PROCEDURE to get deltx and avgy *)
    tarea := tarea + delarea;
    tempy := tempy^.next;
    tempx := tempx^.next;
  END;
tareaall := tarea;
```

```
tempx:=head1; tempx:=tempx^.next;
tempy:=head2; tempy:=tempy^.next;
find_end;       (* call PROCEDURE to find end of peak *)
j:= 1; tarea := 0; sum := 0;
tempx:=head1; tempx:=tempx^.next;
tempy:=head2; tempy:=tempy^.next;
WHILE  j < nend DO
  BEGIN
    IF j > peakstart THEN
    BEGIN
      intg;   (* call PROCEDURE to get deltx and avgy *)
      tarea := tarea + delarea;
      sum := sum + meantx*delarea;
      tend := tempx^.nx/300;
    END;
    j:= j+1;
    tempy := tempy^.next;
    tempx := tempx^.next;
  END;
nEND:= j - 1;
IF tarea <> 0 THEN
avgt:= sum/tarea/300
ELSE avgt := 0;
k:= 1;
tempx:=head1; tempx:=tempx^.next;
tempy:=head2; tempy:=tempy^.next;
WHILE k < nend DO
  BEGIN
    IF k > peakstart THEN
    BEGIN
      intg;
      sumsq := sumsq + sqr(meantx/300 - avgt)*delarea;
    END;
    k := k+1 ;
    tempy := tempy^.next;
    tempx:= tempx^.next;
  END;
IF tarea <> 0 THEN
sigma := sumsq / tarea
ELSE sigma := 0;
CLOSE(filein); RELEASE(heaporg);
END;  (* END of PROCEDURE peaktran *)

(* PROCEDURE to generate output file *)
PROCEDURE outfiles;
  BEGIN
    WRITELN(fileout1,'****** Filename:       ',namein,
            '   ******');
    WRITELN(fileout1,'average retention time    ',
            ,avgt:10:5,'  min.',      ' variance :  ',
            sigma:10:5,' min^2');
    WRITELN(fileout1,'area integrated:', tarea :10:1,
```

```
                ' Integration ended at :',tend:10:2,'
min.',
                '  XBASE:',-ybase:10:4);
      WRITELN(fileout1,'--- end of  ',namein,'total
area:',
                tareaall:10:2,'  slope < ',mini:10:7,' ---
');
      WRITELN(fileout1,' ');
    END;  (* END of outfiles *)

(* BEGIN of main program *)
BEGIN
  REPEAT
    Key := ' ';
    WRITELN('Write output to a file (F) or
             to Printer (P)');
    Key := readkey;WRITELN;
    chkkey;
  UNTIL (Key IN ['F', 'P']) OR (Key = #27);
  CASE key of
  'F' : BEGIN
          WRITELN('Filename for Input');
          READLN(nameout);
          namein1 := nameout+'.inp';
          ASSIGN(filein1,namein1);
          RESET(filein1);
          READLN(filein1,inpend);
          nameout2 :=nameout+'.prn';
          ASSIGN(fileout, nameout2);
          rewrite(fileout);
          nameout1 :=nameout+'.out';
          ASSIGN(fileout1, nameout1);
          rewrite(fileout1);
          FOR ii := 1 to inpend DO
            BEGIN
              peaktran;
              outfiles;

WRITELN(fileout,namein,avgt:10:5,sigma:10:5);
            END;
        END; (* END of 'F' *)
   'P':BEGIN
          Key := ' ';
        FOR ii := 1 to inpend DO
          BEGIN
            peaktran;
            WRITELN(lst,'****** Filename:       ',namein,
                    '   ******');
            WRITELN(lst);
            WRITELN(lst,'average retention time  ',
                    avgt:10:5,'  min.','variance :    ',
                    sigma:10:5,' min^2');
            WRITELN(lst);
```

```
            WRITELN(lst,'area integrated:', tarea :10:1,
                   ' Integration ended at :',tend:10:2,
                   ' min.','  XBASE:',-ybase:10:5);
            WRITELN(lst);
            WRITELN(lst,'***',namein,'total area:',
                    tareaall:10:2,'***');
            WRITELN(lst);
          END
        END; (* END of 'P' *)
  END; (* END of CASE *)
  CLOSE(fileout); CLOSE(fileout1); CLOSE(filein1);
END.
```

APPENDIX I-2.

Program List for the Integration of Analytical Solution

```
c This program has been written for achieving effluent c
c concentration profile of adsorption process in a     c
c soil packed column using analytical solutions        c
c combined with a numerical integration method which   c
c is available in IMSL software in NJIT VAX/VMS system c
c                                                      c
c INPUT DATA required for this program:                c
c   Temp: operation temperature in C                   c
c   z   : column length in cm                          c
c   xv  : linear gas velocity in cm/sec                c
c   xe  : void fraction of soil column                 c
c   ep  : porosity of particle                         c
c   xb  : particle radius in cm                        c
c   xka : equilibrium constant                         c
c   xkf : film mass transfer coefficient in cm/sec     c
c   dl  : axial dispersion coefficient in cm2/sec      c
c   dp  : intraparticle diffusion coeff. in cm2/sec    c
c                                                      c
c OUTPUT gives as concentration as function of time    c
c        in sec.                                       c
c                                                      c
c Program initially written by Jong-In Dong            c
c Modefied by Yo-ping Wu with minor changes to         c
c generate the output in prn format for graphic        c
c uses.                                                c
c                                                      c

      dimension uval(1000)
      character*20 title
      common  t, yka, xv, z, xdp, ep, xb, xe, dl, xkf
      integer interv, nout, mm, nn
      real  bound, errabs, errest, errrel, f, result,
     &      uval, temp
      external f, qdagi, umach
      read(5,1000)title
      read(5,*)
      read(5,*)temp,z,xv,xka,xkf,dl
      read(5,*)
      read(5,*)dp,xe,ep,xb,tlag
1000  format(A12)
      yka = xka * ep
      xdp = dp / ep
      nn  = 36
      bound  = 0.0
      interv = 1
      errabs = 0.0001
      errrel = 0.001
      do 100 i = 1, nn
         tintvl = 10.0
         t = tintvl * float(i) - tlag
```

```
        if(i.gt.12) then
          tintvl = 40.0
          t = 120. + tintvl * float(i-12) - tlag
        else
        end if
        if(i.gt.24) then
          tintvl = 80.0
          t = 600. + tintvl * float(i-24) - tlag
        else
        end if
        if(t.le.0.) then
          result = 0.
          go to 50
        else
        end if

      call
qdagi(f,bound,interv,errabs,errrel,result,errest)

       result = .5 + 2./3.14159 * result
50     uval(i)=result
100    continue
       write (7,205) title,temp, xv, xka,dl, dp
       write (7,200)
       mm = nn/3
       do 110 i = 1, mm
         if(i.le.4) then
          write (7,210) ( ( 10.0*(float(i-1)*3.+float(j)),
     &                    uval(3*(i-1)+j) ), j = 1, 3 )
          write (100,220) ( ( 10.0*(float(i-
1)*3.+float(j)),
     &                    uval(3*(i-1)+j) ), j = 1, 3 )
           go to 110
         end if
         if(i.gt.8) then
           go to 120
         end if
       write (7,210) (((120.+40.*(float(i-5)*3.+float(j))),
     &                    uval(3*(i-1)+j) ), j = 1, 3 )
       write(100,220) (((120.+40.*(float(i-
5)*3.+float(j))),
     &                    uval(3*(i-1)+j) ), j = 1, 3 )
       go to 110
120    write (7,210) (((600.+80.*(float(i-9)*3.+float(j))),
     &                    uval(3*(i-1)+j) ), j = 1, 3 )
       write(100,220)(((600.+80.*(float(i-9)*3.+float(j))),
     &                    uval(3*(i-1)+j) ), j = 1, 3 )
110    continue
200    format(1x,'time(s)  u value   time(s)  u value',
     &        '   time(s)  u value '/)
205    format(//'  [ Concentration Profile Calculation ]',
     &        //'                Chemical =',A12,
     &         /'       Temperature =  ', f4.0, ' deg. C',
```

```
     &        /'  Linear Velocity = ', f5.2, ' cm/sec',
     &        /'                 Ka = ', f6.2,
     &        /'                 Dl = ', f6.2, 'cm^2/sec',
     &        /'                 Dp = ',E9.2,' cm2/sec'///)
210   format( 3 (f7.1, 3x, f7.5, 2x) )
220   format(1x, f7.1, 3x, f7.5 )
      end

      real function f (x)
      common t, xka, xv, z, dp, ep, xb, xe, dl, xkf
      double precision x,hd1,hd2,h1,h2,z2x,z2y,pex,psin
      xm  = xe / (1.-xe)
      xk  = xka + ep
      r1  = xk / xm
      xgama=3. * dp * ep / xb**2
      rf  = xb / (3.*xkf)
      xnu = xgama * rf
      delcof = xgama / ( xm * xv )
      peccof = xv / dl
      ycof   = 2. * dp * ep / ( xk * xb**2 )
      del = delcof * z
      pe  = peccof * z
      if(x.le.50.) then
         vsin = sin(2.*x) / cosh(2.*x)
         vcos = cos(2.*x) / cosh(2.*x)
      else
         vsin=0.
         vcos=0.
      end if
      hd1 = x * ( tanh(2.*x) + vsin ) / ( 1. - vcos ) - 1.
      hd2 = x * ( tanh(2.*x) - vsin ) / ( 1. - vcos )
      h1  = ( hd1 + xnu * (hd1**2+hd2**2) )/
     &        ( (1.+xnu*hd1)**2 + (xnu*hd2)**2 )
      h2  = hd2 / ( (1.+xnu*hd1)**2 + (xnu*hd2)**2 )
      z2x = pe * ( .25 * pe + del * h1 )
      z2y = del * pe * ( 2. * x**2 / ( 3. * r1 ) + h2 )
      y   = ycof * t
      pex = pe / 2. - sqrt ( ( sqrt(z2x**2 + z2y**2)
     &              + z2x ) / 2. )
      psin= y * x**2 - sqrt ( (sqrt(z2x**2 + z2y**2)
     &               - z2x ) / 2. )
      if (x.gt.0.0) then
          f = exp(pex) * sin(psin) / x
      else
          f = 0.0
      end if
      return
      end
```

APPENDIX I-3.
Program List of the Numerical Solution Using Orthogonal Collocation Method

```
C                                                                       C
C This program has been written to estimate concentrationC
C distribution profiles in the adsorption and desorption C
C process in soil columns.  Orthogonal collocation methodC
C was utilized to simulate the mass transfer and IMSL    C
C software was used to solve simultaneous differential   C
C equations.                                             C
C                                                        C
C Basic input data are mass transfer parameter values andC
C two matrices in the radial direction of particles and  C
C particles and axial direction of the column.           C
C                                                        C
C                                                        C
C  Initially written by Jong-in Dong                     C
C  Modefied by Yo-ping Wu with some minor changes which  C
C  can generate the data output to the format for graphicC
C  uses                                                  C
C                                                        C

      PARAMETER ( NEQ = 42, NPARAM=50)

      COMMON AA(30,30), BB(30,30), AAP(30,30), BBP(30,30),
     &    M, N, GAMA, PE, PSI, P0, P1, P2, P3, P4, P5, P6,
     &    P7, P8, PI

      EXTERNAL FCN, DIVPAG, SSET, UMACH

      INTEGER IDO,IEND,IMETH,INORM,NOUT,M,N,TEND

      DOUBLE PRECISION A(1,1),FCN, FCNJ,
     & HINIT, PARAM(NPARAM), X,
     & XEND, Y(NEQ), YPRIME(NEQ),MXSTEP,XV,XR, XL, DP, XK,
     & XE, XKF, DL, EP, CO, P0, P1, P2, P3,P4, P5, P6, P7,
     & P8, PI, ETA,XI,PE,GAMA,ALPA,PSI,AA,BB,AAP, BBP, TOL

C                        INITIALIZE
      INTRINSIC  DFLOAT

      OPEN (5,FILE='MTRX6_6.DAT',STATUS='OLD')
      READ(11,*)
      read(11,*)XV,XR,XL,DP,XK,XE,XKF,DL,EP,CO,TEND

      HINIT=1.0D-7
      MXSTEP=100000.
      INORM=2
      IMETH=1

      CALL SSET(NPARAM,0.0,PARAM,1)
```

```
      PARAM(1)=HINIT
      PARAM(4)=MXSTEP
      PARAM(10)=INORM
      PARAM(12)=IMETH
      N = 7
      M = 8

      DO 110 J = 1, M
         DO 110 I = 1, M
            READ(5,*) AAP(J,I)
110   CONTINUE

      DO 120 J=1, M
         DO 120 I=1, M
            READ(5,*) BBP(J,I)
120   CONTINUE

      DO 130 J=1, N
         DO 130 I=1, N
            READ(5,*) AA(J,I)
130   CONTINUE

      DO 140 J=1, N
         DO 140 I=1, N
            READ(5,*) BB(J,I)
140   CONTINUE

C              PARAMETER CALCULATION

      PI   = XV * XR**2 /XL /DP
      ETA  = XK *(1.-XE) /XE
      XI   = XL * XKF / (XV*XR*XK)
      PE   = XV * XL / DL
      GAMA = 1. / (EP * (1.+XK))
      ALPA = AAP(M,M)*(AAP(1,1)-PE)-AAP(1,M)*AAP(M,1)
      PSI  = 1. / ( XK*PI*XI + AA(N,N) )
      P0   = GAMA * XK * PSI * PI * XI
      P1   = AAP(1,M) / ALPA
      P2   = AAP(M,M) / ALPA
      P3   = AAP(M,1) / ALPA
      P4   = (AAP(1,1)-PE) / ALPA
      P5   = AAP(M,M) / ALPA
      P6   = 3. *ETA *PI *XI / ( XK*PI*XI + AA(N,N) )
      P7   = AA(N,N) * P6
      P8   = PE * CO * PI
C

      IDO=1
      X=0.0D00
      TOL=1.0D-3

      IF( CO .EQ. 0.0D00 ) THEN
```

```
        DO 205 J=1,M-2
          DO 210 K=1,N-1
            Y((J-1)*N+K)=1.0D00
210       CONTINUE
205     CONTINUE

        DO 215 J=1,M-2
         Y(J*N)=1.0D00
215     CONTINUE

      ENDIF

      IF( CO .EQ. 1.0D00 ) THEN

        DO 405 J=1,M-2
          DO 410 K=1,N-1
           Y((J-1)*N+K) = 0.0D00
410       CONTINUE
405     CONTINUE

        DO 415 J=1,M-2
         Y(J*N)=0.0D00
415     CONTINUE

      ENDIF

C                           WRITE TITLE
C       CALL UMACH(2,NOUT)
      WRITE(7,1110)

C                           INTEGRATE ODE

      DO 220 IEND = 1, TEND

        XEND = 0.0D00 + 1.0D00 * DFLOAT(IEND)
        CALL DIVPAG
(IDO,NEQ,FCN,FCNJ,A,X,XEND,TOL,PARAM,Y)
        WRITE(7,1120) X, ( Y(I), I = 1, NEQ )
        WRITE(100,1130)X,Y(NEQ)
220   CONTINUE

C                           FINISH UP
      IDO = 3
      CALL DIVPAG (IDO,NEQ,FCN,FCNJ,A,X,XEND,TOL,PARAM,Y)
C
610   FORMAT(7F9.3)
620   FORMAT(8F9.3)
1110  FORMAT('  T    Q(1)   Q(2)',' Q(3)   Q(4)   Q(5)   Q(6)',
     &'    C(T)'/)
1120  FORMAT(/F6.1, 1X, 6F7.3, F8.3/ (7X, 6F7.3, F8.3))
1130  FORMAT(F6.1,1X,F7.3)
      STOP
      END
```

```
C
      SUBROUTINE FCN (NEQ,X,Y,YPRIME)

      COMMON AA(30,30), BB(30,30), AAP(30,30), BBP(30,30),
     &   M,N, GAMA,PE,PSI, P0,P1,P2,P3,P4,P5,P6,P7,P8, PI
      DOUBLE PRECISION AA, BB, AAP, BBP, GAMA, PE, PSI,
     &   P0, P1, P2, P3, P4, P5, P6, P7, P8, P11, PI,
     &   X, Y(NEQ), YPRIME(NEQ), FIRST_CONST,
SECOND_CONST,
     &   THIRD_CONST, FOURTH_CONST
      INTEGER M, N
      DO 310 J=1,M-2
         DO 320 I=1,N-1
            YPRIME((J-1)*N+I) = 0.0D00
            FIRST_CONST       = 0.0D00
           DO 330 K = 1, N - 1
           FIRST_CONST = GAMA * (BB(I,K)-PSI*BB(I,N)*
     &                   AA(N,K))
           YPRIME((J-1)*N+I) = YPRIME((J-1)*N+I)+
     &                 FIRST_CONST * Y((J-1)*N+K)
330   CONTINUE
      SECOND_CONST = P0 * BB(I, N)
      YPRIME((J-1)*N+I)=YPRIME((J-1)*N+I)+
     & SECOND_CONST*Y(J*N)
320   CONTINUE
310   CONTINUE
      DO 340 J=2,M-1
         YPRIME((J-1)*N)= 0.0D00
         P11= P8 * ( P5 * (BBP(J,1)/PE-AAP(J,1))
     &         - P3 * ( BBP(J,M)/PE-AAP(J,M) ) )
      DO 350 K=2,M-1
         THIRD_CONST = PI * ( BBP(J,K)/PE - AAP(J,K)
     & +(BBP(J,1)/PE-AAP(J,1)) * (P1*AAP(M,K)-P2*AAP(1,K))
     & +(BBP(J,M)/PE-AAP(J,M))*(P3*AAP(1,K)-P4*AAP(M,K)) )
       YPRIME((J-1)*N)=YPRIME((J-1)*N)+
     &     THIRD_CONST*Y((K-1)*N)
350   CONTINUE
      DO 360 I=1,N-1
      FOURTH_CONST    = P6 * AA( N, I )
       YPRIME((J-1)*N)=YPRIME((J-1)*N)-
     & FOURTH_CONST*Y((J-2)*N+I)
360   CONTINUE
      YPRIME((J-1)*N)=YPRIME((J-1)*N)-P11-P7*Y((J-1)*N)
340   CONTINUE
      RETURN
      END
C
      SUBROUTINE FCNJ (NEQ,X,Y,DYPDY)
      INTEGER NEQ
      REAL X,Y(NEQ),DYPDY(*)
      RETURN
      END
```

SECTION II
Oxidation and Pyrolysis of 1,1,1-Trichloroethane in Methane/Oxygen/Argon

1. INTRODUCTION

The management of chemical hazardous wastes is a central political issue and environmental concern (1). High-temperature incineration, which is an expensive option, is increasingly being used as an effective treatment process for the disposal of hazardous waste, because it is a complete conversion process to safe products.

The incineration process is, however, quite complex involving the interaction of a number of chemical, heat transfer, and fluid dynamic phenomena (2). Theoretically, incineration can result in the total conversion of hazardous organic compounds to innocuous thermodynamically controlled end products, such as carbon dioxide and water, and other compounds, such as HCl, which may be easily scrubbed with existing pollution control equipment. In practice, total conversion to innocuous materials cannot be achieved or verified without considerable expense, and for an incinerator of less than optimum design or operation, the most thermally stable components in the waste feed may not be totally decomposed (3). Louw et. al. (4), have noted the drastic operating conditions of more than 1000 K for several minutes which are necessary to prevent incinerators from emitting intolerable amounts of polychlorinated dibenzo dioxins (PCDD).

The emission of hazardous organic compounds from poorly designed or inadequately controlled incinerators represents a potentially significant threat to the environment. Hazardous organic compounds are also subjected to thermal degradation in sources not specifically designed or regulated for their disposal, and hence it is important to obtain knowledge of the thermal decomposition behavior of these organic materials (3).

One important family of hazardous wastes is the halogenated hydrocarbons. Such waste include carbon tetrachloride, trichloroethylene, trichloroethane, vinyl chloride, polychlorinated biphenyls (PCB's) and DDT

(dichlorodiphenyltrichloroethylene) and others. In order to utilize incineration more effectively, and to better assess the applicability and limitation of the incineration process, the chemical kinetic steps involved in this chlorinated hydrocarbon combustion must be understood in more detail. In addition, the manufacture of useful chemicals by the controlled oxidation and pyrolysis of chlorinated hydrocarbons may be possible through the detailed knowledge of their combustion mechanisms (5,6).

Chlorinated compounds are well recognized to inhibit hydrocarbon combustion processes and promote the formation of carbon monoxide, high molecular weight compounds and soot in flames (7,8). This study on the other hand clearly shows that chlorocarbons facilitate or accelerate the rate of hydrocarbon breakdown. Thus two effects of chlorocarbons exist, one in each of the two stages of combustion. The presence of chlorocarbons accelerates the first, hydrocarbons degradation to carbon monoxide stage. While the chlorine reactants or product clearly inhibits oxidation of CO to CO_2 in the second stage.

Graham, Hall and Dellinger (3) have studied the oxidation of a mixture of five priority organic hazardous constituents or POHC's in a 1 mm ID flow reactor at temperatures from 600°C - 900°C. These POHC's consisted of chlorobenzene, carbon tetrachloride, trichloroethylene, freon 113, and toluene. They compiled a list of well over fifty stable products from their partial oxidation study. Twenty seven of these products remained halogenated. These compounds included chlorinated furans, phenols, and polycyclic aromatic hydrocarbons (PAH). All of these are believed to be significantly more toxic than the starting materials (9).

Chang et al (10) studied the high temperature oxidation of C_2HCl_3. Their study revealed the formation of substantial levels of chlorinated hydrocarbon intermediates, including C_2Cl_2, C_2Cl_4, CCl_4, $CHCl_3$ and $COCl_2$ even under

oxygen-rich conditions. Karra et al. (11) investigated the $CH_3Cl/CH_4/O_2/Ar$ flame, they proposed that chlorine has a considerable effect on flame chemistry, as evidenced by the enhanced formation of C_2 hydrocarbons, in particular C_2H_2 and C_2H_4, and inhibited CO conversion to CO_2. The increased levels of CO, C_2H_2 and C_2H_4 in flames containing CH_3Cl is consistent with the flame inhibition and soot promoting character of chlorinated hydrocarbons.

The current study was performed in tubular flow reactors of 4 to 16 mm diameter to examine the high temperature dechlorination and thermal reaction of 1,1,1-Trichloroethane in Methane/Oxygen/Argon mixtures and to utilize the intermediate reagent and products to formulate a detailed reaction mechanism based on fundamental thermochemical and kinetic principles for this system. We characterize reactant loss and product formation as function of both time and temperatures and we developed a detailed kinetic model to accurately describe the reaction process.

2. PREVIOUS STUDIES

1,1,1-trichloroethane, also referred to as methyl chloroform and alpha-trichloroethane, is a colorless, nonflammable liquid with an odor similar to that of chloroform. It is commonly used by the industry for degreasing and cleaning agent. It has a vapor pressure at 127 torr at 25°C and a boiling point of 74.1°C at 760 torr (12).

Barton and Onyon (13) studied the thermal decomposition of 1,1,1-trichloroethane in a batch reactor throughout the temperature range 635.7 to 707 K and pressure range 10 to 120 mm Hg. The reaction yielded 1,1-dichloroethylene and HCl products almost exclusively. They found that the decomposition rate in packed reactor was slower than in empty one indicating that surfaces inhibited the reaction. They proposed the packed reactor has a large surface to volume ratio so the recombination of some radicals to terminate the chain reactions occurred at a faster rate and slowed the overall process. The initiation steps suggested by Barton and Onyon are as follows:

$$CH_3CCl_3 \rightarrow CH_2CCl_2 + HCl$$

$$CH_3CCl_3 \rightarrow CH_3CCl_2 + Cl$$

Their results showed that the wall inhibited the decomposition reaction because the proposed "key" free radical CH_3CCl_2 was consumed faster at the wall. They reported that the global first order rate constant for homogeneous unimolecular decomposition can be represented by $10^{14} \times e^{(-54,000/RT)}$ sec.

Benson and Spokes (14), using the very low pressure technique, covered a high temperature range 890 to 1265 K (so that the reactor was operated at gas flow rates from 10^{15} to 10^{16} molecules/sec. and most of the collisions made by reactant molecules were with wall rather than with other gas molecule). They calculated the homogeneous rate constant of the thermal decomposition of 1,1,1-trichloroethane at the high pressure limit. Their corresponding high pressure rate

equation is $10^{13.8} x\ e^{(-51700/RT)}$ sec.

Chang and Bozzelli (15) investigated reactor modeling and used their model in the calculation of homogeneous bulk and wall rate constants from laminar flow reactor analysis on the reaction of 1,1,1-trichloroethane diluted in hydrogen in the temperature range 828 to 954 K. The activation energies of bulk and wall reaction were determined to be 25.3 Kcal/mol and 37.9 Kcal/mol, respectively. The major products from the reaction were observed to be 1,1-dichloroethylene, chloroform, 1,1-dichloroethane, trichloroethylene, dichloromethane, 1,1,1,2-tetrachloroethane and HCl.

Won and Bozzelli (16) studied the thermal decomposition of a dichloromethane/1,1,1-trichloroethane mixture diluted in hydrogen at 1 atmosphere total pressure in a tubular flow reactor. The thermal degradation was analyzed systematically over temperature range from 748 to 1083 K and three different surface to volume ratio flow reactor. They found that complete decay occurs at around 843 K for 1,1,1-trichloroethane and about 1083 K for dichloromethane at 1 second residence time. An increase in surface to volume ratio of the reactor tube was observed to accelerate the species decomposition in hydrogen, but it had no effect on the distribution of major products. Their study demonstrated that selectivity to HCl formation can result from thermal reaction of dichloroethane/1,1,1-trichloroethane mixture and showed that synergistic effects of 1,1,1-trichloroethane decomposition parent (small amount of reaction to CH_3CCl_2. + Cl) relative to molecular elimination (CH_2CCl_2 + HCl) accelerated the rate of dichloromethane decomposition.

Huybrechts et. al (17) studied the pyrolysis of 1,1,1- trichloroethane with CCl_4 and mixture of CCl_4 + HCl in static quartz reaction vessel between 587 and 658 K at pressures between 40 and 152 torr. They found that the

dehydrochlorination is the only significant reaction and is accelerated by the HCl product. They also reported that the addition of CCl_4 can accelerate the dehydrochlorination of 1,1,1-trichloroethane. The rate constant for their system is $10^{(13.85\pm0.03)}*e^{(-54000\pm100/RT)}$.

Nelson et. al. (18) investigated the mechanisms for oxidation of CH_3CCl_2 and CCl_3CH_2 radicals through the atmospheric degradation of CH_3CCl_3. They studied the reaction of OH radical with CH_3CCl_3 in 1 atm of Argon at 359, 376, and 402 K using pulse radiolysis combined with UV kinetic spectroscopy. They reported the rate constant for OH + CH_3CCl_3 is $(5.4\pm3)10^{-12}\exp(-3570\pm890/RT)$ $cm^3molecule^{-1}s^{-1}$.

3. EXPERIMENTAL METHOD

A schematic diagram of the reactor system is shown in Figure 1. The high temperature tubular flow reactor was operated isothermally and isobarically in the range 773 K - 1073 K, and at 1 atm total pressure.

Argon was used as both a carrier and dilution gas. One part of the argon flow was passed through a two stage saturation bubbler to pick up 1,1,1-trichloroethane, which was held at 0°C using an ice bath. The other part of argon flow was used to achieve the desired molar ratio between argon, methane, oxygen and 1,1,1-trichloroethane. The methane and oxygen were added into the flow before entering the reactor and were preheated to 180 °C to limit cooling at the reactor entrance (60 cm preheat). Three quartz reactor tubes were utilized in this study: 4 mm, 10.5 mm, or 16 mm ID. The reactor tube was housed in a three zone Lindberg electric tube furnace. The reactor effluent was monitored using two on line gas chromatographs (GC's), one with Flame Ionization Detector and one with Thermal Conductivity Detector. The outlet lines between reactor and GC analysis were heated to 110°C to limit condensation.

When the inlet switching valves were properly selected the mixture (CH_3CCl_3, CH_4 and O_2) was transferred directly from the bubbler to the GC samplers via a reactor bypass line. This was necessary to determine the GC peak area which corresponded to the input (initial) concentration of mixture.

The reactor outlet gases were passed through heated transfer lines, with a loosely packed plug of glass wool to trap any solid like carbon, then to the GC samplers and the exhaust. The bulk of the outlet gases, however, was passed through a sodium-bicarbonate flask to neutralize the HCl, and then released to the atmosphere via a fume hood.

A. Temperature Measurement and Control

The three zone furnace equipped with three independent temperature controllers (NANMAC CORP., Framingham Centre, Mass).

The quartz reactor tube was housed within a three zone electric tube furnace of 18 inches length. The actual temperature profile of the tubular reactor was obtained using type K thermocouple which could be moved coaxially within reactor. The temperature measurements were performed with steady flow of argon gas through reactor. As shown in Figure 2, temperature profiles which were isothermal to within $\pm 3^{o}C$ for 80% of the total furnace length were obtained.

An energy balance calculation was done by Won (19) for the reaction system based upon the experimental observed conversion products and exothermicity. It was determined that the heat of reaction (ΔH_{rxn}), can change the temperature, by $1.5^{o}C$ at most. This is less than 50% of our temperature control error bands and is therefore not considered significant. The reaction conditions determined by the temperature profile with no reaction, are therefore considered accurate and are illustrated in Figure 2.

B. Quantitative Analysis of Reaction Products

Quantitative analysis of the reaction products was performed using a Varian 3700 gas chromatograph with flame ionization detector (FID) and a Varian 1400 gas chromatograph with thermal conductivity detector (TCD). The Varian 3700 GC used a 5 ft. by 1/8 in. OD stainless steel packed column with 1% Alltech AT-1000 on graphpac GB. A 6 ft. by 1/8 in. OD stainless steel column with Carbosphere 80/100 packing for the Varian 1400 GC . The operation conditions of these two GC's and their representative chromatograms were described in more detail by Wu (20). Peak identification with retention time are summarized at Table 1.

Calibration of the flame ionization detector to obtain appropriate molar response factors was done by injecting a known quantity of the relevant compound such as CH_4, C_2H_4, C_2H_6 (flowed through loop at known pressure from a SCOTTY® IV analyzed gases cylinder). CH_2CCl_2, CH_3CCl_3 flowed through from the reactor bypass line through the sampling loop, measure their corresponding response areas. Calibration of the thermal conductivity detector was also done by injecting a known quantity of the relevant compound such as CH_4, CO, CO_2, etc., and then, measuring the corresponding response area. The relative response factors for both detectors, FID and TCD, determined for our compounds are shown in Table 2. The response factors for C_1 compounds are all similar and the response factor for C_2 compounds are ca. twice the response of C_1 compounds on the FID. These results agree with the general principle of flame ionization detector which is well known as a carbon counter (21). The effect of chlorine on the relative response factor appears to be small (less than 10% deviation from hydrocarbons) for our FID operation and the relative response factors of other compounds corresponding to the respective carbon number were used when laboratory standards were not available. The peak area for each component was converted to the equivalent number of moles, based on these response factors.

C. Hydrochloric Acid Analysis

Quantitative analysis of HCl product was performed for reactions in each diameter reactor and each residence time. The samples for HCl analysis were collected independent from GC sampling as illustrated as Figure 1. In this analysis, the effluent was bubbled through a two stage bubbler before being exhausted to the hood. Each stage contained 15 ml of standardized 0.01 M NaOH. The gas was passed through the two stage bubbler until the first stage solution

reached its phenolphthalein end-point (typically 0.5 to 2 minutes). The time required for this to occur was recorded. At this point the bubbling was stopped, the aliquots were combined, and titrated to their end point with standardized 0.01 M HCl.

The HCl produced by reaction was easily calculated; since the concentration and molar flow rate of chlorine as 1,1,1-trichloroethane was known, an estimate of the amount of organic chlorine which remained unaccounted for was available. Several titration were performed using buffered solution (pH 4.7) to discern if CO_2 was affecting the quantitative measurement of HCl. No significant effect was observed due to the relatively low levels of CO_2.

D. Qualitative Analysis of Reaction Products by Mass Spectrometry

The analysis of the reactor outlet gases was performed on a Finnigan 4000 series GC/MS with a 50 m long, 0.22 mm ID methyl silicone stationary phase.

Evacuated 25 ml stainless steel sample cylinders were used for collection of gas samples at the outlet of the reactor. The samples was then injected into the GC/MS via a six port gas sampling valve. The sample was cryogenically focused inside the GC oven, 20 cm loop at front of GC column, with liquid nitrogen.

A sample chromatogram from the Mass Spectrometer analysis is shown in Figure 3.

E. Computer Codes Used for the Kinetic Model

i. THERM

Our thermo data is based upon the evaluated thermochemical data in literature. When experimentally based thermodynamic data were not available, the values were estimated using THERM computer code (24,27).

THERM is the computer code which can be used to estimate, edit, or enter thermodynamic property data for gas phase radicals and molecules using Benson's Group Additivity Method (25). All group contributions considered for a species are recorded and thermodynamic properties are generated in NASA polynomial format (for compatibility with CHEMKIN (26)) in addition to listings which are more convenient for thermodynamic, kinetic and equilibrium calculation.

A thermodynamic data base for species with C/H/Cl/O elements is developed at NJIT and used for modeling the kinetic scheme of elementary reactions input to the program. THERMFIT calculated polynomials for heats of formations and entropies at 298 K, as well as heat capacities, from 300 to 1000 K as input to CHEMKIN. These were calculated by group additivity method of Benson (25) when not available in literature on computer code THERM (24,27).

ii. CPFIT

CPFIT (22,24) is a computer code that determine geometric mean frequency. It accepts input in the form of heat capacities versus temperature to 1000 K. in addition to the number of vibrational modes and the number of internal rotors in the molecule. This code fits the heat capacity data in the above range to a five parameter harmonic oscillator model and extends the temperature range to 5000 K. An additional method of estimating the geometric mean frequency of a radical is to take the arithmetic mean of the frequency of the corresponding stable parent molecule (with one more H atom corresponding olefin) and the frequency of the species with one less H atom than the radical of interest.

iii. CHEMACT

CHEMACT (22) is a computer code that uses the QRRK treatment of chemical activation reactions to estimate apparent bimolecular rate constants for various

channels that can result in addition, recombination and insertion reactions. Since these rate constants depend on both pressure and temperature, it is important that the user determine the rate constants for the specific pressure and temperature ranges of interest in the modeling calculation. (This expression is then valid over whatever temperature range was fitted with CHEMACT.) In addition, the user must account for further reactions of the stabilized adducts, which are products of the reaction. The dissociation of stabilized adduct back to reactants is automatically included if the reactions are written reversibly, but, for completeness, dissociation to the other possible products must be explicitly included.

Required Input Data for CHEMACT include:

- Thermodynamic parameters: enthalpy (H_f), entropy (S_f) and heat capacities (C_p) as a function of temperature for reactants, adduct and products of the reaction system are important for accurate results. These parameters are used to determine the well depth, which is the excess energy of the initially formed complex, energies of activation for unimolecular bond cleavage reactions of the energized complex and determination of rate constants for various reaction channels through principles of microscopic reversibility.
- Molecular parameters describing the size, collisional energy transfer and energy levels of the adduct formed by the initial reaction are also needed. These include the mass, number of vibrational modes of the adducts, Lennard-Jones parameters and geometric mean vibrational frequency.
- The bath gas molecule collision diameter, well depth and average energy transferred per collision are needed.

- High pressure limit rate constants for adduct formation and various isomerization and dissociation product channels of the adduct are also needed.

iv. DISSOC

Fall-off corrections for unimolecular decomposition reactions are calculated by the unimolecular Quantum RRK method (23). The DISSOC computer code (22) analyzes unimolecular reaction with unimolecular QRRK analysis for the proper treatment of fall-off dependency and estimates apparent rate constants for various unimolecular dissociation channels. Since these rate constants depend on both pressure and temperature, it is important that the user determine the rate constants for specific pressure and temperature ranges of interest in the modeling calculation. The same input data with CHEMACT computer code is required to run DISSOC program.

v. CHEMKIN

The CHEMKIN computer program package is used in interpreting and integrating the detailed reaction mechanism (model) of the reaction system. The CHEMKIN program (26) reads the user's symbolic description of the reaction mechanism. The thermodynamic data base, which has the appropriate thermodynamic information and mass for all species present in mechanism. The information on the elements, species, and reactions in the mechanism; and finally the CHEMKIN gas phase subroutines, which can be called to return information on the elements, species, reactions, equations of state, thermodynamic properties, chemical production rates, and derivatives of thermodynamic properties relative to any time in the integration. The input to these subroutines are usually the state variables of gas pressure or density, temperature and species composition at initial

time of reaction. The routines can be called with the species composition defined in terms of either mass fraction or molar concentration. Numerical calculations were carried out using the CHEMKIN computer code coupled to LSODE a linear solver of ordinary differential calculations.

The input data requirement to run CHEMKIN program include:

- Detailed reaction mechanism
- Mole fraction of all gases present in the reaction system
- Pressure and temperature at which the reaction system being studied
- Time increment at which the concentration of species present in the system be reported

vi SENKIN

In order to determine the most influential reactions in the mechanism relative to a target species, the SENKIN computer code (28), which has been modified at NJIT, was employed for the calculation of sensitivity gradients. The input data for the execution of SENKIN are similar to those for CHEMKIN.

The results of this analysis contains quantitative information on how the rate coefficients affect the product/reactant concentration. If the model calculations are very sensitive to a specific reaction and it's rate constant, it means that more effort should be put forth to insure an accurate value for that kinetic parameter. On the other hand, if a reaction is not sensitive in the system, it may be possible to eliminate it, and simplify a complex reaction mechanism without influencing the results. The major or more important reaction paths leading from reactants to products are more fully understood from this analysis (29).

The sensitivity and reaction path analysis, also allow, the size of the detailed mechanism to be systematically be reduced. However, this may not be desirable because the reduced mechanism has narrower and more limited range of

applicability. Furthermore, with the availability of fast computers, the usage of detailed reaction mechanisms no longer represents a significant cost factor (30).

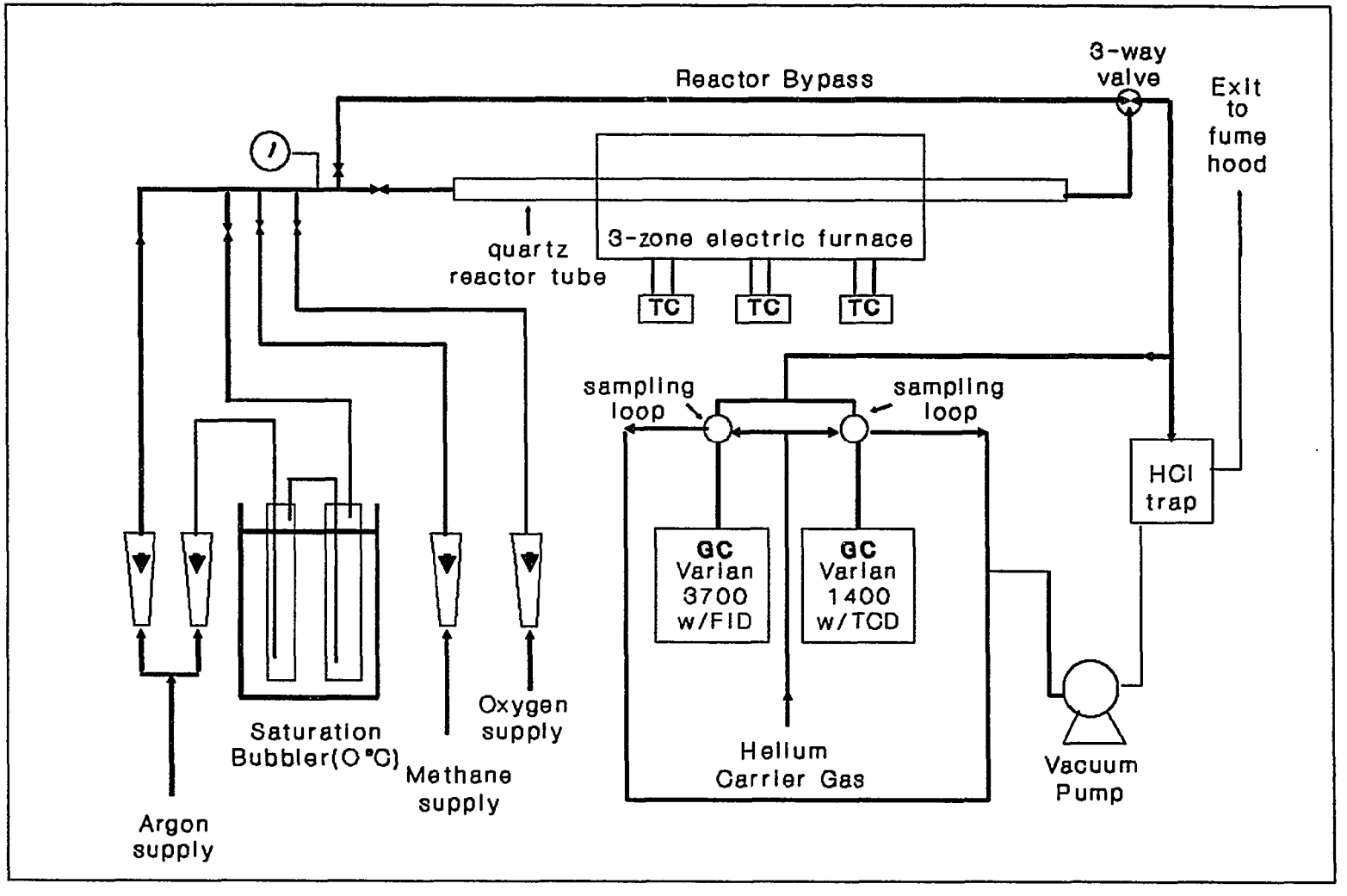

Figure 1. Experimental system

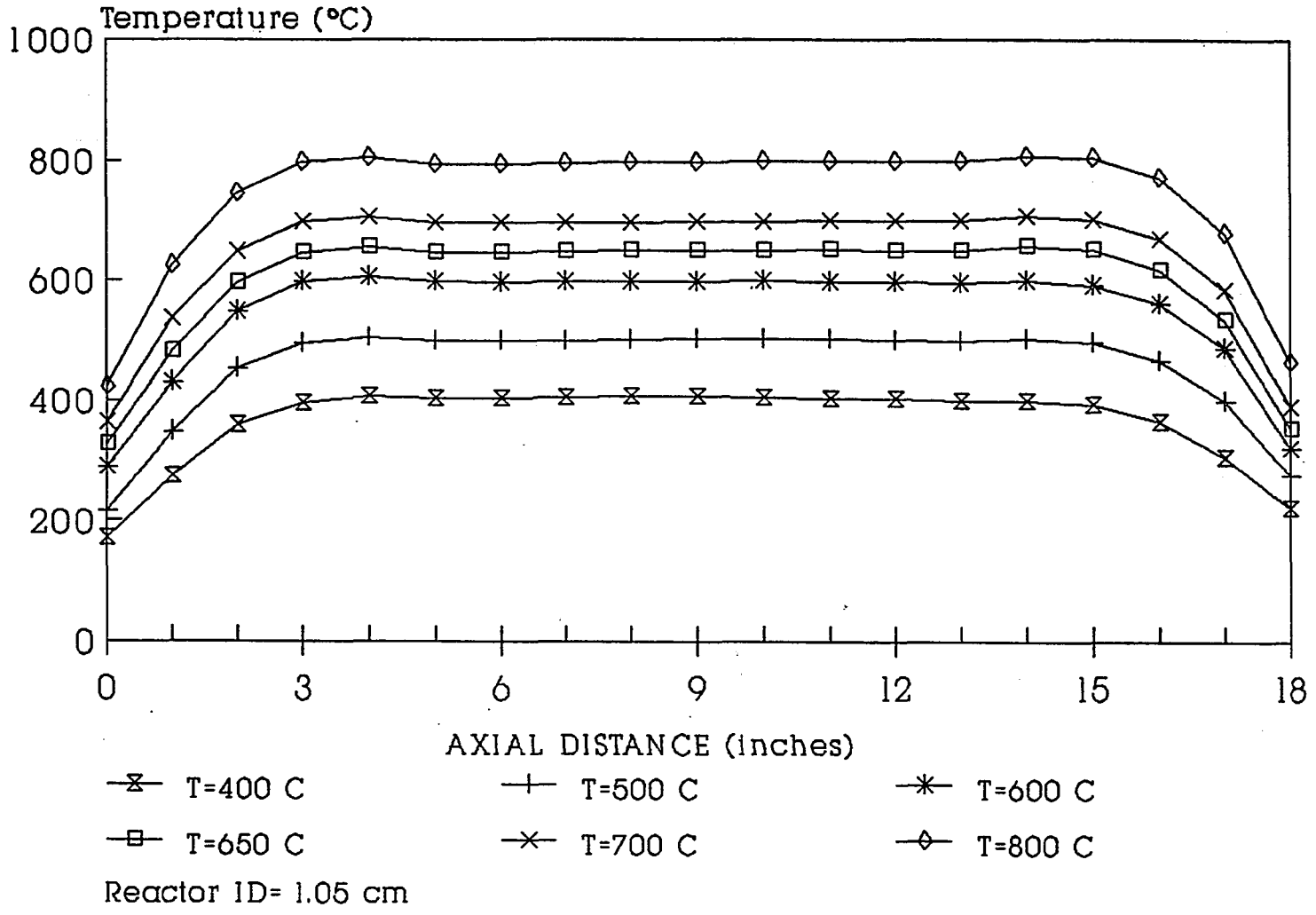

Figure 2. Reactor Temperature Profile

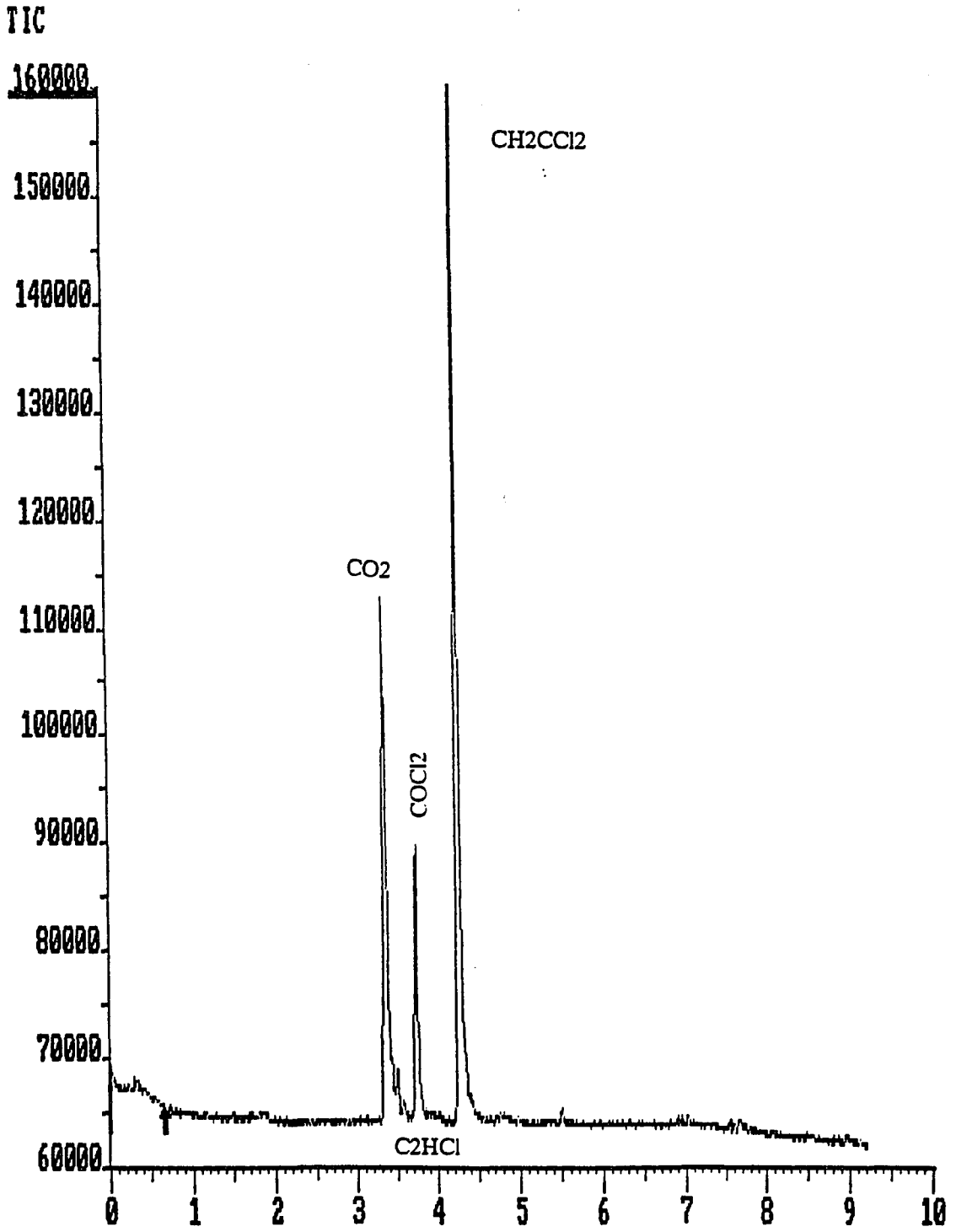

Figure 3. GC/MS Sample Chromatogram in $CH_3CCl_3/CH_4/O_2/Ar$

4. RESULTS AND DISCUSSION

The experimental conditions of the reaction of 1,1,1-trichloroethane/oxygen/ methane mixture with argon are listed below:

Reactants Ratio ($O_2 : CH_4 : CH_3CCl_3$)(Molar Ratios):

1. $O_2 : CH_4 : CH_3CCl_3 = 4.5 : 0 : 0.5$
2. $O_2 : CH_4 : CH_3CCl_3 = 4 : 0.5 : 0.5$
3. $O_2 : CH_4 : CH_3CCl_3 = 3.75 : 0.75 : 0.5$
4. $O_2 : CH_4 : CH_3CCl_3 = 3 : 1.5 : 0.5$
5. $O_2 : CH_4 : CH_3CCl_3 = 0 : 1.5 : 0.5$

(The reaction conditions range from fuel equivalence ratios of 0.2 to 1)

Reactor Temperature (°C) : 500, 525, 550, 575, 600, 650,700, 750, 800.

Effective Reactor length : 30.5 cm.

Reactor Diameter (cm) : 0.4, 1.05, 1.60.

Residence Time Range (sec.) : 0.05 - 1.0 (I.D. = 0.40)

0.3 - 2.0 (I.D. = 1.05)

0.7 - 2.5 (I.D. = 1.60)

Operating Pressure : 1 atm.

Nine temperatures ranging from 500 to 800 °C were studied in the 1.05 cm I.D. reactor, and each temperature study had a minimum of 6 residence time points from 0.3 to 2.0 sec. For the 0.4 cm and 1.6 cm I.D. reactors, experiments at five temperatures ranging from 500 to 700 °C were studied with average residence times in the 0.4 cm I.D. reactor ranging from 0.05 sec. to 1.0 sec. and for the 1.6 cm I.D. reactor ranged from 0.7 sec. to 2.5 sec.

Constant molar ratio of CH_3CCl_3 was maintained at 0.5% through the experiments. The molar ratio of argon was maintained at 95.0% for case 1, 2, 3, 4 and 98.0% for case 5. Oxygen, molar ratios were from 4.5% to 0% and methane ratios were from 0% to 1.5%.

A. Reaction of 1,1,1-Trichloroethane/Oxygen/Methane/Argon Mixture

Experimental results on decomposition of 1,1,1-trichloroethane are in Figure 4a through 4f, which show normalized concentration (C/C_0) as a function of the average residence time for several temperatures studied and each different i.d. reactor.

The 1,1,1-trichloroethane concentration consistently decreased with increasing reaction time for all temperatures. As shown in Figure 5, we found that oxygen up to 4.5% had almost no effect on the 1,1,1-trichloroethane decomposition.

The limited oxygen effect combined with the dominant molecular elimination pathway in excess argon allowed simplification to pseudo-first order kinetics for initial decays in most of these experiments. Integrated rate equation plots for the conversion of CH_3CCl_3 over a range of concentration ratios to fit a first order rate equation are shown in Figure 6a through 6f. Here it is seen that for different values of temperature and diameter, as well as chemical ratios the data fit the integrated first order rate equation well. Decomposition was most rapid in the 4 mm id and slowest with the 16 mm id reactors as show in Figure 7a through 7c. We feel that this trend demonstrates that reagent loss is the result of two reaction paths, in the smaller ID reactor. One, a homogeneous reaction which occurs in the bulk or homogeneous phase of the gas mixture and two, a heterogeneous reaction which occurs on the surface of the flow tube wall. Clearly the relative importance of the wall reaction is greater when the surface to volume ratio (S/V) or relative concentration of the wall surface is greater. We recommend use of the larger ID reactor data for use in modeling as wall loss minimized here. The activation energies and Arrhenius frequency factor for the global reaction (loss) of CH_3CCl_3 in the different reactant set ratios are found

from Arrhenius plots such as in Figure 8. These global Arrhenius equations for each diameter and reactant set ratio are listed in Table 3.

B. Reagent Conversion and Product Distribution

50% conversion of 1,1,1-trichloroethane is observed at reaction temperatures above 550 °C, 1.0 sec residence time, at all different reactor set ratios as shown in Figures set 4. The distributions for major products CH_2CCl_2, C_2H_2, C_2H_4, CO, CO_2 and C_2HCl are shown in Figures set 9 at 1 second residence time for varying temperature and reaction conditions. 1,1-dichloroethylene (CH_2CCl_2) and HCl were the major products over the temperature range from 500 °C to 600 °C, where conversion of CH_3CCl_3 ranged from 5 % to 100 % as shown in both Figure sets 4 and 9. Only a small amount of ethylene, vinyl chloride, chloroacetylene were observed at temperatures below or equal to 600°C.

In Figures set 9, clearly one may see that the major product at 1 sec residence time and below 650°C is 1,1-dichloroethylene which results through loss of HCl (molecular elimination) reaction from 1,1,1-trichloroethane. Above 600°C the carbon monoxide concentration rises exponentially and then levels off to about 93% at 740°C and above. Figure 9b and 9c show that the presence of 0.5% or 0.75% methane has little effect on 1,1,1-trichloroethane conversion, but it serves to stabilize the 1,1-dichloroethylene product to a level where it is not significantly destroyed until temperatures above 750°C at 1 sec residence time in this system. Methane shows a small amount of reaction at 560°C, then significant decomposition above 700°C. At temperature between 600 to 680°C, 1,1-dichloroethylene represents almost 100% of the parent 1,1,1-trichloroethane concentration. Figure 9d and 9e, where the reaction has low (1.5%) or no O_2 and methane concentration constant of 1.5%, show that the 1,1,1-trichloroethane

decomposition and the 1,1-dichloroethylene production and loss, are both similar to conditions for Figure 9 a-c which have more oxygen. The 1,1-dichloroethylene loss is definitely slower at lower [O_2]. CH_4 shows less decomposition and there is more acetylene production at high temperature. There was no carbon monoxide measured below 750°C for the experiments illustrated in Figures 9 b-e, and there was no CO observed before 1 sec residence time.

Figure 10-a shows product distributions of 1,1-dichloroethylene and CO as a function of time above 700°C. Figure 10-b shows that no CO was observed at the lower O_2 concentration at 700°C. Figure 10-c presents product distribution of CH_2CCl_2, CO, CO_2 as a function of time at 800°C. Additional data on the distribution of 1,1-dichloroethylene is also shown in Figure 12a through 12e which is discussed later in this chapter.

The levels of non-chlorinated hydrocarbons are shown to increase with increasing temperature for all reactant ratio sets. The concentration of chlorine containing hydrocarbon products decrease with increasing temperature, residence time and ratio of O_2/CH_4, while HCl formation increased as shown in the chlorine material balance in Appendix II-1.

Formation of CH_2CCl_2 as one of major product from CH_3CCl_3 increases with increasing temperature to a maximum near 600°C at 1.0 sec residence time and is independent of reactant ratio. It then drops quickly with increasing temperature and/or increased levels of O_2. CH_2CCl_2 is the initial stable product in unimolecular reaction of this mixture. As shown in Figure 11, there was an effect from added oxygen on the major product distribution when temperatures were higher than 600°C. Figures 12a through 12e also illustrate CH_2CCl_2 normalized concentration versus residence time for different temperatures. They demonstrate that the CH_2CCl_2 concentration increase with increasing residence

time under 600 °C while its survival temperature window ("stability window") increases with increasing ratio of CH_4 to O_2. This is further illustrated in Figures 9-b through 9-e, and particularly in 9-d and 9-e which show that decreases in $[O_2]$ where CH_4 is held constant, increases the "stability window" of CH_2CCl_2. Further work needs to be performed here to clearly separate the effects of CH_4 and O_2 on the reaction system. Data shown in Figures 9-b through 9-e indicate that CH_4 may have a significant stabilizing effect on 1,1-CH_2CCl_2 in this system.

The increase in CH_2CCl_2 with residence time demonstrates that its rate of formation is faster than its destruction at 600°C and indicate that the CH_2CCl_2 is stable intermediate product in overall reaction. Figure 9 and the mass balance data tables which are in Appendix II-1, show that concentration of CH_2CHCl, CH_2CH_2, CH_3Cl, C_2HCl, increase from 650 to 750°C as the temperature increases. These same products (except C_2H_2) increase in concentration as residence time increases until a mean residence time longer than 0.7 sec occurs. These products then decrease as residence time increases. C_2H_2 increases with increasing residence time for all cases.

C. Effect of Oxygen

As shown in Figure 4, there is almost no effect from oxygen on the decomposition of parent CH_3CCl_3 in our experiments. Oxygen is, in addition, not a significant factor on the formation of CH_2CCl_2 below 600°C. Above 600°C, CH_2CCl_2 drops quickly in the high O_2 ratio set 1 (O_2= 4.5%, Ar= 95%, CH_3CCl_3= 0.5%) with the CH_2CCl_2 decrease more rapid here than for any other case (Figure 11 and Figure set 12). The lower the amount of oxygen, the slower the observed decay of CH_2CCl_2. This also applies to the other products (such as C_2H_2, C_2H_4, etc.) which are formed and then decrease more quickly in reactants ratio set 1 than in

other sets. Generally, a faster decay of compounds which are formed at lower temperature occurs when the temperature is above 650°C, and when more oxygen is in the mixture. The higher ratio of O_2 to CH_4, the lower the required temperature needed to observed formation of CO and CO_2.

Several studies are available on the oxidation of methane in different types of reactors (38,39), but they have investigated temperature regions which are all above 827°C (1100 K). In our study, methane start to react at about 650°C (923 K) where oxygen is present and at about 750°C for the case without oxygen, as illustrated in Figure 13 a-b for varied residence times. The increased methane conversion with respectively higher [O_2] is shown in Figure 14 a and b at 750 and 800°C. Figures 12 a-d along with the mass balance tables in Appendix II-1, show that CH_2CCl_2 decay is more rapid and occurs at lower temperatures e.g. highest conversion for conditions of ratio set 1 with 4.5% O_2.

We found that CO is formed and increases with increasing time in ratio set 1 (4.5% O_2) only for the 650°C reactor temperature. As temperature and O_2 concentration increase CO increases. At 800°C, almost no other products were found except CO, HCl and trace amounts of CO_2 for the case of 4.5% O_2. For the cases with less O_2, the hydrocarbon or halocarbon products were eventually totally converted to HCl and CO or CO_2 at 800°C, and the time needed for this conversion increased with decreasing concentration of oxygen.

D. Comparison of 1,1,1-Trichloroethane/Mixture React with Reactions of Previous Studies

It is valuable to compare the reaction of 1,1,1-trichloroethane in these mixture CH_4/O_2 condition with other published studies on reactions of 1,1,1-trichloroethane to further evaluate effects of CH_4 and O_2 mixtures. Chang (31) studied the thermal decomposition of 1,1,1-trichloroethane diluted in hydrogen

using a similar experimental system over the temperature range of 555 to 681°C and residence times between 0.04 to 1.0 sec where initial 1,1,1-trichloroethane was present at the 5.89% concentration. Figure 15-a shows that conversion trends are very similar for both experimental studies.

Won (19,30) studied the thermal decomposition of 4% di-chloromethane and 4% 1,1,1-trichloroethane mixture diluted in hydrogen using a similar experimental system over the temperature range 475 to 810°C, residence time between 0.05 to 2.0 sec and three different diameter reactors. Figure 15-b shows that the decay of CH_3CCl_3 in Won's study (equal fraction CH_2Cl_2 present) is faster than the present study due to synergistic effects at temperatures below 575°C. The reason for the higher CH_3CCl_3 conversion between these two studies where CH_2Cl_2 was present is the activity of atomic hydrogen and chlorine relative to CH_3 or HO_2 here. Won's system has excess hydrogen in the mixture which provided a rich hydrogen environment for initial radicals to react with.

$$CH_2Cl_2 \rightarrow CH_2Cl + Cl$$

$$Cl + H_2 \rightarrow HCl + H$$

$$H + CH_2Cl_2 \rightarrow HCl + CH_2Cl$$

$$\rightarrow H_2 + CHCl_2$$

$$H + CH_3CCl_3 \rightarrow CH_2CCl_3 + H_2$$

$$H + CH_3CCl_3 \rightarrow CH_3CCl_2 + HCl$$

$$Cl + CH_3CCl_3 \rightarrow CH_2CCl_3 + HCl$$

$$CH_3CCl_2 \rightarrow CH_2CCl_2 + H \text{ (beta scission)}$$

$$CH_2CCl_3 \rightarrow CH_2CCl_2 + Cl \text{ (fast beta scission)}$$

Where in the present study, small amount of HO_2 and CH_3 radicals lead to less reaction with CH_3CCl_3 due to lower reactivity of HO_2 and CH_3 relative to H. In this study, CH_3CCl_3 is just in addition present in a smaller amount, (CH_4 + O_2 +

CH_3CCl_3 =5%). We further point out that radicals produced from either H or Cl abstraction from 1,1,1-CH_3CCl_3 rapidly lead to 1,1-CH_2CCl_2 + another very active radical, such as H or Cl, in the system.

E. Analysis of Addition/Recombination Reactions

The decomposition/stabilization of the energized radical and molecular complexes was modeled using the QRRK calculations. The details of the bimolecular QRRK method are presented by Dean (33), Westmoreland and Dean (34) and Ritter et. al. (35). and its application to a number of chemically activated reaction systems have been previously discussed (33,34,35).

Energized Complex/QRRK theory as presented by Westmoreland and Dean (34) is used for modeling of radical addition reactions to unsaturated bonds and for radical or atom combination reactions. This computer code has been modified by Dean, Ritter and Bozzelli (35) to use gamma function instead of factorials. The QRRK computer code was used to determine the energy dependent rate constants for all reaction channels of the energized complexes and calculates rate constants as function of both temperature and pressure. The use of this formalism is important in determination of accurate rate constants needed for input to the mechanism, specifically in choice of the important reaction paths. This also applied to accurate product distribution prediction from the activated complex.

QRRK analysis of the chemically activated system, using generic estimates or literature values for high pressure rate constants and species thermodynamic properties for the enthalpies of reaction, yields thermodynamically and kinetically plausible apparent rate constants. Figure 16, 18 & 19 illustrate the energy level diagrams and apparent rate constants versus temperature and pressure for

CH_2CCl_2 + H → Products, CH_2CCl_2 + OH → Products and C_2H_2 + O_2 → Products. The input rate parameters used in these calculations and results from the calculations are summarized in APPENDIX II-2. The calculations were performed for each of six pressures between 0.76 torr and 7600 torr.

CH_2CCl_2 + H Reaction

For the CH_2CCl_2 + H system, atomic H can add to the chlorine side carbon of CH_2CCl_2 (ipso addition) to form CH_2CHCl_2 radical as:

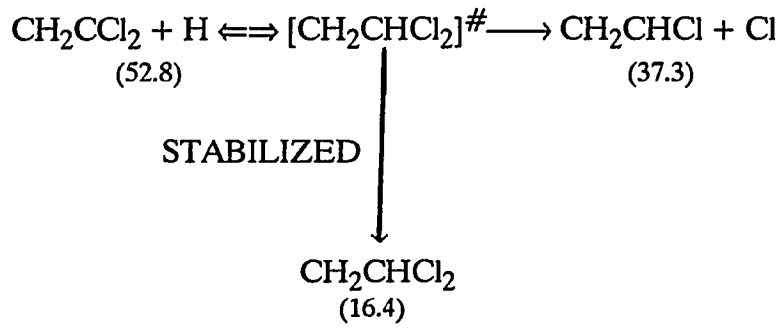

The energy diagram of the reaction system is illustrated in Figure 16 and the calculation results are shown in Figure 17. The $[CH_2CHCl_2]^{\#}$ complex is initially "hot" since, in addition to the thermal energy, it contains energy resulting from the formation of the stronger C-H bond relative to Carbon-Carbon Pi bond broken. Prior to stabilization, it may dissociate back to reactants, become a stabilized radical, or beta scission to CH_2CHCl + Cl. Clearly, the QRRK analysis indicates that all collisions proceed to CH_2CHCl + Cl, the low energy exit channel. A chlorine atom shift which is also feasible for this ipso addition case will result in $CH_2ClCH.Cl$ which will also rapidly beta scission to C_2H_3Cl + Cl, i.e. identical product set.

The non-ipso addition of H atom to CH_2CCl_2 (addition to CH_2 group), as discussed in Won (36), occurs at a higher rate because of a lower barrier to the

addition, and results in CH_3CCl_2. The $[CH_3CCl_2]^{\#}$ radical initially formed can dissociate back to reactants, or isomerize (H shift), and then react to CH_2CHCl + Cl.

The complex has to undergo a 1,2 hydrogen shift to form the CH_2CHCl_2 radical before Cl elimination and formation of CH_2CHCl + Cl can occur. Results from the Chemical Activation QRRK analysis indicate that a smaller fraction of the complex formed is converted to CH_2CHCl + Cl than in the ipso attach.

CH_2CCl_2 + OH Reaction

Unsaturated compounds, such as CH_2CCl_2 in this study, can react with OH radical and are considered important in combustion processes. Won (36) showed the addition of the OH radical at CH_2 side is more favorable than at the CCl_2 side. Due to the instability of the adduct and s slightly higher barrier for ipso addition. The addition reaction will rapidly reverse if the addition is to a site containing only hydrogens.

In the case of OH addition to a site containing chlorine, thermodynamics favor the subsequent displacement of the chlorine as shown in Figure 18. The $[CH_2.CCl_2OH]^{\#}$ activated complex initially formed can dissociated back to reactants, to CH_2CClOH + Cl, or isomerize to $[CH_3CCl_2O.]^{\#}$ and then react to CH_3 + CCl_2O and CH_3CClO + Cl, or either adduct can be stabilized. The measured rate constant, as pointed out by Tsang (37), for this addition at room temperature is smaller than for addition to the non-chlorinated carbon. Since the adduct decomposes rapidly by chlorine elimination rather than reverse reaction at higher temperatures, it has the decisive effect of placing an oxygen atom (OH) on the carbon. The result is reversion of the C_2 carbon system to C_1 carbons which react rapidly to CO and H_2O.

C_2H_2 + O_2 Reaction

C_2H_2 is one of the important observed products in the experiment and direct reactions of C_2H_2 with O_2 have been reported in the literatures<40>. We, therefore, decided to analyze the C_2H_2 + O_2 reaction in order to properly include it in our mechanism.

The energy level diagram for the C_2H_2 + O_2 reaction is shown in Figure 19. Molecular O_2 is a triplet and will add to C_2H_2 to form ^{3}[HC=CHOO.]$^\#$ (triplet state). ^{3}[HC=CHOO.]$^\#$ can further isomerize through a hydrogen shift to ^{3}HC=COOH or ^3H_2C=C.OO.. The triplet can undergo singlet-triplet crossing and convert to a singlet, then cyclize to Cy(C_2H_2OO) (see Figure 19). The [Cy(C_2H_2OO)]$^\#$ will go to OHC-CHO then react to form two HCO radicals. ^3H_2C=COO. can undergo beta scission to CH_2=C=O + ^{3}O. We note that an appreciable activation energy, ca. 11 kcal/mole in this case, is required to convert the spin of the system from its triplet state, ^{3}[HC=CHOO.]$^\#$, to the singlet state of the product before ring closure to the lower energy product [Cy(C_2H_2OO)]$^\#$ can occur. The calculation result from Chemical Activation QRRK analysis, as shown in Figure 20, shows that formation of the triplet complex is endothermic by 34 Kcal/mol and once formed, it will rapidly react back to reactants and only a small fraction (9.7E-5) will react to form HCO at 1073 K. While this reaction does not appear to be too important, it is very important to include it accurately or omit it rather than have it much faster than it should be in the mechanism.

F. Kinetic Mechanism and Modeling

The reaction mechanism and decomposition kinetics for 1,1,1-CH_3CCl_3/O_2/CH_4 mixture in Ar are developed.

The initial reactions for unimolecular decomposition of CH_3CCl_3 include:

	A (1/s)	E (Kcal/mol)		
$CH_3CCl_3 \rightarrow CH_3CCl_2 + Cl$	1.05E16	71.2	(ΔHr)	(1)
$CH_3CCl_3 \rightarrow CH_2CCl_2 + HCl$	6.31E13	51.7	(ΔHr+42)	(2)
$CH_3CCl_3 \rightarrow CH_3 + CCl_3$	9.1E16	85.7	(ΔHr)	(3)

(kinetic data sources are referenced in the source part of Table 4, the listing of the detail mechanism)

It is observed from the above kinetic listing that reaction (2) dominates the other pathways by more than three orders of magnitude at temperatures below 600 ^oC. This is consistent with our experimental results. CH_2CCl_2 and HCl are the major products detected below 600 ^oC.

The major product from the destruction of 1,1,1-CH_3CCl_3, 1,1-CH_2CCl_2, is relatively stable, as compared to CH_3CCl_3 or other chloroethanes. This is because simple bond cleavage or HCl molecular elimination from the 1,1-CH_2CCl_2 has relatively high energy requirements. 1,1-CH_2CCl_2, therefore, reacts by addition/combination and abstraction processes. Oxy radicals (O, OH, HO_2), Cl and H atoms and hydrocarbon radicals (HCs) now contributes to the destruction of CH_2CCl_2 and need to be considered in the mechanism.

The destruction of CH_2CCl_2 occurs primarily by hydrophobic and hydrophilic species as follows:

Hydrophobic Process

The H atom abstracts Cl from CH_2CCl_2:

$$CH_2CCl_2 + H \rightarrow CH_2CCl + HCl \qquad (4)$$

Hydrophilic Process

Hydrophilic species (OH, O, HO_2, O_2, Cl and ClO) selectively abstract a H atom from CH_2CCl_2 as:

$$CH_2CCl_2 + \begin{bmatrix} OH \\ O \\ HO_2 \\ O_2 \\ Cl \\ ClO \end{bmatrix} \rightarrow CHCCl_2 + \begin{bmatrix} H_2O \\ OH \\ H_2O_2 \\ HO_2 \\ HCl \\ HOCl \end{bmatrix} \quad (5)$$

The chlorovinyl radicals, which are produced by the above abstraction reactions, may react with molecular oxygen in extremely exothermic reactions that lead to stable oxy-containing products as follow:

$$CH_2CCl + O_2 \rightarrow CH_2O + CClO \quad (6)$$

$$CHCCl_2 + O_2 \rightarrow HCO + CCl_2O \quad (7)$$

For the destruction of methane, there are several important metathesis or abstractions reactions:

$$CH_4 + Cl \rightarrow CH_3 + HCl \quad (8)$$

$$CH_4 + O_2 \rightarrow CH_3 + HO_2 \quad (9)$$

$$CH_4 + O \rightarrow CH_3 + OH \quad (10)$$

$$CH_4 + H \rightarrow CH_3 + H_2 \quad (11)$$

$$CH_4 + OH \rightarrow CH_3 + H_2O \quad (12)$$

$$CH_4 + HO_2 \rightarrow CH_3 + H_2O_2 \quad (13)$$

Once the methyl radical is formed, it can react with oxygen or radicals species as follow:

$$CH_3 + O_2 \rightarrow CH_3OO \quad (14)$$

$$CH_3 + O_2 \rightarrow CH_3O + O \quad (15)$$

$$CH_3 + O_2 \rightarrow CH_2O + OH \quad (16)$$

$$CH_3 + O \rightarrow CH_3O \quad (17)$$

$$CH_3 + O \rightarrow CH_2O + H \quad (18)$$

$$CH_3 + OH \rightarrow CH_3O + H \quad (19)$$

$$CH_3 + OH \rightarrow CH_2 + H_2O \quad (20)$$

$$CH_3 + HO_2 \rightarrow CH_3O + OH \quad (21)$$

A detailed mechanism of elementary reactions is developed and listed in Table 4 together with the rate parameters and corresponding sources.

This kinetic mechanism consists of 339 elementary reactions with 99 species. Elementary reaction rate parameters for abstraction reactions are based upon literature comparison, thermodynamics and thermochemical methods of Benson (25). QRRK calculations (34,35), as described in previous section, were used to estimate apparent rate parameters for addition, combination and dissociation reactions (1 atm).

Experimental data are compared with model predictions in Figure 21 and 22 for reagent decomposition and product distribution between 500 and 800°C. Figure 21 shows a comparison of CH_4, CH_3CCl_3, CH_2CCl_2 and CO from model and experimental results. Figure 22 is a comparison of model calculation with the experimental data for minor products such as C_2H_4, C_2H_2, C_2H_3Cl and C_2HCl. Predictions for loss of the two reagents and product distribution match experiment well, although C_2HCl is a little over predicted by the model. Figure 23 and 24 illustrate the calculated concentration of reactants and products versus reaction time at 700 °C and show good agreement with the experimentally observed data for decay of reactants and formation of products. Figures 21 and 22 show the small difference seen between calculated and experimental values for reagents and products at 1 sec residence time. Figures 23 and 24 show the model and experiment comparison at 700°C for varied times. As shown in Figure 21 and 22, the reagent (CH_3CCl_3, CH_4) and major products (CH_2CCl_2), model prediction match the experiment data well in the lower temperature range (500 -

700°C). As temperature increases above 700°C, the model result shows slower decay of CH_4 and CH_2CCl_2 than the experiment and the resulting lower formation of hydrocarbons, such as C_2H_2.

To determine the most influential reactions in the large scheme of Table 4, a sensitivity analysis computer code SENS was applied. We point out that sensitivity is a function of time of reaction, initial conditions, temperature plus other parameters and it is therefore difficult to indicate quantitative sensitivities for all conditions. We therefore discuss the important sensitivities and relative orders for general condition described in this experimental program.

As a representative example, results showing the most influential reactions on the formation or loss of products from the sensitivity analysis, reactant ratio set 3 (O_2:CH_4:CH_3CCl_3:Ar= 3.75: 0.75: 0.5: 95) are given in Table 5 at two temperatures. The important reactions can be summarized with respect to the selected species as follows:

CH_3CCl_3

The primary reaction responsible for the destruction of CH_3CCl_3 below 873 K is unimolecular decomposition:

$$CH_3CCl_3 = CH_2CCl_2 + HCl.$$

The abstraction reaction of $CH_3CCl_3 + Cl = CCl_3CH_2 + HCl$ is a minor channel for destruction of CH_3CCl_3.

The simple decomposition channels:

$$CH_3CCl_3 = CH_3CCl_2 + Cl \text{ and}$$

$$CH_3CCl_3 = CH_3 + CCl_3$$

will become more important with increasing temperature.

CH_4

The major reactions responsible for decay of CH_4 are:

$CH_4 + O = CH_3 + OH$

$CH_4 + OH = CH_3 + H_2O$

$CH_4 + Cl = CH_3 + HCl$

As shown, Cl, O and OH react with CH_4 and result in the acceleration of CH_4 destruction. Cl abstraction is relatively rapid and accelerates initiation of the hydrocarbons breakdown leading to more production of higher molecular weight hydrocarbons through combination of CH3 radical species.

The reactions which produce Cl, OH and O, such as

$CH_3CCl_3 = CH_3CCl_2 + Cl$

and $H + O_2 = O + OH$ are therefore important to the destruction of CH_4.

CH_2CCl_2

CH_2CCl_2 is the major intermediate product in oxidation and pyrolysis of 1,1,1-CH_3CCl_3 and is formed from the destruction of CH_3CCl_3 through

$CH_3CCl_3 = CH_2CCl_2 + HCl$

CH_2CCl_2 is not as reactive as CH_3CCl_3 and its conversion does not become important until higher temperatures are effected. The major reaction responsible for the decay of CH_2CCl_2 is

$CH_2CCl_2 + Cl = CCl_2CH + HCl.$

The following reactions:

$CH_2CCl_2 + H = CCl_2CH + H_2$

$CH_2CCl_2 + CH_3 = CH_2CCl + CH_3Cl$

$CCl_2CH = C_2HCl + Cl$

$CCl_2CH + O_2 = COCl_2 + HCO$

$CH_2CCl = C_2HCl + H$

$HClC_2 + O_2 = CHCl + CO_2$

and $HClC_2 + O_2 = CHClO + CO$ are the minor channels and will become more important with increasing temperature.

HCl

Hydrogen chloride is formed primarily from the unimolecular decomposition (HCl elimination) of CH_3CCl_3,

$CH_3CCl_3 = CH_2CCl_2 + HCl$

Attack CH_2CCl_2 by Cl also contributes to HCl formation,

$CH_2CCl_2 + Cl = CCl_2CH + HCl$

The minor reaction pathways responsible for the formation or loss of HCl are

$CH_2CCl_2 + H = CH_2CCl + HCl$

$CH_4 + Cl = CH_3 + HCl$

$CH_3 + CH_2Cl = C_2H_4 + HCl$

$O + HCl = OH + Cl$

$OH + HCl = Cl + H_2O$

$Cl + H_2 = HCl + H$

$Cl + HO_2 = HCl + O_2$

C_2H_3Cl

The formation of C_2H_3Cl is dominated by

$CH_2CCl_2 + H = C_2H_3Cl + Cl$ (an addition/elimination reaction) and

$CH_2CCl + HCl = C_2H_3Cl + Cl$

H and CH_3 react with C_2H_3Cl, such as

$C_2H_3Cl + H = C_2H_4 + Cl$

$C_2H_3Cl + CH_3 = C_2H_3 + CH_3Cl$

are the major pathways for the destruction of C_2H_3Cl at higher temperatures

(above 600 °C). As temperature is increased, the Cl addition to the C_2H_3Cl will accelerate the decay of C_2H_3Cl. Since the formation of C_2H_3Cl comes from H addition to CH_2CCl_2. The concentration of C_2H_3Cl is also strongly affected by reactions of CH_2CCl_2, such as:

$$CH_2CCl_2 + CH_3 = CH_2CCl + CH_3Cl$$

$$CH_2CCl_2 + Cl = CCl_2CH + HCl$$

$$CCl_2CH + O_2 = COCl_2 + HCO$$

and $CH_2CCl + O_2 = CClO + CH_2O$.

C_2H_2

The reactions:

$$C_2H_3Cl = C_2H_2 + HCl$$

$$C_2HCl + H = C_2H_2 + Cl$$

$C_2H_3 + O_2 = C_2H_2 + HO_2$ are primarily responsible for the formation of C_2H_2. The beta scission of C_2H_3 to C_2H_2 + H will also contribute to the formation of C_2H_2 at higher temperatures.

C_2H_4

The following reactions:

$C_2H_3Cl + H = C_2H_4 + Cl$ and

$CH_3 + CH_2Cl = C_2H_4 + HCl$

are most important for the formation of C_2H_4.

The reaction of Cl or OH with C_2H_4, such as

$C_2H_4 + OH = CH_3 + CH_2O$ and

$C_2H_3 + HCl = C_2H_4 + Cl$

are responsible for the destruction of C_2H_4.

CO

Unimolecular dissociation of HCO = CO + H is the major pathway to the form CO. The following reactions (in the order of reaction number) also indicate high sensitivity toward the formation of CO:

$CH_2CCl_2 + CH_3 = CH_2CCl + CH_3Cl$

$CH_2CCl_2 + Cl = CCl_2CH + HCl$

$CCl_2CH = C_2HCl + Cl$

$CCl_2CH + O_2 = COCl_2 + HCO$

$CH_2CCl = C_2HCl + H$

$HClC_2 + O_2 = CHCl + CO_2$

$C_2H_6 = 2\,CH_3$

$CH_4 + O_2 = CH_3 + HO_2$

$CH_3 + HO_2 = CH_3O + OH$

CO_2

The major reactions (in the order of reaction number) for the formation of CO_2 are:

$CO + OH = CO_2 + H$

$CO + HO_2 = CO_2 + OH$

$CO + O = CO_2$

The important reaction pathways to form the CO_2 are the same as in the case of CO.

C_2HCl

The reaction responsible for the concentrations of C_2HCl are:

$CCl_2CH = C_2HCl + Cl$

$CH_2CCl = C_2HCl + H$

The unimolecular reaction of $CH_2CCl_2 = C_2HCl + HCl$ will become more important with increasing temperature. The reactions which effect (control) CCl_2CH and CH_2CCl radicals, such as

$$CH_2CCl_2 + CH_3 = CH_2CCl + CH_3Cl$$

$$CH_2CCl_2 + Cl = CCl_2CH + HCl$$

$$CCl_2CH = C_2HCl + Cl$$

$$CCl_2CH + O_2 = COCl_2 + HCO$$

and $CH_2CCl + O_2 = CClO + CH_2O$, are also considered important to C_2HCl levels.

Table 1 Average Retention Time of Products

Table 1-a Flame Ionization Detector

Compound	Average Retention Time (min.)
CH_4	1.40
C_2H_2	1.96
C_2H_4	2.28
C_2H_6	2.60
CH_3Cl	4.30
CHCCl	6.70
CH_2CHCl	8.24
CH_2Cl_2	10.72
CH_2CCl_2	12.60
CH_3CHCl_2	13.66
CHClCHCl	14.17
CH_3CCl_3	15.40
$CHClCCl_2$	16.70
C_6H_6	17.90
$CH_2ClCHCl_2$	20.95

Table 1-b Thermal Conductivity Detector

Compound	Average Retention Time (min.)
Air	1.20
CO	2.10
CH_4	4.83
CO_2	8.20

Table 2 Relative Response Factor of Several Compounds

Table 2-a Flame Ionization Detector

Compound	Relative Response Factor (RRF)
Methane	1.00
Acethylene	2.13
Ethylene	1.87
Ethane	1.83
Propyne	3.16
Propene	3.24
Propane	3.20
Butane	4.03
Dichloromethane	0.93
1,1,1-Trichloroethane	1.73
1,1-Dichloroethylene	1.96
Chloroform	0.92
Tetrachloromethane	1.10
1,1,2-Trichloroethane	1.96

Table 2-b Thermal Conductivity Detector

Compound	Relative Response Factor (RRF)
Methane	1.00
Carbon monoxide	1.56
Carbon dioxide	1.32

Corrected area = measured area/RRF

Table 3. Rate Constants For $CH_3CCl_3 + CH_4 + O_2$ in excess Ar

$O_2 : CH_4 : CH_3CCl_3 : Ar = 4.5 : 0 : 0.5 : 95$	
Reactor I.D. (cm)	k_{expt}
0.4	$1.24 * 10^{12}\ e^{(-45588/RT)}$
1.05	$9.29 * 10^{12}\ e^{(-49009/RT)}$
1.6	$2.36 * 10^{12}\ e^{(-47102/RT)}$

$O_2 : CH_4 : CH_3CCl_3 : Ar = 4 : 0.5 : 0.5 : 95$	
Reactor I.D. (cm)	k_{expt}
0.4	$5.71 * 10^{11}\ e^{(-44404/RT)}$
1.05	$1.77 * 10^{12}\ e^{(-46233/RT)}$
1.6	$3.06 * 10^{12}\ e^{(-47627/RT)}$

$O_2 : CH_4 : CH_3CCl_3 : Ar = 3.75 : 0.75 : 0.5 : 95$	
Reactor I.D. (cm)	k_{expt}
0.4	$6.17 * 10^{12}\ e^{(-48429/RT)}$
1.05	$2.44 * 10^{12}\ e^{(-46799/RT)}$
1.6	$1.47 * 10^{12}\ e^{(-46420/RT)}$

$O_2 : CH_4 : CH_3CCl_3 : Ar = 3 : 1.5 : 0.5 : 95$	
Reactor I.D. (cm)	k_{expt}
0.4	$3.98 * 10^{11}\ e^{(-43875/RT)}$
1.05	$1.18 * 10^{12}\ e^{(-45588/RT)}$
1.6	$1.28 * 10^{12}\ e^{(-46267/RT)}$

$O_2 : CH_4 : CH_3CCl_3 : Ar = 0 : 1.5 : 0.5 : 98$	
Reactor I.D. (cm)	k_{expt}
0.4	$1.78 * 10^{12}\ e^{(-46378/RT)}$
1.05	$2.58 * 10^{12}\ e^{(-46837/RT)}$
1.6	$7.11 * 10^{11}\ e^{(-45388/RT)}$

For ratio sets 2,3,4 and 5 the overall rate constant for 1.05 cm reactor I.D. is $(1.99 \pm 0.65) * 10^{12} \exp(-(46364 \pm 587)/RT)$.

Table 4. Detailed Mechanism for $CH_3CCl_3/CH_4/O_2$ Reaction System

	REACTIONS	A@	n	Ea$	SOURCES
1.	CH3CCL3 = CH2CCL2 + HCL	6.30E13#	0.00	51.70	1
		3.35E13*	0.00	51.20	DISSOC
2.	CH3CCL3 = CH3CCL2 + CL	1.10E16#	0.00	68.30	2
		4.59E14*	0.00	66.60	DISSOC
3.	CH3CCL3 = CH3 + CCL3	9.10E16#	0.00	85.70	3
		2.05E14*	0.00	77.70	DISSOC
4.	CH3CCL3+CL=CCL3CH2+HCL	2.51E12	0.00	3.60	4
5.	CH3CCL3+OH=CCL3CH2+H2O	5.81E12	0.00	3.96	5
6.	CH3CCL3+O=CCL3CH2+OH	6.50E12	0.00	4.00	6
7.	CH3CCL3 + H = CH3CCL2 + HCL	3.00E13	0.00	5.20	6
8.	CH3CCL3+O2=CCL3CH2+HO2	1.00E13	0.00	46.80	6
9.	CH3CCL2+CH4 =CH3CHCL2+CH3	1.58E12	0.00	22.63	7
10.	CH3CCL2 = CH2CCL2 + H	2.60E13	0.00	41.40	8
11.	CH3CCL2 + H = CH3CHCL2	5.93E10	0.00	-7.55	QRRK1
12.	CH3CCL2 + H =C2H3CL +HCL	4.69E12	0.00	-0.70	QRRK1
13.	CCL3CH2 = CH2CCL2 + CL	1.35E10	0.00	7.60	6
14.	CCL3CH2 + H = CH3CCL3	5.60E36	-7.89	6.12	QRRK2
15.	CCL3CH2+H= CH2CCL2+HCL	2.02E12	0.00	-1.58	QRRK2
16.	CCL3CH2+H=CH3CCL2+CL	2.65E13	0.00	1.16	QRRK2
17.	CH2CCL2 = C2HCL + HCL	1.04E14#	0.00	73.70	9
		4.10E13*	0.00	72.70	DISSOC
18.	CH2CCL2 = CH2CCL + CL	1.17E16#	0.00	86.60	10
		1.40E14*	0.00	81.70	DISSOC
19.	CH2CCL2 + H = CH2CCL+HCL	1.20E13	0.00	5.50	11
20.	CH2CCL2 + H = CHCL2CH2	7.21E24	-4.89	7.92	QRRK3
21.	CH2CCL2 + H = C2H3CL+CL	1.00E13	0.00	5.80	QRRK3
22.	CH2CCL2 + H = CCL2CH + H2	1.58E13	0.00	6.00	6
23.	CH2CCL2+OH=CH2CCL2OH	1.41E30	-6.46	5.02	QRRK4
24.	CH2CCL2+OH=CH2CCLOH+CL	2.56E13	-0.50	2.00	QRRK4
25.	CH2CCL2 +OH=CH3CCLO+CL	1.21E05	1.15	11.88	QRRK4
26.	CH2CCL2 + OH = CH3 + COCL2	4.23E03	1.75	11.69	QRRK4
27.	CH2CCL2 + OH = CH2OHCCL2	1.36E10	0.00	-4.71	QRRK5
28.	CH2CCL2 + OH = CHCL2CH2O	1.45E05	0.00	7.17	QRRK5

Table 4. (cont'd)

	REACTIONS	A@	n	Ea$	SOURCES
29.	CH2CCL2+ OH = CHCL2CHO + H	1.65E09	0.00	13.30	QRRK5
30.	CH2CCL2 + OH = CHCL2 + CH2O	2.28E10	0.00	12.40	QRRK5
31.	CH2CCL2 + OH = CCL2CH + H2O	3.65E12	0.00	6.00	6
32.	CH2CCL2 + O2 = CCL2CH + HO2	1.06E13	0.00	61.60	6
33.	CH2CCL2 + O = CH2CCL2O	1.06E06	0.00	1.16	QRRK6
34.	CH2CCL2 + O = CH2 + COCL2	2.55E11	0.00	5.40	QRRK6
35.	CH2CCL2 + O = CCL2CH + OH	7.59E12	0.00	6.00	6
36.	CH2CCL2+CH3=CH2CCL+CH3CL	6.00E12	0.00	10.30	6
37.	CH2CCL2 + CL = CCL2CH + HCL	2.00E13	0.00	7.00	6
38.	CCL2CH = C2HCL + CL	5.72E14#	0.00	19.60	12
		1.00E10*	0.00	14.40	DISSOC
39.	CCL2CH + O2 = COCL2 + HCO	2.11E12	0.00	-0.60	6
40.	CH2CCL +CH4 = C2H3CL +CH3	2.90E11	0.00	7.20	13
41.	CH2CCL + OH = C2HCL + H2O	1.50E13	0.00	0.0	14,15
42.	CH2CCL + H = C2H3CL	1.24E31	-6.19	4.98	QRRK7
43.	CH2CCL + H = C2H3 + CL	1.02E14	0.00	0.08	QRRK7
44.	CH2CCL + H = C2H2 + HCL	8.34E11	0.00	-2.12	QRRK7
45.	CH2CCL + O2 = CH2CCLOO	6.63E27	-5.55	3.87	QRRK8
46.	CH2CCL + O2 = CH2CCLO + O	6.31E12	0.00	21.40	QRRK8
47.	CH2CCL + O2 = CH2OCCLO	2.85E22	-4.52	3.66	QRRK8
48.	CH2CCL + O2 = CCLO + CH2O	1.16E12	0.00	-1.09	QRRK8
49.	CH2CCL + O2 = H + CHOCCLO	1.97E11	0.00	-1.10	QRRK8
50.	CH2CCL + HCL = C2H3CL + CL	1.32E11	0.00	0.0	16
51.	CH2CCL = C2HCL + H	6.00E13#	0.00	40.60	17,18
		8.24E11*	0.00	35.50	DISSOC
52.	CHOCCLO + H = H2 + COCCLO	1.00E14	0.00	3.00	82
53.	CHOCCLO + O = OH + COCCLO	1.05E14	0.00	0.70	83
54.	CHOCCLO+OH=COCCLO+H2O	1.00E14	0.00	0.30	84
55.	CHOCCLO+CL=COCCLO+HCL	1.91E14	0.00	0.30	85
56.	COCCLO = CO + CCLO	4.20E13	0.00	20.48	86
		2.29E09	0.00	4.00	DISSOC
57.	CH3CHCL2 = C2H3CL + HCL	4.30E13#	0.00	57.70	19
		1.98E13*	0.00	55.40	DISSOC

Table 4. (cont'd)

	REACTIONS	A@	n	Ea$	SOURCES
58.	CH2CLCH2CL=C2H3CL +HCL	6.40E10	0.00	47.00	20
59.	CH2CLCH2CL = C2H4 + CL2	1.00E13	0.00	72.00	20
60.	CH2CLCH2CL+O=CH2CLCHCL+OH	4.99E12	0.00	5.01	5
61.	CH2CLCH2CL+OH=CH2CLCHCL+H2O	1.32E11	0.00	0.	21
62.	CH2CLCH2CL+CL=CH2CLCHCL+HCL	2.97E13	0.00	2.16	22
63.	CH2CLCHCL = C2H3CL + CL	6.50E13	0.00	19.84	23
64.	C2H3CL = C2H2 + HCL	5.30E13#	0.00	68.70	24
		1.99E13*	0.00	67.90	DISSOC
65.	C2H3CL = C2H3 + CL	4.08E15#	0.00	91.70	25
		1.16E14*	0.00	83.10	DISSOC
66.	C2H3CL + H = C2H3 + HCL	1.00E13	0.00	6.50	11
67.	C2H3CL + H = C2H4 + CL	1.34E13	0.00	3.32	QRRK9
68.	C2H3CL + H = CH2CLCH2	7.66E08	0.00	-1.67	QRRK9
69.	C2H3CL + OH = CH2CCL + H2O	4.90E12	0.00	4.50	26
70.	C2H3CL + OH = CH2CHCLOH	2.08E08	0.00	-5.93	QRRK10
71.	C2H3CL + OH = CH2CHOH + CL	2.67E12	0.00	1.50	QRRK10
72.	C2H3CL + OH = CH3 + CHCLO	4.20E09	0.00	11.60	QRRK10
73.	C2H3CL + OH = CH3CHO + CL	2.58E07	0.00	13.80	QRRK10
74.	C2H3CL + OH = CHCHCL + H2O	3.70E12	0.00	4.20	27
75.	C2H3CL + O = CHCHCL + OH	2.00E12	0.00	5.20	6
76.	C2H3CL + O = CH2CHCLO	1.95E07	0.00	-4.63	QRRK11
77.	C2H3CL + O = CH2 + CHCLO	2.76E11	0.00	4.17	QRRK11
78.	C2H3CL + O = C.H2CHO + CL	3.25E12	0.00	1.05	QRRK11
79.	C2H3CL + O = HCO + CH2CL	3.71E09	0.00	3.32	QRRK11
80.	C2H3CL + O = CH2CHO. + CL	1.07E10	0.00	5.07	QRRK11
81.	C2H3CL + O2 = CHCHCL + HO2	1.40E13	0.00	57.40	6
82.	C2H3CL + O2 = CH2CCL + HO2	1.10E13	0.00	56.00	6
83.	C2H3CL + CH3 = C2H3 + CH3CL	2.67E11	0.00	9.80	6
84.	C2H3CL + CL = CHCHCL + HCL	5.00E13	0.00	7.00	28
85.	C2H5CL = C2H4 + HCL	3.24E13#	0.00	56.60	29
		2.79E13*	0.00	56.40	DISSOC
86.	C2H5CL = C2H5 + CL	2.18E15#	0.00	79.50	17,30
		1.66E37*	-6.71	90.90	DISSOC

Table 4. (cont'd)

	REACTIONS	A@	n	Ea$	SOURCES
87.	C2H5CL = CH3 + CH2CL	6.84E15#	0.00	90.90	30
		1.44E39*	-7.26	98.31	DISSOC
88.	CH2CCLOH+O = H+CH2O+CCLO	5.00E12	0.00	2.00	31
89.	CH2CCLOH+H=CH2CHOH+CL	5.00E12	0.00	6.00	31
90.	CH2CCLOH+OH=CH2CCLO+H2O	5.00E12	0.00	5.00	31
91.	CH2CCLOH+CL=CHCCLOH+HCL	3.00E13	0.00	7.00	32
92.	CH2CCLOH+CL= CH2CCLO+HCL	3.00E13	0.00	2.50	5,33
93.	CHCCLOH = HCCOH + CL	4.40E09	0.00	2.20	31,34
94.	CH2CCLO = CH2CO + CL	5.00E13	0.00	6.15	31,35
95.	C2HCL + H = C2H + HCL	1.00E13	0.00	7.00	36
96.	C2HCL + H = C2H2 + CL	2.00E13	0.00	2.10	37
97.	C2HCL + OH = HCCOH + CL	2.50E05	2.30	13.50	38,39
98.	C2HCL + OH = CH2CO + CL	1.10E-4	4.50	-1.00	38,39
99.	C2HCL + OH = CH2CL + CO	2.40E-4	4.00	-2.00	38,39
100.	C2HCL + OH = C2CL + H2O	1.70E07	2.00	13.50	38,39
101.	C2HCL + O = C2CL + OH	1.58E15	-0.6	15.00	38,40
102.	C2HCL + O = CHCL + CO	5.10E06	2.00	1.90	38,40
103.	C2HCL + O = CHCO + CL	5.10E06	2.00	1.90	38,40
104.	C2HCL + O2 = C2CL + HO2	6.00E12	0.00	75.00	14,41
105.	C2HCL + H2 = CH2CCL + H	1.20E12	0.00	64.98	14,42
106.	C2HCL = HCLC2	3.98E13	0.00	43.00	31
107.	C2HCL + CL = C2CL + HCL	7.50E13	0.00	12.40	81
108.	C2CL + O2 = CO + CCLO	5.00E13	0.00	1.50	43,44
109.	C2CL + H2 = C2HCL + H	3.50E12	0.00	2.10	43,45
110.	C2CL + CH4 = C2HCL + CH3	1.20E13	0.0	0.	46,47
111.	CHCL + O2 = CCLO + OH	1.00E12	0.0	0.	38,48
112.	CHCL + O2 = CHCLO + O	1.00E12	0.0	0.	38,48
113.	HCLC2 + O2 = CHCL + CO2	2.50E12	0.0	0.	31
114.	HCLC2 + O2 = CHCLO + CO	2.50E12	0.00	0.	31
115.	CHCO + H = CH2S + CO	1.00E14	0.00	0.	38
116.	CHCO + O = H + 2CO	1.00E14	0.00	0.	38
117.	CHCO + O2 = 2CO + OH	1.60E12	0.00	0.85	38
118.	CHCO + CHCO = C2H2 + 2CO	1.00E13	0.00	0.	38

Table 4. (cont'd)

	REACTIONS	A@	n	Ea$	SOURCES
119.	CH3CL = CH3 + CL	2.63E15#	0.00	81.60	49
		2.40E13*	0.00	77.20	DISSOC
120.	CH3CL + H = CH3 + HCL	1.00E14	0.00	7.60	4
121.	CH3CL + CL = CH2CL + HCL	1.30E14	0.00	3.60	4
122.	CH3CL + CL = CH3 + CL2	1.00E14	0.00	25.00	4
123.	CH3CL + OH = CH2CL + H2O	1.32E12	0.00	2.30	4
124.	CH3CL + O = CH2CL + OH	1.92E13	0.00	7.99	5
125.	CH3CL + CH3 = CH4 + CH2CL	3.30E11	0.00	9.40	4
126.	CH3CL + O2 = CH2CL + HO2	2.00E13	0.00	52.70	50
127.	CH3CL + HO2 = CH2CL + H2O2	9.00E10	0.00	8.50	51
128.	CH2CL + CH2CL = CH2CLCH2CL	2.04E11	0.00	-4.51	52
129.	CH2CL + CH2CL = C2H3CL + HCL	2.14E12	0.00	2.54	52
130.	CH2CL+CH2CL=CH2CLCH2 +CL	1.11E11	0.00	6.23	52
131.	CCL3 + OH = CCL3OH	9.13E09	0.00	-5.50	52
132.	CCL3 + OH = COCL2 + HCL	1.62E13	0.00	-0.30	52
133.	CCL3 + OH = CCL2OH + CL	8.65E12	0.00	4.30	52
134.	CCL3 + O2 = CCL3OO	7.33E06	0.00	-13.50	52
135.	CCL3 + O2 = CCL3O + O	1.14E14	0.00	50.50	52
136.	CCL3 + O2 = COCL2 + CLO	1.11E10	0.00	6.30	52
137.	CCL3 + O = CCL3O	8.60E07	0.00	-3.10	52
138.	CCL3 + O = COCL2 + CL	1.98E13	0.00	0	52
139.	CCL3 + CH3 = CH2CCL2 + HCL	7.88E11	0.00	-1.80	52
140.	CCL3 + CH3 = CH3CCL2 + CL	3.80E13	0.00	1.90	52
141.	CCL3 + HO2 = CCL3OOH	5.50E07	0.00	-8.60	52
142.	CCL3 + HO2 = CCL3O + OH	5.81E12	0.00	-0.10	52
143.	COCL2 = CCLO + CL	1.30E12	0.00	68.00	53
144.	COCL2 + OH = CCLO + HOCL	1.00E13	0.00	15.00	54
145.	COCL2 + O = CCLO + CLO	2.00E13	0.00	17.00	6
146.	COCL2 + O2 = CCLO + CLOO	5.40E13	0.00	73.60	6
147.	COCL2 + H = CCLO + HCL	5.00E13	0.00	2.50	6
148.	COCL2 + CH3 = CCLO + CH3CL	1.90E13	0.00	12.90	6
149.	COCL2 + CL = CCLO + CL2	3.20E14	0.00	23.50	6
150.	CH3CHO = CH3 + HCO	3.80E15	0.00	78.50	5

Table 4. (cont'd)

	REACTIONS	A@	n	Ea$	SOURCES
151.	CH3CHO + OH = CH3CO + H2O	3.40E12	0.00	-0.60	55
152.	CH3CHO + O = CH3CO + OH	5.00E12	0.00	1.80	56
153.	CH3CHO+HO2=CH3CO+H2O2	1.50E11	0.00	9.00	46
154.	CH3CHO + O2 = CH3CO + HO2	1.00E13	0.00	38.90	46
155.	CH3CHO + CH3 = CH3CO+ CH4	8.50E10	0.00	6.00	56
156.	C2H6 = CH3 + CH3	7.94E16#	0.00	89.40	57
		3.64E16*	0.00	89.50	DISSOC
157.	C2H6 = C2H5 + H	1.26E16#	0.00	98.00	57
		2.03E14*	0.00	92.30	DISSOC
158.	C2H6 = C2H4 + H2	2.29E17	0.00	67.64	5
159.	C2H6 + H = C2H5 + H2	6.61E13	0.00	9.70	4
160.	C2H6 + CH3 = C2H5 + CH4	5.75E11	0.00	11.60	4
161.	C2H6 + CL = C2H5 + HCL	4.64E13	0.00	0.18	55
162.	C2H6 + O = C2H5 + OH	3.00E07	2.00	5.10	56
163.	C2H6 + OH = C2H5 + H2O	6.30E06	2.00	0.60	56
164.	C2H6 + HO2 = C2H5 + H2O2	6.00E12	0.00	19.30	56
165.	C2H6 + O2 = C2H5 + HO2	4.04E13	0.00	50.87	14
166.	C2H6 + CCL3 = C2H5 + CHCL3	2.04E14	0.00	18.10	4
167.	C2H5 = C2H4 + H	4.31E12	1.19	37.20	14
168.	C2H5 + H = CH3 + CH3	5.10E14	0.00	2.85	QRRK12
169.	C2H5 + O2 = C2H4 + HO2	8.89E28	-5.43	9.92	59
170.	C2H5 + O2 = C2H5OO	1.66E55	-13.49	15.03	59
171.	C2H5 + O2 = C2H5O + O	3.24E14	-0.65	28.63	59
172.	C2H5 + O2 = CH2CH2OOH	1.02E50	-12.40	15.46	59
173.	C2H5 + O2 = CH3CHO + OH	5.89E12	-0.77	9.36	59
174.	C2H5 + CH2O = C2H6 + HCO	4.93E10	2.81	5.86	14
175.	C2H5 + C2H4 = C2H3 + C2H6	1.68E13	0.00	22.16	5
176.	C2H5 + C2H5 = C2H4 + C2H6	1.40E12	0.00	0.	14,56
177.	C2H5 + OH = C2H4 + H2O	2.41E13	0.00	0.	14
178.	C2H5 + HO2 = C2H4 + H2O2	3.01E11	0.00	0.	14
179.	C2H5 + O = CH2O + CH3	1.61E13	0.00	0.	14
180.	C2H5 + O = C2H4 + OH	5.00E13	0.00	0.	60
181.	C2H5 + O = CH3CHO + H	5.00E13	0.00	0.	61

Table 4. (cont'd)

	REACTIONS	A@	n	Ea$	SOURCES
182.	C2H5 + CL2 = C2H5CL + CL	7.58E12	0.00	-0.24	62
183.	C2H4 = C2H3 + H	2.00E16#	0.00	110.00	46
		2.82E15*	0.00	108.00	DISSOC
184.	C2H4 + O = C.H2CHO + H	5.82E12	0.00	1.53	87
185.	C2H4 + O = CH3 + HCO	2.70E30	-4.54	39.49	87
186.	C2H4 + O = CH2O + CH2	2.50E13	0.00	5.00	63
187.	C2H4 + O2 = C2H3 + HO2	4.22E13	0.00	57.62	14
188.	C2H4 + OH = CH2CH2OH	2.59E49	-11.9	16.75	87
189.	C2H4 + OH = CH2CHOH + H	3.95E12	0.00	10.50	87
190.	C2H4 + OH = CH3 + CH2O	1.29E11	0.00	9.08	87
191.	C2H4 + OH = Ch3CHO + H	3.21E11	0.00	9.80	87
192.	C2H4 + OH = C2H3 + H2O	1.45E13	0.00	4.18	65
193.	C2H4 + H = C2H3 + H2	1.50E14	0.00	10.20	60
194.	C2H4 + H2 = C2H5 + H	1.02E13	0.00	68.15	14
195.	C2H4 + AR = C2H2 + H2 + AR	2.60E17	0.00	79.29	56
196.	C2H4 + CH3 = CH4 + C2H3	3.60E-1	4.00	9.50	46
197.	C2H4 + HO2 = CH3CHO + OH	6.03E09	0.00	15.80	14
198.	C2H3 = C2H2 + H	3.16E12	0.00	38.30	57
199.	C2H3 + HCL = C2H4 + CL	3.97E11	0.00	0.67	16
200.	C2H3 + CL2 = C2H3CL + CL	5.24E12	0.00	-0.50	62
201.	C2H3 + H = C2H2 + H2	9.64E13	0.00	0.	14
202.	C2H3 + OH = C2H2 + H2O	3.01E13	0.00	0.	14
203.	C2H3 + H2O2 = C2H4 + HO2	1.21E10	0.00	-0.60	14
204.	C2H3 + CH2O = C2H4 + HCO	5.42E03	2.81	5.86	14
205.	C2H3 + O2 = C2H3OO	2.26E38	-8.10	8.45	66
206.	C2H3 + O2 = CH2CHO + O	9.86E14	-0.59	5.03	66
207.	C2H3 + O2 = C2H2 + HO2	2.77E22	-3.30	6.57	66
208.	C2H3 + O2 = CYC2H3OO	1.12E36	-8.18	9.40	66
209.	C2H3 + O2 = CH2OCHO	3.01E28	-6.24	7.31	66
210.	C2H3 + O2 = CH2O + HCO	1.65E26	-4.34	6.70	66
211.	C2H3 + O2 = CHOCHO + H	1.47E23	-3.83	6.24	66
212.	C2H2 = C2H + H	5.83E15#	0.00	127.90	67
		1.16E13*	0.00	124.00	DISSOC

Table 4. (cont'd)

	REACTIONS	A@	n	Ea$	SOURCES
213.	C2H2 + CH3 = CH4 + C2H	1.81E11	0.00	17.29	14
214.	C2H2 + O = CH2CO	1.70E11	0.00	0.	68
215.	C2H2 + O = CHCO + H	2.96E12	0.00	2.19	87
216.	C2H2 + O = CH2 + CO	3.54E12	0.00	0.39	87
217.	C2H2 + O2 = HCO + HCO	1.20E11	0.00	44.50	QRRK13
218.	C2H2 + O2 = C2H + HO2	1.20E13	0.00	74.50	14
219.	C2H2 + OH = HCCOH + H	4.51E12	0.00	14.40	87
220.	C2H2 + OH = C.H2CHO	5.07E26	-4.95	5.80	87
221.	C2H2 + OH = CH2CO + H	5.91E11	0.00	2.17	87
222.	C2H2 + OH = CH3CO	1.66E22	-4.00	4.93	87
223.	C2H2 + OH = CO + CH3	2.63E12	0.00	0.75	87
224.	C2H2 + OH = C2H + H2O	1.44E04	2.68	12.00	14
225.	C2H2 + HO2 = CH2CO + OH	6.02E09	0.00	7.98	14
226.	C2H2 + CL = C2H + HCL	1.57E14	0.00	16.90	71
227.	C2H2 = H2C2	3.98E13	0.00	52.60	72
228.	H2C2 + O2 = CH2 + CO2	5.00E12	0.00	0.	31
229.	H2C2 + O2 = CH2O + CO	5.00E12	0.00	0.	31
230.	C2H + O2 = CO + HCO	5.00E13	0.00	1.50	43
231.	C2H + H2 = C2H2 + H	3.50E12	0.00	2.10	43
232.	C2H + C2H4 = C2H3 + C2H2	1.20E13	0.00	0.	46
233.	CH4 = CH3 + H	3.72E15#	0.00	103.80	14
		7.43E13*	0.00	101.00	DISSOC
234.	CH4 + CH3O = CH3 + CH3OH	1.57E11	0.00	8.84	14
235.	CH4 + O2 = CH3 + HO2	7.90E13	0.00	56.00	38
236.	CH4 + O = CH3 + OH	1.20E07	2.1	7.60	38
237.	CH4 + H = CH3 + H2	2.20E04	3.0	8.74	56
238.	CH4 + OH = CH3 + H2O	1.60E06	2.1	2.46	56
239.	CH4 + CL = CH3 + HCL	3.09E13	0.00	3.60	4
240.	CH4 + HO2 = CH3 + H2O2	1.81E11	0.00	18.60	14
241.	CH3 + H = CH2 + H2	9.00E13	0.00	15.10	38
242.	CH3 + CH2CL = C2H4 + HCL	1.88E13	0.00	2.00	QRRK14
243.	CH3 + CH2CL = C2H5 + CL	2.43E13	0.00	6.10	QRRK14
244.	CH3 + O2 = CH3O + O	2.05E19	-1.57	29.23	38

Table 4. (cont'd)

	REACTIONS	A@	n	Ea$	SOURCES
245.	CH3 + O2 = CH3OO	2.58E33	-7.18	5.30	73
246.	CH3 + O2 = CH2O + OH	3.04E10	0.00	11.70	74
247.	CH3 + O = CH2O + H	8.94E13	-0.03	0.	73
248.	CH3 + O = CH3O	6.76E15	-2.14	0.60	73
249.	CH3 + OH = CH3OH	1.12E41	-8.44	11.80	73
250.	CH3 + OH = CH3O + H	1.54E19	-1.74	7.60	73
251.	CH3 + OH = CH2O +H +H	5.30E12	0.00	0.	64
252.	CH3 + OH = CH2 + H2O	7.50E06	2.00	5.00	38
253.	CH3 + HO2= CH3O + OH	2.00E13	0.00	0.	60
254.	CH3O + O2 = CH2O + HO2	1.00E13	0.00	7.17	56
255.	CH3O = CH2O + H	1.96E14	0.00	25.07	5
256.	CH3O + CH3 = CH2O + CH4	2.40E13	0.00	0.	14
257.	CH2O = CO + H2	4.52E15	0.00	35.30	5
258.	CH2O + H = HCO + H2	2.50E13	0.00	3.99	56
259.	CH2O + O2 = HCO + HO2	1.79E13	0.00	38.91	5
260.	CH2O + O = HCO + OH	3.50E13	0.00	3.51	56
261.	CH2O + HO2 = HCO + H2O2	1.00E12	0.00	8.00	75
262.	CH2O + OH= HCO + H2O	3.00E13	0.00	1.19	76
263.	CH2O + CL = HCO + HCL	4.40E13	0.00	0.	55
264.	CH2O + CH3 = HCO + CH4	1.00E11	0.00	6.00	56
265.	CHCLO = HCO + CL	4.30E11	0.00	72.30	53
266.	CHCLO = CO + HCL	8.60E10	0.00	34.10	53
267.	CHCLO + OH = CCLO + H2O	7.50E12	0.00	1.20	6
268.	CHCLO + O = CCLO + OH	8.80E12	0.00	3.50	6
269.	CHCLO + O2 = CCLO + HO2	4.50E12	0.00	41.80	6
270.	CHCLO + CL = CCLO + HCL	2.40E13	0.00	0.50	6
271.	CHCLO + CH3 = CCLO + CH4	2.50E10	0.00	6.00	6
272.	CHCLO + CH3 = HCO + CH3CL	1.49E13	0.00	8.80	6
273.	HCO + AR = CO + H + AR	2.50E14	0.00	13.30	6
274.	HCO + CH3 = CH4 + CO	1.00E12	0.00	0.	6
275.	HCO + O2 = CO + HO2	3.00E13	0.00	0.	56
276.	HCO + OH = CO + H2O	5.00E13	0.00	0.	56
277.	HCO + O = CO + OH	3.00E13	0.00	0.	56

Table 4. (cont'd)

	REACTIONS	A@	n	Ea$	SOURCES
278.	HCO + HO2 = CO + H2O2	5.00E12	0.00	0.	6
279.	HCO + H = CO + H2	2.00E14	0.00	0.	56
280.	HCO + CL = CO + HCL	1.50E13	0.00	0.	6
281.	CCLO = CO + CL	1.30E14	0.00	8.00	6
282.	CCLO + O2 = CO2 + CLO	1.00E13	0.00	0.	31
283.	CCLO + H = CO + HCL	3.50E16	-0.79	5.00	77
284.	CH2CO = CH2 + CO	3.00E14	0.00	70.90	5,38
285.	CH2CO + H = CH3 + CO	1.13E13	0.00	3.43	38
286.	CH2CO + H = CHCO + H2	5.00E13	0.00	8.00	38
287.	CH2CO + OH = CHCO + H2O	7.50E12	0.00	2.00	38
288.	CH2CO + OH = HCO + CH2O	2.80E13	0.00	0.	70
289.	CH2CO + O = CH2O + CO	1.70E12	0.00	1.40	61
290.	CH2CO + O = CH2 + CO2	1.75E12	0.00	1.35	38
291.	CH2CO + O = CHCO + OH	1.00E13	0.00	8.00	38
292.	CH2S + AR = CH2 + AR	1.00E13	0.00	0.	38
293.	CH2S + CH4 = 2CH3	4.00E13	0.00	0.	38
294.	CH2S + C2H6 = CH3 + C2H5	1.20E14	0.00	0.	38
295.	CH2S + O2 = CO + OH + H	3.00E13	0.00	0.	38
296.	CH2S + H2 = CH3 + H	7.00E13	0.00	0.	38
297.	CH2S + H = CH2 + H	2.00E14	0.00	0.	38
298.	CH2 + H = CH + H2	1.00E18	-1.56	0.	38
299.	CH2 + OH = CH + H2O	1.13E07	2.00	3.00	38
300.	CH2 + OH = CH2O + H	2.50E13	0.00	0.	38
301.	CH2 + CO2 = CH2O + CO	1.10E11	0.00	1.00	38
302.	CH2 + O = CO + 2H	5.00E13	0.00	0.	38
303.	CH2 + O = CO + H2	3.00E13	0.00	0.	38
304.	CH2 + O2 = CO2 + 2H	1.60E12	0.00	1.00	38
305.	CH2 + O2 = CH2O + O	5.00E13	0.00	9.00	38
306.	CH2 + O2 = CO2 + H2	6.90E11	0.00	0.50	38
307.	CH2 + O2 = CO + H2O	1.90E10	0.00	-1.00	38
308.	CH2 + O2 = CO + OH + H	8.60E10	0.00	-0.50	38
309.	CH2 + O2 = HCO + OH	4.30E10	0.00	-0.50	38
310.	CH2 + CH3 = C2H4 + H	3.00E13	0.00	0.	38

Table 4. (cont'd)

	REACTIONS	A@	n	Ea$	SOURCES
311.	CH2 + CHCO = C2H3 + CO	3.00E13	0.00	0.	38
312.	CH2 + CH2 = C2H2 + H2	4.00E13	0.00	0.	38
313.	CO + OH = CO2 + H	4.40E06	1.50	-0.70	56
314.	CO + HO2=CO2+OH	1.51E14	0.00	23.60	56
315.	CO + O2 = CO2 +O	2.50E13	0.00	47.60	56
316.	CO + O = CO2	3.00E14	0.00	3.00	78
317.	H + OH + AR = H2O + AR	7.50E23	-2.6	0.	79
318.	H + O + AR = OH + AR	2.29E14	0.0	3.90	4
319.	H + O2 = O + OH	2.20E14	0.00	16.79	76
320.	O2 + AR = AR + O + O	1.85E11	0.5	95.56	79
321.	H + HO2=OH + OH	1.50E14	0.00	1.00	60,79
322.	H + HO2 = H2 + O2	2.50E13	0.00	0.69	60,79
323.	H2 + HO2 = H2O2 + H	3.01E13	0.00	26.03	14
324.	O + HO2 = OH + O2	2.00E13	0.00	0.	60,79
325.	O + H2O = OH + OH	1.50E10	1.14	17.20	56
326.	O + H2 = H + OH	1.08E04	2.80	5.92	14
327.	H + H2O = H2 + OH	4.60E08	1.60	18.60	76
328.	OH + HO2=H2O + O2	2.00E13	0.00	0.	76
329.	O + HCL = OH + CL	5.24E12	0.00	6.40	4
330.	OH + HCL = CL + H2O	2.45E12	0.00	1.10	4
331.	CL + CL + AR = CL2 + AR	2.34E14	0.00	-1.80	4
332.	CL + H2 = HCL + H	7.94E13	0.00	5.30	58
333.	CL + HO2= HCL + O2	1.08E13	0.00	0.10	80
334.	CL + HO2 = CLO + OH	2.42E13	0.00	2.30	80
335.	CL2 + OH = HOCL + CL	8.43E11	0.00	1.80	80
336.	HOCL + O = OH + CLO	6.03E12	0.00	4.40	80
337.	CLO + CO = CL + CO2	6.03E11	0.00	7.35	80
338.	CH3 + CLO = CH3CL + O	6.00E12	0.00	4.00	31
339.	CH3 + CLO = CH3O + CL	9.00E12	0.00	1.00	31

@ Unit of A factor are cc/(mol sec.) for bimolecular reactions and 1/sec for unimolecular reactions.; $ Unit of Ea is Kcal/mol; # High pressure limit value
* Apparent rate constants by DISSOC computer code analysis
Pressure dependent : rate expression given for 760 torr.
Temperature range : 773 - 1273 K

DISSOC : apparent rate constant by DISSOC computer code analysis
QRRK : apparent rate constant by CHEMACT computer code analysis

SOURCES

1. $A = 10^{13.72} * 10^{(-4/4.6)} * 9$, $E_a=51.7\ (\Delta H_r + 42.7)$ (E_a ref: Benson, S.W. and G. N. Spokes, 11 th Symposium, 95,1966).

2. A factor based upon entropy change for reverse. A_{-1} taken as that for $iC_4H_9 + CH_3$ (A=2.0E+13), $E_a = \Delta H_r - RT$.

3. A factor based upon entropy change for reverse. A_{-1} taken as that for $CH_3 + 1\text{-}C_4H_9$ (A = 2.0 E+13), $E_a = \Delta H_r - RT$.

4. Kerr, J.A. and S. J. Moss, "Handbook of Bimolecular and Termolecular Gas Reaction, Vol.I & II", CRC Press Inc. (1981).

5. National Institute of Standard and Technology Chemical Gas Kinetics Database v. 2.0 (1990).

6. Won, Y. S., Ph.D. Thesis, NJIT (1991).

7. A factor based upon entropy change for reverse. A_{-1} taken as that for $n\text{-}C_4H_{10} + CH_3 = 2\text{-}C_4H_9 + CH_4$ (A = 3.98E+11), Ea from Evans-Polanyi Plot.

8. A factor based upon entropy change for reverse. A_{-1} taken as that for $CH_3CCl_2 = CH_2CCl_2 + H$ (A =1.6E+13), $E_a = \Delta H_r + 2.0$.

9. $A = 10^{13.72} * 2$, $E_a = \Delta H_r + 45$ (ref: Zabel, F., Int. J. of Chem. Kinetics, 9 (1977): 651.).

10. A factor based upon entropy change for reverse. A_{-1} taken as that for $C_3H_5 + CH_3$ (A = 2.0 E+13), $E_a = \Delta H_r - RT$.

11. Barat, R.B. and J. W. Bozzelli, "Reaction of Atomic Hydrogen with Vinyl Chloride", submitted to J. Phys. Chem. (1988), (A factor taken as 1.2 of that for $2\text{-}C_4H_9 + H_2$).

12. A_{-1} taken as that for $C_2H_2 + Cl$ (A=2.0E13, Ref:Source 5.) and microscopic reversibility, $E_a = \Delta H_r + 2.0$.

13. A factor based upon entropy change for reverse. A_{-1} taken as that for $C_2H_4 + CH_3 = C_2H_3 + CH_4$ (A = 1.58E+11), E_a taken as $C_2H_3 + H_2$, $E_a=7.4$.

14. Tsang, W. and R. F. Hampson, J. of Phys. Chem. Ref. Data, 15 (1986): 1087.

15. A factor taken as 1/2 of that for C_2H_3 + OH (A=3.0E13, Ref: source 14).

16. Russell,J.J., S. M. Senkan, J. A. Seetula and D. Gutman, J. of Phys. Chem., 93, 13 (1989): 5184.

17. Allara, D.L. and R. Shaw, J. of Phys. Chem. Ref. Data, 9 (1980): 523.

18. A_{-1} taken as that for C_2H_2 + H (A=1.0E14, Ref: source 17) and microscopic reversibility, $E_a = \Delta H_r + 2.0$.

19. $A = 10^{13.72} * 10^{(-4/4.6)} * 6$, $E_a = \Delta H_r + 40.8$.

20. Barton,D. H. R. and K. E. Howlett, J. Chem. Soc., 155 (1949).

21. Howard, C.J. and K. M. Evenson, J. Chem. Phys., 64 (1976): 4303.

22. Tschuikow-Roux, E., F. Faraji and J. Niedzielski, Int. J. Chem. Kinet., 18 (1986): 513.

23. Wolfrum, J., Laser Chem., 6 (1986): 125.

24. $A = 10^{13.72} * 1$, $E_a = \Delta H_r + 45$ (ref: Zabel, F., Int. J. Chem. Kinetics, 9 (1977): 651.

25. A factor based upon ΔS for reverse, A_{-1} taken as that for C_2H_5 + CH_3 (A = 2.0 E+13, Dean, A.M., J. of Phys. Chem, 89 (1985): 4600.), E_a = 91.7.

26. A= 1/4 * A(C_2H_3Cl + OH) (Ref: Liu and Jonah, J. of Phys. Chem, 93 (1989): 4092.).

27. A= 1/6 * A(C_2H_3Cl + OH) (Ref: Liu and Jonah, J. of Phys. Chem, 93 (1989): 4092).

28. Manion, J.A. and R. Louw, J. Chem. Perk. Trans., 2 (1988): 1547.

29. Benson,S.W., "Thermochemical Kinetics", 2nd ed., John Wiley & Son (1976).

30. A_{-1} taken as that for C_2H_5 + CH_3 (A=2.0E13, Ref:Source 17), $E_a = \Delta H_r - RT$.

31. estimation of this work.

32. A and E_a taken as that for CH_2CCl_2 + Cl.

33. A and E_a estimated from R-OH + Cl of Source 5.

34. A_{-1}=1E13, Ea_{-1}= 1.85(kcal/mol).

35. $E_a = \Delta H_r + 2$.

36. A taken as that for C_2H_3Cl + H, E_a= 7.0.

37. A taken as that for C_2H_3Cl + H, $E_a = E_a(C_2H_3Cl + H)-1$.

38. Miller, J.A. and C. T. Bowman, Pro. Ener. Comb. Sc., Vol 15 (1989): 287.

39. A taken as 1/2 of that for C_2H_2 + OH (Ref: source 38).

40. A taken as 1/2 of that for C_2H_2 + O (Ref: source 38).

41. A taken as 1/2 of that for $C_2H_2 + O_2$ (Ref: source 14).

42. A taken as 1/2 of that for $C_2H_2 + H_2$ (Ref: source 14).

43. Warnatz, J. Combust. Sci. and Technol., 34 (1983): 177.

44. A and E_a taken as that for $C_2H + O_2$ (Ref: source 43).

45. A and E_a taken as that for $C_2H + H_2$ (Ref: source 43).

46. Dean's mechanism.

47. A and Ea taken as that for $C_2H + CH_4$ (Ref: source 46).

48. A and Ea taken as that for $CH_2 + O_2$ (Ref: source 38).

49. A factor based upon entropy change for reverse. A_{-1} taken as that for CH_3 + CH_3 (A = 2.5 E+13, Ref:Source 17), $E_a = \Delta H_r$ - RT.

50. A factor taken as 1/2 of that for $CH_4+O_2 = CH_3 + HO_2$ (A=4.0E13, Ref: source 14), $E_a = \Delta H_r + 0.5$.

51. A factor taken as 1/2 of that for $CH_4 + HO_2 = CH_3 + H_2O_2$ (A=1.81E11, Ref: source 14), $E_a = \Delta H_r + 3$.

52. result of QRRK calculation from Won, Y.S., Ph. D. Thesis, NJIT (1991).

53. result of DISSOC calculation from Won, Y.S., Ph.D. Thesis, NJIT (1991).

54. Chang, W.D. et. al., Combust. Sci. and Technol., 49 (1986): 107.

55. Atkinson, R., D. L. Baulch, R. A. Cox, R. F. Hampson, Jr., J. A. Kerr and J. Troe, J. of Phys. Chem. Ref. Data, 18 (1989): 881.

56. Warnatz, J.,(1984) in Combustion Chemistry (W. C. Gardiner, Jr.,Ed.) Springer-Verlag, New York.

57. Dean, A.M., J. Phys. Chem., 89 (1985): 4600.

58. Ritter, E., J. W. Bozzelli and A. M. Dean, J. Phys. Chem., 94, (1990): 2493.

59. Bozzelli, J.W. and A. M. Dean, J. Phys. Chem., 94, 8 (1990): 3313.

60. Hennessy, R. J., C. Robinson and D. B. Smith, Twenty-first Symposium (International) on Combustion/The Combustion Institute (1986): 761-772.

61. Hasan, K. Md., M.Sc. Thesis, NJIT (1990).

62. Timonen, R. S., J.J. Russell, D. Sarzynski and D. Gutman, J. Phys. Chem., 91 (1987): 1873-1877.

63. Peeters, J. and G. Mahnen, Combust. Inst. European Symp., Academic Press., London, 1 (1973): 53.

64. Olson, D. B. ,and W. C. Gardiner, Jr., Combust. Flame, 32 (1978): 151.

65. Liu, A.-D., W. A. Mulac and C. D. Jonah, Int. J. Chem. Kinet., 19 (1987): 25.

66. Bozzelli, J.W. and A. M. Dean, paper submitted to J. Phys. Chem..

67. A_{-1} = 1.81E14 (Ref:source 14) and microscopic reversibility, $E_a = \Delta H_r - RT$.

68. Gaedtke, H., K. Glaenzer, H. Hippler, K. Luther and J. Troe, Sym. Int. Combust. Proc., 14 (1973): 295.

69. Axelsson, E.I., K. Brezinsky and C. K. Westbrook et. al., The Canadian and Western State Sections of the Combust. Inst., April (1986), Banff, Alberta, Canada.

70. Vandooren, J and P. J. Van Tiggelen Symp. Inst. Combust. Proc, 16 (1977): 1133.

71. Weissman, M. and S. W. Benson, Int. J. of Chem. Kinetics, 16 (1984): 307.

72. $E_a = \Delta H_r + 12$, A estimated by this work.

73. Dean, A.M. and P. R. Westmoreland, Int. J. of Chem. Kinetics, Vol 19 (1987): 207-228.

74. Yu, H.H., M.Sc. Thesis, NJIT (1990).

75. Cathonnet, M. et. al., 19th Symposium (International) on Combustion/The Combustion Institute (1982): 167.

76. Warnatz, J., H. Bockhorn, A. Moser and H. W. Wenz, Nineteenth Symposium (International) on Combustion/ The Combustion Institute (1982): 197-209.

77. Barat, R.B. et. al., Combust. Sci and Technol., 74 (1990): 361.

78. Baldwin, R.R., D. Jackson, A. Melvin and B. N. Rossiter, Int. J. Chem. Kinet., 4 (1972): 277.

79. Miller, J.A., R. E. Mitchell, M. D. Smooke and R. J. Kee, Nineteenth Symposium (International) on Combustion/ The Combustion Institute (1982): 181-196.

80. Demore, W.B., D. M. Golden, R. F. Hampson, C. J. Howard, M. J. Kurylo, M. J. Molina, A. R. Ravishankara and S. P. Sander, JPL publication, 87-41 (1987).

81. A= 1/2 of that for C_2H_2 + Cl, $E_a = \Delta H + 0.5$.

82. A taken as that for CCC + H (Ref: source 17), $E_a = 3.0$.

83. A taken as that for CCC + O (Ref: source 4), $E_a = 0.7$.

84. A taken as that for CCC + OH (Ref: source 4), $E_a = 0.3$.

85. A taken as that for CCC + Cl (Ref: source 4), $E_a = 0.3$.

86. A_{-1} taken as that for CO + C_2H_3 and CO + C_2H_5 (1.51E11, Ref: source 14), Ea = ΔH + 8 = 20.48.

87. Yu, Q.R., M. Sc. Thesis, NJIT (1992).

Table 5. Sensitivity Analysis Summary

Residence Time = 1.0 sec, Temp.= 873K

Species	S	Reaction No. Most Important Reactions	Important Reactions
CH_4	>0	1	19, 22, 37, 38, 48, 51, 112, 119, 156, 235, 242, 275, 316, 322, 328, 332, 333
	<0	2, 36	6, 35, 39, 49, 111, 113, 127, 236, 239, 240, 244, 246, 253, 273, 314, 319, 329
CH_3CCl_3	>0		19, 21, 22, 24, 31, 37, 39, 48, 51, 112, 119, 126, 156, 158, 169, 235, 237, 238, 239, 242, 275, 316, 322, 328, 330, 332, 333
	<0	1, 2, 4	5, 6, 7, 10, 35, 36, 38, 49, 111, 113, 127, 161, 236, 240, 244, 246, 253, 273, 314, 319, 329, 334
CH_2CCl_2	>0	1, 39, 156, 235	4, 48, 51, 55, 87, 112, 119, 126, 169, 199, 237, 238, 239, 275, 316, 322, 328, 330, 332, 333
	<0	2, 36, 38, 253	6, 19, 21, 22, 24, 35, 37, 49, 111, 113, 127, 161, 236, 240, 242, 244, 273, 314, 319, 321, 329, 334
C_2H_3Cl	>0	2, 6, 21, 35, 36, 38, 49, 50, 111, 113, 127, 161, 236, 244, 253, 273, 319, 329	3, 8, 9, 10, 12, 18, 24, 31, 34, 37, 40, 53, 57, 62, 102, 103, 121, 124, 129, 168, 184, 186, 207, 210, 238, 240, 243, 246, 251, 255, 264, 313, 314, 315, 323, 326, 327, 330, 334, 339
	<0	1, 19, 22, 39, 48, 51, 112, 119, 156, 158, 235, 237, 242, 275, 316, 332, 333	4, 5, 7, 20, 47, 52, 55, 64, 66, 67, 69, 71, 78, 83, 87, 92, 95, 96, 114, 120, 126, 128, 147, 169, 192, 193, 199, 206, 233, 239, 249, 254, 288, 305, 306, 321, 322, 324, 328, 337, 338
C_2H_2	>0	2, 6, 35, 36, 37, 38, 49, 96, 111, 113, 127, 161, 199, 207, 236, 240, 244, 253, 273, 314, 319, 329, 333	3, 8, 10, 17, 18, 24, 31, 34, 53, 64, 66, 83, 88, 95, 102, 103, 121, 124, 136, 167, 168, 174, 184, 186, 192, 193, 196, 213, 226, 243, 246, 255, 304, 313, 315, 323, 326, 327, 330, 334, 337, 339
	<0	1, 19, 21, 22, 39, 48, 51, 112, 119, 156, 158, 169, 206, 235, 237, 239, 242, 275, 316, 322, 328, 332	4, 5, 7, 9, 11, 12, 20, 47, 50, 52, 55, 67, 87, 92, 108, 114, 120, 126, 128, 129, 147, 198, 210, 211, 216, 221, 223, 225, 228, 229, 230, 233, 238, 247, 249, 254, 288, 305, 306, 321, 324, 338
C_2H_4	>0	2, 6, 10, 35, 38, 49, 113, 156, 158, 161, 236, 239, 244, 253, 273, 319	3, 8, 24, 34, 50, 53, 67, 85, 102, 103, 111, 124, 127, 163, 167, 168, 174, 238, 240, 242, 243, 255, 304, 314, 321, 329, 330, 334, 337, 339
	<0	1, 7, 22, 36, 37, 39, 48, 119, 199, 235, 237, 275, 316, 332, 333	4, 11, 12, 19, 20, 21, 31, 47, 51, 55, 87, 96, 112, 114, 126, 128, 129, 169, 173, 184, 186, 192, 193, 196, 206, 210, 233, 246, 247, 249, 254, 306, 322, 324, 328, 338

Residence Time = 1.0 sec, Temp.= 873K

Species	S	Most Important Reactions	Important Reactions
CO	>0	2, 6, 19, 35, 36, 38, 49, 51, 111, 113, 127, 236, 244, 253, 273, 319, 329	3, 8, 10, 17, 18, 24, 34, 53, 54, 55, 102, 103, 114, 121, 124, 147, 148, 161, 174, 184, 207, 210, 238, 239, 240, 246, 255, 304, 314, 321, 323, 326, 327, 330, 334, 339
	<0	1, 37, 39, 112, 156, 235, 242, 275, 316, 332, 333	4, 5, 7, 12, 20, 21, 22, 31, 40, 47, 48, 50, 87, 96, 119, 120, 126, 128, 129, 158, 169, 192, 193, 196, 199, 206, 233, 237, 247, 249, 254, 288, 306, 313, 322, 324, 328, 338
CO_2	>0	2, 36, 37, 38, 49, 112, 113, 161, 199, 244, 253, 273, 313, 314, 316, 319, 334, 337	3, 8, 10, 17, 18, 22, 31, 34, 46, 55, 66, 83, 127, 136, 148, 168, 186, 192, 193, 196, 206, 240, 243, 246, 255, 282, 293, 304, 315, 323, 327
	<0	1, 6, 19, 21, 35, 39, 48, 51, 111, 119, 156, 235, 236, 237, 239, 242, 275, 329, 332, 333, 339	4, 5, 7, 11, 12, 20, 24, 47, 50, 52, 53, 78, 87, 95, 96, 102, 103, 114, 120, 124, 126, 128, 129, 146, 147, 158, 169, 184, 207, 210, 211, 233, 238, 247, 249, 254, 281, 305, 308, 322, 324, 328, 338
C_2HCl	>0	2, 22, 35, 37, 38, 111, 113, 127, 236, 244, 253, 273, 314, 319, 329	3, 6, 8, 10, 17, 18, 31, 34, 49, 53, 102, 103, 121, 124, 147, 161, 174, 184, 207, 210, 240, 255, 304, 315, 321, 323, 326, 330, 334, 337
	<0	1, 36, 39, 51, 112, 114, 156, 235, 239, 242, 275, 316, 332, 333	4, 5, 7, 12, 19, 20, 21, 47, 48, 55, 87, 92, 95, 96, 108, 119, 126, 128, 129, 158, 169, 192, 193, 196, 199, 206, 233, 237, 238, 246, 247, 249, 254, 288, 306, 322, 324, 328, 338, 339
CH_3Cl	>0	2, 6, 35, 36, 38, 111, 113, 127, 236, 239, 244, 253, 273, 314, 319, 329	3, 8, 10, 17, 18, 24, 34, 49, 50, 53, 102, 103, 124, 148, 174, 207, 210, 238, 240, 255, 304, 321, 323, 326, 330, 334, 337
	<0	1, 22, 37, 39, 112, 156, 235, 242, 275, 316, 333	4, 7, 12, 19, 20, 21, 31, 47, 48, 51, 55, 87, 92, 95, 96, 114, 119, 120, 126, 128, 129, 158, 161, 169, 192, 193, 196, 199, 206, 233, 237, 243, 246, 247, 249, 254, 288, 306, 322, 324, 328, 332, 338, 339
HCl	>0	36, 38, 253	1, 2, 6, 19, 21, 24, 35, 37, 49, 51, 55, 111, 113, 114, 127, 147, 161, 236, 244, 273, 314, 319, 329, 334
	<0	39, 156	22, 48, 87, 112, 119, 126, 158, 169, 199, 235, 237, 238, 242, 275, 316, 322, 328, 330, 332, 333

Residence Time=1.0 sec, Temp.= 1023K

Species	S	Most Important Reactions	Important Reactions
CH_4	> 0	1, 156, 242, 316	19, 21, 39, 48, 49, 51, 55, 66, 87, 95, 96, 108, 112, 114, 119, 120, 121, 126, 128, 129, 192, 193, 196, 198, 199, 206, 223, 233, 235, 237, 273, 305, 306, 314, 322, 328, 332, 333
	< 0	2, 36, 37, 244	17, 18, 22, 31, 35, 38, 53, 92, 102, 103, 111, 113, 124, 143, 147, 148, 184, 207, 210, 228, 236, 238, 243, 246, 253, 275, 284, 304, 319, 326, 329, 330
CH_3CCl_3	> 0	2, 17, 22, 37, 38, 50, 111, 113, 210, 236, 244, 246, 253, 329, 332	3, 10, 18, 24, 31, 35, 40, 49, 53, 55, 58, 62, 69, 78, 92, 102, 103, 124, 140, 143, 158, 184, 186, 207, 211, 215, 216, 220, 221, 228, 229, 237, 243, 247, 251, 273, 284, 295, 304, 308, 309, 313, 314, 315, 326, 327, 339
	< 0	1, 19, 21, 36, 39, 48, 51, 87, 96, 112, 114, 128, 129, 147, 156, 198, 199, 206, 235, 239, 242, 316, 319, 333	4, 6, 7, 47, 52, 64, 66, 67, 83, 91, 95, 107, 108, 119, 120, 121, 123, 126, 127, 136, 148, 169, 192, 193, 196, 223, 233, 238, 240, 249, 275, 285, 286, 287, 288, 305, 306, 307, 321, 322, 328, 330, 334, 337
CH_2CCl_2	> 0	1, 39, 48, 51, 96, 112, 114, 128, 156, 199, 235, 239, 242, 316	10, 47, 54, 55, 66, 67, 83, 87, 95, 119, 121, 123, 126, 129, 147, 148, 158, 169, 192, 193, 196, 198, 206, 233, 237, 238, 249, 275, 288, 305, 306, 322, 328, 330, 333, 338
	< 0	2, 17, 19, 21, 22, 35, 36, 37, 38, 111, 113, 236, 244, 253, 319, 329	18, 24, 31, 34, 49, 50, 53, 78, 92, 102, 103, 107, 108, 120, 124, 127, 143, 161, 184, 186, 207, 210, 211, 215, 216, 228, 240, 243, 246, 273, 284, 295, 304, 308, 313, 314, 315, 321, 326, 332, 334
C_2H_3Cl	> 0	2, 21, 35, 36, 37, 38, 49, 111, 113, 128, 129, 210, 236, 244, 253, 329, 332	9, 17, 18, 31, 34, 53, 58, 62, 92, 102, 103, 123, 124, 130, 143, 148, 161, 168, 184, 186, 207, 211, 215, 216, 228, 229, 237, 238, 243, 246, 247, 251, 273, 284, 288, 295, 304, 308, 313, 315, 326, 327, 330, 339
	< 0	1, 19, 22, 39, 40, 48, 50, 51, 64, 67, 87, 96, 112, 114, 120, 147, 156, 199, 206, 235, 239, 242, 316, 319, 333	4, 10, 24, 47, 52, 55, 66, 69, 71, 78, 83, 91, 95, 107, 108, 119, 126, 127, 158, 169, 192, 193, 196, 198, 233, 240, 249, 275, 285, 305, 306, 314, 321, 322, 328, 334, 338
C_2H_2	> 0	2, 17, 18, 22, 31, 35, 37, 38, 49, 64, 96, 111, 113, 207, 210, 236, 244, 246, 253, 273, 319, 329, 332	3, 24, 34, 40. 46, 50, 53, 58, 62, 78, 88, 92, 102, 103, 124, 127, 143, 161, 168, 186, 211, 213, 220, 226, 237, 243, 251, 284, 295, 304, 308, 309, 313, 314, 315, 323, 326, 327, 330, 334, 337, 339
	< 0	1, 19, 21, 36, 39, 48, 51, 87, 112, 114, 119, 120, 128, 129, 147, 156, 198, 199, 206, 235, 238, 239, 242, 275, 316, 333	4, 7, 10, 47, 52, 54, 55, 66, 67, 71, 83, 91, 95, 107, 108, 121, 123, 126, 148, 169, 192, 193, 196, 215, 216, 221, 223, 225, 228, 229, 230, 233, 249, 285, 288, 305, 306, 307, 321, 322, 328, 338
C_2H_4	> 0	2, 17, 18, 21, 22, 35, 37, 38, 67, 111, 113, 156, 236, 242, 243, 244, 253, 273, 314, 319, 329	3, 6, 10, 24, 31, 34, 46, 49, 53, 54, 58, 62, 78, 85, 87, 92, 102, 103, 120, 123, 124, 127, 143, 147, 161, 168, 174, 207, 210, 211, 213, 215, 216, 228, 238, 240, 284, 295, 304, 308, 309, 313, 315, 321, 323, 326, 327, 330, 334, 337

Residence Time=1.0 sec, Temp.= 1023K

Species	S	Most Important Reactions	Important Reactions
C_2H_4	< 0	1, 36, 48, 51, 96, 112, 114, 128, 129, 192, 193, 196, 199, 206, 235, 275, 316, 332, 333	4, 7, 19, 40, 47, 50, 55, 64, 66, 83, 91, 95, 107, 108, 119, 121, 126, 148, 158, 169, 173, 184, 186, 198, 230, 233, 237, 239, 246, 247, 249, 288, 305, 306, 322, 328, 338
CO	> 0	2, 17, 18, 19, 22, 35, 36, 37, 38, 49, 51, 111, 113, 210, 236, 244, 253, 329, 332	21, 24, 31, 34, 40, 50, 53, 58, 62, 69, 78, 92, 102, 103, 108, 114, 120, 124, 127, 143, 147, 148, 161, 186, 207, 211, 215, 216, 223, 228, 229, 230, 243, 246, 247, 273, 284, 288, 295, 304, 308, 309, 319, 326, 327, 339
	< 0	1, 39, 87, 96, 112, 128, 129, 156, 199, 206, 235, 239, 242, 316, 333	10, 47, 48, 52, 55, 64, 66, 67, 83, 91, 95, 119, 121, 123, 126, 158, 169, 192, 193, 196, 198, 213, 233, 237, 238, 249, 275, 305, 306, 313, 314, 315, 322, 328, 330, 334, 338
CO_2	> 0	2, 17, 18, 22, 35, 37, 38, 111, 113, 236, 244, 253, 313, 314, 319	24, 31, 34, 46, 49, 50, 53, 64, 66, 67, 83, 92, 102, 103, 120, 124, 143, 161, 168, 169, 186, 192, 193, 196, 198, 199, 206, 228, 243, 246, 275, 284, 304, 315, 326, 329, 334, 337
	< 0	1, 36, 39, 48, 51, 87, 96, 112, 114, 128, 129, 156, 235, 238, 239, 242, 316, 333	4, 6, 19, 21, 47, 52, 54, 55, 91, 95, 108, 119, 121, 123, 126, 127, 148, 158, 207, 210, 211, 223, 233, 237, 247, 249, 273, 305, 306, 321, 322, 324, 327, 328, 330, 332, 338, 339
C_2HCl	> 0	1, 17, 21, 22, 37, 38, 111, 113, 114, 120, 147, 319	7, 19, 31, 52, 55, 64, 67, 119, 124, 127, 143, 206, 207, 228, 235, 240, 273, 284, 285, 304, 314, 316, 321, 330, 333, 334
	< 0	2, 36, 39, 49, 51, 96, 112, 128, 239, 242, 244, 253, 332	18, 24, 34, 35, 48, 50, 53, 83, 87, 92, 95, 102, 103, 107, 108, 121, 126, 129, 148, 156, 168, 186, 192, 193, 196, 198, 199, 210, 230, 236, 237, 238, 243, 246, 275, 288, 313, 327, 329, 339
CH_3Cl	> 0	36, 37, 38, 111, 113, 236, 239, 253, 319	1, 7, 17, 18, 22, 34, 35, 53, 78, 83, 92, 102, 103, 124, 127, 143, 147, 148, 184, 186, 207, 210, 211, 228, 238, 240, 244, 273, 284, 304, 314, 315, 321, 326, 329, 330, 334
	< 0	39, 51, 112, 114, 120, 128, 129, 156, 199, 235, 242, 316, 332	2, 10, 19, 21, 24, 31, 48, 49, 50, 55, 66, 87, 95, 107, 108, 119, 121, 123, 126, 161, 168, 169, 192, 193, 196, 198, 206, 230, 233, 237, 243, 246, 247, 249, 275, 288, 305, 306, 313, 322, 327, 328, 333
HCl	> 0	17, 19, 22, 36, 37, 38, 111, 113, 236, 244, 253, 319	2, 18, 21, 24, 31, 35, 40, 49, 50, 53, 58, 62, 64, 78, 92, 102, 103, 120, 124, 127, 143, 147, 148, 161, 184, 186, 207, 210, 211, 228, 243, 246, 273, 284, 304, 313, 314, 315, 326, 327, 329, 332, 334
	< 0	1, 39, 51, 112, 114, 128, 156, 199, 235, 239, 242, 316	48, 55, 66, 83, 87, 95, 96, 107, 108, 119, 121, 123, 126, 129, 158, 169, 192, 193, 196, 198, 206, 233, 238, 249, 275, 288, 305, 306, 322, 328, 330, 333

S: Sensitivity CoefficientMost Important: $10^{-2} \leq |S|$; Important: $10^{-4} \leq |S| < 10^{-2}$

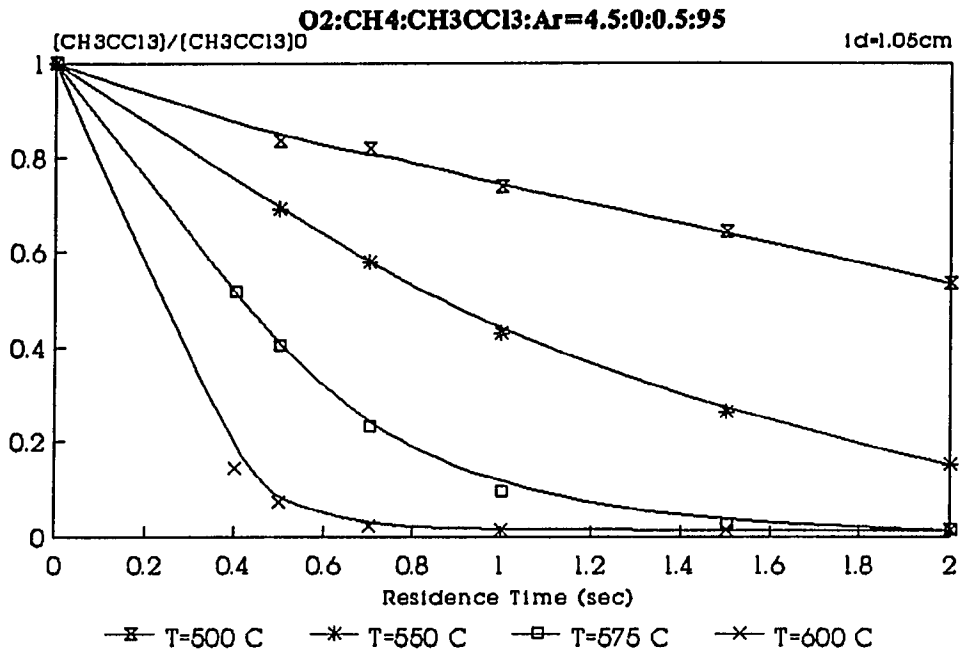

Figure 4-a. 1,1,1 Trichloroethane Decay Curve in Ratio Set 1

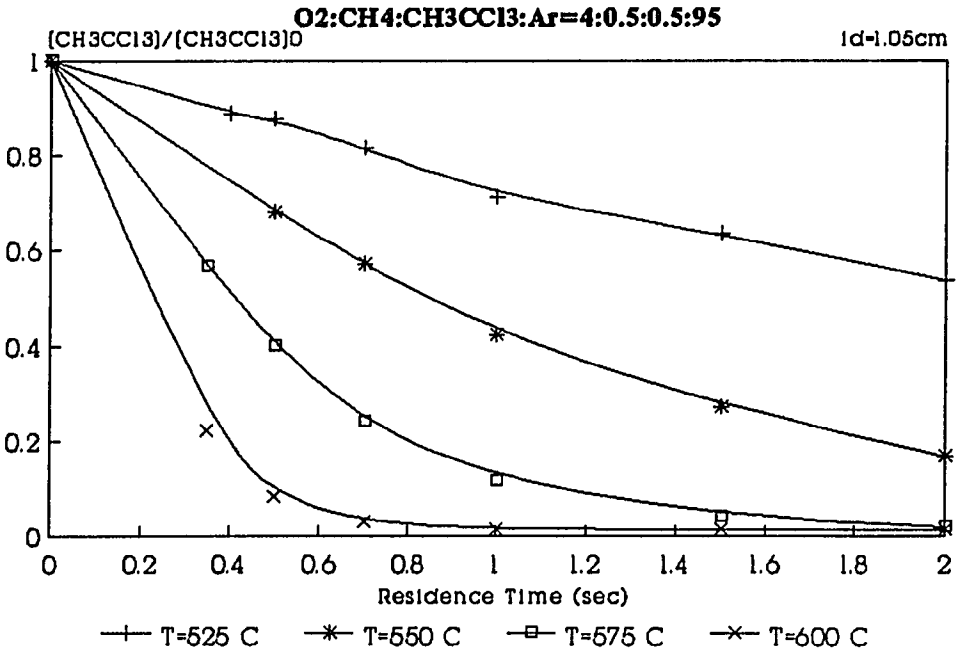

Figure 4-b. 1,1,1 Trichloroethane Decay Curve in Ratio Set 2

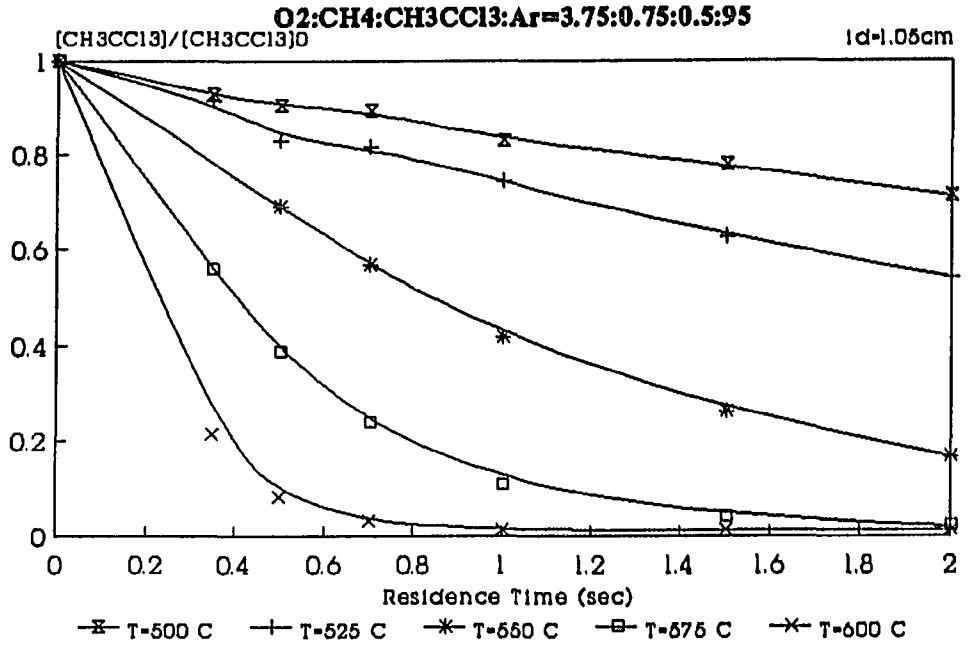

Figure 4-c. 1,1,1 Trichloroethane Decay Curve in Ratio Set 3

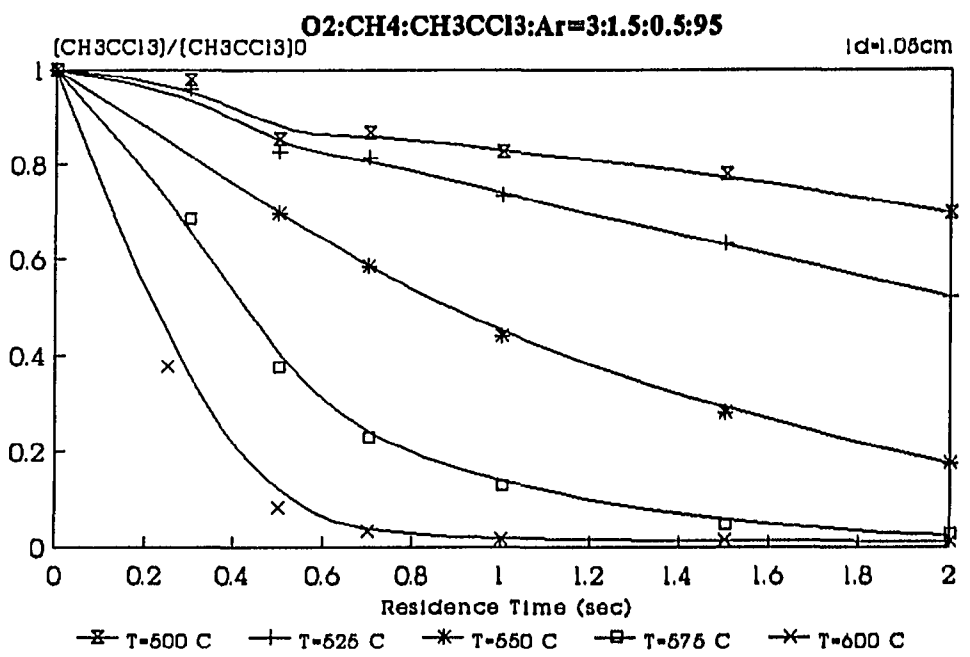

Figure 4-d. 1,1,1 Trichloroethane Decay Curve in Ratio Set 4

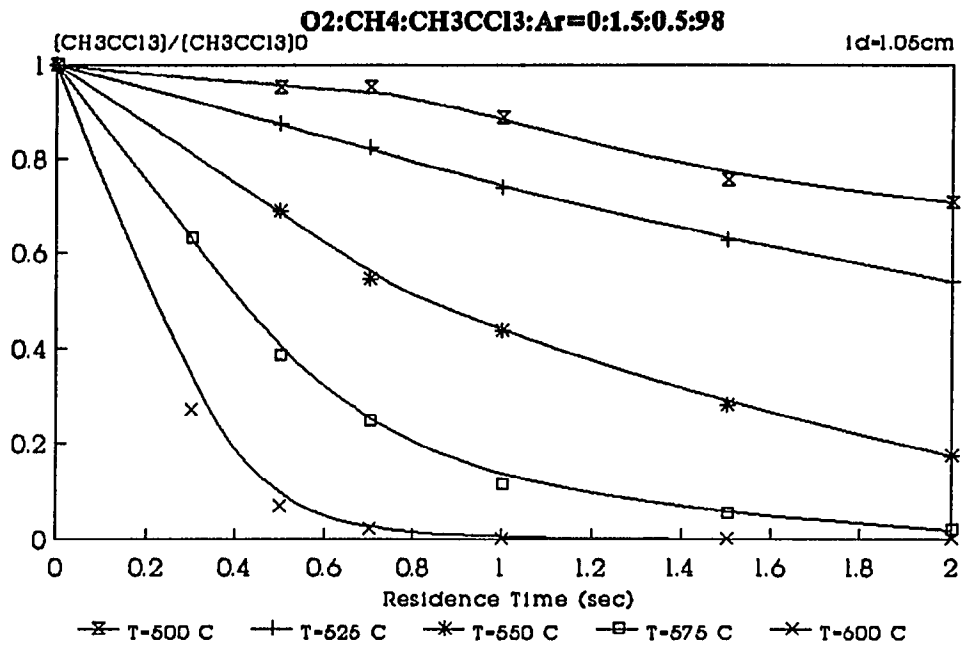

Figure 4-e. 1,1,1-Trichloroethane Decay in Ratio Set 5

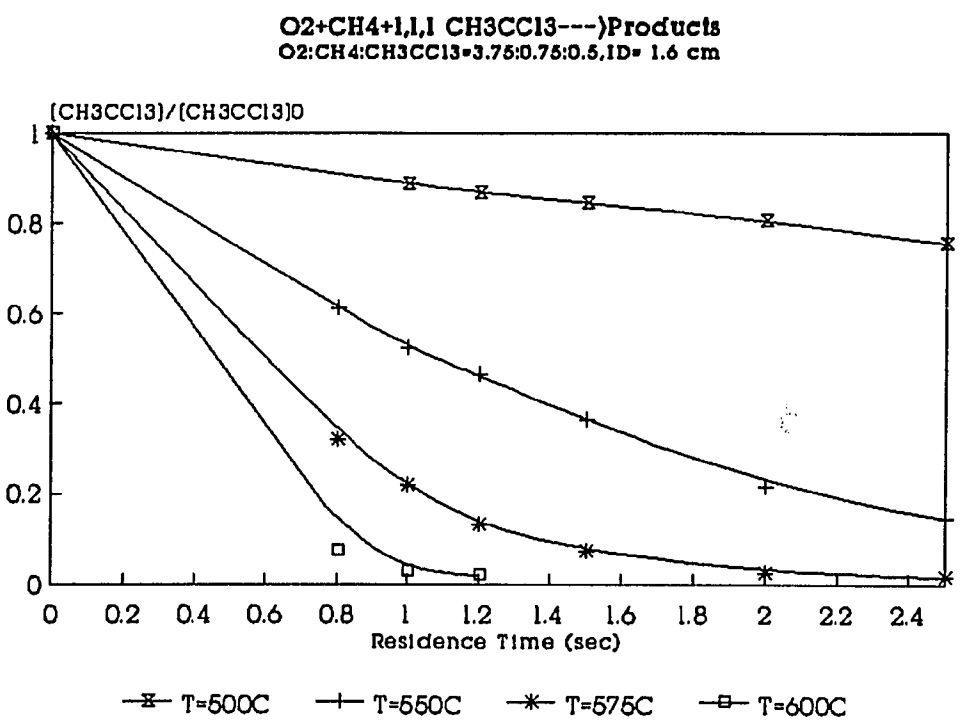

Figure 4-f. 1,1,1-CH3CCl3 Decay in Ratio Set 3 and 1.6 cm ID

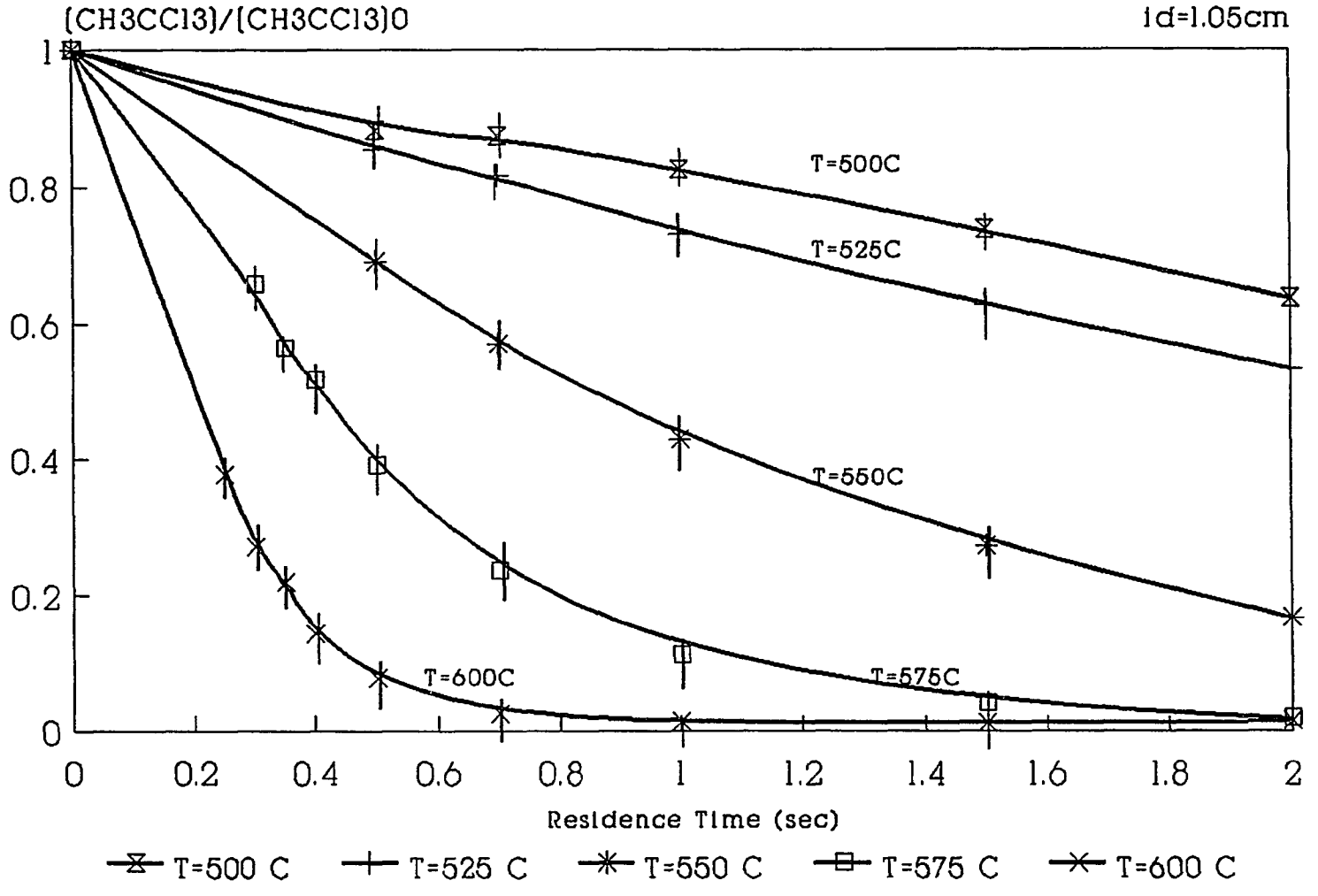

Figure 5. 1,1,1-CH3CCl3 Decay for all Reactants Ratio Sets (Distribute at the same range) vs. Time

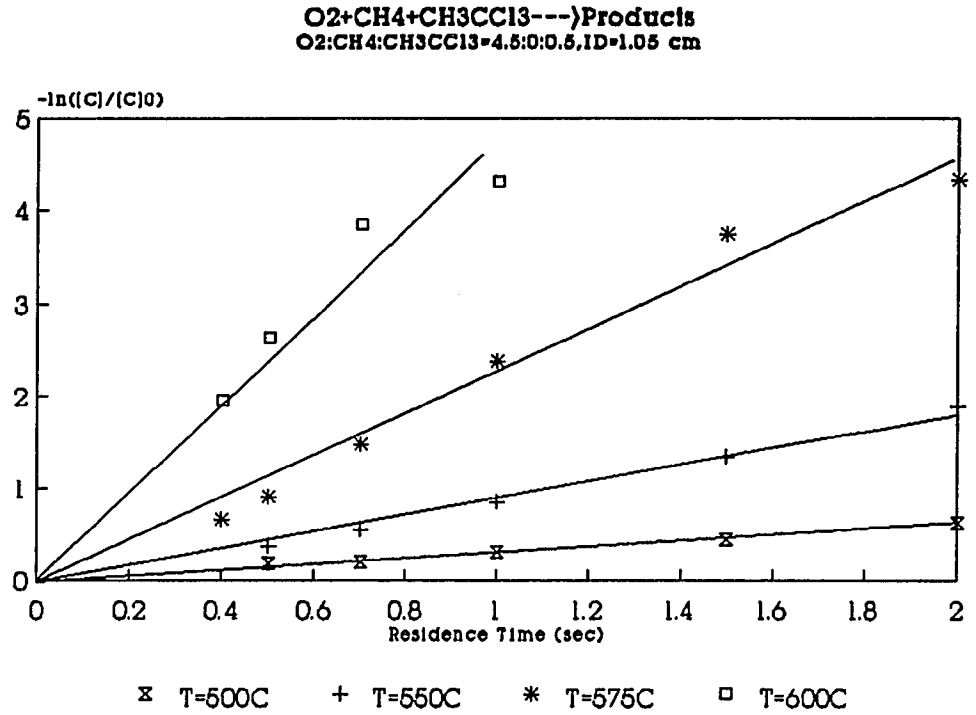

Figure 6-a. 1st-Order Kinetics Fit of CH3CCl3 Decomposition

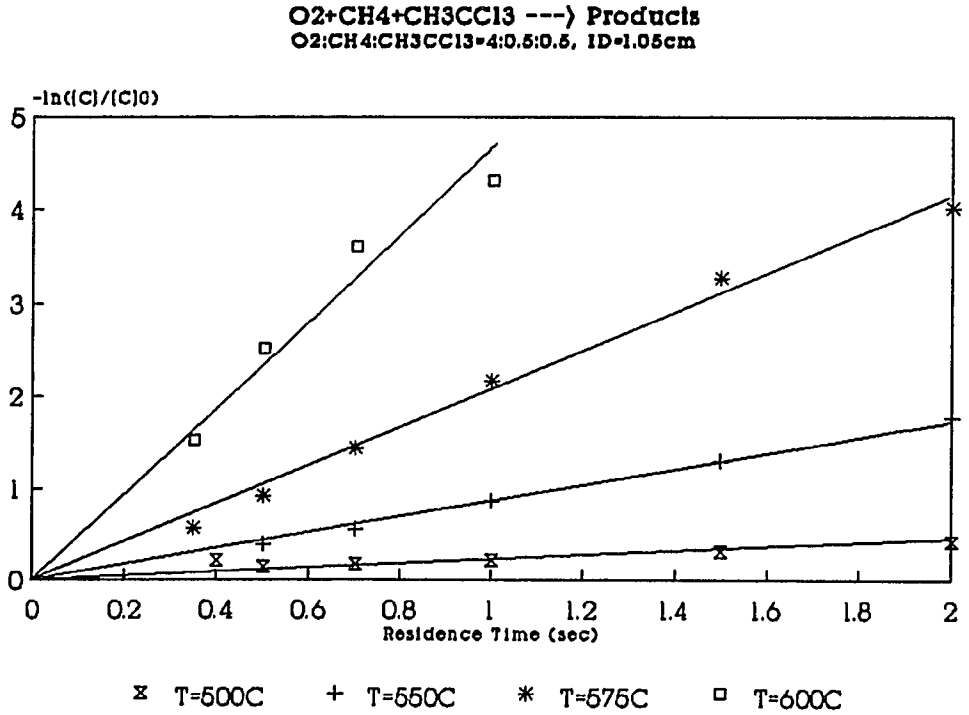

Figure 6-b. 1st-Order Kinetics Fit of CH3CCl3 Decomposition

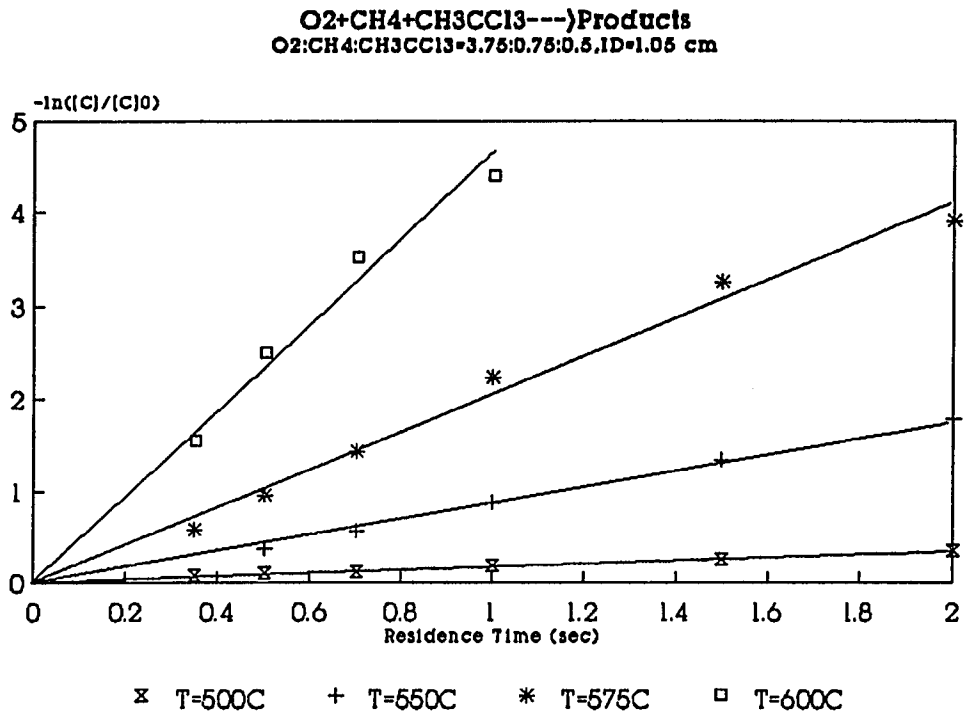

Figure 6-c. 1st-Order Kinetics Fit of CH3CCl3 Decomposition

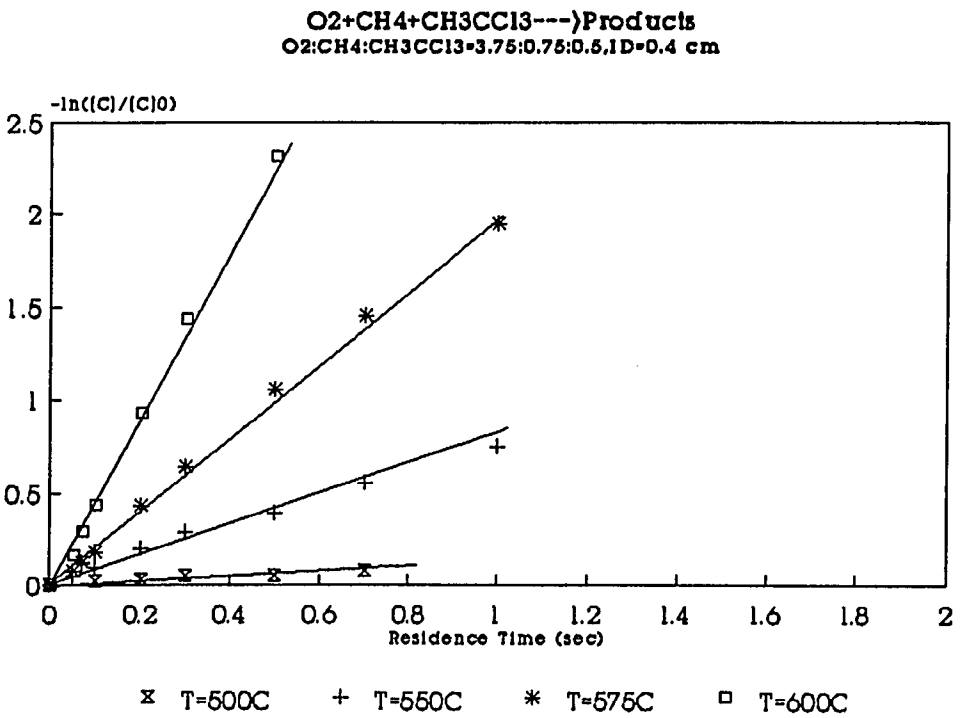

Figure 6-d. 1st-Order Kinetics Fit of CH3CCl3 Decomposition

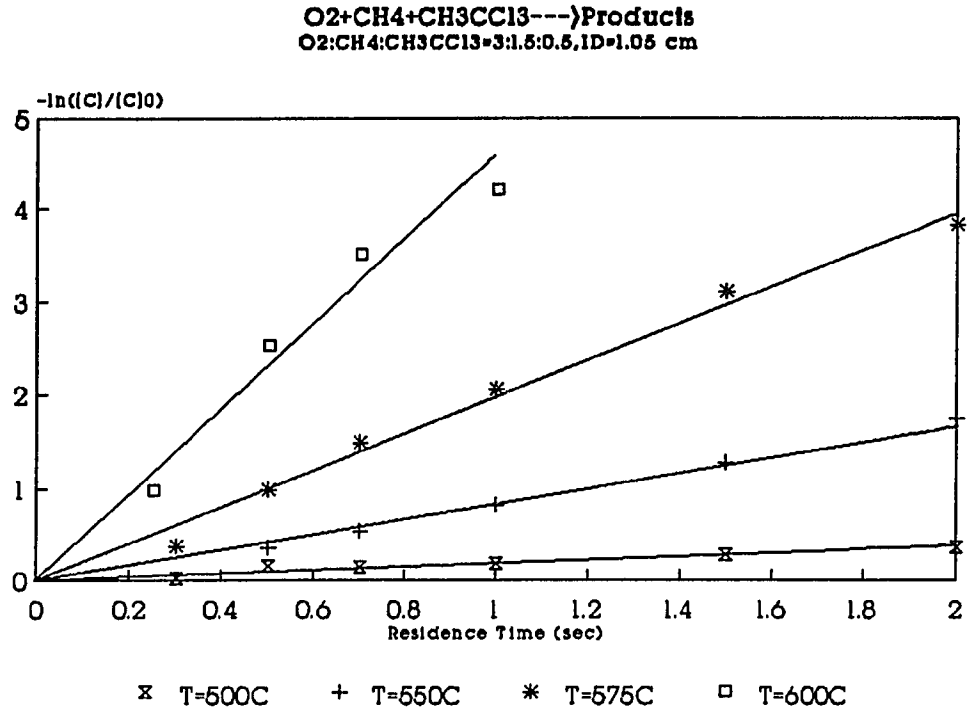

Figure 6-e. 1st-Order Kinetics Fit of CH3CCl3 Decomposition

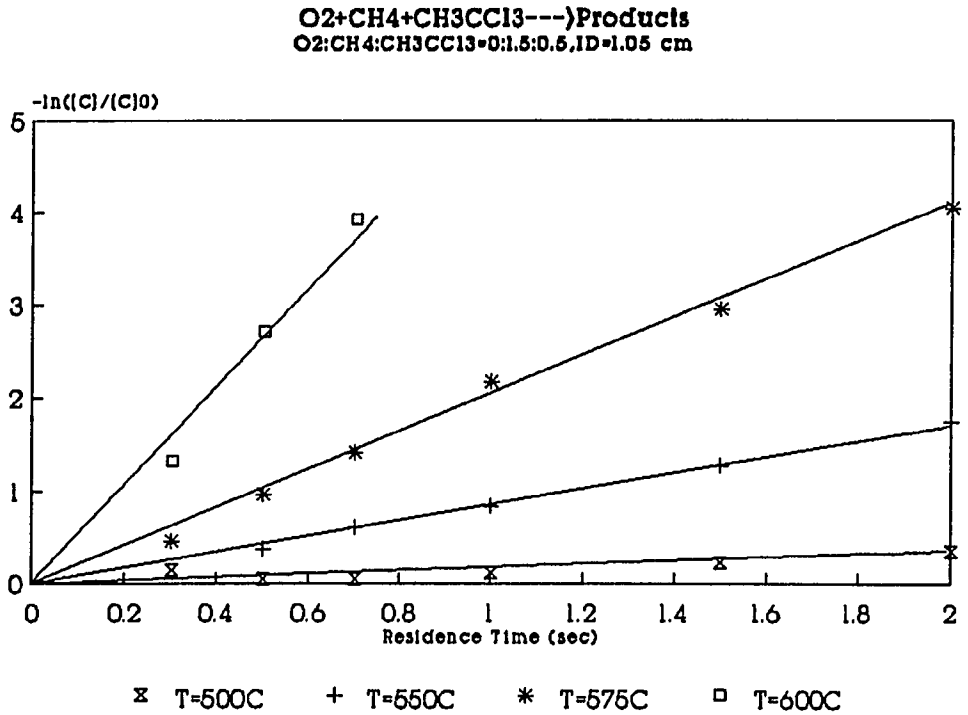

Figure 6-f. 1st-Order Kinetics Fit of CH3CCl3 Decomposition

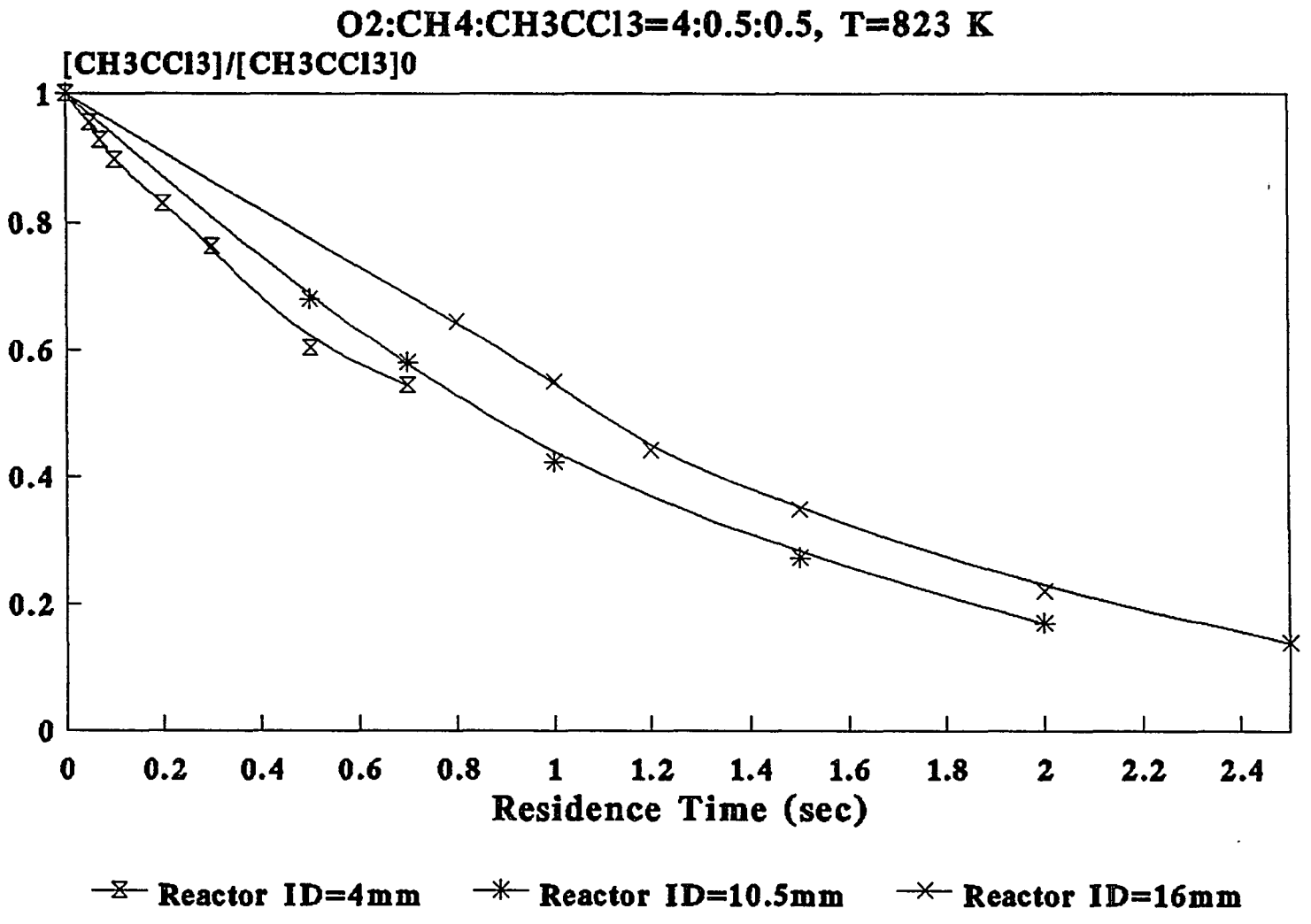

Figure 7-a. 1,1,1-Trichloroethane Decay in varied Reactors

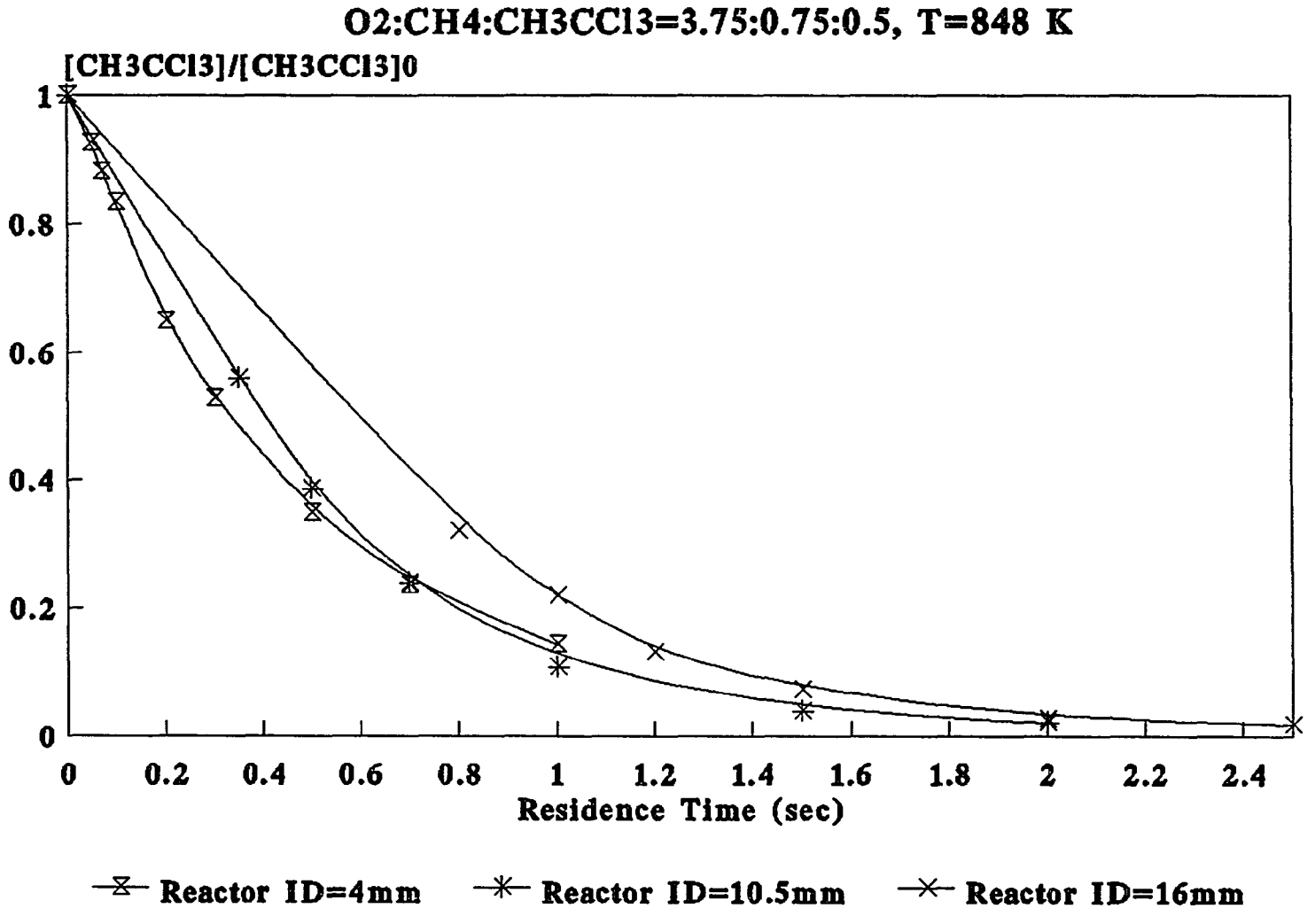

Figure 7-b. 1,1,1-Trichloroethane Decay in varied Reactors

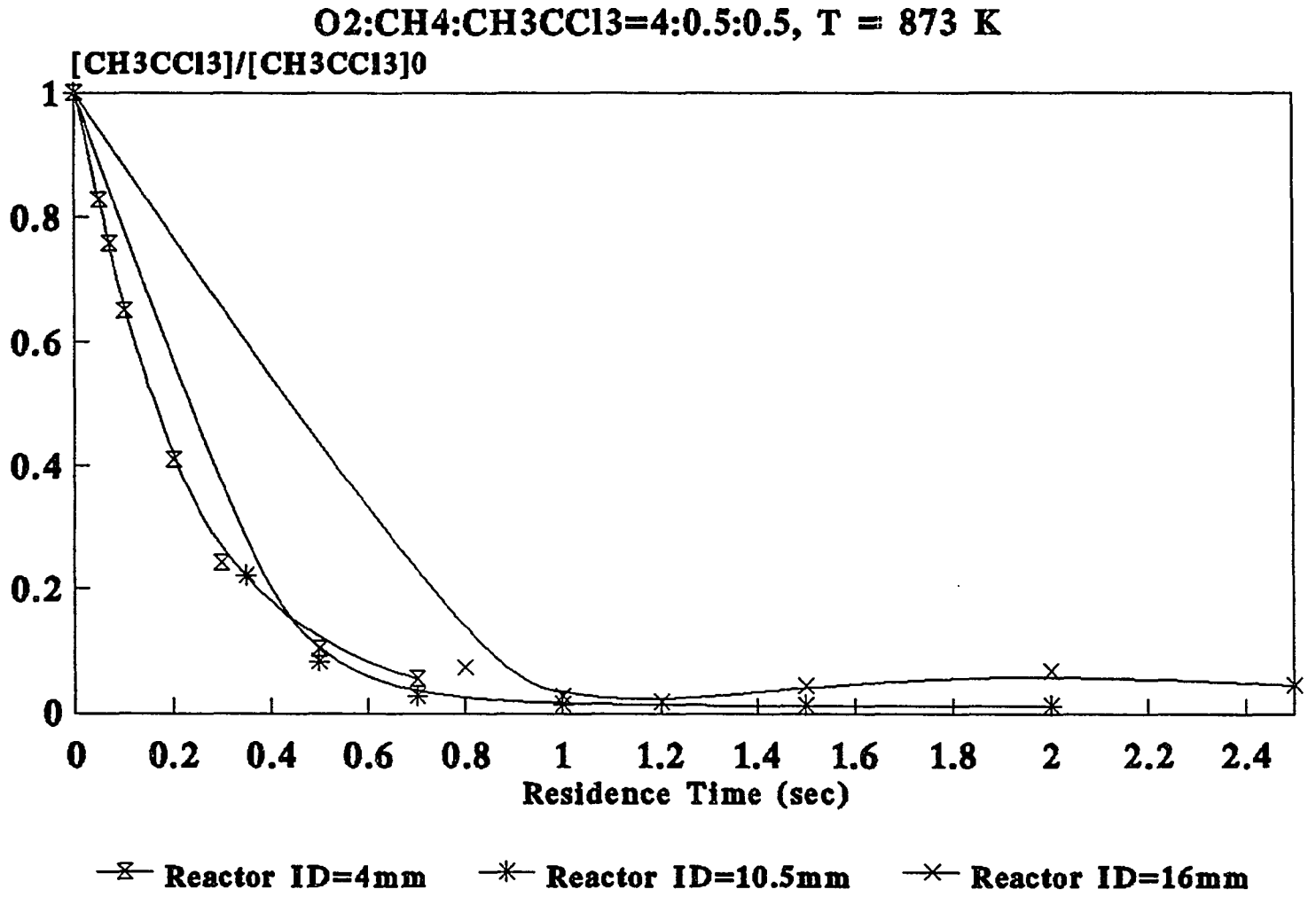

Figure 7-c. 1,1,1-Trichloroethane Decay of varied Reactors

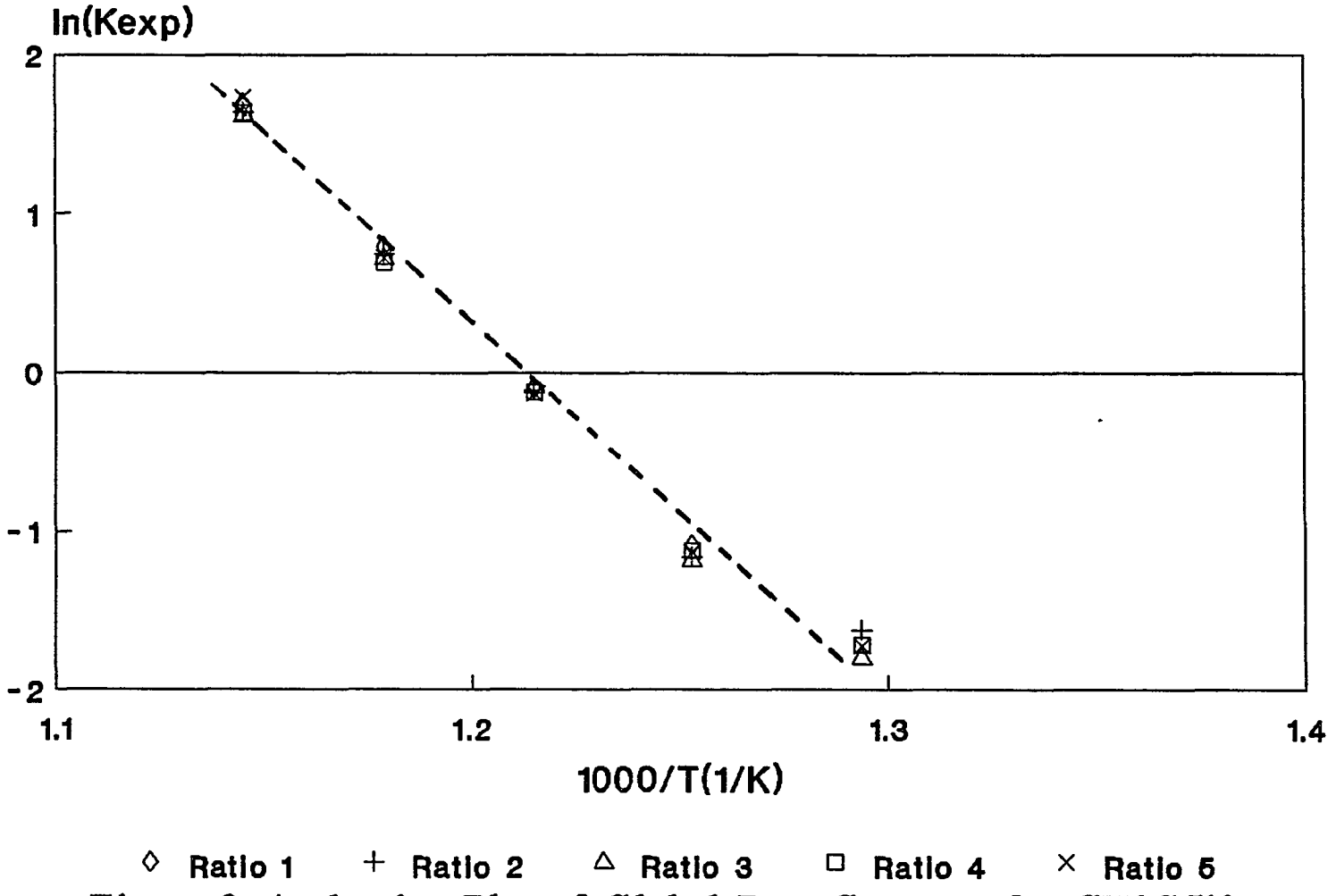

Figure 8. Arrhenius Plot of Global Rate Constant for CH3CCl3

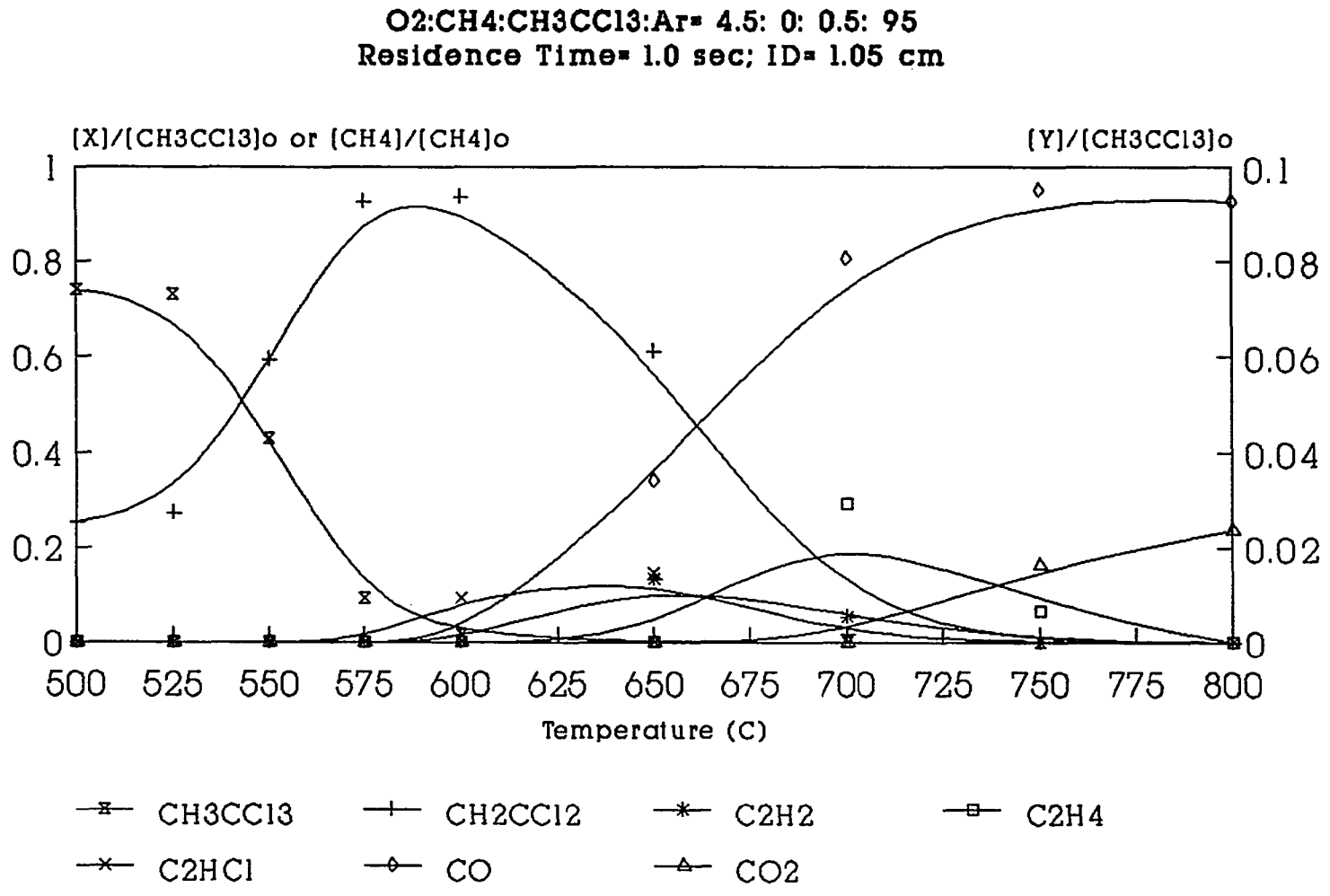

Figure 9-a. Product Distribution for Ratio Set 1.

X: CH3CCl3, CH2CCl2, CO, CO2
Y: C2H2, C2H4, C2HCl

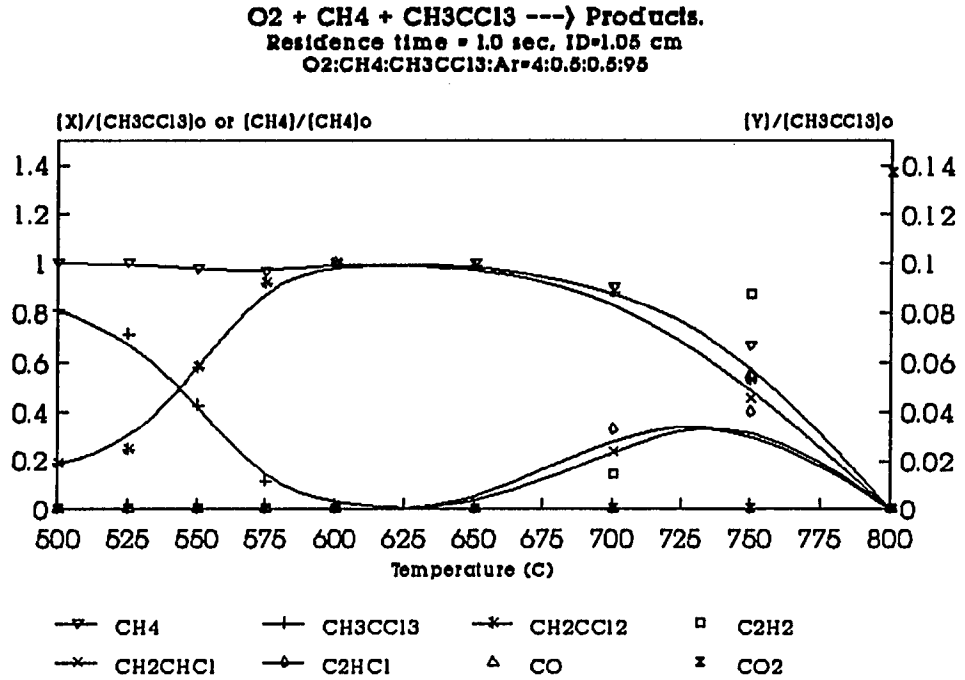

Figure 9-b. Product Distribution for Ratio Set 2

X: CH3CCl3, CH2CCl2, CO, CO2
Y: C2H2, C2H3Cl, C2HCl

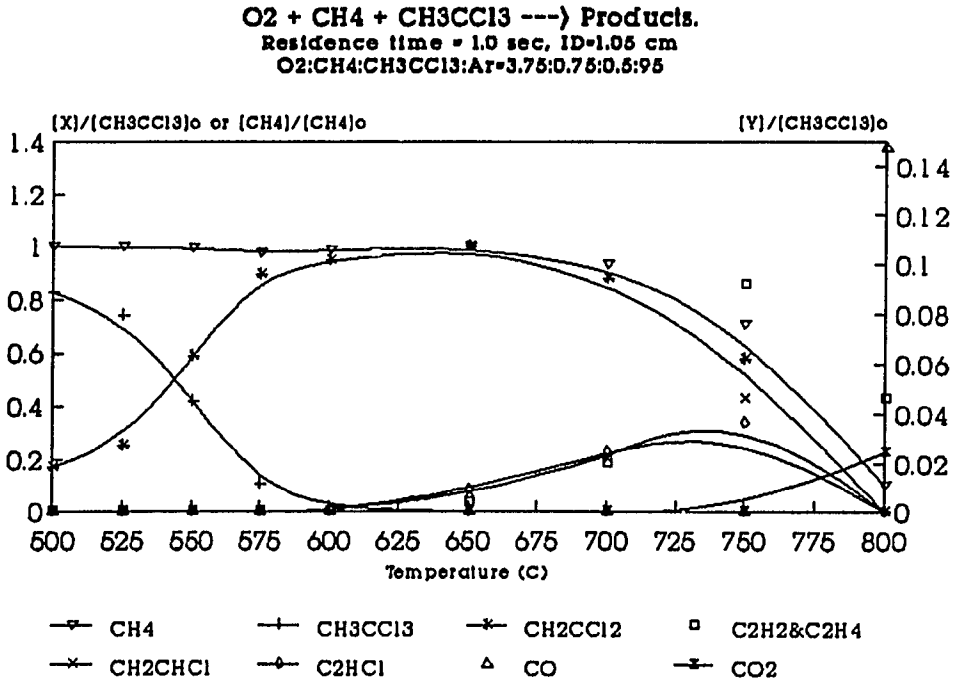

Figure 9-c. Product Distribution for Ratio Set 3

X: CH3CCl3, CH2CCl2, CO, CO2
Y: C2H2, C2H4, C2H3Cl, C2HCl

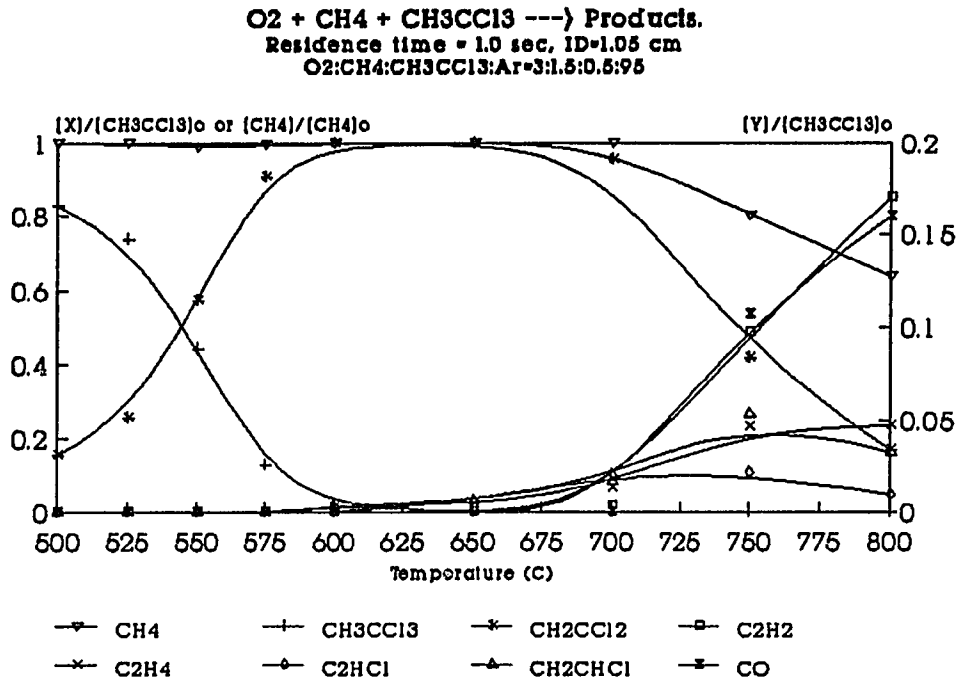

Figure 9-d. Product Distribution for Ratio Set 4.

X: CH3CCl3, CH2CCl2, CO
Y: C2H2, C2H4, C2H3Cl, C2HCl

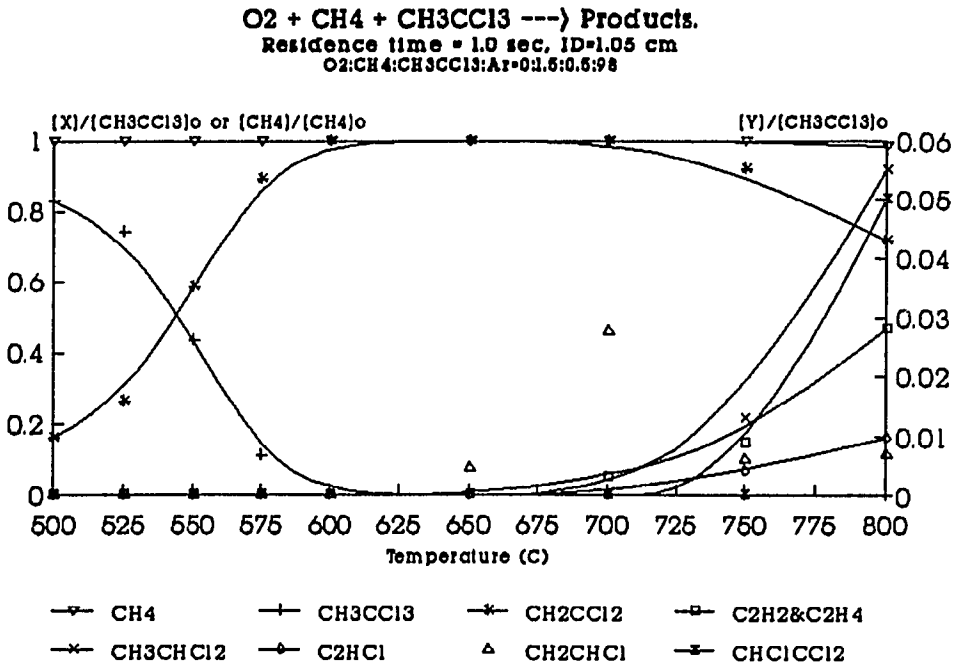

Figure 9-e. Product Distribution for Ratio Set 5.

X: CH3CCl3, CH2CCl2,C2HCl
Y: C2H2, C2H4, CH3CHCl2, CH2CHCl,
CHClCCl2

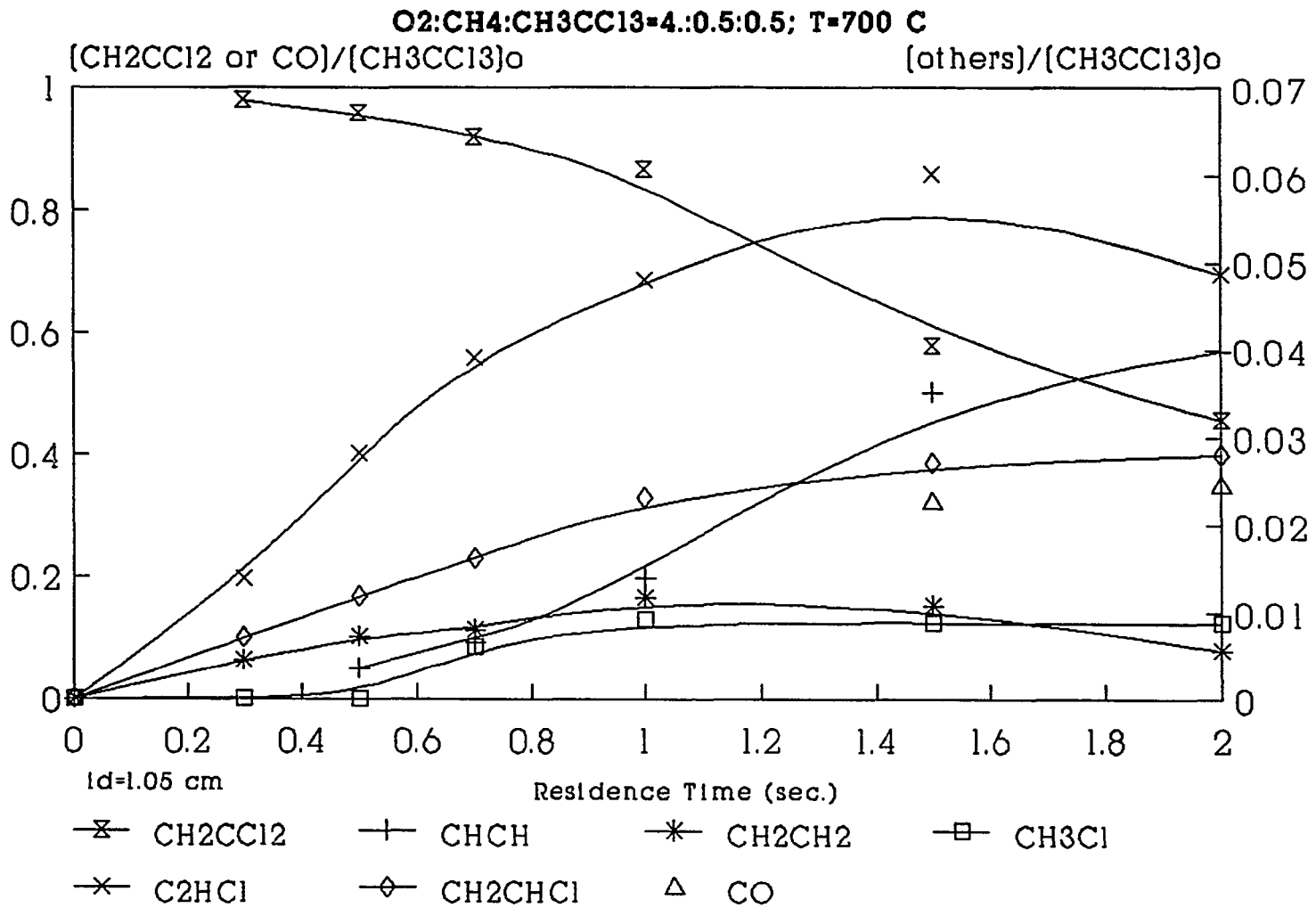

Figure 10-a. Product Distribution For Ratio Set 2 at 700C

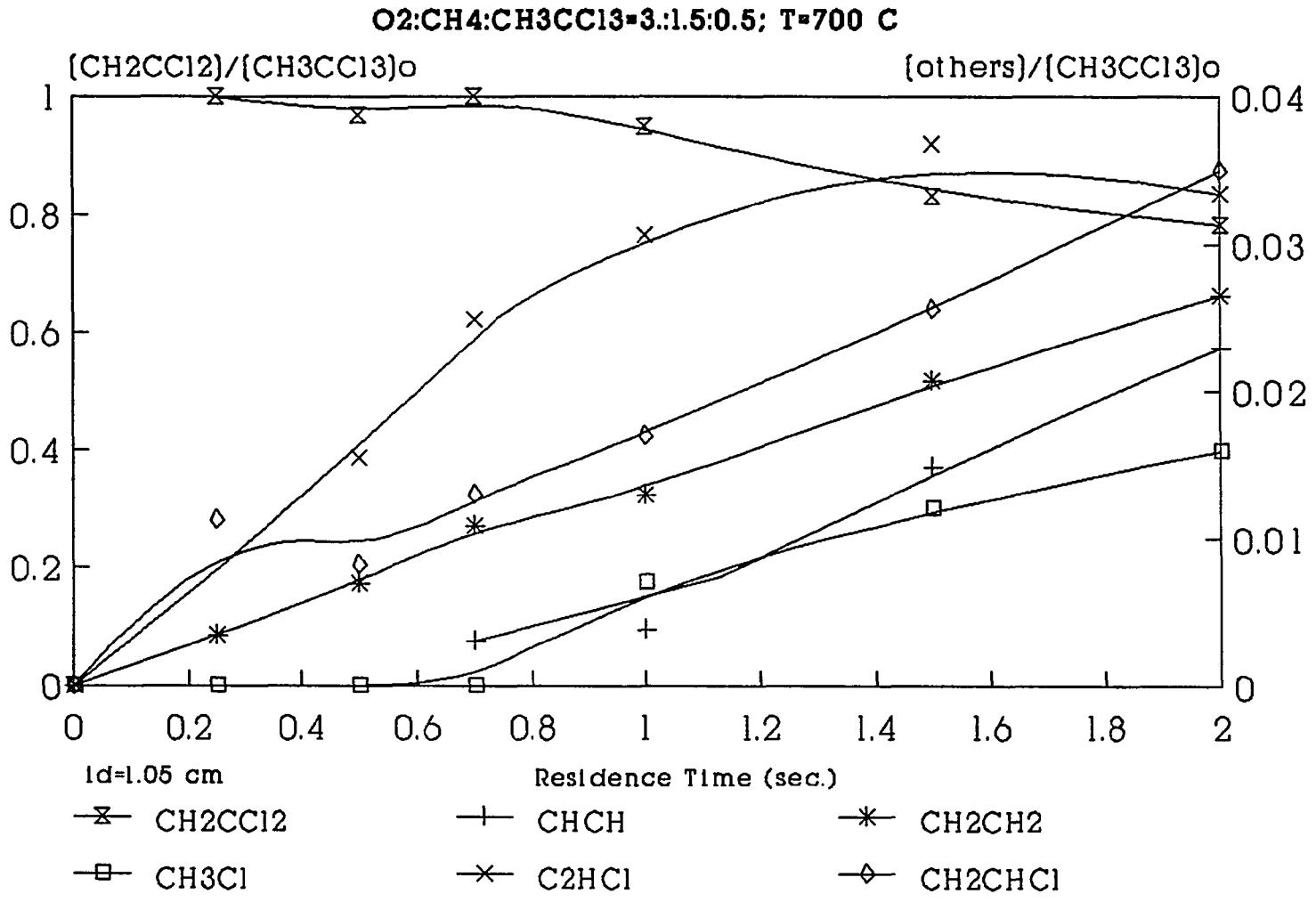

Figure 10-b. Product Distribution for Ratio Set 4 at 700C

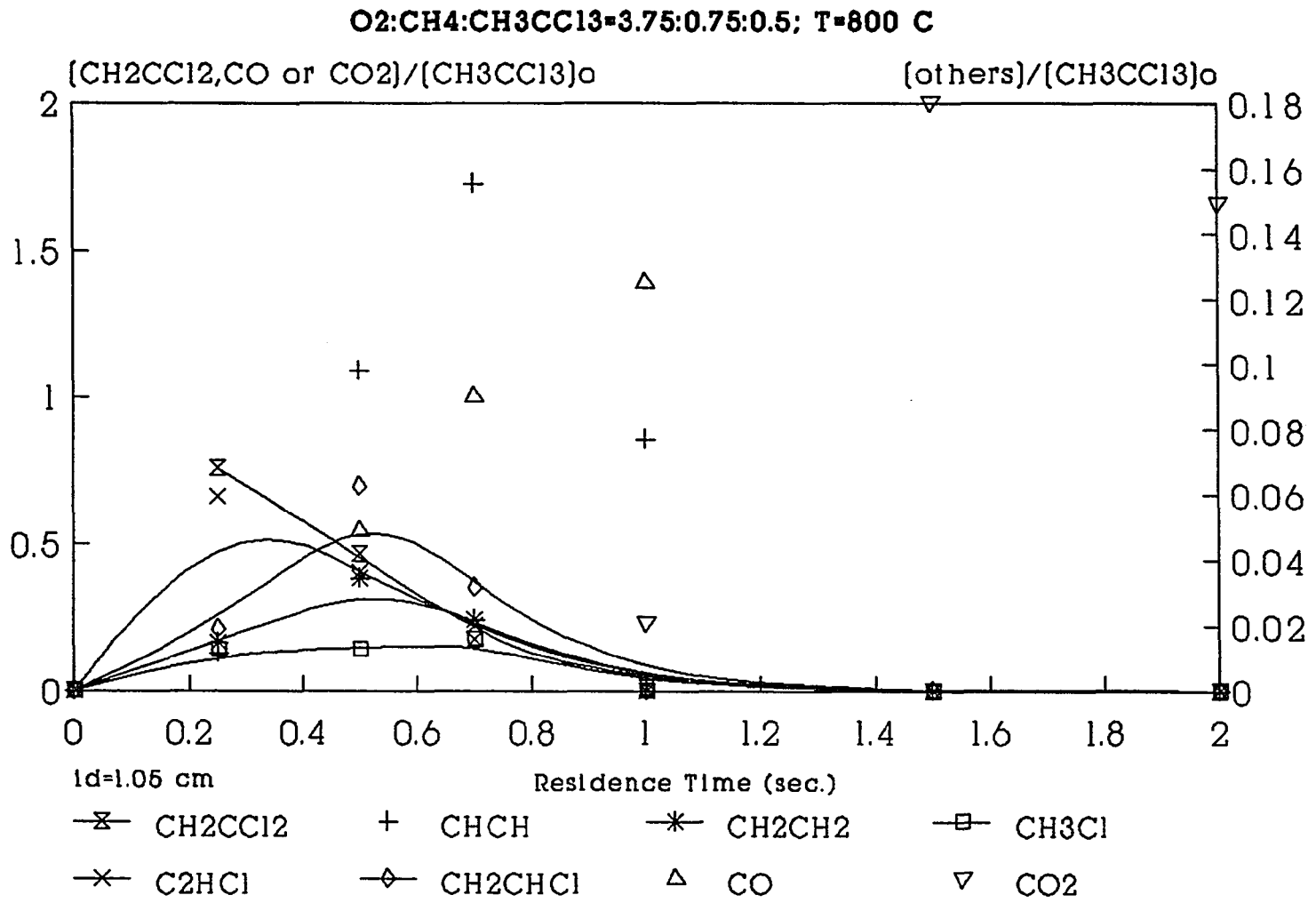

Figure 10-c. Product Distribution for Ratio Set 3 at 800 C

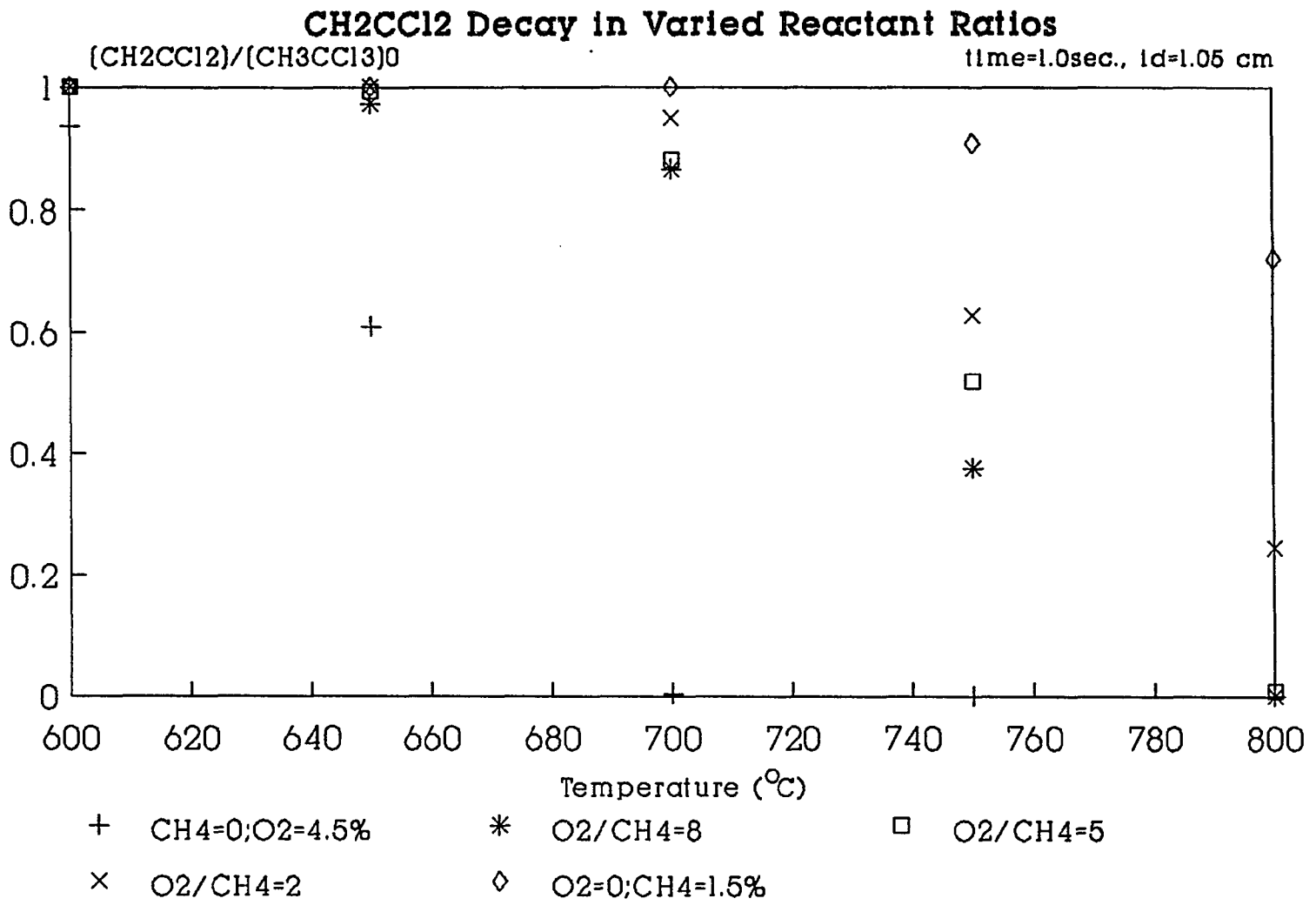

Figure 11. 1,1-Dichloroethylene Distribution versus Temp.

CH3CCl3=0.5%

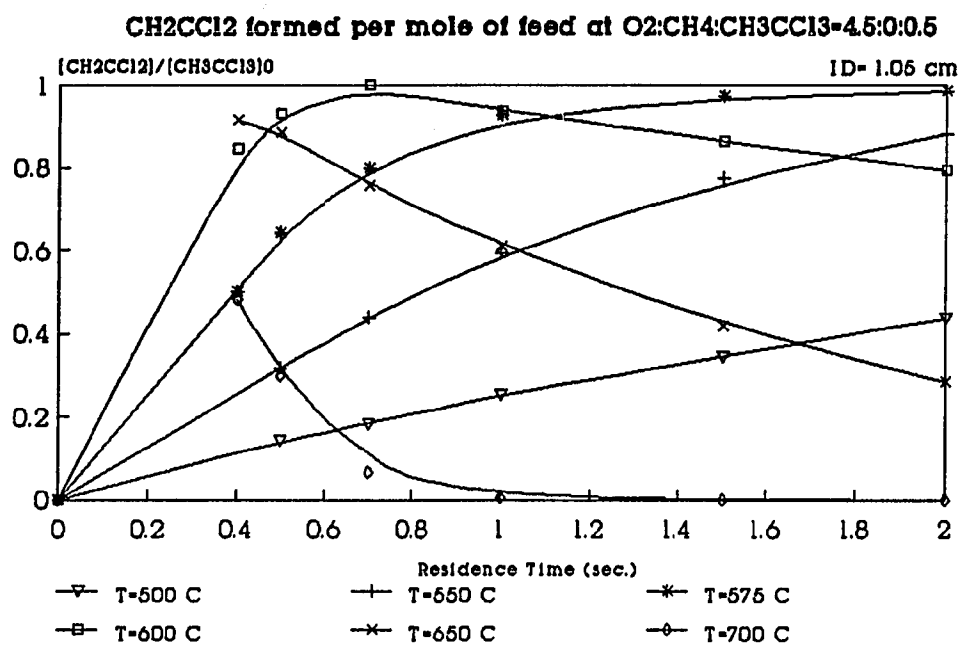

Figure 12-a. CH2CCl2 Distribution for Ratio Set 1

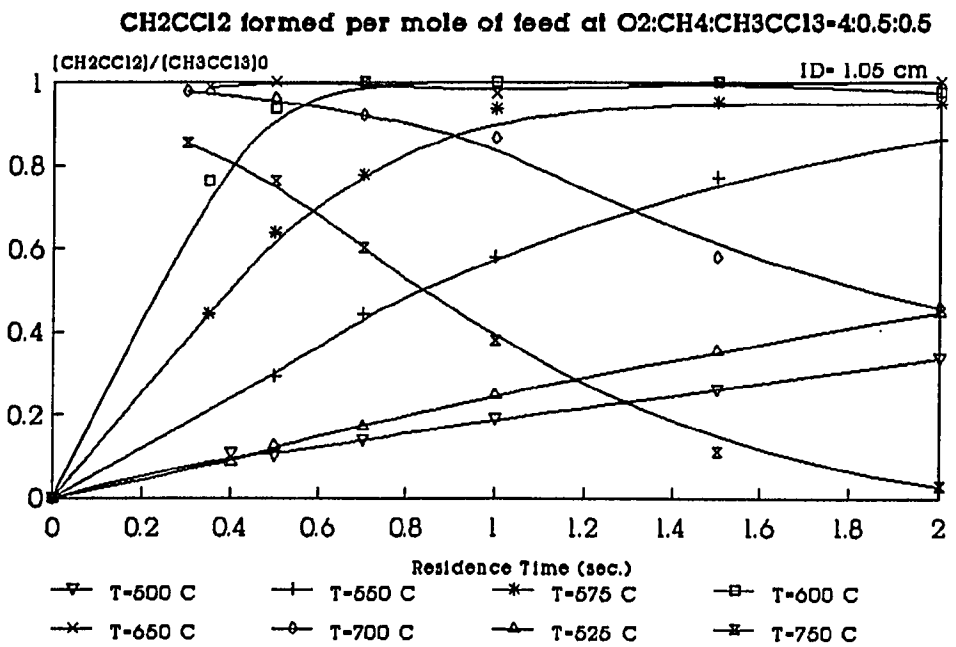

Figure 12-b. CH2CCl2 Distribution for Ratio Set 2

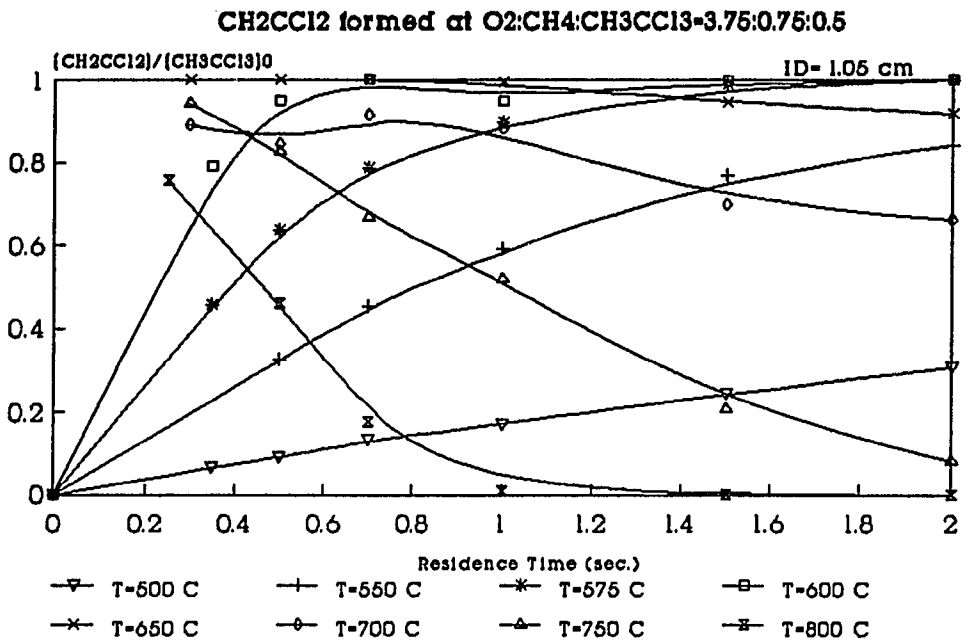

Figure 12-c. CH2CCl2 Distribution for Ratio Set 3

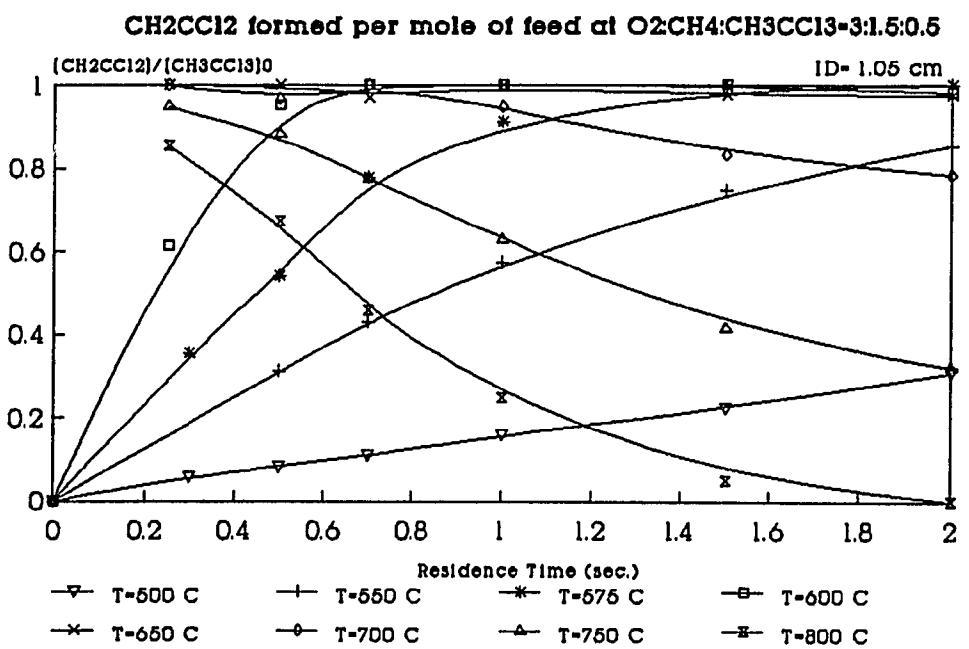

Figure 12-d. CH2CCl2 Distribution for Ratio Set 4

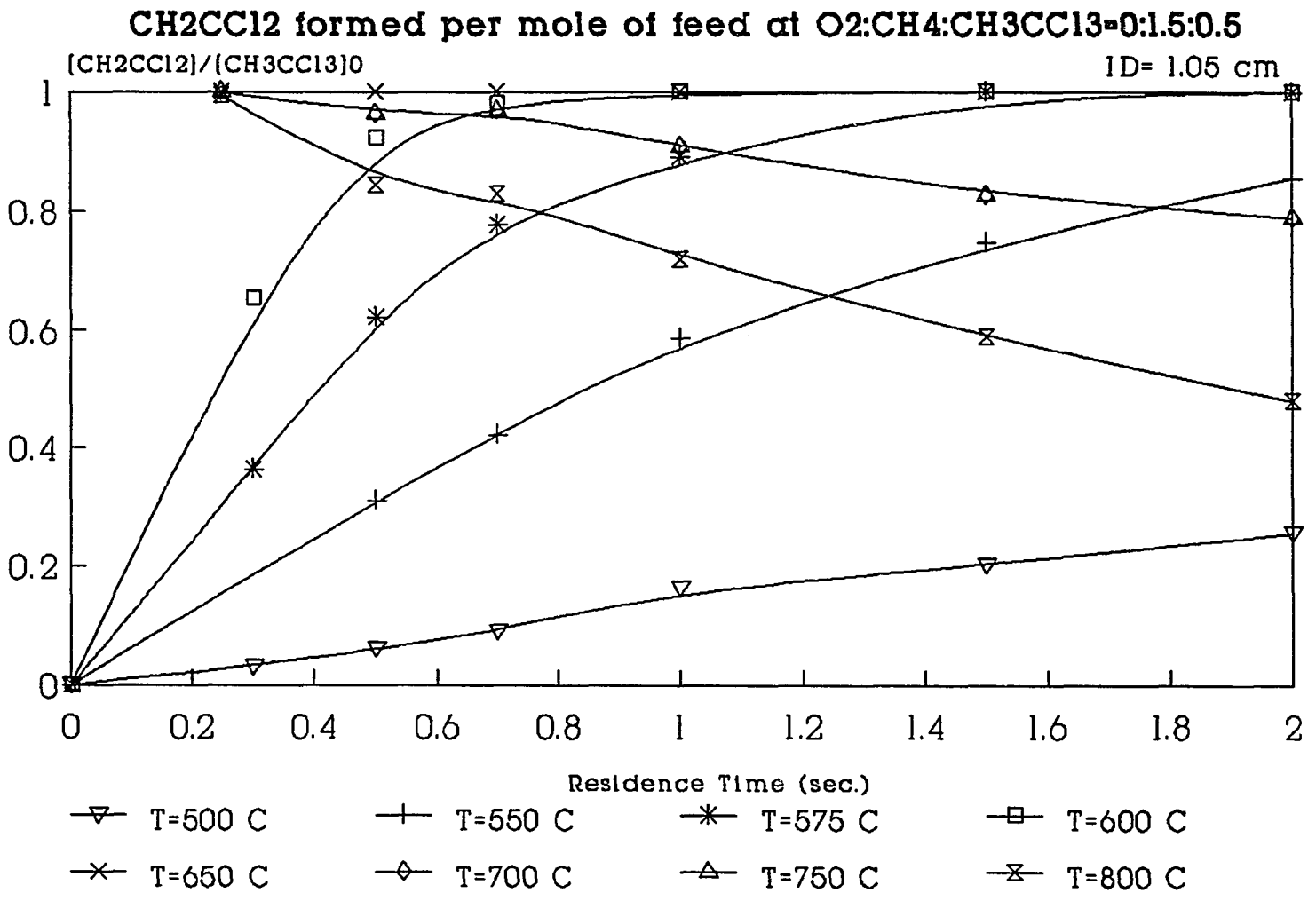

Figure 12-e. CH2CCl2 Distribution vs Time for Ratio Set 5

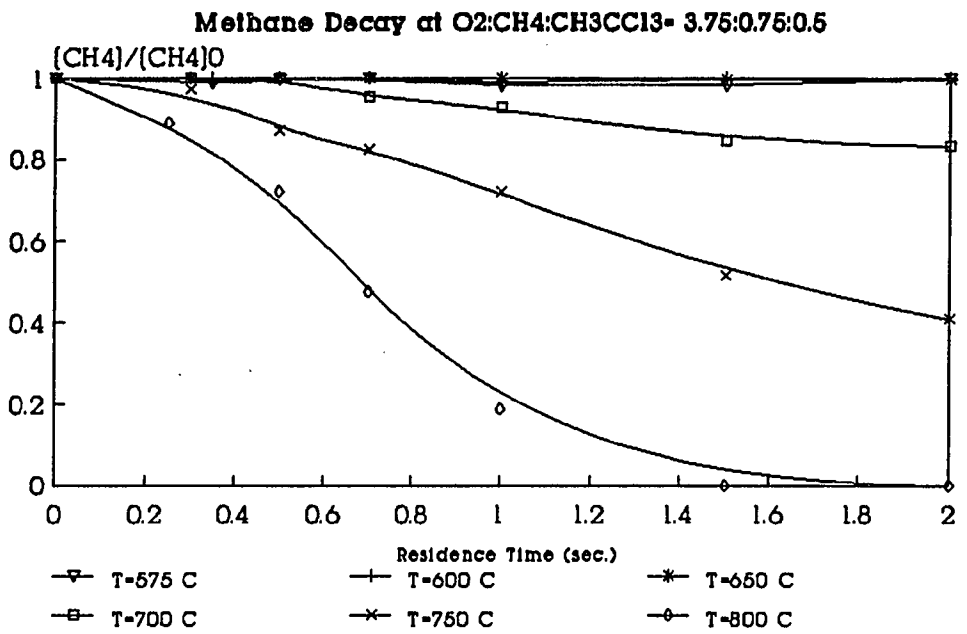

Figure 13-a. Methane Deacy Distribution ,id=1.05cm

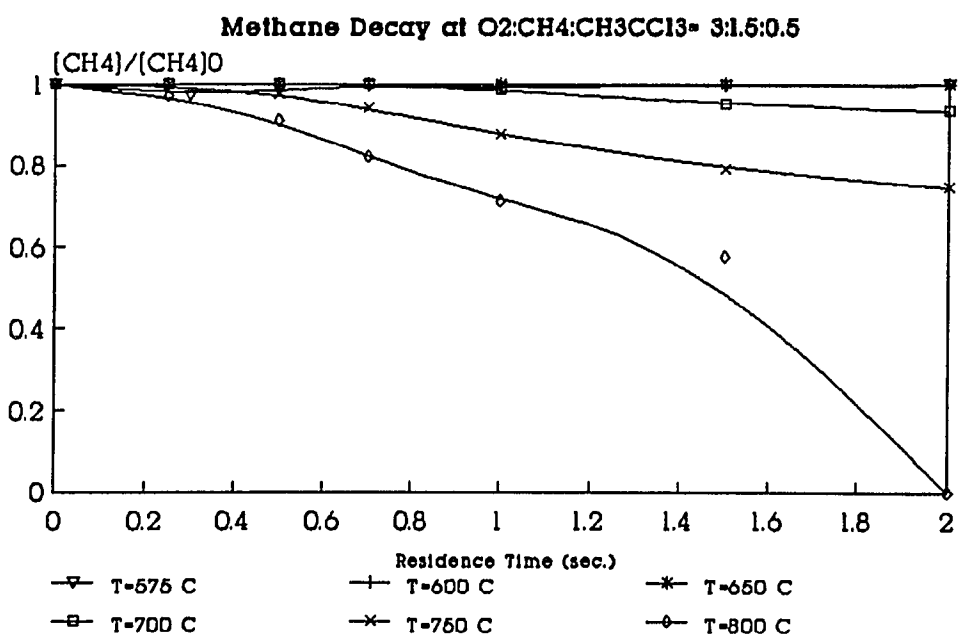

Figure 13-b. Methane Deacy Distribution ,id=1.05cm

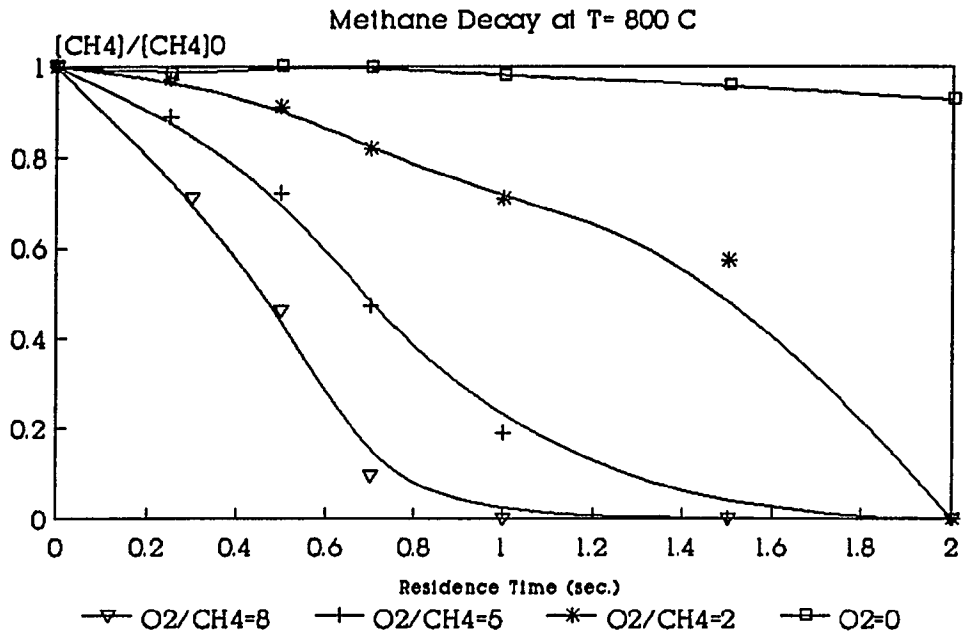

Figure 14-a. Methane Decay vs Time at 800 C

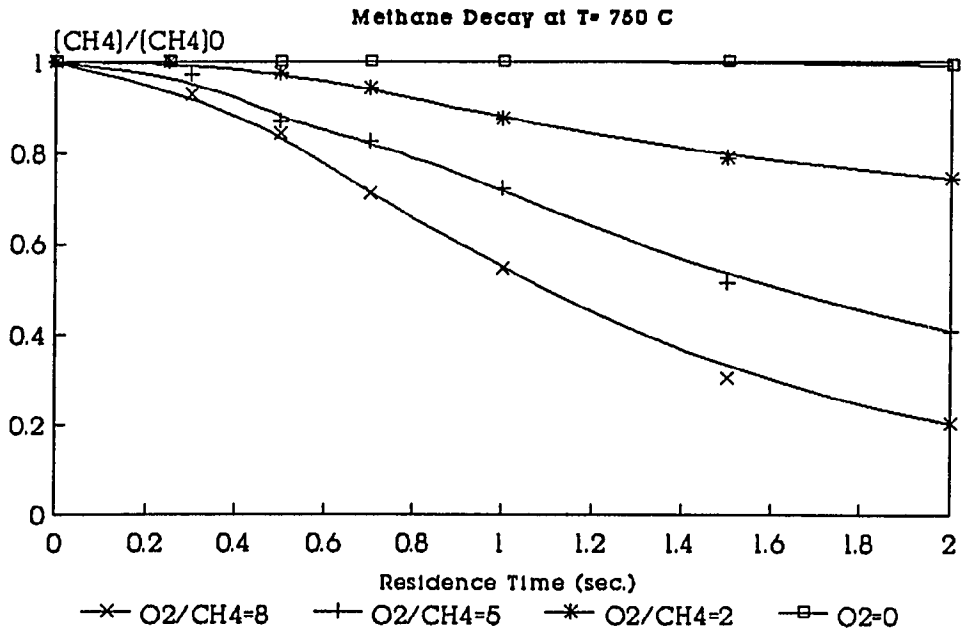

Figure 14-b. Methane Decay vs Time at 750 C

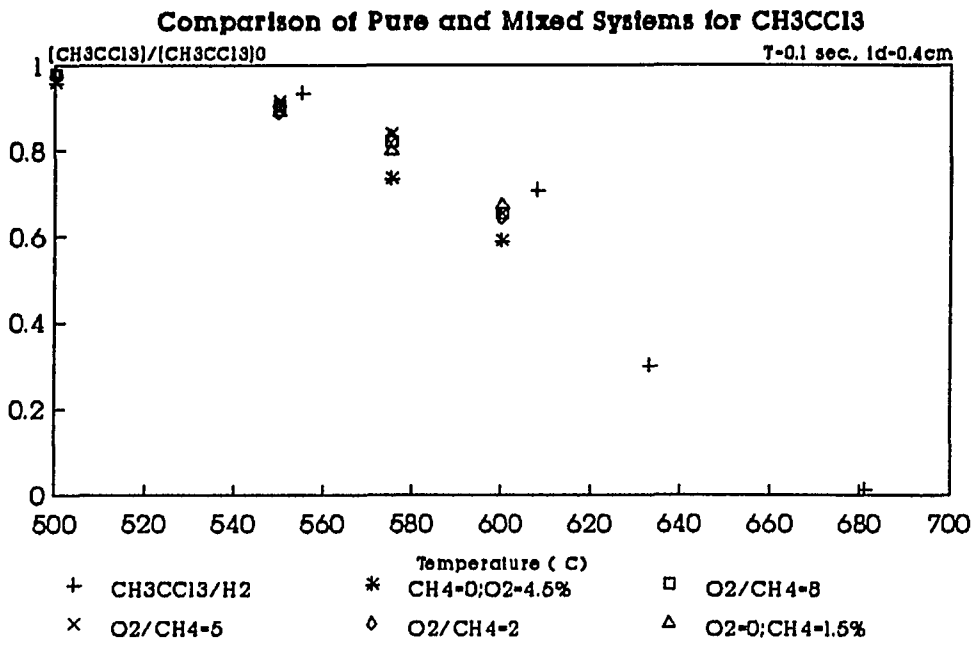

Figure 15-a.

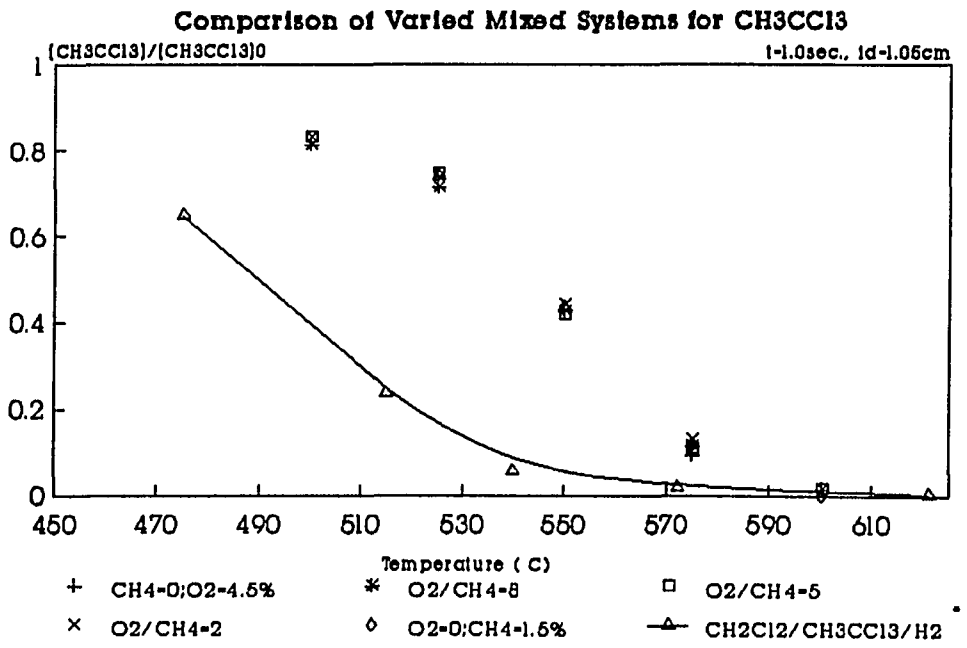

* equal fraction CH2Cl2 added difference from present study due to synergistic effects.

Figure 15-b.

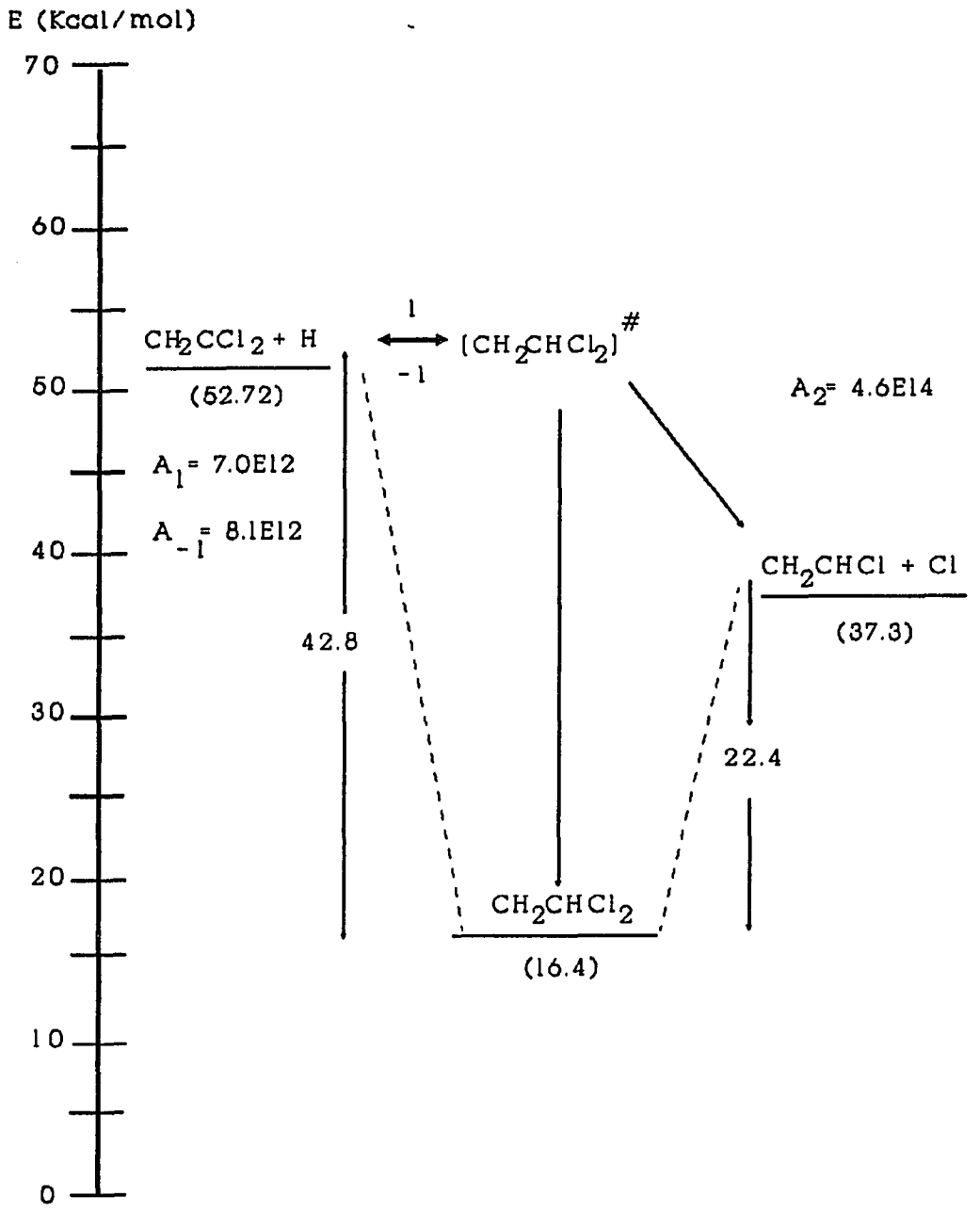

Figure 16. Energy Diagram for CH2CCl2 + H

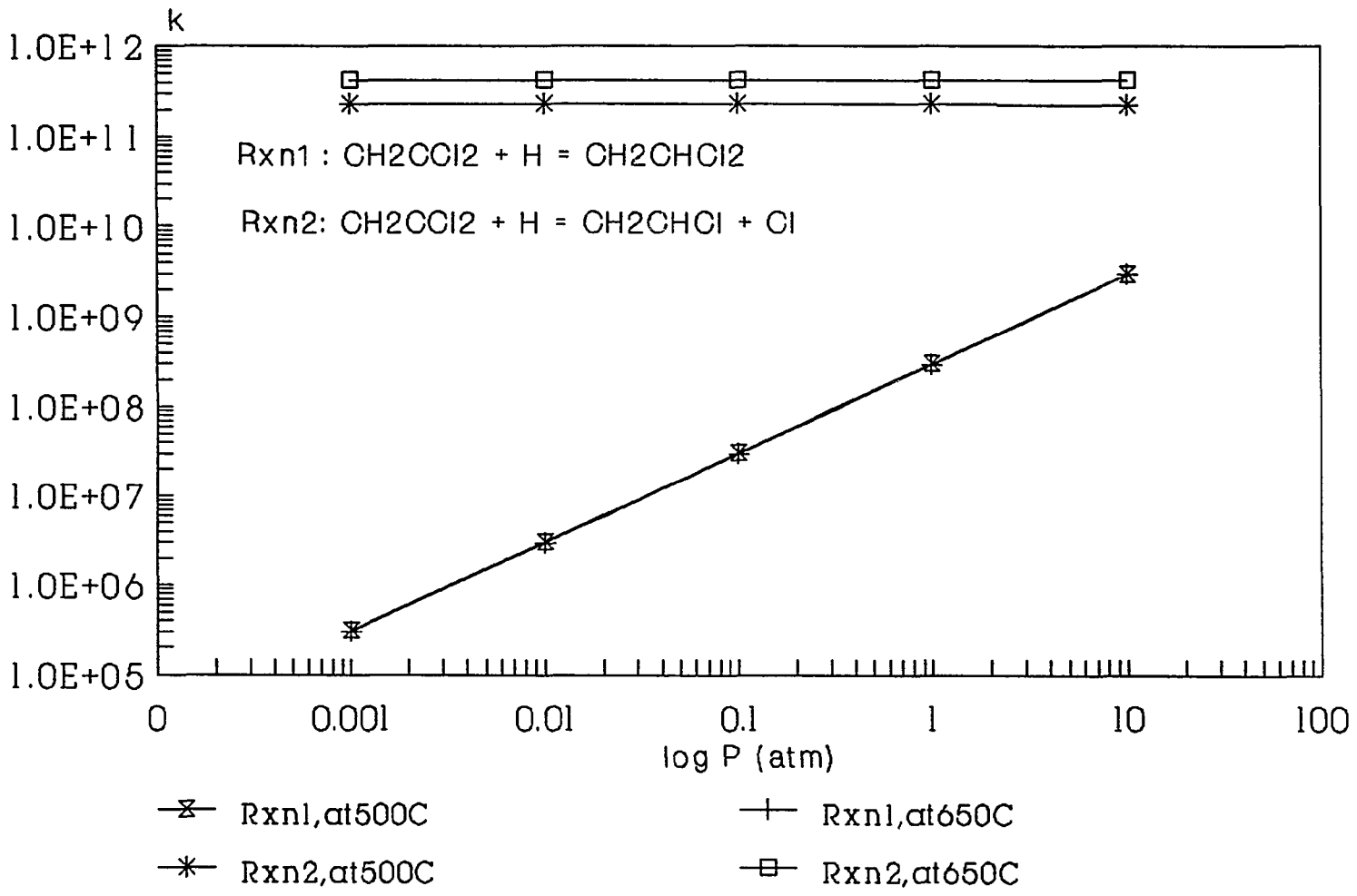

Figure 17. Results of Activated Complex Theory Calculation for Reaction CH2CCl2+ H

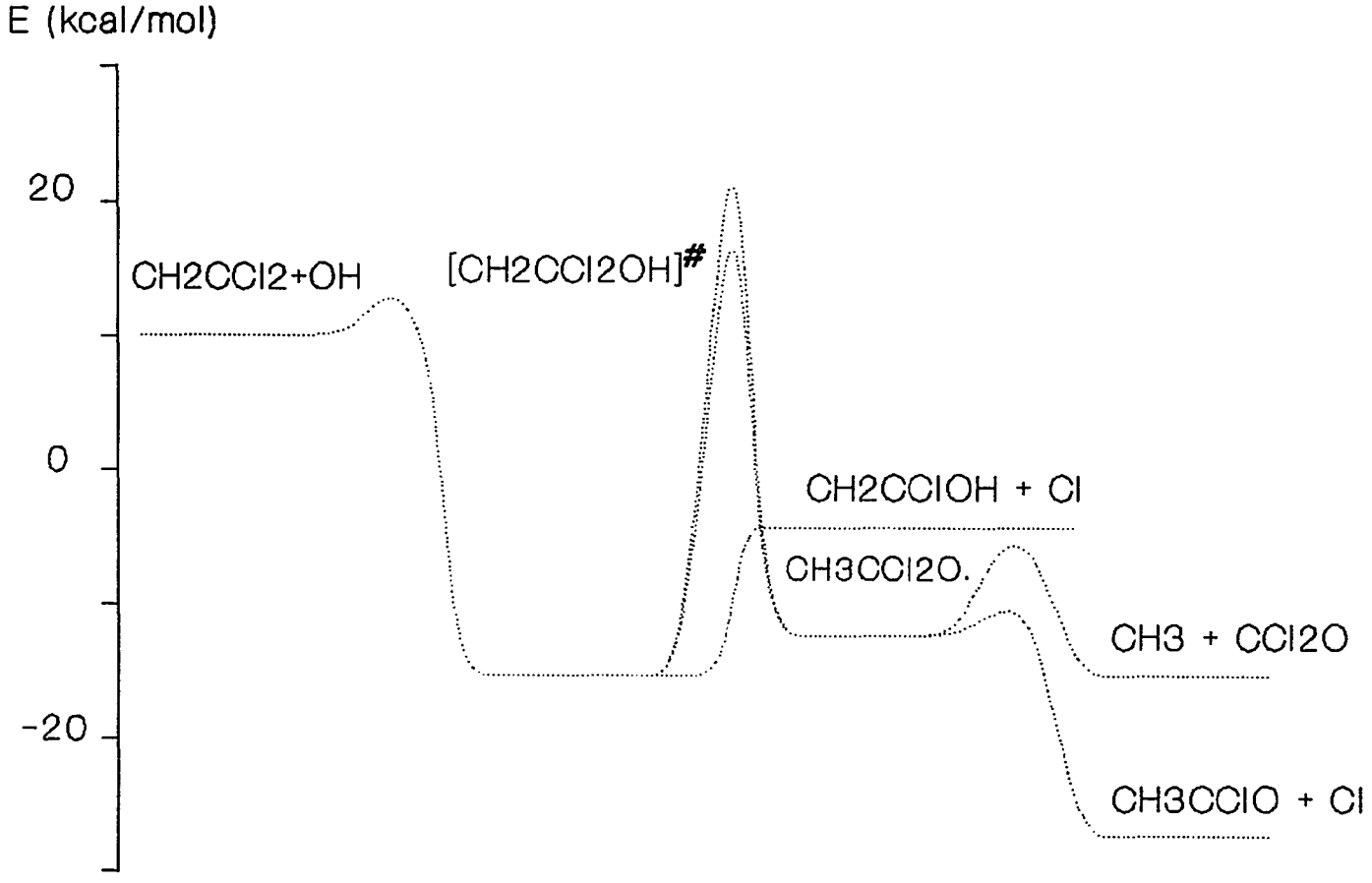

Figure 18. Potential Energy Diagram for CH2CCl2 + OH.

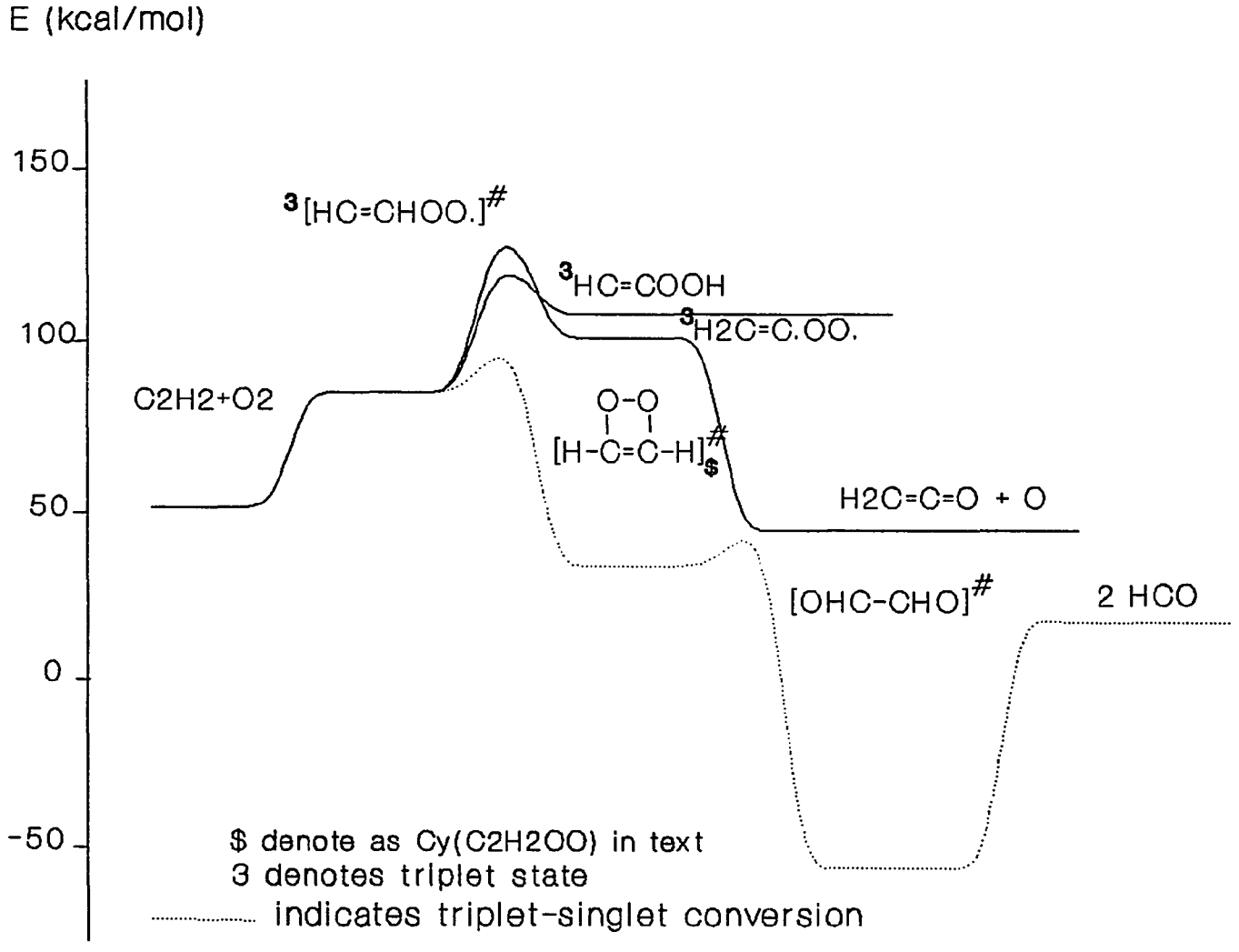

Figure 19. Potential Energy Diagram for C2H2 + O2.

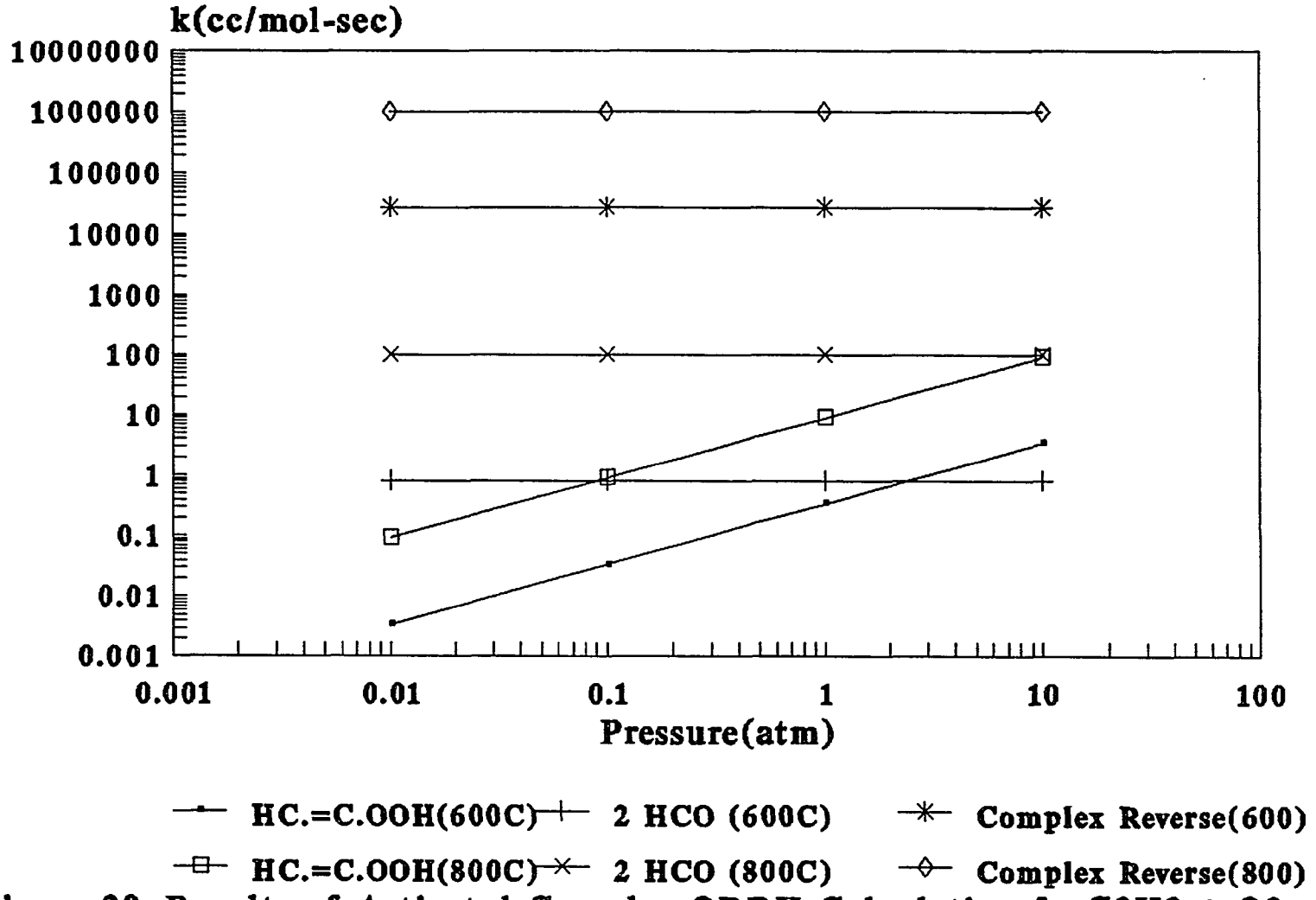

Figure 20. Results of Activated Complex QRRK Calculation for $C_2H_2 + O_2$

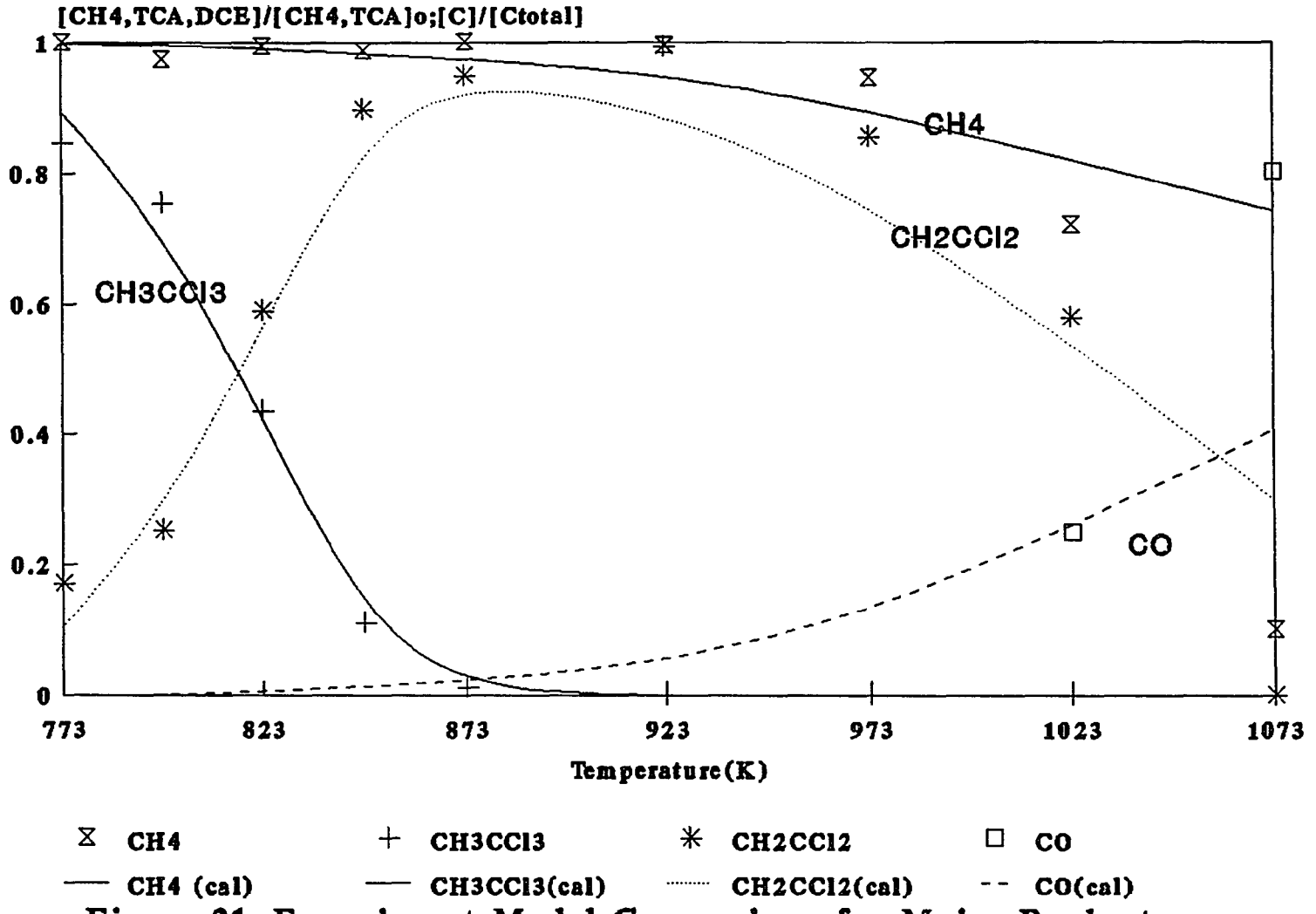

Figure 21. Experiment-Model Comparison for Major Products of O2:CH4:TCA=3.75:0.75:0.5 at RT=1.0sec, ID=1.05cm

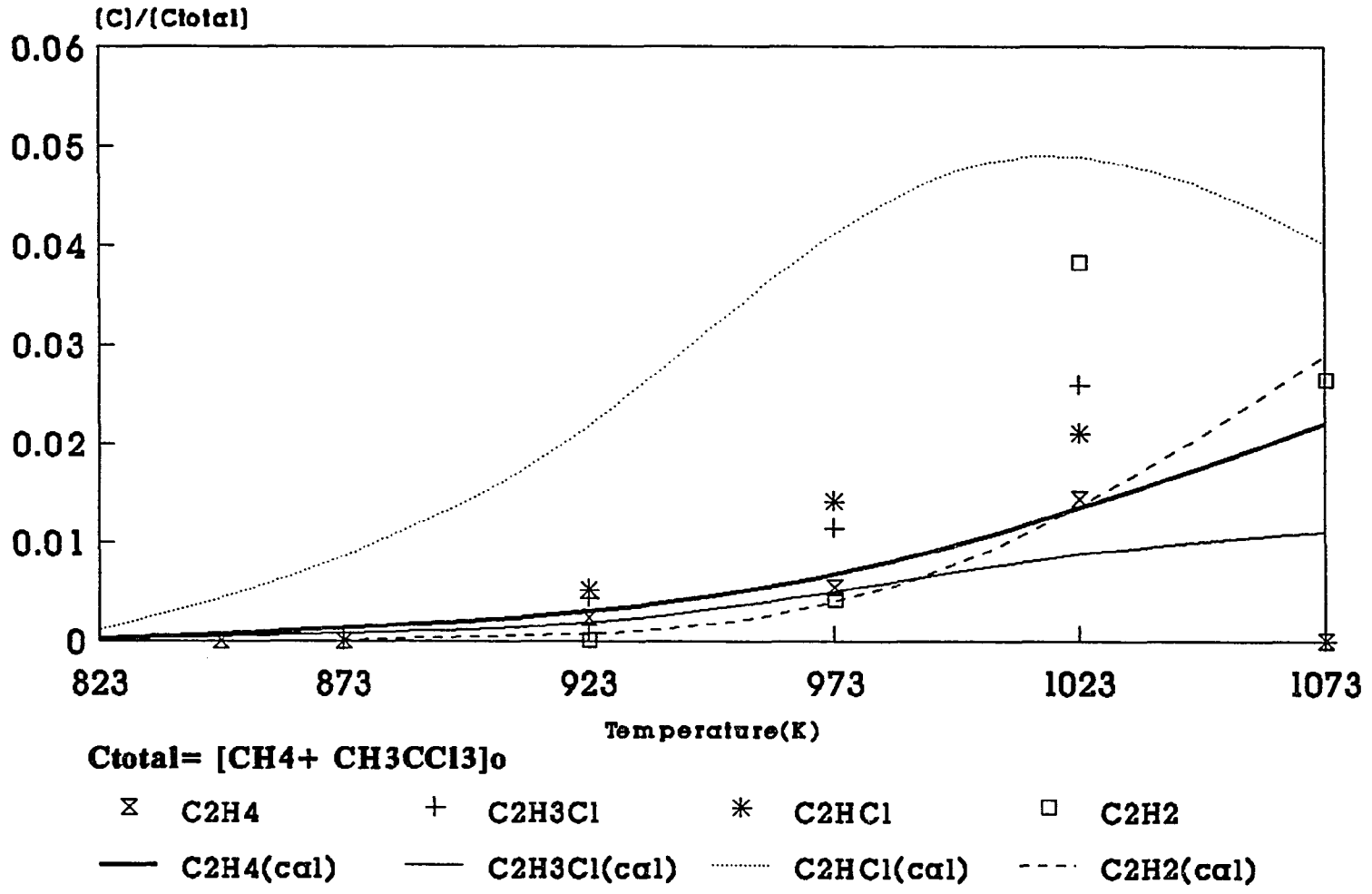

Figure 22. Experiment-Model Comparison for Minor Products for O2:CH4:TCA=3.75:0.75:0.5 at RT=1.0sec; ID=1.05cm

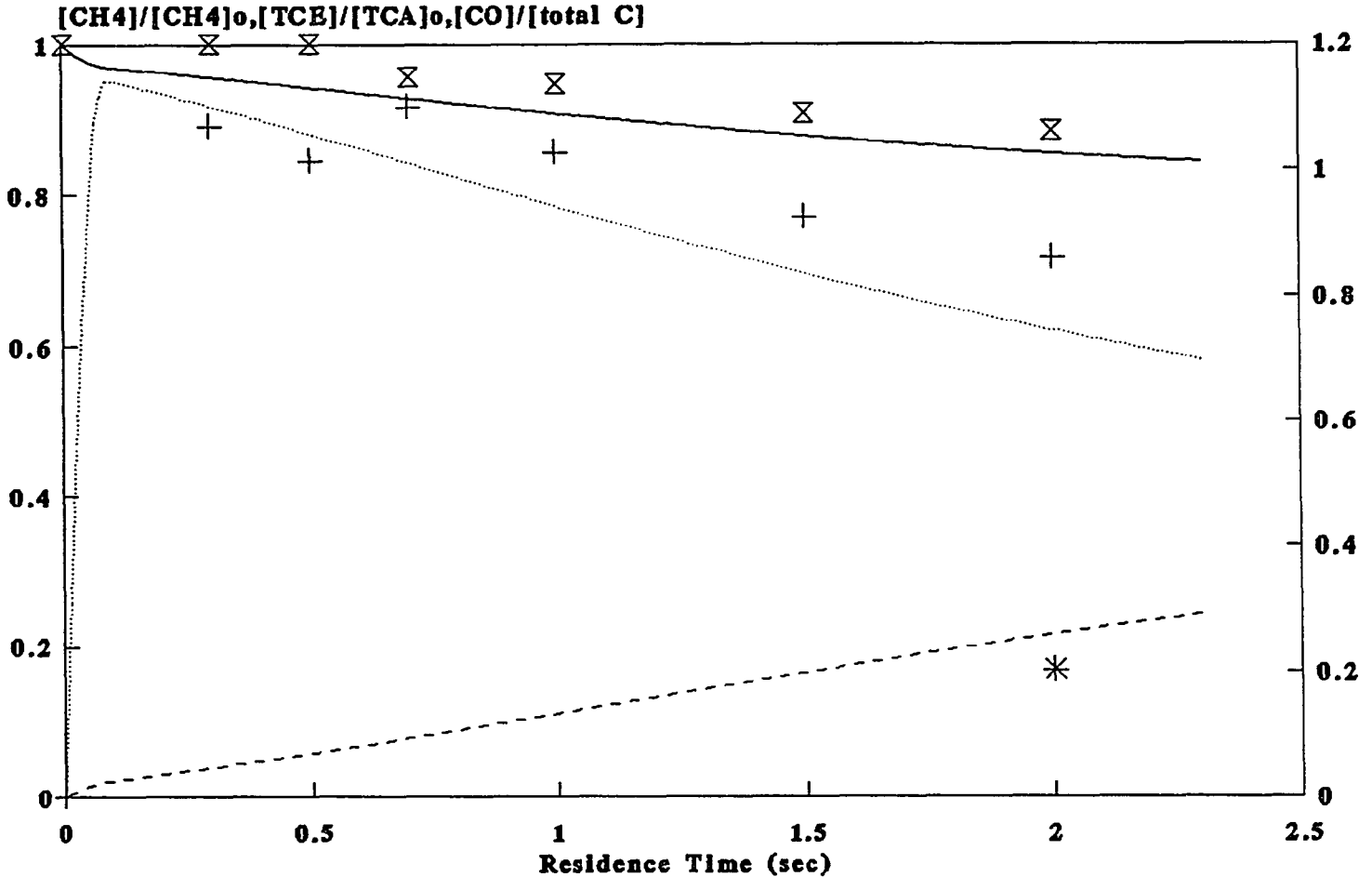

⧖ CH4 + CH2CCl2 ✳ CO — CH4(cal) ····· CH2CCl2(cal) - - - CO(cal)

Figure 23. Experiment-Model Comparison of Major Products for O2:CH4:TCA=3.75:0.75:0.5 at 973 K; ID= 1.05 cm

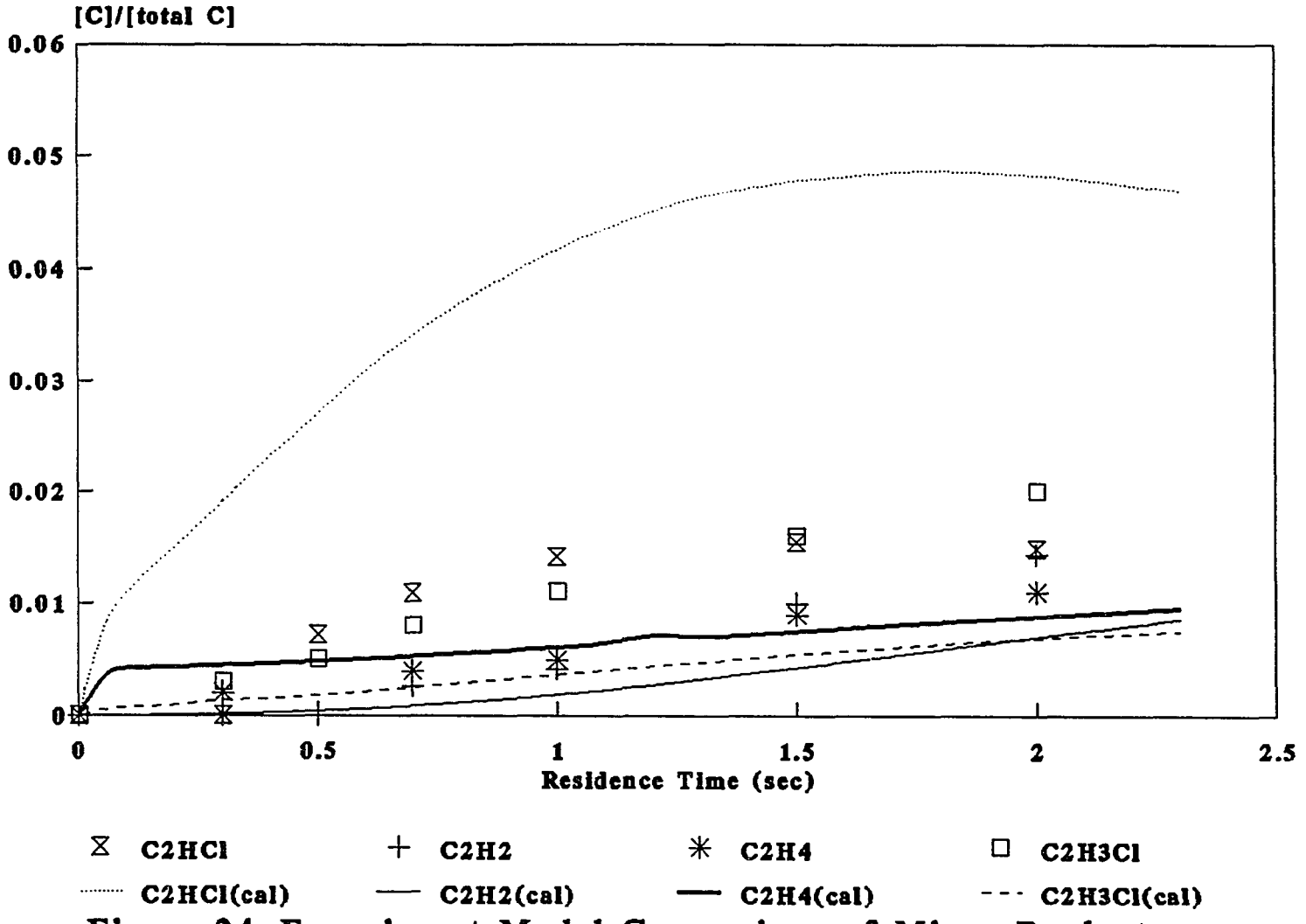

Figure 24. Experiment-Model Comparison of Minor Products for O2:CH4:TCA= 3.75:0.75:0.5 at 973 K; ID=1.05cm

5. CONCLUSIONS

The thermal decomposition of 1,1,1-trichloroethane in methane/oxygen mixtures and argon bath gas was carried out at 1 atmosphere total pressure in tubular flow reactors. Temperature ranged from 500 to 800°C, with the average residence times in the range from 0.05 to 2.5 seconds. Five reactants ratio sets range from fuel equivalence ratios of 0.2 to 1 in three size flow reactors (4, 10.5, 16 mm ID) were studied.

Complete decay (ca. 99%) for the 1,1,1-trichloroethane at 1 second residence time occurs at about 600°C for all the reactants ratio sets. The major products for 1,1,1-trichloroethane decomposition are 1,1-dichloroethylene and HCl. The number and quantity of chlorinated products decrease with increasing temperature and residence time. Oxygen has almost no effect on the conversion of 1,1,1-trichloroethane in our study because this species decays by low E_a unimolecular HCl elimination. Formation of CH_2CCl_2 as one of the major products from CH_3CCl_3 increases with increasing temperature to a maximum near 600°C at 1.0 sec residence time and is independent of reactant ratio. It then drops quickly with increasing temperature and increased O_2. Faster decay of compounds, such as C_2H_3Cl, C_2H_2, C_2H_4, C_2HCl, formed at lower temperature occurs when the reactor temperature is above 650°C, and higher oxygen levels are present in the mixture. Higher ratios of O_2 to CH_4, lead to formation of CO and CO_2 at lower temperature. The major products above 750°C are HCl, C_2HCl and non-chlorinated hydrocarbons: C_2H_2, C_2H_4, CO and CO_2.

An increase in surface to volume ratio of reactor tube was observed to accelerate the decomposition process in this study, but it had no effect on distribution of principal products.

This study demonstrates that a select ratio of oxygen/methane can be used to optimize the operate conditions to get non-chlorinated hydrocarbons and HCl

from thermal reaction of chlorocarbon mixture.

A detailed kinetic reaction mechanism was developed and used to model results obtained from the experimental reaction system. A sensitivity analysis of the model was done to show the most important reactions in the mechanism. The kinetic reaction mechanism includes 339 elementary reaction steps involving stable compounds and free radical species with the addition, beta scission and recombination type reactions all analyzed by QRRK theory.

We conclude that the primary decomposition reaction pathway for 1,1,1-trichloroethane is $CH_3CCl_3 \rightarrow CH_2CCl_2 + HCl$. High pressure limit rate constants obtained in this study for the initial decomposition of CH_3CCl_3 were determined to be:

	A (1/sec)	Ea(Kcal/mole)
$CH_3CCl_3 \rightarrow CH_2CCl_2 + HCl$	6.31E13	51.7
$CH_3CCl_3 \rightarrow CH_3CCl_2 + Cl$	1.05E16	71.2
$CH_3CCl_3 \rightarrow CH_3 + CCl_3$	9.10E16	85.7

Rate constants for 500 - 1000 ^{o}C and 1 atm are:

	A (1/sec)	Ea(Kcal/mole)
$CH_3CCl_3 \rightarrow CH_2CCl_2 + HCl$	3.35E13	51.2
$CH_3CCl_3 \rightarrow CH_3CCl_2 + Cl$	4.59E14	66.6
$CH_3CCl_3 \rightarrow CH_3 + CCl_3$	2.05E14	77.7

6. BIBLIOGRAPHY

1. Senser, D. W., V. A. Cundy, and J. S. Morse, Combust. Sci. and Tech., Vol. 51 (1987): 209-233.

2. Miller, D. L., V. A. Cundy and R. A. Matula, Proceedings of the Ninth Annual Research Symposium on Incineration and Treatment of Hazardous Waste, USEPA-600/9-84-015, July (1984): 113-128.

3. Graham, J. L., D. L. Hall and B. Dellinger, Environ. Sci. Tech. Vol. 20, No. 7 (1986).

4. Louw, R., J. H. M. Dijks and P. Mulder, Chemistry and Industry, October (1983): 759-7603.

5. Russell, J. J., J. A. Seetula, D. Gutman and S. M. Senkan, J. Phys. Chem., 93 (1989): 1934-1938.

6. Chang, W.-D. and D. M. Senkan, Environ. Sci. Technol., 23 (1989): 442-450.

7. Valeiras, H., A. K. Gupta and S. M. Senkan, Combust. Sci. Tech. 36 (1984): 123.

8. Fristrom, R.M. and P. Van Tiggelen, Seventeenth Symposium (International) on Combustion, The Combustion Institute, p. 802.

9. Deichman, W., Patty's Industrial Hygiene and Toxicology, Vol. II B, 3rd ed., ed. by G. Clayton and F. Clayton, New York : Wiley Interscience, (1981): 3650-3675.

10. Chang, W. D. S. B. Karra, and S. M. Senkan, Combust. Sci. and Tech., Vol. 49 (1986): 107-121.

11. Karra, S.B., D. Gutman and S. M. Senkan, Combust. Sci. and Tech., Vol. 60 (1988): 45-62.

12. CRC Handbook of Chemistry and Physics, 63rd ed.

13. Barton, D. H. R. and P. F. Onyon, J. Am. Chem. Soc. 72 (1950): 988.

14. Benson, S. W., and G. N. Spokes, Symp. Comb., 11 (1966): 95.

15. Chang, S.H. and J. W. Bozzelli, AIChE. J., 33 (1987): 1207.

16. Won, Y.S. and J. W. Bozzelli, The American Society of Mechanical Engineering Annual Meeting, HTD-Volume 104 (1988): 131-135.

17. Huybrechts, G., Y. Hubin and B. Van Mele, Int. J. of Chem. Kinetics, Vol. 21 (1989): 575-591.

18. Nelson, L., I. Shanahan, H. W. Sidebottom, J. Treacy and O. J. Nielsen, Int. J. of Chem. Kinetics, Vol. 22 (1990): 577.

19. Won, Y.S., M.Sc. Thesis. NJIT , Appendix 2 (1988).

20. Wu, Y.P., M.Sc. Thesis, NJIT (1989).

21. Leathard, D.A. and Shwrlock, Identification Techniques in Gas Chromatography, Wiley, New York (1970).

22. Dean, A. M., J. W. Bozzelli and E. R. Ritter, Combust. Sci. and Technol., 80 (1991): 63.

23. Robison, P.J. and K. A. Holbrook, Unimolecular Reactions, John-Wiley, N.Y. (1972).

24. Ritter, E.R., Ph. D. Thesis, NJIT (1989).

25. Benson, S.W., Thermochemical Kinetics, 2nd ed., Wiley, New York (1976).

26. Kee, R.J., T. H. Miller and T. H. Jefferson, CHEMKIN: A General-Purpose, Problem-Independent, Transportable, Fortran Chemical Kinetics Code Package, SANDIA Report, SAND80-8003, UC-4 (1980).

27. Ritter, E.R. and J. W. Bozzelli, The Eastern Section of the Combustion Institute, 1988 Technical Meeting, 29-1.

28. Lutz, A.E., R. J. Kee and J. A. Miller., SENKIN: A Fortran Program for Predicting Homogeneous Gas Phase Chemical Kinetics With Sensitivity Analysis, SAND 87-8248. UC-4 (1988).

29. Chang, W.D., Ph.D. Dissertation, Illnois Institute of Technology, IL (1988).

30. Karra, S.B. and S. M. Senken, Ind. Eng. Chem. Rev., 27 (1988): 1163.

31. Chang, S.H., Doctoral Dissertation, NJIT (1985).

32. Won, Y.S. and J. W. Bozzelli, The Eastern Section of the Combustion Institute, 1988 Technical Meeting, 24-1.

33. Dean, A.M., J. Phys. Chem., 89 (1985): 4600.

34. Westmoreland, P.R. and A. M. Dean, AIChE J., 32 (1986):171.

35. Ritter, E. and J. W. Bozzelli and A. M. Dean, J. Phys. Chem., 94 (1990): 2493.

36. Won, Y.S., Ph.D. Thesis, NJIT (1991).

37. Tsang, W., Combust. Sci. and Technol., 74 (1990): 99.

38. Rotzoll, G., Combust. Sci. and Tech., Vol 47 (1986): 275- 298.

39. Lifshitz, A., K. Scheller, A. Burcat and G. B. Skinner, Combustion & Flame, 16 (1971): 311-321.

40. Miller, J. A. and C. T. Bowman, Prog. Energy Combust. Sci., Vol 15 (1989): 287-338.

APPENDIX II

APPENDIX II-1-a. Material Balance for 100 Moles Carbon
$O_2 : CH_4 : CH_3CCl_3 = 4.5 : 0 : 0.5$
Reactor Diameter : 1.05 cm; Residence Time : 1.0 sec.

Species (%)	Temperature (°C) 525	550	575	600	650	700	750	800
CH_3CCl_3	73.17	32.00	9.17	1.36	-	-	-	-
CH_2CCl_2	27.12	59.60	92.68	94.22	60.98	1.56	-	-
CHCH	-	-	-	-	1.34	0.54	-	-
C_2HCl	-	-	-	0.21	0.97	-	-	-
CH_2CHCl	-	-	-	-	0.66	-	-	-
$CHClCCl_2$	-	-	-	-	0.68	-	-	-
CO	-	-	-	-	34.15	80.49	95.12	92.68
CH_2CH_2	-	-	-	-	-	2.93	0.66	-
Total	100.29	91.60	101.85	95.79	98.78	85.52	95.78	92.68

APPENDIX II-1-b. Material Balance for 100 Moles Carbon
$O_2 : CH_4 : CH_3CCl_3 = 4 : 0.5 : 0.5$
Reactor Diameter : 1.05 cm; Residence Time : 1.0 sec.

Species (%)	Temperature (°C) 500	525	550	575	600	650	700	750	800
CH_4	32.90	29.80	32.41	32.25	32.25	33.22	30.94	22.80	-
CH_3CCl_3	54.56	45.44	28.50	7.54	0.95	-	-	-	-
CH_2CCl_2	12.65	15.73	38.76	61.40	70.36	63.52	57.00	34.20	-
CHCH	-	-	-	-	-	-	0.91	5.70	-
CH_2CH_2	-	-	-	-	-	0.26	0.77	1.27	-
CH_3Cl	-	-	-	-	-	-	0.60	0.91	-
C_2HCl	-	-	-	-	-	-	1.41	1.74	-
CH_2CHCl	-	-	-	-	-	-	1.51	2.93	-
CO	-	-	-	-	-	-	-	35.83	-
CO_2	-	-	-	-	-	-	-	-	89.58
Total	100.11	90.97	99.67	101.19	103.56	97.00	93.14	105.38	89.58

APPENDIX II-1-c. Material Balance for 100 Moles Carbon
$O_2 : CH_4 : CH_3CCl_3 = 3.75 : 0.75 : 0.5$
Reactor Diameter : 1.05 cm; Residence Time : 1.0 sec.

Species (%)	Temperature (°C) 500	525	550	575	600	650	700	750	800
CH_4	43.44	41.20	42.04	40.08	41.48	41.90	40.50	30.73	4.33
CH_3CCl_3	48.32	41.76	24.44	6.54	0.73	-	-	-	-
CH_2CCl_2	10.00	14.25	34.50	54.61	55.73	58.66	50.28	33.52	-
CHCH	-	-	-	-	-	-	0.52	3.91	2.65
CH_2CH_2	-	-	-	-	-	0.24	0.63	1.4	-
CH_3Cl	-	-	-	-	-	-	0.49	0.88	-
C_2HCl	-	-	-	-	-	0.35	0.93	1.39	-
CH_2CHCl	-	-	-	-	-	0.43	1.20	2.65	-
CO	-	-	-	-	-	-	-	25.14	79.61
CO_2	-	-	-	-	-	-	-	-	13.13
Total	101.76	97.21	100.98	101.23	97.94	101.58	94.55	99.62	99.72

APPENDIX II-1-d. Material Balance for 100 Moles Carbon
$O_2 : CH_4 : CH_3CCl_3 = 3 : 1.5 : 0.5$
Reactor Diameter : 1.05 cm; Residence Time : 1.0 sec.

Species (%)	Temperature (°C) 500	525	550	575	600	650	700	750	800
CH_4	60.25	65.63	59.77	58.50	61.62	61.52	59.57	46.88	36.13
CH_3CCl_3	34.77	27.15	17.24	5.41	0.59	-	-	-	-
CH_2CCl_2	6.60	9.37	22.46	38.67	40.04	40.04	38.09	17.58	8.11
CH_2CH_2	-	-	-	-	0.11	0.20	0.52	1.95	2.25
CH_2CHCl	-	-	-	-	0.14	0.26	0.67	2.25	1.56
CHCH	-	-	-	-	-	-	0.16	4.10	8.11
CH_3Cl	-	-	-	-	-	-	0.28	1.07	0.83
C_2HCl	-	-	-	-	-	0.17	0.54	0.61	0.32
CO	-	-	-	-	-	-	-	22.46	38.09
Total	101.62	102.15	99.47	102.58	102.50	102.19	99.93	96.90	95.40

APPENDIX II-1-e. Material Balance for 100 Moles Carbon
$O_2 : CH_4 : CH_3CCl_3 = 0 : 1.5 : 0.5$
Reactor Diameter : 1.05 cm; Residence Time : 1.0 sec.

Species (%)	Temperature (°C) 500	525	550	575	600	650	700	750	800
CH_4	60.84	74.24	61.05	57.90	61.86	62.51	62.51	61.54	58.61
CH_3CCl_3	27.06	19.29	17.08	4.08	-	-	-	-	-
CH_2CCl_2	6.60	6.85	22.97	37.44	41.05	38.10	40.05	35.17	29.30
CH_2CHCl	-	-	-	-	-	0.18	1.07	0.23	0.28
CHCH	-	-	-	-	-	-	-	0.18	0.85
CH_2CH_2	-	-	-	-	-	-	0.12	0.18	0.30
C_2HCl	-	-	-	-	-	-	0.12	1.76	4.43
CH_3CHCl_2	-	-	-	-	-	-	-	0.50	2.25
CH_2Cl_2	-	-	-	-	-	-	-	-	1.07
$CHClCCl_2$	-	-	-	-	-	-	-	-	2.05
C_6H_6	-	-	-	-	-	-	-	-	0.62
Total	94.50	100.38	101.10	99.42	102.91	100.79	103.87	99.56	99.76

APPENDIX II-1-f. Material Balance for 100 Moles Chlorine
$O_2 : CH_4 : CH_3CCl_3 = 4.5 : 0 : 0.5$
Reactor Diameter : 1.05 cm; Residence Time : 1.0 sec.

Species (%)	Temperature (°C) 550	575	600	650	700	750	800
CH_3CCl_3	32.43	9.28	1.39	-	-	-	-
CH_2CCl_2	40.17	62.50	63.73	40.98	0.31	-	-
CH_3Cl	-	-	-	0.36	-	-	-
CH_2CHCl	-	-	-	0.23	-	-	-
C_2HCl	-	-	0.10	0.49	-	-	-
HCl	18.60	30.59	35.83	49.18	77.05	95.08	104.92
Total	91.20	102.37	101.05	91.24	77.36	95.08	104.92

APPENDIX II-1-g. Material Balance for 100 Moles Chlorine
$O_2 : CH_4 : CH_3CCl_3 = 4 : 0.5 : 0.5$
Reactor Diameter : 1.05 cm; Residence Time : 1.0 sec.

Species (%)	Temperature (°C) 500	525	550	575	600	650	700	750	800
CH_3CCl_3	81.40	68.13	42.79	11.42	1.38	-	-	-	-
CH_2CCl_2	12.60	15.71	38.72	61.93	67.98	66.10	58.33	26.23	-
CH_3Cl	-	-	-	-	-	-	0.62	0.85	-
CH_2CHCl	-	-	-	-	-	-	0.77	0.90	-
C_2HCl	-	-	-	-	-	-	0.71	0.61	-
HCl	6.44	8.28	18.22	28.58	30.37	35.59	41.67	67.21	109.68
Total	100.44	92.12	99.73	101.93	99.73	101.69	102.10	95.80	109.68

APPENDIX II-1-h. Material Balance for 100 Moles Chlorine
$O_2 : CH_4 : CH_3CCl_3 = 3.75 : 0.75 : 0.5$
Reactor Diameter : 1.05 cm; Residence Time : 1.0 sec.

Species (%)	Temperature (°C) 500	525	550	575	600	650	700	750	800
CH_3CCl_3	83.58	73.01	42.27	10.84	1.24	-	-	-	-
CH_2CCl_2	11.51	16.59	39.85	60.35	63.43	67.74	60.00	35.59	0.58
CH_3Cl	-	-	-	-	-	-	0.58	1.29	-
CH_2CHCl	-	-	-	-	-	0.26	0.72	1.58	-
C_2HCl	-	-	-	-	-	0.17	0.47	0.70	-
HCl	6.59	7.77	18.39	27.16	30.52	33.87	38.33	59.32	95.16
Total	101.68	97.37	100.51	98.35	95.19	102.04	100.10	98.48	95.74

APPENDIX II-1-i. Material Balance for 100 Moles Chlorine
$O_2 : CH_4 : CH_3CCl_3 = 3 : 1.5 : 0.5$
Reactor Diameter : 1.05 cm; Residence Time : 1.0 sec.

Species (%)	Temperature (°C) 500	525	550	575	600	650	700	750	800
CH_3CCl_3	83.08	67.80	44.33	12.91	1.50	-	-	-	-
CH_2CCl_2	10.52	15.59	38.48	61.54	68.31	68.33	63.93	42.62	16.67
CH_2CHCl	-	-	-	-	0.12	0.22	0.56	1.41	1.82
CH_3Cl	-	-	-	-	-	-	0.48	1.26	1.82
C_2HCl	-	-	-	-	-	0.08	0.27	0.31	0.16
HCl	6.44	8.08	19.07	27.51	30.66	35.00	36.07	52.46	71.21
Total	100.04	91.47	101.88	101.96	100.59	103.63	101.31	98.06	91.68

APPENDIX II-1-j. Material Balance for 100 Moles Chlorine
$O_2 : CH_4 : CH_3CCl_3 = 0 : 1.5 : 0.5$
Reactor Diameter : 1.05 cm; Residence Time : 1.0 sec.

Species (%)	Temperature (°C) 500	525	550	575	600	650	700	750	800
CH_3CCl_3	67.07	38.54	44.03	11.62	-	-	-	-	-
CH_2CCl_2	10.93	9.12	39.47	60.51	69.51	67.24	69.49	61.02	48.39
CH_2CHCl	-	-	-	-	-	0.16	0.92	0.20	0.23
CH_3CHCl_2	-	-	-	-	-	-	-	1.14	3.71
CH_2Cl_2	-	-	-	-	-	-	-	-	3.55
$CHClCCl_2$	-	-	-	-	-	-	-	-	5.00
C_2HCl	-	-	-	-	-	-	0.06	0.88	2.21
HCl	5.95	9.09	19.06	27.29	30.45	34.48	33.90	40.68	48.39
Total	83.95	56.75	102.56	99.42	99.96	101.88	104.37	103.92	111.48

APPENDIX II-2.

QRRK 1

$$CH_3CCl_2 + H \overset{1}{\Longleftrightarrow} [CH_3CHCl_2]^{\#} \overset{2}{\longrightarrow} CH_2CHCl + HCl$$

$$\overset{3}{\longrightarrow} CH_3CHCl + Cl$$

$$\longrightarrow CH_3CHCl_2 \text{ (Stab.)}$$

k	A	Ea	source
1	2.0 E+13	0.0	a
-1	4.2 E+14	93.2	a
2	4.3 E+13	57.9	b
3	6.2 E+15	76.3	c
<v> = 797.2/cm			d
L-J Parameters:	σ = 5.103 Å	ε/k = 435.9 ^{o}K	e

a. A_1 factor taken as 1/2 that for H + CH_3CH_2 (A= 4.0 E+13), A_{-1} and Ea_{-1} from thermodynamics and microscopic reversibility, (ref: Allara,D.L. and Shaw,R.J., J. Phys. Chem. Ref. Data, 9 (1980): 523)

b. Transition State Theory (this study): loss of a rotor, degeneracy= 6, A_2 = $10^{13.72} * 10^{(-4/4.6)} * 6$, $E_a = \Delta H + 41.0$ (Ea ref: Weissman, M. and Benson, S.W., Inter. J. Chem. Kinet., 16 (1984): 941)

c. A_3 factor based upon entropy change for reverse. A_{-3} factor taken as that for 2-C_3H_7 + CH_3 (A = 1.6E+13, ref: Allara and Shaw as note a.), $E_a = \Delta H - RT$.

d. Shimanouchi,T., Tables of Molecular Vibration Frequencies Consolidated Vol.I, Natl. Stand. Ref. Data Ser. (U.S. Natl. Bur. Stand.) (1972) NSRDS-NBS 39. (refer to CH_2ClCH_2Cl)

e. Activated complex L-J parameters are estimated using critical property data tabulated in Reid, Prausnitz and Poling (The Properties and Gases and Liquids, 3th ed., RPP in abbrev.)

* Units of A factor are cc/(mol sec) for bimolecular reactions and 1/sec for unimolecular reactions. ΔHr taken as from stabilized adduct

CALCULATED APPARENT FORWARD REACTION RATE CONSTANTS

Bath Gas	P (torr)	Product Channel	A (cc/mole s)	E_a (Kcal/mole)
AR	760.0	CH_3CHCl_2	5.98 E+11	-7.54
		$CH_2CHCl + HCl$	4.73 E+12	-0.70
		$CH_3CHCl + Cl$	5.06 E+13	3.33

QRRK 2

$$CCl_3CH_2 + H \overset{1}{\Longleftrightarrow} [CH_3CCl_3]^{\#} \overset{2}{\longrightarrow} CH_2CCl_2 + HCl$$

$$\overset{3}{\longrightarrow} CH_3CCl_2 + Cl$$

$$\longrightarrow CH_3CCl_3 \text{ (Stab.)}$$

k	A	Ea	source
1	2.0 E+13	0.0	a
-1	2.5 E+15	94.9	a
2	6.3 E+13	51.7	b
3	1.1 E+16	68.3	c
<v> = 732.8/cm			d
L-J Parameters:			e
	σ= 5.72 Å	ε/k = 498.0 °K	

a. A_1 factor taken as 1/2 that for H + CH_3CH_2 (A= 4.0 E+13). A_{-1} and Ea_{-1} from thermodynamics and microscopic reversibility (ref: Allara,D.L. and Shaw,R.J., J. Phys. Chem. Ref. Data, 9 (1980): 523)

b. Transition State Theory (this study): loss of a rotor, degeneracy= 9, $A_2 = 10^{13.72} * 10^{(-4/4.6)} * 9$, $E_a = \Delta H + 42.7$. (E_a ref: Benson, S.W. and Spokes, G.N., 11th Symposium (1966): 95)

c. A_3 factor based upon entropy change for reverse. A_{-3} factor taken as that for i-C_4H_9 + CH_3 (A = 2.0E+13, ref: Allara and Shaw). $E_a = \Delta Hr - RT$

d. Shimanouchi,T., Tables of Molecular Vibration Frequencies Consolidated Vol.I, Natl. Stand. Ref. Data Ser. (U.S. Natl. Bur. Stand.) (1972) NSRDS-NBS 39. (refer to CH_2ClCH_2Cl)

e. Activated complex L-J parameters are estimated using critical property data tabulated in Reid, Prausnitz and Poling (The Properties and Gases and Liquids, 3th ed.)

CALCULATED APPARENT FORWARD REACTION RATE CONSTANTS

Bath Gas	P (torr)	Product Channel	A (cc/mole s)	n	Ea (Kcal/mole)
AR	760.0	CH_3CCl_3	5.60E36	-7.89	6.12
		CH_2CCl_2 + HCl	2.02E12		-1.58
		CH_3CCl_2 + Cl	2.65E13		1.16

QRRK3

$$CH_2CCl_2 + H \overset{1}{\Longleftrightarrow} [CH_2CHCl_2]^{\#} \overset{2}{\longrightarrow} CH_2CHCl + Cl$$
$$\longrightarrow CH_2CHCl_2 \text{ (Stab.)}$$

k	A	Ea (Kcal/mol)	source
1	7.00 E+12	6.5	a
-1	8.05 E+12	42.8	a
2	4.62 E+14	22.4	b
<v> = 736/cm			c
Lennard-Jones Parameters :	σ= 5.103 Å	ε/k = 435.91 °K	d

a A_1 factor taken as 1/2 that for C_2Cl_4 + H . Ea estimated from addition reaction of C_2Cl_4 + H and C_2H_4 + H and reverse reaction (k_{-1}) from thermodynamics (ref: Tsang, W., 23rd Symposium on Combustion, Orleans, France (1990) and NIST Chemical Kinetic Database (Version 2.0) (1990))

b A_2 based upon ΔS for $CH_2CHCl + Cl = CH_2CHCl_2$ with A_{-2} = 2.0 E+13 and Ea_{-2} = 1.5 (ref: Kerr, J.A. and Moss, S.J. ,"Handbook of Bimolecular and Termolecular Gas Reaction Vol. I & II", CRC Press Inc. (1981))

c Shimanouchi,T., Tables of Molecular Vibration Frequencies Consolidated Vol.I, Natl. Stand. Ref. Data Ser. (U.S. Natl. Bur. Stand.) (1972) NSRDS-NBS 39. (refer to $CH_2ClCHCl$)

d Activated complex L-J parameters are estimated using critical property data tabulated in Reid, Prausnitz and Poling (The Properties and Gases and Liquids, 3th ed.)

CALCULATED APPARENT FORWARD REACTION RATE CONSTANTS

Bath Gas	P (torr)	Product Channel	A (cc/mole s)	n	Ea (Kcal/mole)
AR	760.0	CH_2CHCl_2	7.21E24	-4.89	7.92
		$CH_2CHCl + Cl$	1.00E13		5.80

QRRK4

$$CH_2CCl_2 + OH \overset{1}{\Longleftrightarrow} [C.H_2CCl_2OH]^{\#} \overset{2}{\longrightarrow} CH_2CClOH + Cl$$

$$\overset{4}{\Longleftrightarrow} [CH_3CCl_2O]^{\#}$$

$$\overset{5}{\longrightarrow} CH_3CClO + Cl$$

$$\overset{6}{\longrightarrow} CH_3 + CCl_2O$$

k	A	Ea	Source
1	2.90E12	2.2	a
-1	2.05E14	30.6	b
2	2.55E13	17.6	c
4	1.23E12	38.4	d
-4	1.63E13	35.0	e
5	2.87E15	2.0	f
6	2.24E14	7.7	g
$\langle v \rangle = 958.2\ cm^{-1}$			h
LJ PARAMETERS:	$\sigma = 5.19$ Å	$\varepsilon/k = 649.1\ ^{o}K$	i

a. A_1, E_1 taken as 1/2 that for C_2Cl_4 + OH (Ref: NIST fit).

b. Reverse reaction (k_{-1}) from thermodynamics.

c. A_{-2} taken as that for Cl + unsaturated species (A=1.50E13, ref: Kerr, J.A. and Moss, S.J. ,"Handbook of Bimolecular and Termolecular Gas Reaction Vol. I & II", CRC Press Inc. (1981) and NIST) and microsopic reversibility , $E_a = \Delta Hr + 1.0$.

d. Transition State Theory: loss of 2 rotors and degeneracy,
$A_4 = 10^{13.72} * EXP(-7/R) * 1 = 1.23E12$. $Ea_4 = RS + \Delta Hr + Ea_{abs} = 26 + 3.4 + 9 = 38.4$.

Ea_{abs}: $CH_3 + ROH \longrightarrow CH_4 + RO.$ (K-M I, 199)
$CH_3 + CH_3OH \longrightarrow CH_4 + CH_3O.$, $E_a = 9.0$
$CH_3 + CH_3CH_2OH \longrightarrow CH_4 + CH_3CH_2O.$, $E_a = 9.4$.

e. Reverse reaction (k_{-4}) from thermodynamics.

f. A_{-5} taken as that for Cl + unsaturated species (A=1.5E13, ref: Kerr, J.A. and Moss, S.J. ,"Handbook of Bimolecular and Termolecular Gas Reaction Vol. I & II", CRC Press Inc. (1981) and NIST) and microscopic reversibility, $E_a = \Delta Hr + 2 = 2$.

g. A_{-6} taken as that for $C_2C{=}C$ + C. (A=1.41E11 Ref: Kerr & Moss, II), Ea_{-6} = 7.7 and microscopic reversibility.

h. From "CPFIT" program and Cp data.

i. Calculated from critical properties (estimated by using Lydersen method) for CH_3CCl_2OH (Ref: RPP).

CALCULATED APPARENT FORWARD REACTION RATE CONSTANTS

Bath Gas	P (torr)	Product Channel	A (cc/mole s)	n	Ea (Kcal/mole)
Ar	760	CH_2CCl_2OH	1.41E30	-6.46	5.02
		CH_2CClOH + Cl	2.56E13	-0.50	2.0
		CH_3CCl_2O	2.51E01		11.6
		CH_3CClO + Cl	1.21E05	1.15	11.88
		CH_3 + CCl_2O	4.23E03	1.75	11.69

QRRK5

$$CH_2CCl_2 + OH \overset{1}{\Longleftrightarrow} [CH_2OHCCl_2.]^{\#} \overset{2}{\longrightarrow} CCl_2CHOH + H$$

$$\overset{4}{\Longleftrightarrow} [CHCl_2CH_2O.]^{\#}$$

$$\overset{5}{\longrightarrow} CHCl_2CHO + H$$

$$\overset{6}{\longrightarrow} CHCl_2 + CH_2O$$

k	A	Ea	Source
1	2.72E12	2.4	a
-1	1.65E14	28.9	b
2	7.36E13	36.2	c
4	1.23E12	38.4	d
-4	1.63E13	35.0	e
5	6.88E13	19.7	f
6	4.93E14	15.6	g
$\langle v \rangle = 958.2\ cm^{-1}$			h
LJ PARAMETERS:	$\sigma = 5.19$ Å	$\varepsilon/k = 649.1\ ^{o}K$	i

a. A_1 taken as 1/2 that for C_2H_4 + OH (Ref: NIST fit).

b. Reverse reaction (k_{-1}) from thermodynamics.

c. A_{-2} taken as 1/2 of that for H + C_2H_4 (A=1.8E13, Ref:NIST fit), E_{-2} = 2.8, and microscopic reversibility.

d. Transition State Theory: loss of 2 rotors and degeneracy=1,
$A_4 = 10^{13.72} * EXP(-7/R) * 1 = 1.23E12$. $Ea_4 = RS + \Delta Hr + Ea_{abs} = 26 + 3.4 + 9 = 38.4$.
Ea_{abs}: $CH_3 + ROH \longrightarrow CH_4 + RO.$ (K-M I, 199),
$CH_3 + CH_3OH \longrightarrow CH_4 + CH_3O.$, $E_a = 9.0$,
$CH_3 + CH_3CH_2OH \longrightarrow CH_4 + CH_3CH_2O.$, $E_a = 9.4$.

e. Reverse reaction (k_{-4}) from thermodynamics.

f. A_{-5} taken as 1/2 of that for H + C_2H_4 (A=1.8E13, Ref:NIST fit),
$E_a = \Delta Hr + 2.6$.

g. A_{-6} taken as that for CC.C + C=C (A=6.92E10, Ref: Kerr, J.A. and Parsonage, M.J., "Evaluated kinetic data on gas phase addition reactions: reactions of atoms and radicals with alkenes, alkynes and aromatic compounds, Butterworths, London (1972)), Ea_{-6} = 7.0 and microscopic reversibility.

h. From "CPFIT" program and Cp data.

i. Calculated from critical properties (estimated by using Lydersen method) for CH_3CCl_2OH (Ref: RPP).

CALCULATED APPARENT FORWARD REACTION RATE CONSTANTS

Bath Gas	P (torr)	Product Channel	A (cc/mole s)	Ea (Kcal/mole)
Ar	760	CH_2OHCCl_2	1.36E10	-4.7
		$CHCl_2CH_2O$	1.45E05	7.2
		$CHCl_2CHO + H$	1.65E09	13.3
		$CHCl_2 + CH_2O$	2.28E10	12.4

QRRK6

$$CH_2CCl_2 + O \overset{1}{\Longleftrightarrow} [CH_2.CCl_2O.]^{\#} \overset{2}{\longrightarrow} {}^3CH_2 + CCl_2O$$

$$[CH_2.CCl_2O.]^{\#} \overset{3}{\longrightarrow} CH_2.CClO + Cl$$

k	A	Ea	Source
1	5.90E11	4.5	a
-1	1.00E13	31.0	b
2	1.72E14	7.5	c
3	9.50E14	1.0	d
$\langle v \rangle = 853.8\ cm^{-1}$			e
LJ PARAMETERS:	$\sigma = 5.19$ Å	$\varepsilon/k = 649.1\ ^oK$	f

a. A_1 taken from CH_2CCl_2 + O (A=5.90E11, Ref: Cvetanovic, R.J., J. Phys. Chem., Ref. Data, 16 (1987): 261).

b. Reverse reaction (k_{-1}) from thermodynamics.

c. A_{-2} taken as 2 of that for C. + $C_2C{=}C \longrightarrow (CH_3)_3CC$. (A=2.0E11, Ea=8.9, Ref: Allara,D.L. and R. J. Shaw, J. Phys. Chem. Ref. Data, 9 (1980): 523), Ea = 7.5, and microscopic reversibility.

d. A_{-3} taken as 1/3 of that for Cl + C_2Cl_4 (2.49E13, Atkinson,R. and S. M. Aschmann, Int. J. of Chem. Kinetic., 19 (1987): 1097), Ea_3=1.0.

e. From "CPFIT" program and Cp data.

f. Calculated from critical properties (estimated by using Lydersen method) for CH_3CCl_2OH (Ref: RPP).

CALCULATED APPARENT FORWARD REACTION RATE CONSTANTS

Bath Gas	P (torr)	Product Channel	A (cc/mole s)	Ea (Kcal/mole)
Ar	760	CH_2CCl_2O	1.06E06	1.16
		CH_2 + CCl_2O	2.55E11	5.40
		CH2.CClO+Cl	3.63E11	4.18

QRRK7

$$CH_2CCl + H \overset{1}{\Longleftrightarrow} [CH_2CHCl]^{\#} \overset{2}{\longrightarrow} CH_2CH + Cl$$

$$\overset{3}{\longrightarrow} CHCH + HCl$$

$$\longrightarrow CH_2CHCl \text{ (Stab.)}$$

k	A	Ea	source
1	1.0 E+14	0.0	a
-1	3.0 E+15	104.1	a
2	7.9 E+16	87.6	b
3	5.3 E+13	68.7	c
$\langle v \rangle$ = 1344.3 cm^{-1}			d
L-J Parameters :	σ = 4.644 Å	ε/k = 349 ^{o}K	e

a A_1 factor taken as that for H + 2-C_4H_9. A_{-1} based upon entropy change for reverse. (Ref: Allara,D.L. and R. J. Shaw, J. Phys. Chem. Ref. Data, 9 (1980): 523).

b A_2 factor based upon entropy change for reverse. $CH_2CH + CH_3 = CH_2CHCH_3$ with A = 1.8 E+13 and Ea = 0.0 (ref: Dean, A.M., J. Phys. Chem., 89 (1985): 4600).

c Transition State Theory (this study): loss of no rotor and degeneracy, $A_3 = 10^{13.72} * 1$, $E_a = \Delta Hr + 45$ (Ea ref: Zabel, F., Inter. J. Chem. Kinetics, 9 (1977): 651).

d see note (d) in QRRK1, Geometric mean frequency estimated as follows:
$\langle v \rangle_{CH2CHCl} = \langle v \rangle_{CH2CH2} - \Delta\langle v \rangle$,
$\Delta\langle v \rangle = \langle v \rangle_{CH3CH3} - \langle v \rangle_{CH3CH2Cl}$.

e see note (e) in QRRK1.

CALCULATED APPARENT FORWARD REACTION RATE CONSTANTS

Bath Gas	P (torr)	Product Channel	A (cc/mole s)	n	Ea (Kcal/mole)
AR	760.0	CH_2CHCl	1.24E31	-6.19	4.98
		$CH_2CH + Cl$	1.02E14		0.07
		CHCH + HCl	8.34E11		-2.12

QRRK8

$$CH_2CCl + O_2 \overset{1}{\Longleftrightarrow} [C.H_2CClOO.]^{\#} \overset{2}{\longrightarrow} CH_2CClO + O$$

$$\overset{4}{\Longleftrightarrow} [CH_2O.CClO]^{\#}$$

$$\overset{5}{\longrightarrow} CH_2O + CClO$$

$$\overset{6}{\longrightarrow} H + CHOCClO$$

k	A	Ea	Source
1	3.00E12	2.0	a
-1	1.23E15	36.0	b
2	2.67E15	56.5	c
4	4.79E12	15.0	d
-4	7.35E12	78.6	e
5	1.20E14	17.8	f
6	2.50E13	19.7	g
$\langle v \rangle = 781.9\ cm^{-1}$			h
LJ PARAMETERS:	$\sigma = 4.957$ Å	$\varepsilon/k = 454.09\ ^oK$	i

a. A_1 taken from $CH_2CCl + O_2$ in Russell, J.J., J. A. Seetula, D. Gutman and S.M. Senkan, J. Phys. Chem., 93 (1989): 1934-1938.

b. Reverse reaction (k_{-1}) from thermodynamics.

c. A_{-2} taken as that for $C_2H_3O + O$ (A=2E13), and microsopic reversibility, $E_a = \Delta Hr + 6$ ($C_2H_3 + O_2$, Ref: Bozzelli, J. W. and A. M. Dean, paper submitted to J. Phys. Chem.).

d. Transition State Theory: loss of a rotors and degeneracy= 1,
$A_4 = 10^{13.55} * EXP(-4/R) * 1 = 4.79E12$. $Ea_4 = 15$ (estimated in this work).

e. Reverse reaction (k_{-4}) from thermodynamics.

f. A_{-5} taken as that $C_2H_4 + iC_3H_5$ (A=6.3E10, Ref: Allara,D.L. and R. J. Shaw, J. Phys. Chem. Ref. Data, 9 (1980): 523) and microscopic reversibility, $E_a = \Delta Hr + 7.7 = 17.8$.

g. A_{-6} taken as 1/2 of that for H + C_2H_4 (Ref: NIST fit), E_{-6} = 2.8 and microscopic reversibility h. From "CPFIT" program and Cp data.

i. Calculated from critical properties (estimatedby using Lydersen method) for $CH_2CClOOH$ (Ref: RPP).

CALCULATED APPARENT FORWARD REACTION RATE CONSTANTS

Bath Gas	P (torr)	Product Channel	A (cc/mole s)	n	Ea (Kcal/mole)
Ar	760	CH_2CClOO	6.63E27	-5.55	3.87
		CH_2CClO + O	6.31E12		21.4
		$CH_2O.CClO$	2.85E22	-4.51	3.66
		CH_2O + CClO	1.16E12		-1.09
		H + CHOCClO	1.97E11		-1.10

QRRK9

$$CH_2CHCl + H \overset{1}{\Longleftrightarrow} [CH_2CH_2Cl]^{\#} \overset{2}{\longrightarrow} CH_2CH_2 + Cl$$
$$\longrightarrow CH_2CH_2Cl \text{ (Stab.)}$$

k	A	Ea	source
1	1.33 E+13	5.8	a
-1	1.27 E+13	45.5	a
2	1.15 E+14	20.7	b
$\langle v \rangle = 1265.3\ cm^{-1}$			c
L-J Parameters :	$\sigma = 4.898$ Å	$\varepsilon/k = 300\ ^{o}K$	d

a A_1 factor taken as 1/3 that for C_2H_4 + H. E_a estimated from addition reaction of C_2Cl_4+H and C_2H_4+H. Reverse reaction (k_{-1}) from thermodynamics (ref: Tsang, W., 23rd Symposium on Combustion, Orleans, France (1990) and NIST Chemical Kinetic Database (1990)).

b A_2 factor based upon entropy change for reverse. A_{-2} taken as that for CH_2CH_2 + Cl (A_{avg}=5.9E+13, from NIST database).

c see note (d) in QRRK1 (refer to CH_3CH_2Cl).

d see note (e) in QRRK1.

CALCULATED APPARENT FORWARD REACTION RATE CONSTANTS

Bath Gas	P (torr)	Product Channel	A (cc/mole s)	Ea (Kcal/mole)
AR	760.0	CH_2CH_2Cl	7.66E08	-1.67
		CH_2CH_2 + Cl	1.33E13	3.30

QRRK10

$$CH_2CHCl + OH \overset{1}{\Longleftrightarrow} [C.H_2CHClOH]^{\#} \overset{2}{\longrightarrow} CH_2CHOH + Cl$$

$$\overset{4}{\Longleftrightarrow} [CH_3CHClO]^{\#}$$

$$\overset{5}{\longrightarrow} CH_3 + CHClO$$

$$\overset{6}{\longrightarrow} CH_3CHO + Cl$$

k	A	Ea	Source
1	2.72E12	1.5	a
-1	9.82E13	33.2	b
2	1.32E14	20.6	c
4	1.23E12	38.4	d
-4	1.63E13	35.0	e
5	8.21E14	2.0	f
6	2.74E14	15.2	g
$\langle v \rangle = 1085.7\ cm^{-1}$			h
LJ PARAMETERS:	$\sigma = 4.985$ Å	$\varepsilon/k = 596\ ^{o}K$	i

a. A_1 taken as 1/2 that for C_2H_4 + OH, also referred to OH + C_2HCl_3 and OH + C_2Cl_4 (Ref: NIST fit).

b. Reverse reaction (k_{-1}) from thermodynamics.

c. A_{-2} taken as that Cl + unsaturated species (ca. A=1.5E13 Ref: Kerr, J.A. and Moss, S.J. ,"Handbook of Bimolecular and Termolecular Gas Reaction Vol.I & II", CRC Press Inc. (1981) and NIST) and microscopic reversibility.

d. Transition State Theory: loss of two rotors and degeneracy,
$A_4 = 10^{13.72} * EXP(-7/R) * 1 = 1.23E12$. $Ea_4 = RS + \Delta Hr + Ea_{abs} = 26 + 3.4 + 9 = 38.5$.
Ea_{abs}: $CH_3 + ROH \longrightarrow CH_4 + RO$. (Ref: Kerr & Moss II, 199),
$CH_3 + CH_3OH \longrightarrow CH_4 + CH_3O.$, Ea = 9.0,
$CH_3 + CH_3CH_2OH \longrightarrow CH_4 + CH_3CH_2O.$, Ea = 9.4.

e. Reverse reaction (k_{-4}) from thermodynamics.

f. A_{-6} = 3.16E11 (C. + CC=C $\longrightarrow$ $(CH_3)_2CC$. Ref: Allara,D.L. and R. J. Shaw, J. Phys. Chem. Ref. Data, 9 (1980): 523), Ea_{-6} = 2.0 and microscopic reversibility.

g. A_{-5} = 1.50E13 (Cl + unsaturated species Ref: Kerr, J.A. and S. J. Moss, "Handbook of Bimolecular and Termolecular Gas Reaction Vol.I & II", CRC Press Inc. (1981) and NIST), Ea_{-5} = 9.1 and microscopic reversibility, $E_a = \Delta Hr + 9 = 15.2$.

h. From "CPFIT" program and Cp data.

i. Calculated from critical properties (estimated by using Lydersen method) for $CH_3CHClOH$ (Ref: RPP).

CALCULATED APPARENT FORWARD REACTION RATE CONSTANTS

Bath Gas	P (torr)	Product Channel	A (cc/mole s)	Ea (Kcal/mole)
Ar	760	$CH_2CHClOH$	2.08E08	-5.93
		CH_2CHOH + Cl	2.67E12	1.50
		CH_3CHClO	1.58E03	8.42
		CH_3 + CHClO	4.20E09	11.60
		CH_3CHO + Cl	2.58E07	13.80

QRRK11

$$CH_2CHCl + O \overset{1}{\Longleftrightarrow} {}^3[CH_2.CHClO.]^{\#} \overset{2}{\longrightarrow} {}^3CH_2 + CHClO$$

$$\overset{3}{\longrightarrow} CH_2.CHO + Cl$$

$$\overset{4}{\Longleftrightarrow} {}^3[CH_2ClC.HO.]^{\#}$$

$$\overset{5}{\longrightarrow} CHO + CH_2Cl$$

$$\overset{6}{\longrightarrow} CH_2CHO. + Cl$$

k	A	Ea	Source
1	3.40E12	1.1	a
-1	7.35E12	30.9	b
2	1.49E14	23.9	c
3	4.98E14	15.0	d
4	7.10E12	24.0	e
-4	1.25E13	32.1	f
5	2.78E14	15.0	g
6	2.36E15	22.7	h
$\langle v \rangle$ = 1023.5 cm^{-1}			i
LJ PARAMETERS:	σ = 4.985 Å	ε/k = 596.4 ^oK	j

a. A_1 taken from C_2H_3Cl + O (A=3.4E12, Ref: Cvetanovic, B.J., J. Phys. Chem., Ref. Data, 16 (1987): 261).

b. Reverse reaction (k_{-1}) from thermodynamics.

c. A_{-2} taken as 2 that for C. + CC=C$\longrightarrow$ $(CH_3)_2CC$. (A=3.16E11, E_a=9.1 Ref: Allara,D.L. and R. J. Shaw, J. Phys. Chem. Ref. Data, 9 (1980): 523), $E_a = \Delta Hr$ + 9, and microscopic reversibility.

d. A_{-3} taken as 1/2 of that for Cl + C=C (A=5.0E13), $Ea_3 = \Delta H + 8 = 15$.

e. Transition State Theory: loss of a rotors and degeneracy= 1,
$A_4 = 10^{13.72} * EXP(-4/R) * 1 = 7.1E12$. $Ea_4 = Rs + Ea_{abs} = 17 + 7 = 24$.

f. Reverse reaction (k_{-4}) from thermodynamics.

g. A_{-5} taken as 1/2 of that for HCO + C_2H_4 and HCO + C_3H_6 (NIST data base), $Ea_5=\Delta H + 5.5 = 15.0$.

h. A_{-6} taken as that for Cl + CC=C (A=1.50E14, Atkinson, R. and S. M. Aschmann, Int. J. Chem. Kinet., 17 (1985): 33).

i. From "CPFIT" program and Cp data.

j. Calculated from critical properties (estimated by using Lydersen method) for $CH_3CHClOH$ (Ref: RPP).

CALCULATED APPARENT FORWARD REACTION RATE CONSTANTS

Bath Gas	P (torr)	Product Channel	A (cc/mole s)	Ea (Kcal/mole)
Ar	760	CH_2CHClO	1.95E07	-4.63
		CH_2 + CHClO	2.76E11	4.17
		CH_2.CHO + Cl	3.25E12	1.05
		CH_2ClC.HO.	2.75E04	-1.68
		CHO + CH_2Cl	3.71E09	3.32
		CH_2CHO. + Cl	1.07E10	5.07

QRRK12

$$CH_3CH_2 + H \overset{1}{\Longleftrightarrow} [CH_3CH_3]^{\#} \overset{2}{\longrightarrow} CH_3 + CH_3$$

$$\longrightarrow CH_3CH_3 \text{ (Stab.)}$$

k	A	Ea	source
1	1.8 E+14	0.0	a
-1	1.3 E+16	100.7	a
2	8.0 E+16	90.4	a
$\langle v \rangle = 1509\ cm^{-1}$			b
L-J Parameters:	$\sigma = 4.342$ Å	$\varepsilon/k = 246.8\ ^{o}K$	c

a Dean, A.M., J. Phys. Chem., 89 (1985): 4600.

b see note (d) in QRRK1.

c see note (e) in QRRK1.

CALCULATED APPARENT FORWARD REACTION RATE CONSTANTS

Bath Gas	P (torr)	Product Channel	A (cc/mole s)	Ea (Kcal/mole)
AR	760.0	CH_3CH_3	4.93E12	-5.21
		$CH_3 + CH_3$	5.10E14	2.85

QRRK13

$$C_2H_2 + O_2 \overset{1}{\Longleftrightarrow} {}^3[C.H{=}CHOO]^{\#} \overset{2}{\longrightarrow} {}^3CH.{=}C.OOH$$

$$\overset{3}{\longrightarrow} {}^3CH_2{=}C.OO.$$

$$\overset{3b}{\longrightarrow} CH_2{=}C{=}O + O$$

$$\overset{4}{\Longleftrightarrow} [Cy(C_2H_2OO)]^{\#}$$

$$\overset{5}{\Longleftrightarrow} [OHCCHO]^{\#}$$

$$\overset{6}{\longrightarrow} HCO + HCO$$

k	A	Ea	Source
1	5.00E12	34.0	a
-1	6.30E13	0.	b
2	1.50E13	35.0	c
3	3.98E13	43.8	d
3b	1.38E12	0.	e
4	1.50E12	11.0	f
-4	1.00E14	61.0	g
5	1.10E14	8.0	h
-5	1.50E13	92.0	i
6	4.30E17	72.0	j
$\langle v \rangle = 776.2\ cm^{-1}$			k
LJ PARAMETERS:	$\sigma = 4.8$ Å	$\varepsilon/k = 481.\ ^oK$	l

a. A_1 estimated as 5.0E12 at this work, $E_a = \Delta Hr$.

b. Reverse reaction (k_{-1}) from thermodynamics.

c. Transition State Theory: loss of 1 rotors and degeneracy,
$A_2 = 10^{13.55} * EXP(-4/R) * 1 = 1.5E13$. $Ea_2 = RS + \Delta Hr + Ea_{abs} = 19.8 + 6 + 9.2 = 35$.

d. Transition State Theory: degeneracy=1, $A_3 = 10^{13.55} * 1 = 3.98E13$.
$Ea_3 = RS + \Delta Hr = 28 + 15.8 = 43.8$.

e. A_{-3b} =3.2E11 from CRC.

f. A_4 taken as 1/10 of that for Transition State Theory = $10^{13.55}$ EXP(-4/R)/10 = 1.5E12, Ea_4 = 11.

g. Reverse reaction (k_{-4}) from thermodynamics.

h. Transition State Theory: loss of 1 rotors and degeneracy, A_5 = $10^{13.55}$ * EXP(-4/R) * 1 = 1.5E13, Ea=8.

i. Reverse reaction (k_{-5}) from thermodynamics.

j. A_{-6} take as 2.0E13 and microscopic reversibility, E_a = ΔHr =72.

k. From "CPFIT" program and Cp data.

l. Calculated from critical properties (estimated by using Lydersen method) for CCCOH (Ref: RPP).

CALCULATED APPARENT FORWARD REACTION RATE CONSTANTS

Bath Gas	P (torr)	Product Channel	A (cc/mole s)	Ea (Kcal/mole)
Ar	760	HCO + HCO	1.20E11	44.5

QRRK14

$$CH_2Cl + CH_3 \overset{1}{\Longleftrightarrow} [CH_2ClCH_3]^{\#} \xrightarrow{2} C_2H_4 + HCl$$

$$\xrightarrow{3} C_2H_5 + Cl$$

$$\longrightarrow CH_2ClCH_3 \text{ (Stab.)}$$

k	A	Ea	Source
1	2.00 E+13	0.0	a
-1	1.63 E+17	90.6	a
2	3.24 E+13	56.6	b
3	2.17 E+15	79.5	c
<v> = 1265.3 cm^{-1}			d
L-J Parameters:	σ = 4.898 Å	ε/k = 300 °K	e

a. A_1 factor taken as that for $CH_3CH_2 + CH_3$ (A =2.5 E+13). A_{-1} based upon entropy change for reverse. (Ref: Allara,D.L. and R. J. Shaw, J. Phys. Chem. Ref. Data, 9 (1980): 523), E_a = 0.0 (BE ref: Weissman, M and S. W. Benson, J. Phys. Chem., 87 (1983): 243).

b Benson,S.W., "Thermochemical Kinetics", John Wiley & Son, 2nd ed., NY (1976).

c A_{-3} taken as that $CH_3CH_2 + CH_3$ (A = 2.0 E+13) and microscopci reversibility, $E_a = \Delta Hr - RT$.

d see note (d) in QRRK1.

e see note (e) in QRRK1.

CALCULATED APPARENT FORWARD REACTION RATE CONSTANTS

Bath Gas	P (torr)	Product Channel	A (cc/mole s)	Ea (Kcal/mole)
AR	760.0	CH_2ClCH_3	8.79E11	-4.45
		$C_2H_4 + HCl$	1.88E13	1.96
		$C_2H_5 + Cl$	2.43E13	6.08